

UC-NRLF

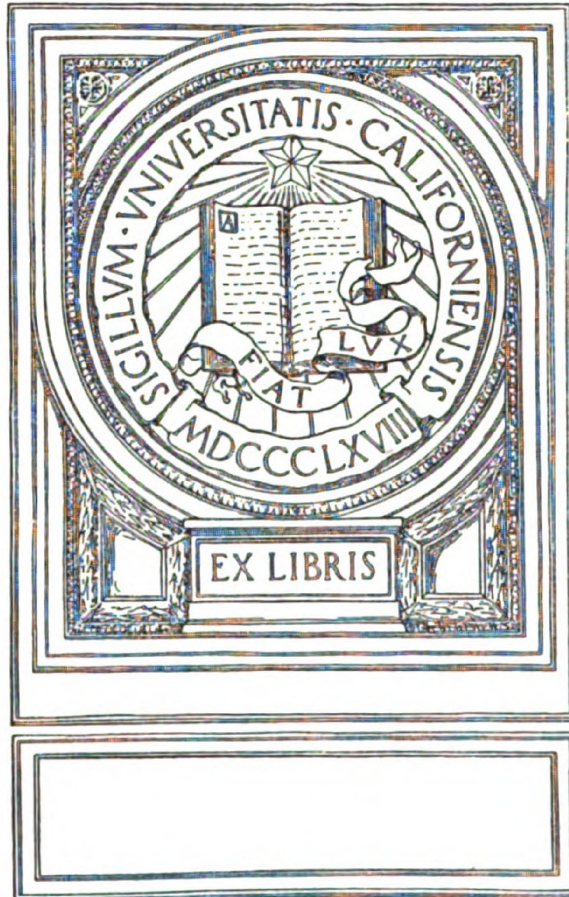


B 4 211 149

THE PHYSICS OF
RADIATION THERAPY

HAROLD ELFORD JOHNS, Ph.D.

UNIVERSITY OF CALIFORNIA
MEDICAL CENTER LIBRARY
SAN FRANCISCO



**THE PHYSICS OF
RADIATION THERAPY**

Publication Number 116
AMERICAN LECTURE SERIES®

A Monograph in
The BANNERSTONE DIVISION of
AMERICAN LECTURES IN RADIATION THERAPY

Edited by
MILTON FRIEDMAN, M. D.

Associate Professor of Radiology, New York University Post-Graduate Medical School
Associate Radiologist, University Hospital
Attending Radiotherapist, Hospital for Joint Diseases
Visiting Radiation Therapist, Bellevue Hospital
Senior Consultant in Radiation Therapy, Veterans Administration
Consultant, Walter Reed General Hospital
Consultant in Radiation, National Bureau of Standards
and United States Public Health Service
Washington, D. C.

The Physics *of* Radiation Therapy

By

HAROLD ELFORD JOHNS, M.A., PH.D., F.R.S.C.

Professor of Physics, University of Saskatchewan

Physicist, Saskatchewan Cancer Commission

Saskatoon, Saskatchewan, Canada

R895
J6
1953



CHARLES C THOMAS · PUBLISHER
Springfield · Illinois · U.S.A.

CHARLES C THOMAS • PUBLISHER
BANNERHOUSE HOUSE
301-327 East Lawrence Avenue, Springfield, Illinois

Published simultaneously in the British Commonwealth of Nations by
BLACKWELL SCIENTIFIC PUBLICATIONS, LTD., OXFORD, ENGLAND

Published simultaneously in Canada by
THE RYERSON PRESS, TORONTO

This monograph is protected by copyright. No
part of it may be reproduced in any manner
without written permission from the publisher.

Copyright 1953, by CHARLES C THOMAS • PUBLISHER

Library of Congress Catalog Card Number: 53-10948

..

Printed in the United States of America

PREFACE

THIS book is an expansion of a set of notes, *The Physical Basis of Radiotherapy*, which was printed privately and in limited numbers by the Saskatchewan Cancer Commission. It is written with the object of supplying students and physicians with the fundamental physical principles basic to an understanding of radiotherapy.

No detailed discussion of elementary electricity and mechanics has been included, since this may be found in any number of physics text books. Throughout, the concept of the energy of a photon of radiation rather than its wavelength has been emphasized. A detailed discussion of the methods by which an x-ray beam can give up its energy to tissue has been included. Special emphasis has been placed, throughout, on the concept of energy absorption in tissue, which I feel is fundamental. The nature of the distribution of radiation in space has been emphasized and a number of practical examples in radiotherapy have been included. The methods by which depth dose data and isodose distributions may be used in clinical work are indicated. In addition, a discussion of energy absorption in bone, fat and muscle has been included. Description of radium dosage has followed closely the Manchester system. A section on high energy devices (in particular, the betatron) and the use of radioactive isotopes has been added.

To increase the practical application of this book, I have added an appendix. This includes depth dose data based upon a comprehensive experimental survey of the depth dose which has been obtained from a variety of types of radiations. Great care has been taken in compiling this data to determine how the depth dose depends upon focal skin distance and area. A number of isodose distributions for the more commonly used types of radiation have been included. Experimentally determined spectral distributions of radiations are also presented.

I am indebted to Professor W. V. Mayneord for many of the basic ideas of energy absorption and the distributions of radiation in space, which were so ably presented in a course of lectures in 1946 at the Toronto General Hospital. The original set of notes followed closely



this set of lectures and it gives me pleasure to acknowledge Professor Mayneord's contribution. I am grateful to Dr. F. W. Spiers for his kind permission to include some of his basic work on the absorption of energy in a heterogeneous medium; to Dr. W. J. Meredith for his excellent tables on the use of radium; and to the originators of the Manchester system of radium dosage.

Much of the material included in this book has been used during the past two years in courses of lectures given to the staffs of the clinics of the Saskatchewan Cancer Commission. I am indebted to these various staff members for many suggestions and ideas concerning the book. In particular I am grateful to acknowledge the encouragement given me by the late Dr. A. W. Blair, former Director of Cancer Services for Saskatchewan, and by Dr. T. A. Watson, present Director. Thanks are also due to Dr. C. C. Burkell and Dr. A. Becker of the staff of the Saskatoon Cancer Clinic for their careful reading of the script and for their many helpful suggestions; and to Dr. E. L. Harrington, professor of Physics, University of Saskatchewan, for his continual encouragement. I am grateful to the many publishers who have made published material available for this book. The support of the Saskatchewan division of the Canadian Cancer Society was most acceptable.

Finally, to Dr. Milton Friedman, editor of the Radiation Therapy Series of the *American Lecture Series*, who asked me to prepare this script for publication, I wish to acknowledge the many helpful suggestions which were freely given.

HAROLD E. JOHNS

University of Saskatchewan
Saskatoon, Canada

CONTENTS

I	THE STRUCTURE OF MATTER AND RADIATION	3
	Atoms; Elemental Particles; The Nucleus; Extra Nuclear Structure; Energy Levels; Electromagnetic Radiation; Quantum Nature of Radiation; The Electromagnetic Spectrum; Radiation of Energy.	
II	THE PRODUCTION AND PROPERTIES OF X-RAYS	17
	The X-ray Tube; Simple Self Rectified X-ray Circuit; Anode Construction; X-ray Circuit Using Valve Rectification; Comparison between Valve Rectifiers and X-ray Tubes; Full Wave Rectification; Villard Voltage Doubling Circuit; The Production of X-rays; Characteristic Radiation; White Radiation; The Angular Distribution of X-rays.	
III	THE ABSORPTION OF X-RAYS BY MATTER	35
	Apparent Linear Absorption Coefficient; The Absorption of X-rays; Electronic and Mass Absorption Coefficients; Photoelectric Absorption; Compton Absorption; Pair Production; Total Apparent Absorption Coefficients; Total Real Absorption Coefficients; The Relative Importance of Different Types of Absorption; Summary.	
IV	MEASUREMENT OF QUANTITY OF RADIATION	57
	Methods of Measuring Quantity; The Roentgen; The Standard Ionization Chamber; Precautions in the Use of the Standard Air Chamber; Practical Ionization Chambers; Calibration of an X-ray Machine; Other Types of Radiation Measuring Devices.	
V	THE QUALITY OF X-RAYS	74
	Half Value Layer; The Measurement of Half Value Layer; Filters; Equivalent Wavelength and Kilovoltage; The Variation of Quality within a Scattering Medium.	
VI	THE INTERACTION OF X-RAYS WITH A SCATTERING MEDIUM . .	85
	Phantoms; Surface Backscatter; Percentage Depth Dose; The Variation of Percentage Depth Dose with Area; The Variation of Percentage Depth Dose with Depth; The Variation of Percentage Depth Dose with Half Value Layer; The Variation of Percentage Depth Dose with Focal Skin Distance; Isodose Curves and Surfaces; Summary.	

VII	THE COMBINATION OF X-RAY FIELDS AND THEIR DISTRIBUTIONS IN SPACE	110
	Coplanar Fields; Cancer of the Larynx; Distributions in Planes other than the Principal Plane for Circular Fields; Distribu- tion in Space for Rectangular Fields; Cancer of the Oesophagus; Statement of Dosage in Radiotherapy.	
VIII	ENERGY ABSORPTION	130
	Relation between Energy Absorption and the Roentgen; Inte- gral Dose; Whole Body Irradiation; Energy Flux; Protection Considerations; Energy Absorption in Biological Material; The Effect of Bone and Fat on Depth Dose Data; Comparison of Techniques giving the Same Formal Depth Dose.	
IX	RADIUM AND ITS ACTIVE DEPOSITS	149
	Natural Radioactivity; The Alpha Particle; Beta Decay; The Gamma Ray; Radioactive Disintegration; Radioactive Series from Radium; Radioactive Equilibrium; The Gamma Ray Spec- trum of Radium and its Active Deposits; The Strength of Radioactive Sources; The Decay of Radon; The Growth of the Active Deposits of Radon.	
X	RADIUM DOSAGE	165
	Radium Dosage; Surface Applicators; Distribution Rules for Surface Applicators; Interstitial Planar Implants; Two Plane Implants; Volume Implants; Linear Sources; Radiographic Con- trol of Radium Implants; Examples; Radium Isodose Curves; Cancer of the Cervix; Beta Ray Applicators; Summary.	
VI	HIGH ENERGY DEVICES	193
	Introduction; The Cyclotron; The Betatron; The Synchrotron; Fission; The Nuclear Reactor (Pile); The Van De Graaff Gen- erator; The Resonant Transformer; Cobalt 60 Telecurie Units; Protection.	
XII	ARTIFICIAL RADIOACTIVITY	214
	Typical Nuclear Reactions; Stability of Nuclei; Types of Disin- tegrations in Artificial Radioactivity; The Use of Radioactive Material, Tracer Studies; Radio Elements as Therapeutic Agents; Units for Measuring Ionizing Radiations; Dose Re- ceived during Treatment with Radioactive Isotope; Disintegra- tion Schemes of Radioactive Materials; Dosage Rate from Gam- ma Ray Emitters.	
APPENDIX A	231
	Depth Dose Data	234
	Isodose Distributions	255
APPENDIX B	
	Spectral Distributions	275
AUTHOR INDEX	279
SUBJECT INDEX	281

**THE PHYSICS OF
RADIATION THERAPY**

Chapter I

THE STRUCTURE OF MATTER AND RADIATION

1.01

ATOMS

ALL molecules are made up of atoms. There are 96 known kinds of atoms. These atoms consist of a massive nucleus surrounded by a "cloud" of moving electrons. The nucleus is very small, having a radius of the order of 10^{-12} cm. However, almost all the mass of the atom is concentrated in the nucleus. The planetary electrons move about the nucleus in orbits of about 10^{-8} cm. radius so that the "space" occupied by the atom is large compared with that occupied by the nucleus.

1.02

ELEMENTAL PARTICLES

The nucleus can be broken up by high speed particles and it is found to consist of protons and neutrons. Other particles which appear in nuclear reactions are the positron, the mesotron and the neutrino. The properties of these particles are listed in Table I. The masses of the particles are given in terms of the oxygen atom which is arbitrarily assigned the value 16.00000. The charges of these particles are given in terms of the charge on the proton. This charge is 4.80×10^{-10} e.s.u.*

TABLE I

PROPERTIES OF THE ELEMENTAL PARTICLES

<i>Particle</i>	<i>Mass</i>	<i>Charge</i>	<i>Properties</i>
proton	1.00758	+1	The proton is the nucleus of the hydrogen atom. The hydrogen atom consists of 1 proton in the nucleus and 1 external electron. The mass of the neutral atom is $1.00758 + .00055 = 1.00813$

*The electrostatic unit of charge (e.s.u.) is that charge which when placed 1 cm. from a like charge will repel it with a force of 1 dyne. The dyne is approximately 1/980 of a gram weight.

<i>Particle</i>	<i>Mass</i>	<i>Charge</i>	<i>Properties</i>
			mass units. The proton is one of the fundamental building blocks of all nuclei.
neutron	1.00894	0	The neutron is the other fundamental building block of all nuclei. Neutrons have nearly the same mass as protons. Since the neutron is an uncharged particle it is hard to stop and difficult to detect.
electron	0.00055	-1	The electron has a very small mass compared with the proton. Electrons abound in nature. Every atom contains electrons outside the nucleus. The electron is easily detected. It is sometimes called a negatron.
positron	0.00055	+1	The positron has the same mass as an electron but carries a positive charge. Positrons exist in nature only while they are in motion. A slowly moving or stationary positron quickly combines with an electron to form a burst of radiation.
mesotron	~0.10	± 1	The mesotron is a heavy electron of variable mass which can have either a positive or negative charge. These particles are associated with cosmic ray phenomena and exist in nature for very short periods of time.
neutrino	small mass	0	The neutrino was introduced from theoretical considerations to help explain beta disintegration. The particle has never been detected experimentally.

1.03

THE NUCLEUS

The nucleus consists of protons and neutrons. The number of protons in the nucleus is equal to the number of electrons outside the nucleus. This number is called the *atomic number Z* and ranges from

1 to 96. Because the proton carries a positive charge and the electron an equal negative charge the atom as a whole is neutral. The chemical properties of the atom depend upon the number and arrangement of the outermost electrons of the atom, which in turn depend upon the atomic number Z . This dependence is discussed in greater detail in the next section. The mass of the atom is determined primarily by the number of particles in the nucleus, since the external electrons have very small mass. The total number of particles in the nucleus determines the *mass number* A . Mass numbers range from 1 for hydrogen to 239 for the heaviest atom. Since the mass of the proton and neutron are nearly equal to 1.0 and since the mass of the electron is small, the atomic weight is nearly equal to the mass number A . Atomic weights are, therefore, almost whole numbers in value.

${}^{24}_{12}\text{Mg}$ indicates an atom of magnesium with atomic number 12 and mass number 24. These are 12 protons and 12 neutrons in the nucleus and 12 electrons outside the nucleus. The atomic weight is 23.9924, a value nearly equal to the mass number 24.

Often it will be found that several species of atoms have the same number of electrons outside the nucleus, the same number of protons in the nucleus but different numbers of neutrons in the nucleus. These types of atoms are called *isotopes*. Examples of these are as follows:

Isotopes of Hydrogen

There are three known isotopes of hydrogen represented as ${}^1_1\text{H}$, ${}^2_1\text{H}$, ${}^3_1\text{H}$. All have atomic number $Z=1$, so that each contains 1 proton in the nucleus and 1 electron outside the nucleus. This identical extra nuclear structure gives them all the same chemical properties. ${}^1_1\text{H}$ and ${}^2_1\text{H}$ exist in nature as a mixture in the relative proportions of 99.98% and 0.02% respectively. ${}^2_1\text{H}$ is called heavy hydrogen. The nucleus of heavy hydrogen containing 1 proton and 1 neutron, is widely used in nuclear disintegration experiments and is called the deutron. The atomic weights of these two isotopes are 1.00813 and 2.01471 respectively, being almost equal to the mass numbers 1 and 2.* ${}^3_1\text{H}$ is an unstable isotope of hydrogen which disintegrates to form an isotope of helium.

Isotopes of Helium, ${}^3_2\text{He}$, ${}^4_2\text{He}$ and ${}^6_2\text{He}$

All isotopes of helium have 2 protons in the nucleus and 2 electrons outside the nucleus. The nucleus of ${}^4_2\text{He}$, containing 2 protons and 2

*The mass ${}^1_1\text{H}$ (1.00813) plus 1 neutron (1.00894) is 2.01707. This is greater than the mass of ${}^2_1\text{H}$ (2.01471). The difference in mass corresponds to the energy required to knock a neutron from a ${}^2_1\text{H}$ nucleus (Chapter XII).

neutrons, is a particularly stable combination called an alpha particle. It is widely used in disintegration experiments. ${}^2\text{He}^6$ is unstable and disintegrates to form an isotope of lithium. ${}^2\text{He}^3$ is stable but exists in nature with a very small percentage abundance.

Isotopes of Phosphorus, ${}^{15}\text{P}^{29}$, ${}^{15}\text{P}^{30}$, ${}^{15}\text{P}^{31}$, ${}^{15}\text{P}^{32}$, ${}^{15}\text{P}^{34}$

${}^{15}\text{P}^{31}$ is the only stable isotope of phosphorus. The nucleus contains 15 protons and 16 neutrons. The other isotopes are radioactive. ${}^{15}\text{P}^{32}$ has been used in the treatment of blood disorders.

Isotopes of Cobalt, ${}^{27}\text{Co}^{55}$, ${}^{27}\text{Co}^{56}$, ${}^{27}\text{Co}^{57}$, ${}^{27}\text{Co}^{58}$, ${}^{27}\text{Co}^{59}$, ${}^{27}\text{Co}^{60}$, ${}^{27}\text{Co}^{61}$.

${}^{27}\text{Co}^{59}$, the only stable isotope of cobalt, contains, 27 protons and 32 neutrons. The others disintegrate in a variety of ways to form isotopes of iron and nickel. ${}^{27}\text{Co}^{60}$ shows possibilities of replacing radium as a source of gamma rays for therapeutic work.

In general, as the atomic number is increased the number of known isotopes and the number of stable isotopes increases. For example, naturally occurring tin consists of a mixture of 10 stable isotopes. At least 12 radioactive isotopes of tin have been discovered.

Unstable isotopes disintegrate to form new isotopes and this process will continue until a stable product is reached. Many times it will be found that two elements have the same mass number but different atomic numbers. *Such pairs of atoms are called isobars.* ${}^{26}\text{Fe}^{57}$ and ${}^{27}\text{Co}^{57}$ are isobars with mass number 57. They can be separated chemically since they have different numbers of extra nuclear electrons and hence different chemical properties. For further details concerning the nucleus the reader is referred to Chapter XII.

1.04

EXTRA NUCLEAR STRUCTURE

In discussing x-rays and their effects on atoms we are interested in their extra nuclear structure, that is, the arrangement of the planetary electrons outside the nucleus.

Hydrogen is the simplest atom, consisting of 1 electron moving about the nucleus (Fig. I-1). All isotopes of hydrogen have this simple arrangement of the external electron. Helium, the next simplest atom, has 2 electrons. These two electrons travel in the same orbit spinning in opposite direction (Fig. I-1). This particular electronic configuration is particularly stable and, as a result, it is impossible to make helium interact chemically with any other material. Hydrogen owes its chemical activity to the fact that it would like to acquire one more electron to achieve the dynamic stability of helium.

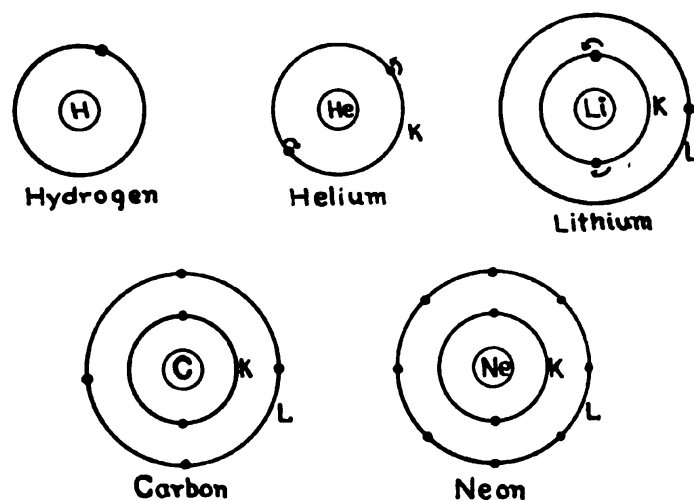


Figure I-1. Schematic diagram showing electron structure for hydrogen, helium, lithium, carbon and neon.

Lithium has three electrons (Fig. I-1). The third electron must be added to a new orbit outside the first one. The two electrons in the inner orbit completely fill this orbit or shell. We refer to this orbit as the K shell. The single electron in the outer orbit or L shell makes lithium a chemically active element.

As one proceeds to higher values of Z in the periodic table the L shell gradually fills up to form beryllium ($Z = 4$) with 2 electrons in the L shell, then boron ($Z = 5$) with 3 electrons, carbon ($Z = 6$) with 4, nitrogen ($Z = 7$) with 5, oxygen ($Z = 8$) with 6, fluorine ($Z = 9$) with 7, and finally neon ($Z = 10$) with 8. The L shell will not hold any more electrons. Diagrams showing the extra nuclear structure for carbon and neon are given in Figure I-1.

Neon, with a completely filled outer shell, is an inert gas and cannot be made to react chemically. Carbon, on the other hand, can form many compounds since it can give up 4 electrons or take on 4 electrons to achieve stability. Oxygen is 2 electrons short of a completed shell. It will try to acquire 2 electrons. Carbon and oxygen can combine to form CO_2 in which case the carbon gives each of the oxygen atoms 2 electrons. This is illustrated in Figure I-2 where carbon is shown sharing two electrons with each of the oxygen atoms. Fluorine, with one electron short of a completed shell, is very active. Sodium ($Z = 11$) is formed with the K and L shells filled and one electron in the M shell. Sodium will thus react with any atom which will take up one electron. Sodium and fluorine will therefore react to form a stable compound. Chlorine is similar in structure to fluorine with one empty place in the M shell. Sodium is shown sharing its extra charge with chlorine in Figure I-2, to form NaCl .

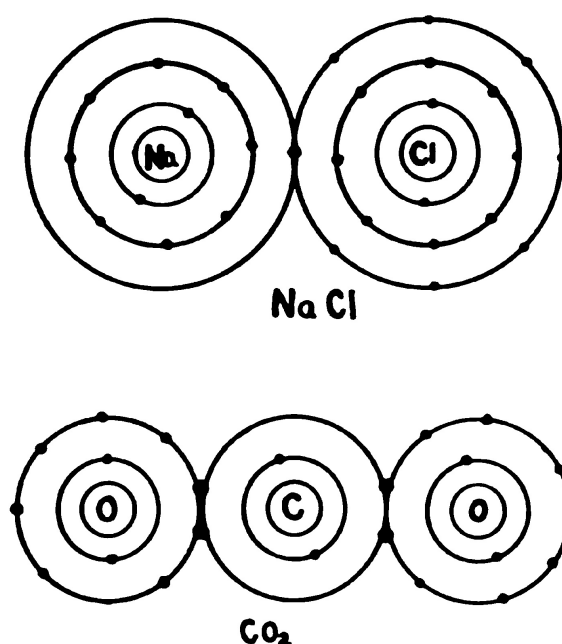


Figure 1-2. Diagram illustrating the combination of an atom of sodium with one of chlorine to form sodium chloride and the combination of two atoms of oxygen with one atom of carbon to form carbon dioxide.

As one proceeds to higher values of Z the extra nuclear structure becomes more and more complicated – the M shell will be filled, then the N and so on. Chemical properties will repeat themselves as the shells fill up. For example, inert gases helium, neon, argon, krypton, etc., will occur as each shell is filled. In a similar way alkaline elements lithium, sodium, potassium, etc., will appear when the outermost shell is occupied by only one electron. In general, the chemical properties and valence will be determined by the number of electrons in the outermost incomplected shell.

1.05

ENERGY LEVELS

Although the electrons are assigned to these definite orbits, it should be emphasized that the orbits do not have any real physical significance. The electron is not confined to these orbits but has a certain definite probability of being almost anywhere. However, the electron will most likely be found near this orbit. There is no friction inside the atom, so the electron can travel about in its orbit with no loss of energy. Although the orbits have no real significance they are characterized by each having a very definite energy.

The fundamental unit of work or energy is the erg.* However,

*Work is measured as the product of the force exerted and the distance through which the force acts. The fundamental physical unit of work is therefore the dyne cm. This unit has been called the erg. 1 dyne cm. = 1 erg.

a more useful energy unit for our purposes is the *electron volt*. It is the amount of energy released when an electron falls through a potential difference of 1 volt. This work is given by the product of the charge and the potential difference through which it falls. Now, 1 electron has a charge of 4.80×10^{-10} e.s.u. and 1 volt is 1/300 of 1 electrostatic unit of potential difference. Hence

$$\begin{aligned} 1 \text{ electron volt (ev.)} &= \frac{1}{300} \times 4.80 \times 10^{-10} \text{ ergs} \\ &= 1.60 \times 10^{-12} \text{ ergs.} \end{aligned} \quad (1-1)$$

For many purposes a unit 1 million times as big, the Mev., is more useful. (The unit Kev. = 1000 ev. is also useful.)

$$1 \text{ Mev.} = 1.60 \times 10^{-6} \text{ ergs.} \quad (1-2)$$

Consider tungsten as an example (Fig. I-3). The binding energies of electrons in the K, L, and M shells are about 70,000 ev., 11,000 ev. and 2500 ev. respectively. This means that, to remove a K electron from the atom, the tungsten atom must be supplied with 70,000 ev. of energy or it must be bombarded with electrons which have fallen through at least 70,000 volts potential difference. To remove an L electron about 11,000 ev. of energy are required.

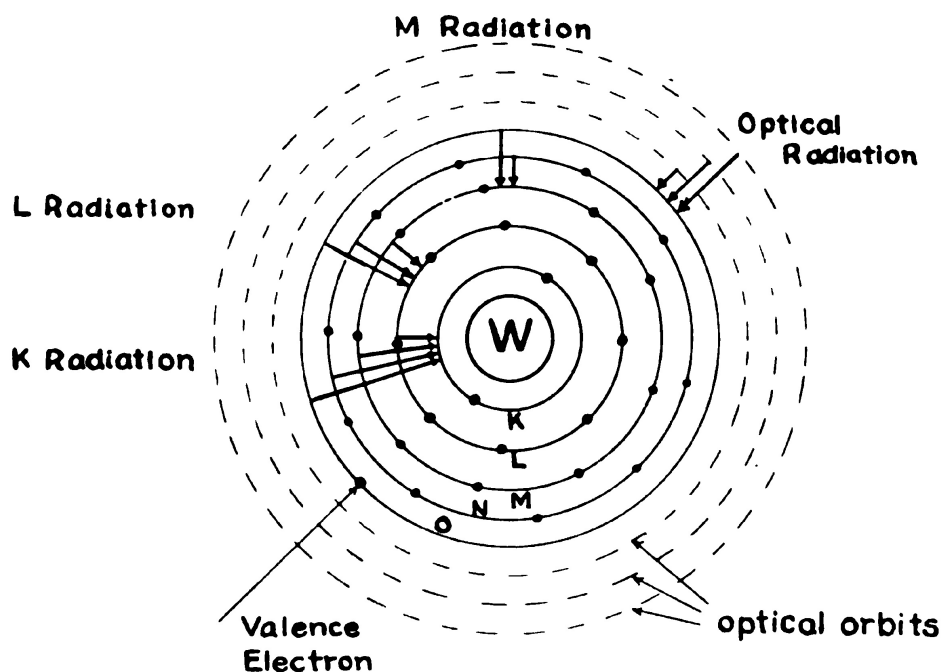


Figure I-3. Schematic diagram for the tungsten atom. X-radiation arises through transitions of electrons to the K, L, and M shells. Optical radiation arises by transitions of the valence electron from optical orbits to the O shell.

In the normal state the outermost valence electron of tungsten is in an O shell. However, by supplying it with energy it can move out into orbits beyond the O shell. These orbits are separated from one another by only a few electron volts energy and are usually referred to as optical orbits. In the normal atom the electrons will always occupy the orbits with the greatest binding energy. However, when the more loosely bound electrons are excited the optical orbits may be filled momentarily. As the electron falls back to its normal orbit, energy is radiated. We find that energy is radiated from the atom whenever an electron falls from an outer orbit into one nearer the nucleus. The nature of this radiated energy is discussed in the next section. For x-ray purposes one is interested in the motion of the tightly bound electrons in the K, L and M shells while the motion of the outer electrons is of importance in determining the optical spectrum of the material.

1.06 ELECTROMAGNETIC RADIATION

Radio waves, heat waves, light waves, ultra violet, x-rays, gamma rays are all examples of electromagnetic radiation. They all travel with a velocity of 3.0×10^{10} cm./sec. or 186,000 miles per second in a vacuum. The velocity is usually referred to as c . Waves of all kinds have associated with them a wavelength λ and a frequency n (Fig. I-4). If a tuning fork makes n vibrations per second and the length of each wave given off is λ then in one second the wave will travel $n\lambda$ cm., i.e., the velocity is equal to $n\lambda$. For electromagnetic waves we have then the very important relation

$$n\lambda = c = 3 \times 10^{10} \text{ cm./sec.} \quad (1-3)$$

This relation enables us to calculate the wavelength of the radiation if the frequency is known, or conversely, the frequency if the wavelength is known. In this formula the frequency is expressed in vibrations per second and the wavelength in cm. The electromagnetic waves which we are interested in are so very short in wavelength

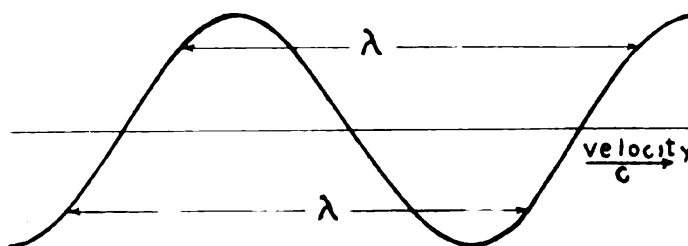


Figure I-4. Diagram of an electromagnetic wave showing the meaning of wavelength.

that it is convenient to express their length in Angstrom units where $1\text{A} = 10^{-8}\text{ cm}$. A wave 0.00005 cm . long or 5000 A has a frequency $n = c/\lambda = 3 \times 10^{10}/0.00005 = 6 \times 10^{14}$ vibrations per second. The wavelength of an electromagnetic wave determines its properties. The wave discussed above (5000 A) can be seen with the human eye and is referred to as green light. Blue light has a shorter wavelength of 4000 A and red light a longer wavelength of 7000 A . If the wavelength is longer than 7000 A the human eye cannot detect it and we refer to the radiation as infra-red. If the wavelength is shorter than 4000 A the radiation is again invisible to the eye and is called ultra-violet. Radiation of 0.1 A is referred to as x-radiation. The properties of electromagnetic radiation depend upon the wavelength of the radiation. As the wavelength becomes very short and the corresponding frequency very large it is necessary to consider the "quantum" nature of the radiation.

1.07 QUANTUM NATURE OF RADIATION

Although for many purposes we can consider all electromagnetic radiations as waves, we must think of them at times as being like small bullets travelling with velocity c and each carrying a certain amount of energy. This bundle of energy is called a quantum or photon. The amount of energy carried by the photon depends upon the frequency of the radiation. If the frequency is doubled the energy of the photon is doubled. The actual amount of energy carried by a photon is given by the important equation

$$\begin{array}{rcccl} E & & h & \times & n \\ \text{energy} & = & \text{Planck's} & & \text{frequency} \\ \text{(ergs)} & & \text{constant} & & \text{(1/sec)} \\ & & \text{(erg. sec).} & & \end{array} \quad (1-4)$$

$$h = 6.61 \times 10^{-27} \text{ erg. sec.}^*$$

As an example, let us calculate the energy carried by one photon of radiation whose wavelength is 1.0 A or 10^{-8} cm . The corresponding frequency is $n = c/\lambda = 3 \times 10^{10}/10^{-8} = 3 \times 10^{18}$ vibrations per second. Hence the energy carried by 1 photon of this radiation is $E = hn = 6.61 \times 10^{-27} \times 3 \times 10^{18} = 19.83 \times 10^{-9}$ ergs. This can be converted to electron volts using equation (1-1) to give $E =$

*Frequency, n , is the number of vibrations per second and is obtained by determining the number of vibrations in a certain time. It is thus a number divided by time in sec. and so has dimensions $1/\text{sec.}$ or sec.^{-1} . Since the energy E is expressed in ergs, Planck's constant must be measured in units $\text{ergs} \times \text{sec.}$ so that when it is multiplied by frequency n measured in $1/\text{sec.}$, the product will be ergs.

$19.83 \times 10^{-9} / 1.60 \times 10^{-12} = 12,400 \text{ ev.} = 12.4 \text{ Kev.}$ That is, one quantum of this wavelength carries with it 12,400 electron volts of energy. If the wavelength is 0.01 A, the frequency will be 100 times as great and the energy of one quantum or photon will be 1,240,000 ev. or 1.24 Mev. A general relation between the energy of the photon in ev. and the wavelength of the radiation in A can be obtained from $E = hn = hc/\lambda$. If E is expressed in ev., and λ in A the relation becomes

$$E \text{ (ev.)} = \frac{12,400}{\lambda \text{ (A)}} \quad (1-5)$$

Using this relation we see that radiation of wavelength 1.0 A carries with it an energy of 12,400 ev. as obtained above. Conversely, it means that to produce radiation of wavelength 1.0 A at least 12,400 ev. of energy must be supplied. The significance of this equation in the production of x-rays will be discussed in the next chapter.

It is readily seen that as the wavelength becomes shorter and shorter, the energy associated with one photon becomes larger and larger. In fact the energy carried by one photon of wavelength 1 A (12,400 ev.) is great enough to trigger a device such as a Geiger counter so that the passage of an individual photon can be recorded. If a Geiger counter is placed in the next room to an operating x-ray machine it will be observed that the photons of radiation are emitted in a discontinuous way. There will be no doubt then as to the quantum nature of radiation. In the case of radiation of long wavelength (low frequency) such as radio waves, the quantum nature is unimportant since each photon will now carry a very small amount of energy. For example, a radio transmitter operating at 300,000 cycles per second ($\lambda = 3 \times 10^{10} / 300,000 = 10^5 \text{ cm.} = 10^{13} \text{ A}$) emits photons of only $1.24 \times 10^{-9} \text{ ev.}$ energy. If the transmitter is operating at a power of 10,000 watts, it will send out into space about 5×10^{31} photons per second. A radio receiver many miles away would receive so many per second that the quantum nature would disappear. The concept of quanta is indispensable when dealing with high energy x-rays and gamma rays.

1.08

THE ELECTROMAGNETIC SPECTRUM

The electromagnetic spectrum includes all electromagnetic radiation from the very long radio waves to the exceedingly short, penetrating gamma rays at the other end of the spectrum. In Table II the

frequency, wavelength, photon energy and properties of the complete spectrum are summarized. It should be emphasized that the regions of the spectrum actually overlap, so that, for example, there is no sudden change in properties as we move from the region of radio waves into the infra red region or from the ultra violet into the x-ray region. It is seen that the quantum of energy for high frequency (short wavelength) radiation becomes very large.

TABLE II
THE ELECTROMAGNETIC SPECTRUM

<i>Frequency (cycles/sec)</i>	<i>Wavelength</i>	<i>Photon Energy</i>	<i>Properties</i>
1.0×10^5	3×10^5 cm.	4.13×10^{-10} ev.	Radio waves ranging from long waves through the broadcast band, to short waves and to ultra short waves in radar. These waves are produced by electrical oscillations and detected by electronic equipment. They will pass through non-conducting layers of materials but are reflected by electrical conductors.
3.0×10^{10}	1.0 cm.	1.24×10^{-4} ev.	
3.0×10^{12}	0.01 cm.	0.0124 ev.	Infra red radiations. These are produced by molecular vibration and the excitation of the outer electrons of the atom. They are generated by heat in stoves, radiators etc. and can be detected by heat devices and films. Most solid materials are opaque to infra red radiations.
3.0×10^{14}	0.0001 cm. (10,000A)	1.24 ev.	

<i>Frequency (cycles/sec)</i>	<i>Wavelength</i>	<i>Photon Energy</i>	<i>Properties</i>
4.3×10^{14}	7000A (0.00007 cm.)	1.77 ev.	Visible light ranging from red through yellow, green and blue to violet. Produced by the excitation of the outer electrons of an atom. Generated in lamps and in gas tubes by electrical discharge. Detected by films, by photoelectric cells and by the eye. Transmitted by materials such as glass.
7.5×10^{14}	4000A	3.1 ev.	
7.5×10^{14}	4000A	3.1 ev.	Ultra violet light. Produced by the excitation of outer electrons in the atom. Detected by films, Geiger counters and ionization chambers. Produces erythema of the skin; kills bacteria and is an agent in the production of Vitamin D.
3.0×10^{16}	100A	124 ev.	
3.0×10^{16}	100A	124 ev.	Soft x-rays. Produced by the excitation of the inner electrons of an atom. Detected by films, Geiger counters and ionization chambers. Have the ability to penetrate very thin layers of material. Of little value in radiology because of their limited power of penetration.
3.0×10^{18}	1A	12,400 ev.	
3.0×10^{18}	1A	12,400 ev.	Diagnostic x-rays and superficial therapy.
3.0×10^{19}	0.1A	124,000 ev.	

<i>Frequency (cycles/sec)</i>	<i>Wavelength</i>	<i>Photon Energy</i>	<i>Properties</i>
3.0×10^{19}	0.1A	124 Kev.	Deep therapy x-rays and gamma rays from radium decay products.
3.0×10^{20}	0.01A	1.24 Mev.	
3.0×10^{21}	0.001A	12.4 Mev.	Radiation from a small betatron.
3.0×10^{22}	0.0001A	124 Mev.	Radiation from a large betatron.
3.0×10^{23}	0.00001A	1240 Mev.	Not yet produced by man.

In the above chart the energy of the photon will also be the energy which is required to produce the radiation. For example 1.24 million volts will be required on an x-ray tube to produce x-rays of wavelength 0.01A. No wavelength shorter than this can be produced by 1.24 Mev., but longer waves are produced. In general, the minimum wavelength $\lambda_{\min.}$ (expressed in angstrom units) which can be produced by V (expressed in kilo-volts) will be given by

$$\lambda_{\min.} (\text{A}) = \frac{12.4}{V(\text{Kev.})} \quad (1-6)$$

This relation comes directly from equation (1-5).

1.09

RADIATION OF ENERGY

To understand the mechanism by which energy can be radiated from an atom let us consider again the energy levels for tungsten (Fig. I-3). Suppose a high speed electron impinges on an atom of tungsten and removes a K electron. This will require at least 70,000 electron volts of energy. In a very short time another electron from the L shell may fall down into the K shell to occupy the vacancy and when this occurs $(70,000 - 11,000) = 59,000$ electron volts of energy will be radiated as a quantum of x-rays. The wavelength of the radiation will be $12.4/59 = 0.211 \text{ A}$.

It may happen that the high speed electron will remove an L, M or N electron instead of the K electron. If the L electron (binding energy 11,000 ev.) is removed and the space filled with an M electron (binding energy 2,500 ev.) then the radiation emitted will have an energy of $11,000 - 2,500 = 8,500 \text{ ev.}$ and a wavelength of $12.4/8.5 = 0.685 \text{ A}$. In all cases the energy of the emitted quantum in electron volts is just the difference between the two binding energies. It is possible for any of the electrons of the atom to be ejected by a high

speed electron, although certain electrons have a higher probability of ejection than others.

To generate visible light from tungsten the valence electron must be excited to an outer optical orbit (Fig. I-3). When it falls back energy will be radiated but the amount will be a few electron volts corresponding to a wavelength in the visible region.

The vacancy in any shell can be filled in many ways. If a K electron is removed an electron may fall into this "hole" from an L shell, and M shell or any other shell. If an electron fills the K shell from the L shell then a "hole" will be left in the L shell and when it is filled L radiation will result. This is illustrated in Figure I-3. Actually the energy level diagram is much more complicated than this, for the L shell is divided into 3 sub shells, the M into 5 and the N into 7.

When we deal with an element of low atomic number the binding energies of the K shell are small. For carbon this energy is 285 ev., for oxygen 528 ev. and for organic tissues we may take the average value of 500 ev. The characteristic K radiation of "tissue" has a wavelength $(12.4/0.500) = 24.8 \text{ A}$ which is very soft and will be absorbed in a very short distance in tissue.

Chapter II

THE PRODUCTION AND PROPERTIES OF X-RAYS

2.01

THE X-RAY TUBE

X-RAYS are produced whenever a substance is bombarded by high speed electrons. The conventional x-ray tube (Fig. II-1) consists of an anode and a cathode assembly placed inside a glass envelope from which all air has been removed. The anode is often a massive piece of copper in the end of which is placed a small tungsten target. The cathode assembly consists of a filament of tungsten wire placed in a shallow focussing cup. When sufficiently energized by the filament supply, electrons are "boiled out" of the surface of the tungsten. Since it is necessary to raise the temperature of the tungsten to a white heat to obtain enough electrons, tungsten, with its high melt-

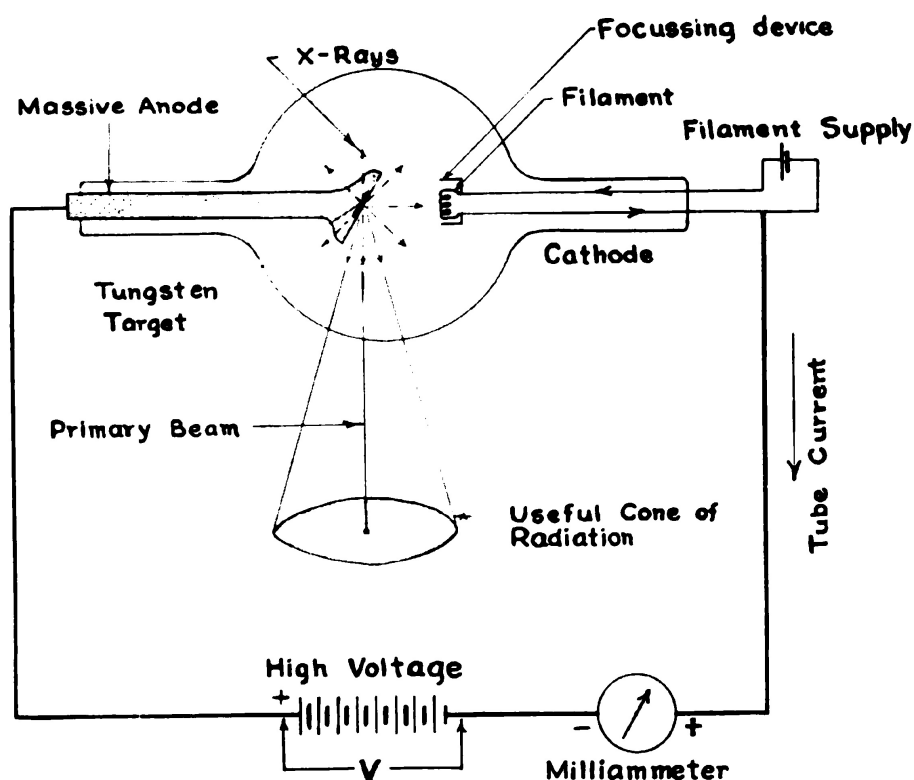


Figure II-1. Schematic diagram of an x-ray tube and the basic x-ray tube circuit.

ing point (3370°C), is almost always used as the source of electrons in an x-ray tube. If a high voltage V is applied between the anode and cathode with the anode positive, the electrons will be accelerated across the evacuated tube and will acquire very high velocities. For example, electrons accelerated by 100 Kv. acquire a velocity of 55% of the velocity of light. When these high speed electrons are suddenly stopped by the target heat is produced and x-rays are radiated. The x-rays are produced by the sudden deceleration of the electrons in passing into the surface layers of the target. The motion of the electrons across the evacuated space in the x-ray tube constitutes an electron current around the circuit in a counter clockwise direction. This is equivalent to a conventional current (the motion of positive charges) in the opposite direction as indicated by the arrow in Figure II-1. This current will be recorded by the milliammeter. Considerable care must be taken by the manufacturer to insure a high vacuum inside an x-ray tube envelope. Presence of air inside the tube will prevent the electrons from acquiring their full speed in falling from cathode to anode because of collisions with the gas molecules. It will also bring about the rapid deterioration and eventual destruction of the hot filament by oxidation. When an x-ray tube goes "soft" the filament almost immediately burns out. For these reasons great care is taken to remove all traces of residual gas occluded in the metal parts of the tube before it is sealed off. The focussing device shown schematically in Figure II-1 is necessary to concentrate the stream of electrons on the tungsten focal spot.

2.02 SIMPLE SELF RECTIFIED X-RAY CIRCUIT

In actual practice x-ray circuits bear little resemblance to that of Figure II-1. However, all circuits contain a filament supply to heat the filament and a high voltage supply to accelerate the electrons across the x-ray tube. The temperature of the filament, controlled by the filament supply, determines the number of electrons which are liberated. Since all the electrons liberated are pulled across to the anode the temperature of the filament determines the tube current. It is found that a slight increase in the filament temperature increases the tube current by a large amount. The high voltage supply determines the speed of the electrons just before they strike the target but has only slight control over the number of electrons which reach the target. The speed of the electrons determines the nature of the x-rays produced. A schematic diagram of a simple self rectified unit is shown in Figure II-2.

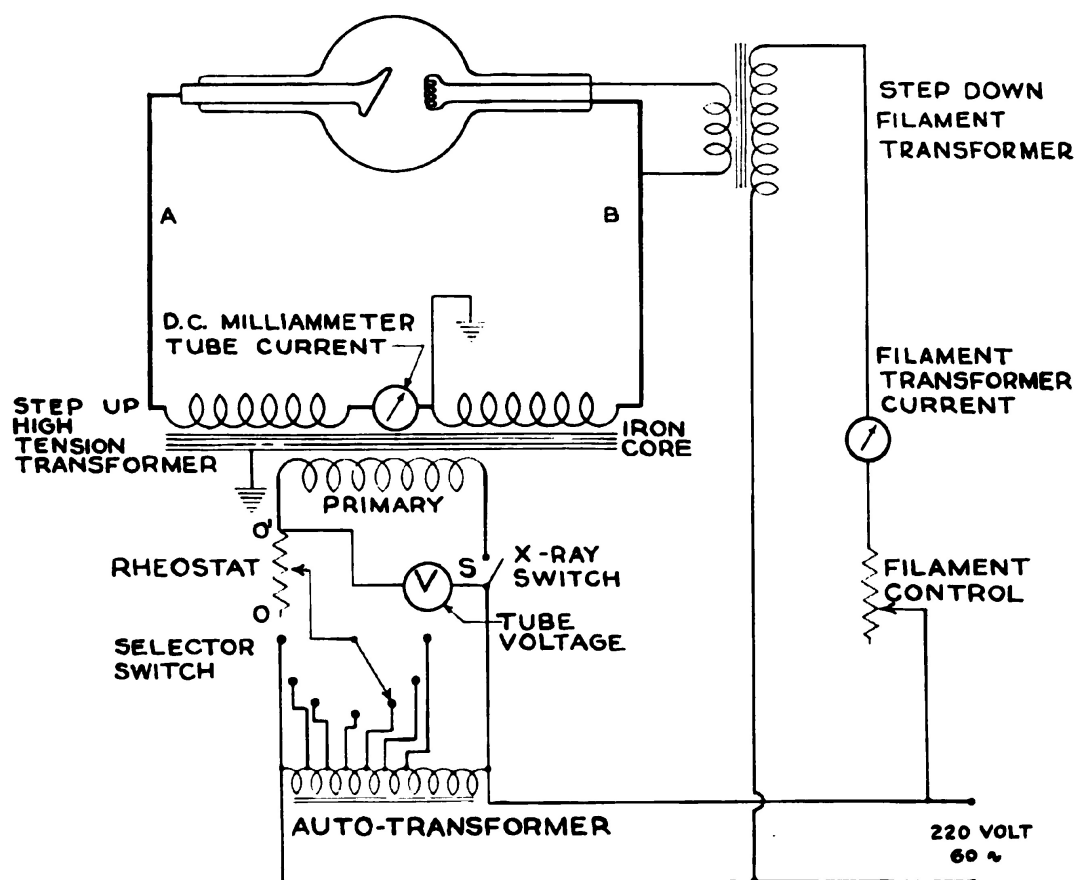


Figure II-2. Schematic diagram of a simple self rectified x-ray circuit showing how the tube voltage and current may be controlled.

The high voltage is varied by the use of an auto transformer and a rheostat. The auto transformer, consisting of a single winding on an iron core, is connected to the 220 volt 60 cycle source of power. By means of a series of contact points and a selector switch it is possible to obtain any voltage from 0 up to 220 volts from this auto transformer. The actual voltage selected is recorded on the voltmeter V. When the x-ray switch S is closed this voltage is applied through the rheostat to the primary of the high tension transformer. The current flowing through the rheostat will cause a voltage drop so that the voltmeter V across the primary of the transformer will now record a smaller voltage than it did before the switch was closed. As the contact on the rheostat is moved from 0 to 0' the voltage across the primary will rise. This means the voltage on the secondary of the transformer will also rise. In most x-ray installations the rheostat must be set with the contact point at 0 before the switch S can be closed. This prevents the sudden application of the high voltage to the x-ray tube. After the switch is closed the contact point may be moved from

0 to 0'. In some installations the voltage V applied to the primary may be varied during operation by adjustment of the rheostat. In others it is necessary to move the contact point all the way to 0' soon after the switch S is closed. It is not permissible to alter the voltage applied to the tube by adjustment of the selector switch while S is closed. If the selector switch is moved from one point to the next under load, excessive sparking will occur because as it moves from one button to the next, the circuit is actually broken. If adjustment of voltage is necessary the switch S should be opened and then the adjustment made. The high voltage applied to the x-ray tube is proportional to the voltage V applied to the primary of the transformer. For this reason the voltmeter V is often calibrated to read directly in kilovolts.

To supply electrons the filament of an x-ray tube is usually excited by about 10 volts at a current of about 6 amperes. This power can be obtained conveniently from the 220 volt 60 cycle mains by the use of a voltage step down transformer. This transformer also serves to isolate the cathode of the x-ray tube from ground potential. When the tube is being operated the cathode alternately goes to a high voltage above ground and then to a high voltage below ground since it is connected to one end of the high voltage transformer. The filament transformer is made with a high enough insulation between the primary and the secondary winding to withstand these large changes in potential. Usually the two windings are placed around the same iron core with the secondary winding spaced a couple of inches from the primary and from the core, and the space filled with insulating transformer oil. The temperature of the filament can be controlled safely by changing the voltage applied to the primary of the filament transformer. Since small changes in filament temperature produce large changes in the electron emission and hence in the tube current, precautions must be taken to hold the filament current constant. This may be done by supplying the power for the filament transformer from a constant voltage transformer (not shown in Fig. II-2). These transformers give an output voltage which is constant for normal variations in the line voltage.

The tube current could be measured by placing a direct current milliammeter anywhere in the main x-ray tube circuit (heavy lines Fig. II-2). However, if it were inserted in either line A or B it could not be placed on the control panel for its potential would fluctuate up and down about ground potential by the high voltage developed in the transformer. In old non-shock proof units it was usually sus-

pended from the ceiling out of the operator's reach. Often the centre point of the secondary winding is connected to the core and to ground and if this is so, the meter may be placed as indicated in Figure II-2. It is now at ground potential and can be safely placed on the control panel. All modern installations are made shockproof by enclosing the x-ray tube in a grounded metal case filled with insulating oil. The tube is made ray proof as well by inserting inside the metal case a lead sheath except in the direction of the useful beam of radiation (Fig. II-1). The tube is connected to the transformer by a flexible rubber insulated cable with an outer grounded metal sheath.

2.03 ANODE CONSTRUCTION

When the high speed electrons strike the target of the x-ray tube more than 99% of their energy is converted into heat in the target while the rest of the energy is radiated in the x-ray beam. This means that, for all practical purposes, all the energy of the electron stream is absorbed by the anode and must be removed from it by some method. The rate at which work is done in an electrical circuit is given by

$$P = VI \quad (2-1)$$

where P is the power expressed in joules* per second or watts, V is the potential difference in volts across the circuit, and I is the current in amperes flowing through the circuit. This energy can be expressed in calories using the relation $4.18 \text{ joules} = 1 \text{ calorie}$.

The energy developed in the anode of an x-ray tube can be calculated using this relation. As an example, consider a deep therapy machine which is designed to operate at 200 Kv. with a current of 30 milliamperes (.030 amperes). The rate at which energy is imparted to the anode is given by $P = VI = 200,000 \times .030 = 6000 \text{ watts}$. This is a very considerable rate of energy production and it is obvious that unless this heat energy is dissipated, the temperature of the anode would soon reach its melting point. Almost all anodes are made by imbedding a piece of tungsten in a massive piece of copper. Copper, with its excellent thermal conductivity, rapidly carries the heat from the tungsten where it is produced. Tungsten, with its high melting point, is unlikely to melt under electron bombardment. If the x-ray

*The fundamental unit of energy, the erg, is too small for practical purposes. A unit 10 million times as big, the joule, is useful ($1 \text{ joule} = 10^7 \text{ ergs}$). Power is the rate of doing work and is measured in joules per second. This unit of power is so important it is called the watt. ($1 \text{ joule/sec.} = 1 \text{ watt}$).

tube is used intermittently for short exposures, such as are required in diagnostic equipment, the copper anode will likely be able to dissipate its heat to the surroundings fast enough by conduction and radiation. However, in a therapy machine which must operate continuously, cooling oil under pressure is often circulated through the centre of a hollow anode.

For diagnostic work, tube currents as large as 500 milliamperes are used for a fraction of a second to obtain a radiograph of a moving part. In order that the shadow picture obtained be sharp, it is necessary that the x-rays originate at a "point." This means the electron stream must be concentrated at a point. However, an intense electron bombardment of a small area for even a short time will raise the temperature of the tungsten to beyond its melting point. This difficulty was overcome by the development of the "line focus" tube in which the electron beam is focussed on a rectangular area on the face of the sloping anode. From below (see Fig. II-1) the x-rays will appear to come from a square. For example, in a typical tube, with the face of the anode inclined at 80° to the tube axis, a focal spot 2 mm. wide and 16 mm. long will appear to be a spot 2 mm. square in the direction of the primary beam (see Fig. II-1). The electron energy is now spread over an area 8 times as great as the apparent size of the focal spot so that a considerable increase in loading is permissible. However, with the anode face set at a large angle the useful cone of radiation (see Fig. II-1) is reduced, for it is limited by the beam of radiation which grazes the surface of the anode. This, then, limits the angle at which the anode may be inclined. If still greater loading is required, the anode can be rotated so that a fresh cool part of the target is continually being brought under the electron stream. The development of such tubes in which the anode is rotated without liquid lubrication inside a vacuum tight glass envelope is indeed a marvel of engineering skill. For further details concerning tube ratings, anode constructions, reference should be made to (2, 6).

2.04 X-RAY CIRCUIT USING VALVE RECTIFICATION

Under severe electron bombardment the tungsten target may reach a temperature at which electron emission from its surface begins. This means that on the half cycle in which the filament is positive, electrons can travel from anode to filament. If this happens the delicate hot filament will be destroyed by electron bombardment and the tube will burn out. If then a tube is operated under conditions in which the target becomes very hot, steps must be taken to prevent electrons

from bombarding the cathode on the "inverse" cycle. In the early days this was done by a mechanical rectifier which reversed the polarity of the high voltage every half cycle so that the anode was always maintained positive with respect to the cathode. Today the same thing is done much more conveniently using high voltage valve rectifiers.

A high voltage valve rectifier consists of an evacuated glass or metal envelope into which are inserted a tungsten filament and an anode. The basic construction is not very different from an x-ray tube. The heated filament supplies electrons which are attracted to the anode when it is positive but repelled by the anode if it is negative. The rectifier will consequently conduct current in the conventional sense from anode to cathode but will not conduct a current in the opposite direction. In Figure II-3 is shown a single rectifier placed in series with the x-ray tube and the secondary of the transformer. The rectifier will conduct a current in the direction indicated. On the half cycle in which A is positive, current can flow through

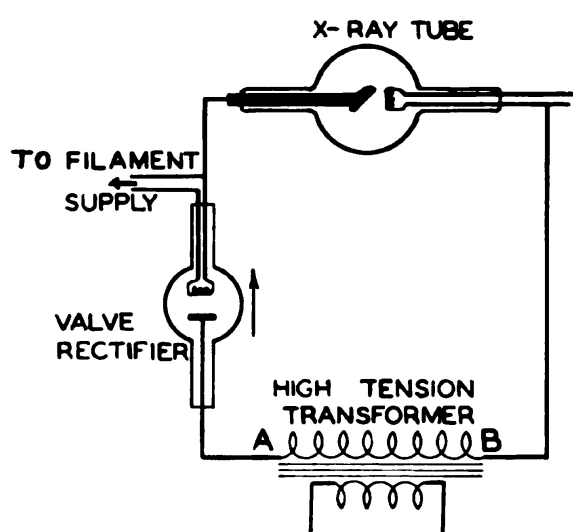


Figure II-3. Diagram showing the basic principles of an x-ray circuit using a half wave rectifier.

the rectifier and x-ray tube but on the next half cycle when B is positive the rectifier will not conduct. Of course the x-ray tube will not conduct either unless its target is hot enough to emit electrons. The rectifier serves little useful purpose if the x-ray tube is being operated at a low enough rating so that the target is cool but does prevent any conduction on the inverse cycle if the target becomes hot.

2.05 COMPARISON BETWEEN VALVE RECTIFIERS AND X-RAY TUBES

From Figure II-3 it is seen that the rectifier and the x-ray tube schematically appear the same and it may well be asked why does the rectifier not produce x-rays and what prevents its anode from getting hot. The answer is found in the way in which the filaments are operated in the two cases. In Figure II-4 is shown the relation

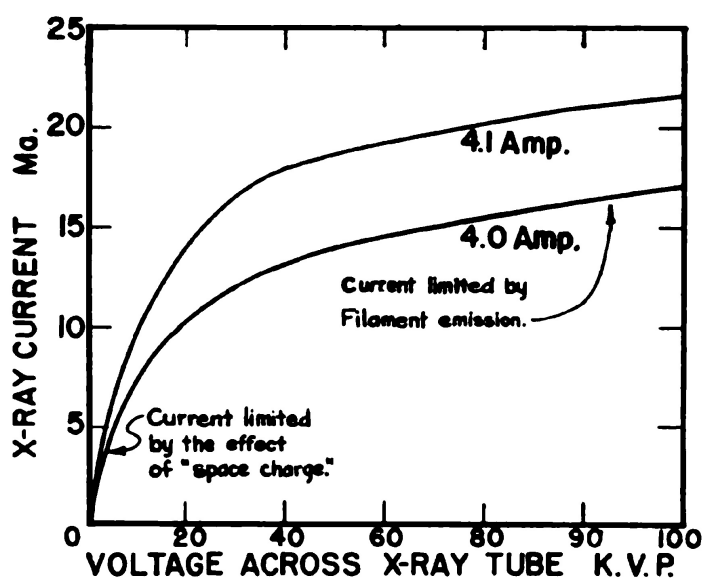


Figure II-4. Graph showing the variation of the current through a General Electric CRT-1 rotating anode x-ray tube as the voltage across the tube is varied. Graphs are shown for filament currents of 4.0 and 4.1 amperes.

between the voltage across a General Electric CRT-1 rotating anode x-ray tube and the current through it. It will be seen that when a few kilovolts is applied across the tube the current is small and is limited by "space charge effects." Surrounding the filament is a cloud of electrons which tend to repel one another back into the filament unless sufficient voltage is applied between anode and cathode to pull them away from the filament as fast as they are produced. When more than 30 or 40 Kv. is applied to the x-ray tube (Fig. II-4) most of the electrons liberated are being pulled to the anode. Under these circumstances an increase in the voltage across the tube does not appreciably increase the tube current. At low voltages the current is limited by space charge effects while at high voltages the current is limited by filament emission. Most x-ray tubes are operated in the region where the current is determined by filament emission and depends on filament current. It is seen that by raising the filament current from 4.0 to 4.1 amp. (i.e., 2.5%) the x-ray current is increased by about 30% (Fig. II-4). This explains the necessity for accurate control of the voltage applied to the filament of an x-ray tube.

In Figure II-5 is shown typical characteristics for a Phillips' high voltage rectifier operating at two different filament currents. The curves are like those for the x-ray tube exhibiting as before the region where space charge effects are important and the region of

saturation effects. However, the voltage scale is very different, a saturation current of 300 Ma. being obtained with only 3 Kv. across the tube (filament current 8.0 amp.). Valve rectifiers are usually used in the region where the current is limited by space charge effects. To make this clear, consider that the x-ray tube and rectifier shown in Figure II-3 have the electrical characteristics of Figures II-4 and II-5 respectively. Suppose that the secondary of the transformer is delivering 80 Kv. and that the filament currents in the x-ray tube and rectifier are 4.0 amp. and 8.0 amp. respectively. From Figure II-4 it is seen that the x-ray current is 15.5 Ma. Examination of Figure II-5 shows that a plate voltage of about 0.3 Kv. is required across the valve to give a current of 15.5 Ma. Consequently, on the conducting cycle the voltage drop across the x-ray tube is 79.7 Kv. and that across the valve 0.3 Kv. Since the energy dissipated is proportional to the voltage across the tube ($P = VI$), almost all the energy will be given to the target of the x-ray tube. The voltage drop across the rectifier is 0.3 Kv., so x-rays will be produced corresponding to this voltage. These however are so "soft" that they would not even get through the glass envelope. Since the power expended in the valve rectifier is very small the anode cannot get hot and consequently will never liberate electrons to cause conduction during the inverse cycle. If the valve were operated with too low a filament voltage so that the saturation current was less than the saturation current in the

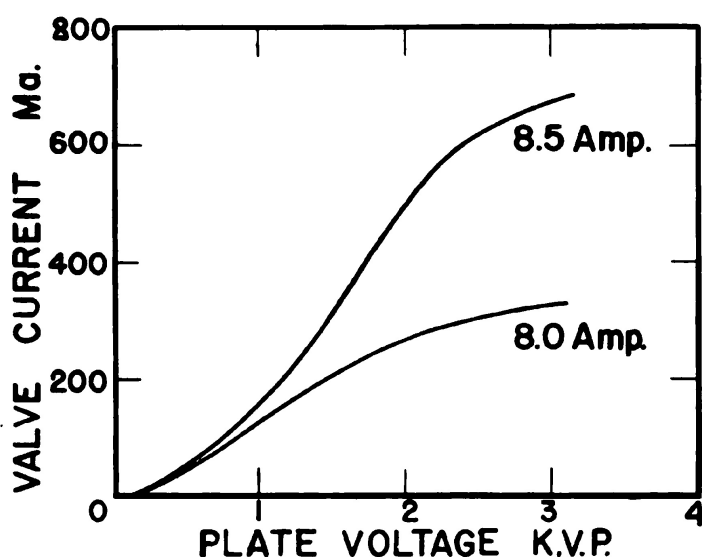


Figure II-5. Graphs showing the variation of the current through a Phillips' rectifier as the voltage across it is varied. Graphs are shown for filament excitations of 8.0 and 8.5 amperes.

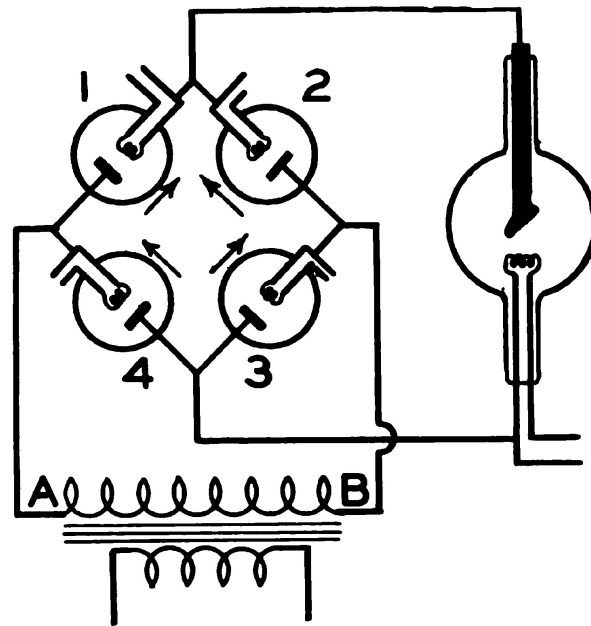


Figure II-6. Diagram showing the use of four valve rectifiers to yield full wave rectification for an x-ray tube.

x-ray tube, the voltage drop would occur in the valve and x-rays would be produced at the anode of the valve.

2.06

FULL WAVE RECTIFICATION

In the circuit shown in Figure II-3 a current flows through the x-ray tube and produces x-rays on every other half cycle. The current in the high voltage circuit is therefore a pulsating direct current and x-rays come from the target in pulses. This causes no serious trouble in a therapy machine but in a diagnostic machine means that the exposures must be longer to get the same x-ray flux. Four valves can be arranged as in Figure II-6 to give full wave rectification and x-rays every half cycle. The four valves are arranged to conduct in the directions indicated. When the end A of the transformer swings positive the current flows in series through valve 1, the x-ray tube, valve 3 and back to the negative end B of the transformer. Valves 2 and 4 do not conduct during this half cycle. On the next half cycle when B swings positive the current flows through valve 2, the x-ray tube, valve 4 and back to the negative end A of the transformer. The current therefore flows through the x-ray tube every half cycle. The filament supplies for the four valves and the x-ray tube are not shown. Although the four valves have filaments which operate on the same voltage, this voltage cannot be taken from the same filament transformer since, for example, the filament of valve 3 and valve 4 are connected directly

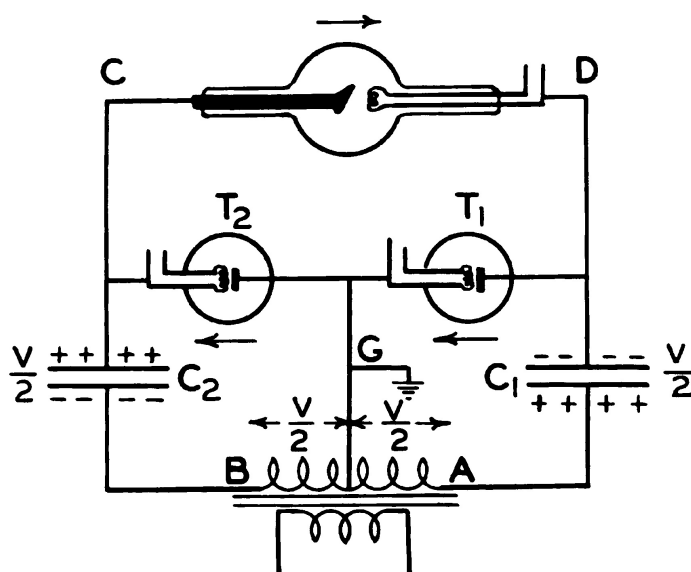


Figure II-7. Diagram showing the use of two valve rectifiers and condensers to yield an intermittent potential for the x-ray tube of twice that developed by the transformer. (Villard Circuit.)

to opposite ends of the high voltage transformer. The filaments of valves 1 and 2 are connected together so can be operated from the same transformer. Consequently three separate filament transformers are required for the four valves and one filament transformer for the x-ray filament supply.

2.07 VILLARD VOLTAGE DOUBLING CIRCUIT

In Figure II-7 is shown an arrangement of two high voltage rectifiers and two condensers which yield a pulsating unidirectional voltage for the x-ray tube whose peak value is twice the peak voltage of the transformer. This basic circuit is very commonly used to develop 200 Kv. for a therapy tube from a 100 Kv. transformer and is called a Villard circuit. The high voltage condenser C_1 and C_2 consists of two parallel metal plates placed close together with an insulating layer of oil between them. When the end A of the transformer goes positive, current flows through C_1 , T_1 , T_2 , C_2 to end B of the transformer. This current charges C_1 and C_2 as indicated. In actual fact the current does not flow through C_1 or C_2 but positive charges from A flow onto the lower plate of C_1 and positive charges from the upper plate of C_1 flow through T_1 and T_2 to the upper plate of C_2 charging it positive and leaving the upper plate of C_1 with a negative charge. The net result is the same as if current actually did flow through the condensers. At the end of the first half cycle C_1 and C_2 are each charged to a potential $V/2$ where V is the peak voltage of the transformer. These

and is called a Villard circuit.
e charges from A flow onto
ak voltage of the transformer.

charges cannot leak off through T_1 and T_2 because they conduct in the opposite direction. The charges will start to flow through the x-ray tube. It will be seen that the centre point of the transformer secondary is grounded and connected to the point between T_1 and T_2 . This connection is unnecessary for the operation of the circuit but usually improves it by preventing excessive voltages from appearing across any component. At the peak of the next half cycle the point B is $V/2$ above ground and the point A, $V/2$ below ground. The voltage across each of the condensers is still $V/2$. Hence the anode of the tube, point C, is $(V/2 + V/2)$ above ground and the cathode, point D, V volts below ground. The total voltage across the tube is $2V$. This argument is based on the assumption that the charge which leaks off the condensers to maintain the x-ray current is a small fraction of the total charge stored. In actual fact the voltage developed across the tube is never quite $2V$. By grounding the centre point of the transformer as in Figure II-7, no point in the circuit ever reaches a point more than V volts above or below ground. This simplifies the problem of insulation. By the use of more rectifiers and condensers in a sort of cascade circuit, it is possible to double the voltage several times to obtain very high voltages.

Many circuits involving rectifiers and condensers have been designed for energizing x-ray tubes but these few examples should illustrate the principles involved. For further details reference should be made to the following (2, 6).

2.08

THE PRODUCTION OF X-RAYS

So far we have discussed a few of the methods which may be used to energize an x-ray tube. We now enquire into the fundamental processes involved in the production of the x-rays when the high speed electron strikes the target. By carefully collimating an x-ray beam and reflecting it from the face of a crystal it is possible to measure the wavelength of the x-rays produced and the relative intensity of the x-rays in the different parts of spectrum. This experiment is very difficult to do and involves many corrections but the general nature of the results which will be obtained are shown in Figure II-8. Here the relative intensity of the x-radiation in a given wavelength band is plotted against the wavelength of the radiation for electrons bombarding a tungsten target. Distributions are shown for 65 Kv., 100 Kv., 150 Kv. and 200 Kv. electrons. The graphs were plotted using an empirical formula due to Kulenkampff (5). The intensity along the vertical axis is in arbitrary units. Examination of

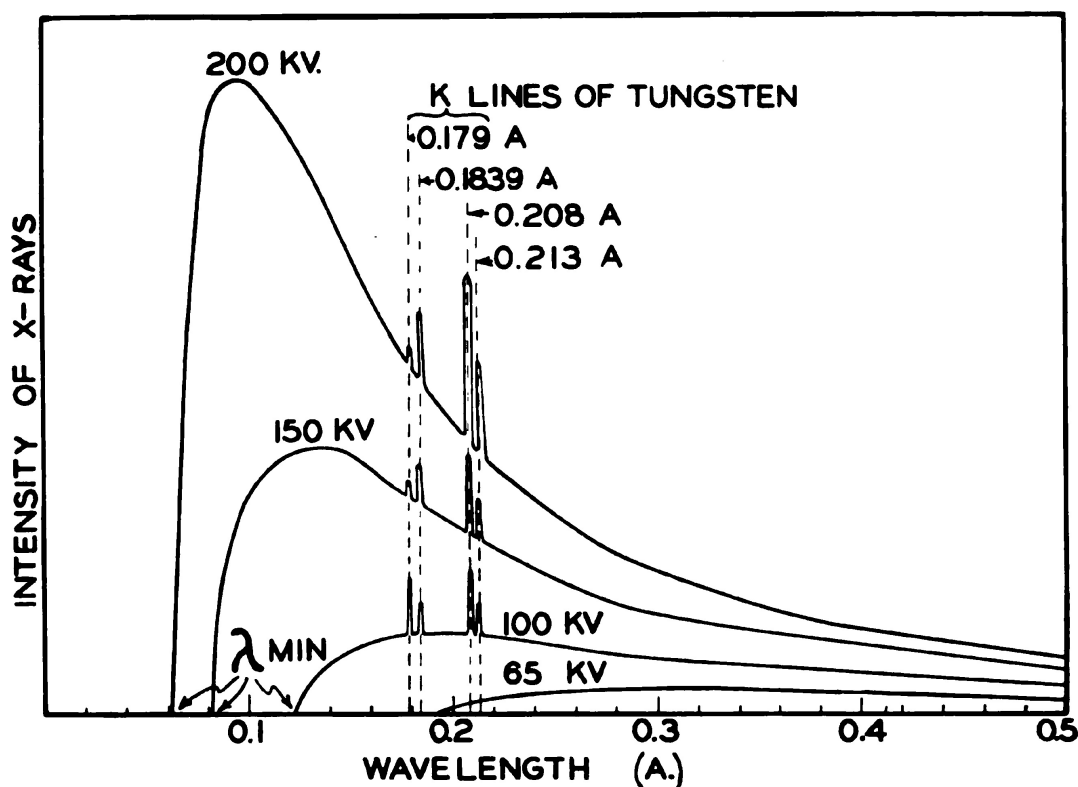


Figure II-8. Graphs showing the variation of intensity with wavelength for four different kilovoltages as calculated using a formula due to Kulenkampff.⁽⁵⁾

Figure II-8 shows that there is a continuous distribution of radiation from very long wavelengths up to a certain minimum wavelength with certain peaks superimposed on this continuous spectrum. The continuous spectrum is often called the “white” radiation because of the similarity of this curve to the continuous optical spectrum obtained from a white light. The peaks which are superimposed on the continuous spectrum are called *characteristic radiation* because they depend on the atomic number of the target material.

2.09 CHARACTERISTIC RADIATION

Characteristic radiation can be readily explained in terms of the energy level diagram for tungsten given in Figure I-3. If a K electron is ejected from the atom of tungsten by the high speed electron, all the K radiation (actually 4 components) can be excited, depending on the way in which the “hole” is filled. For tungsten these wavelengths are 0.213 Å, 0.208 Å, 0.184 Å, and 0.179 Å. If the applied voltage is less than that required to remove the K electron then none of the K series will appear. The shortest wavelength of the K series, 0.179 Å, is emitted when an electron falls from one of the N shells into the K shell so that the voltage required to excite the K lines will

be slightly greater than $12.4/0.179$, or 69.4 Kv. Its actual value is 69.8 Kv., i.e., the binding energy of the K shell. If this voltage or a greater voltage is applied to the x-ray tube *all* the K lines will appear; if the voltage is less than this none will appear. In Figure II-8 all the K radiation appears for 200 Kv., 150 Kv. and 100 Kv. excitation but none appears when 65 Kv. is applied to the tube. At longer wavelength (not shown in Fig. II-8) a group of L lines will appear when the L electron is ejected from the atom and the "hole" subsequently filled. There are 5 main lines in the L spectrum of tungsten ranging from 1.09 A to 1.48 A. The shortest L line (1.09 A) determines approximately the minimum voltage that will excite the L group. A large number of M lines can be excited in a similar way. These wavelengths for tungsten range from 5.16 to 8.98 Angstroms. If a material of lower atomic number than tungsten is used in the target, all the characteristic lines will appear at longer wavelengths. Since characteristic radiation is such a small part of the total radiation shown in Figure II-8 it is of little significance in therapy. However, the characteristic radiation from target materials of lower atomic number is of great importance in diffraction studies.

2.10

WHITE RADIATION

Most of the energy of the radiation from a target is in the continuous spectrum. The mechanism by which it is produced is not subject to simple theoretical treatment because of the complexity of the process involved. As the electrons enter the surface layers of the target they are slowed up by collision with the nuclei and electrons of the target and are deviated from their original direction of motion. Each time the electron suffers a deceleration, energy in the form of x-rays is radiated. This process is very similar to the radiation of energy from an electron which is accelerated in the antenna of a transmitter. The energy of the photon which is emitted will depend on the deceleration which occurs. If the electron is brought to rest in a single collision all its energy will appear as 1 photon of x-rays of wavelength corresponding to the short wavelength limit. If the electron suffers a less drastic collision, a longer wavelength (lower energy photon) will be produced. Since many collisions may be required to bring the electron to rest we expect photons of all energy up to the maximum to be produced as shown in Figure II-8. The minimum wavelength produced depends on only the peak voltage applied to the tube and is given by $\lambda_{\min.} = 12.4/V$ (equation 1-5). The maximum intensity occurs at a wavelength about 1.5 times the minimum

wavelength. For example, with 200 Kv. across an x-ray tube the minimum wavelength produced is 0.062 Å and the maximum intensity occurs at about 0.09 Å, corresponding to an energy of about 140 Kev. It will be seen from Figure II-8 that curves for 200 Kv. and 150 Kv. differ very much in the region of short wavelengths but that at very long wavelengths, the difference between them is not so marked. The total energy radiated from a target is given by the area under the curves of Figure II-8. It is found to vary approximately as the square of the voltage. This means that with the same tube current, there should be 1.8 times as much x-rays radiated when 200 Kv. is applied to the tube instead of 150 Kv. ($200^2/150^2 \approx 1.8$). Examination of Figure II-8 will show that the area under the 200 Kv. curves is about double that under the 150 Kv. curve. Usually the radiation from a tube is filtered so that the longer wavelengths are reduced in intensity more than the short wavelengths. This will reduce the area under the 150 Kv. curve more than that under the 200 Kv. Hence the output in an actual installation is likely to depend on a much higher power of the kilovoltage than 2. For example, if the voltage on a widely used 400 Kv. machine is reduced by 2.5% from 400 Kv. to 390 Kv., the output drops by 17%. For this reason, the voltage on a therapy machine should be set accurately and so maintained during treatment. The empirical curves of Figure II-8 should not be taken too literally since the actual distribution will depend on many other factors such as target construction, filtration and the type of voltage generating apparatus used.

Spectral distributions which were obtained from absorption experiments will be found in the Appendix in Figures B-1, B-2, B-3. Distributions are given for three qualities of radiations. The data shown in Figure II-8 are schematic and are included here to illustrate the principles being discussed in this Chapter.

For a given tube current and voltage, the total amount of radiation depends directly on the atomic number of the target increasing as Z increases. Therefore, for maximum radiation, uranium with atomic number 92 should be used. However, it is necessary to have a high melting point material and for this reason, tungsten ($Z = 74$) is almost universally used as the target material. In some installations gold ($Z = 79$) is used.

When a stream of electrons strikes a target most of the collisions take place with the outer electrons of the atom and do not result in the radiation of x-ray energy. Only a few collisions result in the pro-

duction of x-rays, so that the efficiency of x-ray production is small. Most of the energy of the electron beam is eventually dissipated in the target as heat. In a 100 Kv. tube less than one percent of the electron energy appears in the x-ray beam. As the voltage is raised the process becomes more and more efficient and at very high energies, 20 to 50 Mev., the efficiency approaches 100%. For this reason, in a betatron operating at 20 Mev., no mechanism need be provided to remove heat energy from the target.

2.11 THE ANGULAR DISTRIBUTION OF X-RAYS

If a beam of low energy electrons is incident on a very thin target, it is found that the x-rays are radiated primarily in a direction at right angles to the electron stream. In Figure II-9 (curve A) is shown the experimental results obtained by Honerjäger (3) for the angular distribution of x-rays produced by bombarding a foil of aluminum 200 A thick with 34 Kv. electrons. This angular distribution is for radiation at the short wavelength limit. The distribution in space of the x-rays is found by rotating the curve of Figure II-9 about the axis of the electron beam. The length of the arrows from the target indicate the relative intensity in the different directions. It is seen that the maximum intensity is at an angle of 55° with the direction of the electrons. The intensity in the forward direction is small and the intensity in the backward direction zero. As the energy of the bombarding electrons is increased the two lobes of curve A tip forward to yield in the end a distribution with all the radiation in the forward direction. Curves B and C are theoretical curves as calculated by Schiff (7) for the angular distribution of the radiation produced by bombarding a 0.05 cm. thick tungsten target with 10 and 20 Mev. electrons. These distributions are in essential agreement with a number of experimental results using betatrons.

The distributions of Figure II-9 are for targets so thin that most of the high speed electrons pass right through the target without deviation. In a practical x-ray tube the target is thick enough to stop completely and to deviate widely all the electrons. We now have electrons travelling in many directions in the target so that x-rays will be produced in all directions (see dotted lines of Fig. II-1). The distribution for a thick target cannot be predicted theoretically. For voltages up to 400 Kv. the x-ray beam at right angles to the electron direction is usually used although a number of installations make use of the transmitted x-ray beam. The intensity of the x-ray beam does not vary much as one goes from the primary beam (Fig. II-1) out

to the edge of the useful cone of radiation. Beyond this cone the radiation intensity falls rapidly as one proceeds into the shadow of the target because of the filtration of the target. In 1 and 2 million volt installations it is usual to use the x-ray beam transmitted forward through the target in the direction of the original electrons. This beam is often more intense than the beam produced at right angles because of the effect illustrated in Figure II-9. The target is often made of copper covered with gold. The copper is cooled by circulating water and acts as its own filter. At still higher energies the collimation

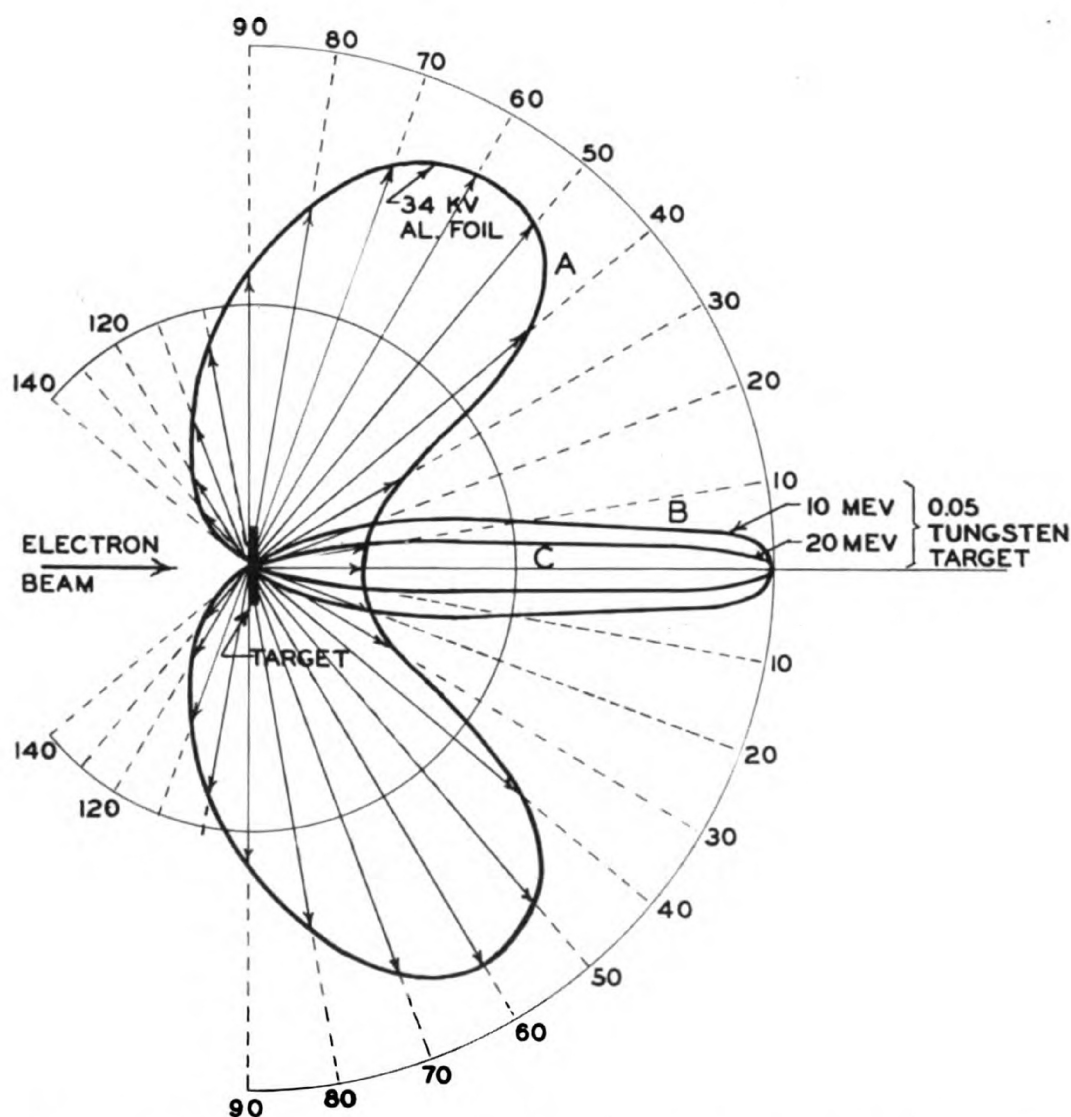


Figure II-9. Polar diagram showing the variation of the intensity of x-rays with angle produced by the electron bombardment of a thin foil. Curve A, 34 Kv. electrons bombarding a thin aluminum foil due to Honerjager⁽³⁾. Curves B and C, 10 and 20 Mev. electrons bombarding a 0.05 cm. tungsten target as calculated by Schiff⁽⁷⁾.

in the forward direction becomes quite severe in spite of electron deviation by the target. From Figure II-9 we see that at 20 Mev. the intensity has fallen to half the forward value at an angle of 5 degrees and the total width of the beam measured out to 50% intensity is about 10 degrees. At 50 Mev. the total angular width measured in the same way is about 4 degrees. This severe collimation offers a difficulty in using these radiations for therapy since great distances from the focal spot must be used to obtain uniform intensity over a 15 cm. circular field. The difficulty has been overcome by the use of a compensating filter which reduces the intensity along the axis of the beam without altering the intensity at the edge of the beam (1, 4).

REFERENCES

1. Adams, G. D.; Almy, G. M.; Dancoff, S. M.; Hanson, A. O.; Kerst, D. W.; Koch, H. W.; Lanzl, E. F.; Lanzl, L. H.; Laughlin, J. S.; Quaster, H.; Riesen, D. E.; Robinson, C. S.; and Skaggs, L. S.: *Am. J. Roentgenol.*, 60:153, 1948.
2. Coolidge, W. D., and Atlee, Z. J.: *Medical Physics*, Chicago, Yr. Bk. Pub., 1944, p. 1395.
3. Honerjäger, R.: *Ann. Physik.*, 38:33, 1940.
4. Johns, H. E., Darby, E. K., Haslam, R. N. H., Katz, L. and Harrington, E. L.: *Am. J. Roentgenol.*, 62:257, 1949.
5. Kulenkampff, H.: *Ann. Physik.*, 69:548, 1922.
6. Robertson, J. K.: *Radiology Physics*, New York, Van Nostrand, 1948, p. 65.
7. Schiff, L.: *Physical Rev.*, 70:87, 1946.

Chapter III

THE ABSORPTION OF X-RAYS BY MATTER

INTRODUCTION

WHEN an x-ray beam passes through an absorbing medium, the energy of the beam is converted into the motion of high speed electrons. It is these high speed electrons which produce the biological effect. The process by which this absorption takes place is complicated, but some understanding of the process is essential to a radio-therapist. The x-ray photons may interact with the absorber to produce high speed electrons by three distinct mechanisms known as the photoelectric process, the Compton process and pair production. These processes will be discussed in detail in the following sections but first such things as absorption coefficients must be defined.

3.01 APPARENT LINEAR ABSORPTION COEFFICIENT

Suppose a device which can record the number of photons which pass through it in one second is placed in an x-ray beam at the point P (Fig. III-1). Let the number of photons recorded per second be N_0 . If a slab of material of thickness x is placed in the path of the x-rays, a number N of the photons will be stopped and the number

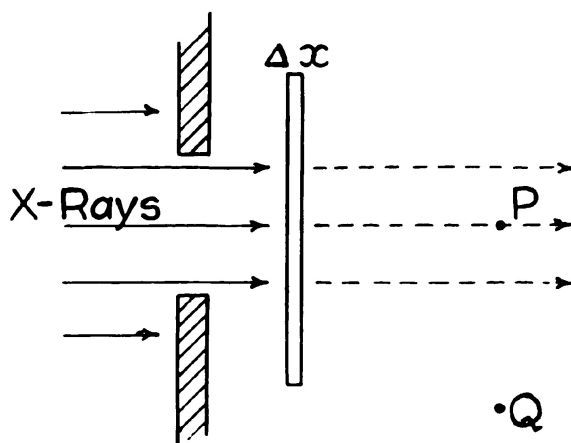


Figure III-1. Diagram illustrating how the absorber of thickness Δx reduces the intensity of radiation at P.

reaching P will be reduced. A photon cannot be partially stopped by the atoms in the slab of material. It will either come close enough to the atom to interact and thus be removed from the beam or it will not be affected at all. Hence the number N which are removed will depend directly on the number of photons present. If N_0 is doubled, then the chances of an interaction will be doubled. N will also depend directly on the thickness, x. If x is doubled the number of atoms placed in the beam is doubled and so the chance of interaction is doubled. Mathematically, we may say that N varies as the product of N_0 and x. Symbolically this can be written

$$N = \mu N_0 x \quad (3-1)$$

where μ , the constant of proportionality, is called the linear absorption coefficient, or more correctly the apparent linear absorption coefficient. μ depends in a complicated way on the atomic number Z of the absorbing material and the wavelength λ of the radiation but for given values of Z and λ it has a definite value. Its dependence on λ and Z will be discussed later. For the present it should be considered as a constant.

By rearranging equation (3-1) we obtain $\mu = N/N_0 \times 1/x$. Since N/N_0 is the ratio of two numbers and x is a thickness, μ may be expressed in units $1/\text{cm.}$ or cm^{-1} . Suppose $\mu = 0.01 \text{ cm}^{-1}$. Substituting this value in equation (3-1) we obtain $N = 1/10 N_0$ for $x = 1 \text{ cm.}$ which means 1/10 of the photons are stopped by 1 cm. of the absorber. *The linear absorption coefficient is therefore numerically equal to the fractional number of photons removed from the beam per cm. of absorber.* Since the number of photons which pass through a square cm. per second determines the intensity I of the beam of radiation, equation (3-1) can equally well be written

$$\Delta I = -\mu I \Delta x \quad (3-2)$$

I, the intensity, is proportional to N_0 of equation (3-1), ΔI , the change in intensity is proportional to N the number of photons stopped, and the thickness of the absorber is written here as Δx rather than x for reasons which will appear later. ΔI thus gives the change in intensity of the beam produced by the absorber of thickness Δx .^{*} The negative sign merely indicates that as the thickness of absorber is increased the intensity is decreased. By an argument similar to the one above, it follows that *the linear absorption coefficient is equal to the fractional reduction in intensity produced by 1 cm. of absorber.*

^{*} Δ placed in front of a quantity such as x indicates a small thickness x or an "increment" in x. Later we will see that it is necessary to consider Δx as being made very small.

3.02

THE ABSORPTION OF X-RAYS

To illustrate the use of the linear absorption coefficient, let us determine how the intensity of an x-ray beam is reduced as successive layers of absorber 1 cm. thick are placed in a beam. Suppose $\mu = 0.10 \text{ cm}^{-1}$ and that the original intensity of the beam is 100. The first 1 cm. slab will absorb 10% of 100 leaving a beam of intensity 90. The next layer will absorb 10% of the radiation which reaches it, i.e., 10% of 90 or 9.0. Hence the radiation intensity transmitted by two layers is 81. This type of calculation can be extended to yield the results shown in the first three columns of Table III.

cm. slab to the back of the slab

TABLE III

ILLUSTRATING THE ABSORPTION OF AN X-RAY BEAM WHEN THE
LINEAR ABSORPTION COEFFICIENT IS 0.10 cm^{-1}

<i>Thickness of Absorber</i> (x)	<i>Changes in in- tensity pro- duced per cm.</i> (ΔI)	<i>Intensity (I) Transmitted</i> (equation 3-2)	<i>Intensity (I) Transmitted</i> (equation 3-3)
0	0	100.0	100.0
1	10	90.0	90.5
2	9	81.0	81.9
3	8.1	72.9	74.1
4	7.3	65.6	67.0
5	6.5	59.1	60.7
6	6.0	53.1	54.9
7	5.4	47.7	49.7
8	4.9	42.8	44.9
9	4.4	38.4	40.6
10	3.9	34.5	36.8
11	3.5	31.0	33.3
12	3.2	27.8	30.1
13	2.9	24.9	27.2
14	2.6	22.3	24.7
15	2.3	20.0	22.3
16	2.1	17.9	20.2

From column (2) it is seen that as layers of absorber are added the reduction in intensity produced by each layer gets smaller and smaller but the percentage reduction produced by each layer is always 10%. The calculations shown in the first three columns of Table III are only approximately correct, for it is assumed that the intensity is 100 from the front face of the first 1 cm. slab to the back of the slab,

whereas the intensity at the back of the slab is really only 90. Hence the amount absorbed will be less than the value 10 given in column (2) and the transmitted intensity will be greater than the value 90 given in column (3). To obtain a more accurate result we may divide the first slab into 10 layers 1 mm. thick. The first layer will absorb 1% of 100 leaving 99 incident on the second slab. This process can be continued exactly as in Table III to yield a transmitted intensity of 90.45 for 10 slabs 1 mm. thick. To obtain the correct solution a very large number of layers each very thin should be considered. That is, Δx in equation (3-2) should be made very small and the calculations carried through for a very large number of these very thin layers. Such a task would be formidable and fortunately need not be done since the problem can be solved by the calculus to give the equation

$$I = I_0 e^{-\mu x} \quad (3-3)$$

where I is the intensity transmitted by a layer of material of thickness x and μ is the linear absorption coefficient. I_0 is the original intensity, and e is the base of the natural logarithms with the value 2.718. This equation need not be understood in detail for graphical methods are available for handling it. It merely puts in mathematical form the calculations which have been indicated in Table III. Equation (3-3) can be used to calculate the absorption by any thickness of material whereas equations (3-1) and (3-2) are only applicable when the fraction absorbed, by the layers of material under consideration, is

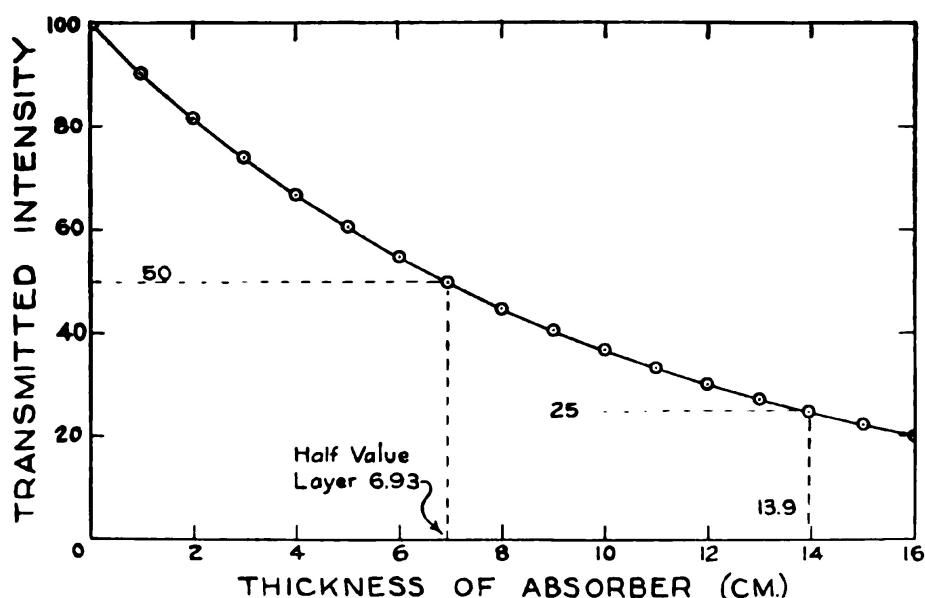


Figure III-2. Graph showing how the intensity of an x-ray beam is reduced by an absorber whose linear absorption coefficient is $\mu = 0.10 \text{ cm.}^{-1}$.

small. In column (4), Table III, is given the intensity transmitted as calculated by equation (3-3). Comparison of the last two columns shows that the agreement is fair, indicating that equation (3-2) is reasonably satisfactory even when the fraction absorbed by each layer is 10%. If the absorption coefficient were 10 times as great, layers 1/10 as thick should be considered. Conversely, if the absorption coefficient were very small, much thicker layers could be considered.

The values given in column (4) of Table III are plotted on ordinary graph paper in Figure III-2 and on semilogarithm paper in Figure III-3. From Figure III-2 we see that the curve becomes quite flat as it approaches the X axis. Even when very thick layers of absorber are used, there will be some transmitted intensity. We cannot refer to a thickness which will absorb all the radiation since theoretically all the radiation can never be absorbed but we can conveniently think of the thickness which is required to absorb half the radiation. This thickness, known as the half value layer (H.V.L.), is related to the linear absorption coefficient μ by the important relation.*

*This equation follows from equation (III-3). If x is the H.V.L. then $I = \frac{1}{2}I_0$ and $\frac{1}{2} = e^{-\mu x}$ or $e^{\mu x} = 2$. Now $e^{0.693} = 2$ so $\mu x = 0.693$.

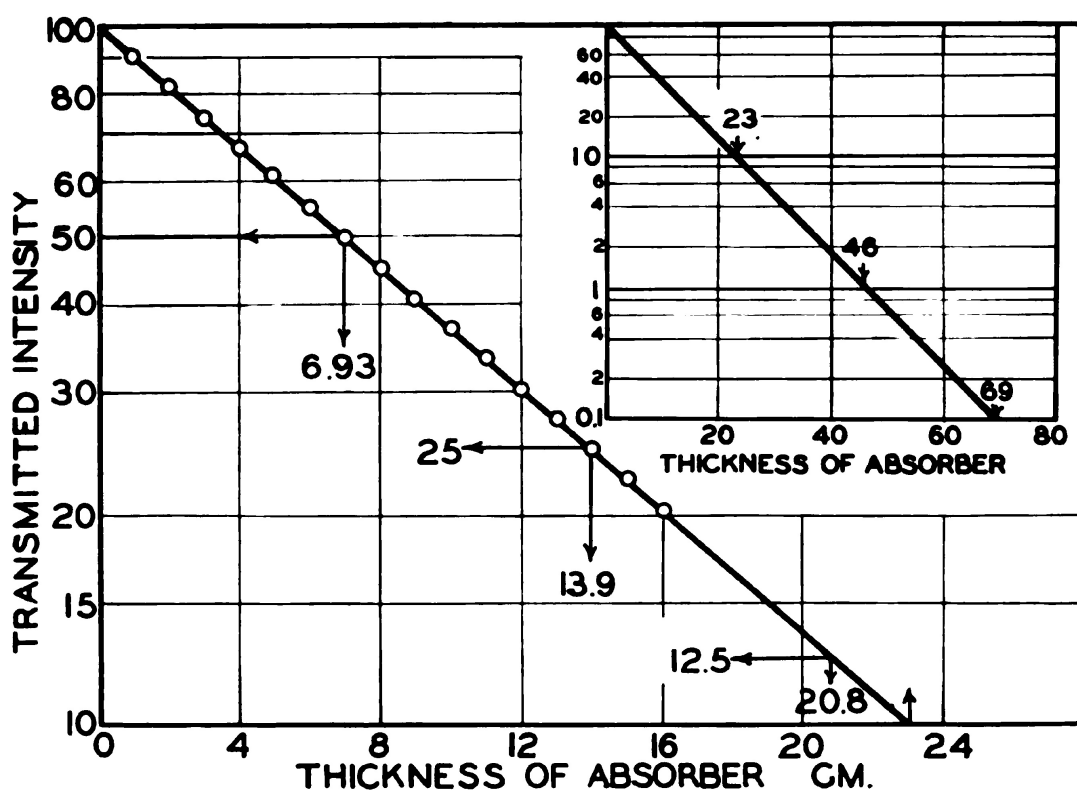


Figure III-3. Graph showing how the intensity of an x-ray beam is reduced by an absorber whose linear absorption coefficient is $\mu = 0.10 \text{ cm}^{-1}$. The transmitted intensity is plotted on a logarithmic scale.

$$\mu \cdot (\text{H.V.L.}) = 0.693 \quad (3-4)$$

For the case considered ($\mu = 0.10$) we obtain from equation (3-4) the value 6.93 cm. for the H.V.L. This checks with Table III and the graph of Figure III-2 where we see that 6.93 cm. does reduce the intensity to 50%. The next 6.93 cm. (total 13.86 cm.) reduces the intensity to one-half of 50%, i.e., 25%. The next 6.93 cm. will reduce the intensity to 12.5%. This type of exponential decrease is very conveniently represented graphically on semilogarithm paper because a straight line relation is obtained. Examination of the vertical scale of Figure III-3 will show that the distance from 10 to 20 is greater than from 20 to 30 which in turn is greater than from 30 to 40, etc. These distances actually correspond to the logarithms of the numbers. Measurement will show that the distance from 100 to 50 on the vertical scale is the same as from 50 to 25 or from 25 to 12.5, or in fact from any number to half the number. Since successive layers 6.93 cm. thick reduce the intensity in turn from 100 to 50 to 25 to 12.5 etc., the curve plotted in Figure III-2 must appear as a straight line in Figure III-3. It should be noted that the scale goes from 100 to 10. This is called a cycle. If a greater range is to be represented, double cycle paper going from 1 to 10 and then from 10 to 100 should be used. In the insert of Figure III-3 is shown the data plotted on triple cycle paper. It is seen that 23, 46 and 69 cm. are required to reduce the intensity from 100 to 10, to 1 and to 0.1 respectively. This emphasizes the fact that with exponential absorption, an infinite thickness is required to reduce the intensity to zero. A selection of semilogarithmic paper with 1, 2 and 3 cycles should be available in a radiotherapy department for plotting absorption data and the decay of radioactive materials which follows the same law.

3.03 ELECTRONIC AND MASS ABSORPTION COEFFICIENTS

We now enquire into the mechanisms by which the intensity of the radiation at P (Fig. III-1) is reduced by the absorbing layer. If a measuring device is placed at Q it will be found that some radiation reaches Q when the absorber is in place. This is called *scattered radiation*. The reduction in intensity ΔI recorded at P does not therefore mean that all the radiation ΔI was absorbed in the layer. It does mean that it was either absorbed or diverted. In general, both take place and some is absorbed and some diverted. For this reason μ is more correctly referred to as the *apparent linear absorption coefficient*.

When x-rays are used in therapy we are primarily interested in the energy which is absorbed by the tissue. The biological effect

must depend in some way on the energy absorbed. We certainly would not expect to observe any biological effect if the radiation passed through a subject without absorption. The question arises then as to how energy can be extracted by an absorbing medium from an x-ray beam. There is ample evidence to show that this can be done only by first converting the stream of photons into motion of electrons. When the x-ray beam interacts with matter, the electrons of the absorbing material may be set in motion by three distinct mechanisms known as photoelectric absorption, Compton absorption and pair production. These will be discussed in detail in the next three sections. The high speed electron, whatever its origin, in turn gives up its energy to the tissue by causing ionization along its path. On the average, an electron loses 32.5 ev. of energy for each ion pair produced in air. Electron paths in air can be made visible in a cloud chamber photograph (see Fig. IX-1).

Since x-rays are absorbed by interaction with the electrons of the material, the absorption of a layer Δx thick will depend on the number of electrons present in the layer. If the layer were compressed to half the thickness it would still have the same number of electrons and still absorb the same fraction of the x-rays but of course its linear absorption coefficient (absorption per cm.) would be twice as great as before. Linear absorption coefficients will therefore vary greatly as the density of the material is changed. Much more fundamental absorption coefficients are the *electronic absorption coefficient* (represented by $\kappa\mu$) and the *mass absorption coefficient* (represented by μ/ρ where ρ is the density*). In absorption work it is often convenient to measure the "thickness" of an absorber in gm./cm.². A thickness of 10 gm./cm.² means that one square cm. of the absorber has a mass of 10 gm. The mass absorption coefficient is the fractional reduction in intensity produced by a layer of "thickness" 1 gm./cm.². It has dimensions cm.²/gm.† It can be obtained from the linear absorption coefficient by dividing the latter by the density ρ . Suppose an absorber has density 2.0 and a linear absorption coefficient of 0.14 cm.⁻¹. The mass absorption coefficient is $0.14/2.0 = .07$ cm.²/gm. The electronic absorption coefficient $\kappa\mu$ gives the fractional reduction in intensity produced by one electron in an area of 1 cm.². It has dimensions cm.²/electron. The mass absorption coefficient can be obtained from the electronic one by multiplying the latter by N_0 , the number of elec-

*Density ρ is defined as the mass per unit volume and is measured in gm./cm.³.

†Mass absorption coefficient = $\frac{\mu}{\rho} = \frac{\text{cm}^{-1}}{\text{gm/cm}^3} = \frac{\text{cm}^2}{\text{gm}}$

trons per gm. The relation between the three coefficients is summarized as follows:

linear absorption coefficient μ cm^{-1}

mass absorption coefficient $\frac{\mu}{\rho}$ $\text{cm}^2/\text{gm.}$ (3-5)

electronic absorption coefficient $\mu_e = \frac{\mu}{\rho} \cdot \frac{1}{N_0}$ $\text{cm}^2/\text{electron}$

In Table IV is shown the density, the effective atomic number \bar{Z} , and the number of electrons per gm. (N_0) for a number of materials. The values given for fat, bone and muscle are those determined experimentally by Spiers (7). The meaning of the effective atomic number \bar{Z} when referred to materials like water, air, etc. will be discussed later. The number of electrons per gm., N_0 , is almost constant for all materials except for hydrogen (see footnote to Table IV).

TABLE IV
DATA CONCERNING ABSORBING MATERIALS*

<i>Material</i>	<i>Density gm/cm³</i>	<i>Effective Atomic Number \bar{Z}</i>	<i>Number of electrons per gm. $N_0 = NZ/A$</i>
Hydrogen	0.0000899	1	5.97×10^{23}
Carbon	2.25	6	3.01×10^{23}
Oxygen	0.001429	8	3.01×10^{23}
Aluminum	2.7	13	2.90×10^{23}
Copper	8.9	29	2.75×10^{23}
Lead	11.1	82	2.38×10^{23}
Air	0.001293	7.64	3.03×10^{23}
Water	1.00	7.42	3.34×10^{23}
Muscle	1.00	7.42	3.36×10^{23}
Subcutaneous Fat	0.91	5.92	3.48×10^{23}
Bone	1.85	13.8	3.00×10^{23}

Since electrons may be set into motion by three distinct mechanisms, we separate the total coefficient μ into a part for the photo-electric absorption, a part for the Compton process and a part for

* N is Avogadro's Number 6.02×10^{23} which gives the number of atoms present in 1 atomic wt. (A) of the material. For example 16 gm. of oxygen contain 6.02×10^{23} atoms. N/A gives the number of atoms per gm. of material. Each atom contains Z electrons so the number of electrons per gm. $N_0 = ZN/A$. Since all nuclei contain approximately equal numbers of protons and neutrons Z/A will be approximately 0.5 and N_0 will be approximately 3×10^{23} . In Table IV we see that hydrogen is an exception. The ratio Z/A falls from 0.5 to about 0.4 for heavy elements so that the number of electrons per gm. in lead is slightly less than for low atomic number materials.

pair production. The absorption coefficient for the photoelectric effect is represented by τ , for the Compton effect by σ , and for pair production by π . The corresponding mass coefficients are τ/ρ , σ/ρ and π/ρ , and the electronic coefficients are ${}_e\tau$, ${}_e\sigma$, ${}_e\pi$. The total coefficient is the sum of these, that is

$$\mu = \tau + \sigma + \pi, \quad \frac{\mu}{\rho} = \frac{\tau}{\rho} + \frac{\sigma}{\rho} + \frac{\pi}{\rho} \quad \text{and} \quad {}_e\mu = {}_e\tau + {}_e\sigma + {}_e\pi \quad (3-6)$$

In the next three sections the three mass absorption coefficients will be discussed. The corresponding electronic and linear coefficients may be obtained from the relations given in (3-5).

3.04 PHOTOELECTRIC ABSORPTION

Suppose a quanta of energy $h\nu$ (Fig. III-4) is directed at an atom in such a way that an electron from the K shell is removed. This electron will have kinetic energy $(h\nu - E_k)$ where E_k is the binding energy of the K shell. This electron is called a photoelectron. In this type of absorption all the energy of the quantum is given to the photoelectron and to its removal from the atom. The quantum thus disappears and in its place we have a high speed photoelectron and an excited atom. After a short time another electron will fill the K shell and produce characteristic radiation, which will be radiated from the absorber as fluorescent or characteristic scattered radiation. To illustrate this, suppose the absorbing layer (Fig. III-1) is tungsten and the incident x-ray photons have an energy of 150,000 ev. each. Suppose that a K electron is ejected (binding energy 70,000 ev.) and that eventually the hole in the K shell is filled by an electron from the outermost shell. As far as the point P (Fig. III-1) is concerned the measuring instrument will indicate that one quantum has been absorbed with

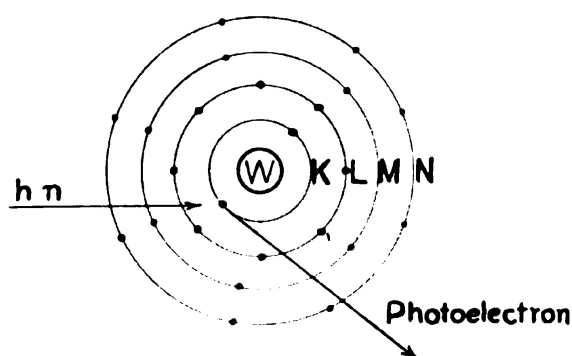


Figure III-4. Diagram illustrating the absorption of a photon by the photoelectric process.

TABLE V
MASS ABSORPTION COEFFICIENTS cm^2/gm

ENERGY		WATER							LEAD Z = 82					COPPER Z = 29	
(1)	(2)	(3)	(4)	(5)	(6)	(7)	(8)	(9)	(10)	(11)	(12)				
	Photo- electric τ/ρ	Compton σ/ρ	σ_a/ρ	Pair π/ρ	π_a/ρ	Total Real $\tau + \sigma_a + \pi_a$ ρ	Photo- Electric τ/ρ	Compton σ/ρ	Pair π/ρ	Total μ/ρ $\tau + \sigma + \pi$ ρ	Total μ/ρ $\tau + \sigma + \pi$ ρ				
5 Kv.	39.7	0.218	0.00209			39.7	780	0.156		780	185				
10 Kv.	4.80	0.214	0.00401			4.80	131	0.153		131	215				
20 Kv.	0.58	0.206	0.00752			0.587	33	0.147		33.1	32.5				
40 Kv.	0.070	0.194	0.0130			0.0830	48	0.138		48.1	4.80				
100 Kv.	0.0042	0.164	0.0228			0.0270	5.5	0.117		5.62	0.465				
200 Kv.	0.00051	0.136	0.0294			0.0299	0.874	0.097		0.971	0.152				
400 Kv.		0.106	0.0328			0.0328	0.147	0.0756		0.223	0.0920				
1 Mv.		0.0713	0.0311			0.0311	0.0193	0.0507		0.0700	0.0590				
2 Mv.		0.0489	0.0260	0.00044	0.00022	0.0262	0.0064	0.0348	0.00392	0.0451	0.0419				
4 Mv.		0.0322	0.0194	0.00185	0.00139	0.0208	0.0026	0.0230	0.0164	0.0420	0.0330				
10 Mv.		0.0171	0.0117	0.00478	0.00430	0.0160		0.0122	0.0392	0.0514	0.0310				
20 Mv.		0.0101	0.00739	0.00724	0.00687	0.0143		0.00715	0.0611	0.0682	0.0336				
40 Mv.		0.00581	0.00448	0.00981	0.00955	0.0140		0.00415	0.0822	0.0863	0.0391				
100 Mv.		0.00272	0.00218	0.0133	0.0132	0.0154		0.00194	0.1038	0.1057	0.0477				

*Photoelectric coefficients were obtained from Compton and Allison (2) for low energies, Victoreen (8) for medium energies and Hume *et al.* (5) for high energies. Compton coefficients were obtained from Lea (6) for low and medium energies and from Appleyard *et al.* (1) for high energies. Pair production coefficients were obtained from Heitler (5). Photoelectric coefficients for water were taken from Lea (6). Much of this data has been ably compiled in a Ph.D. thesis by C. M. Davison (3).

energy 150,000 ev. In actual fact the tungsten has absorbed only the photoelectron (energy 80,000 ev.) and the rest of the energy 70,000 ev. has been reradiated by the absorber.

If we replace the tungsten absorber by tissue quite a different state of affairs arises. The binding energy of the K shell is 500 ev. for tissue so that the photoelectron acquires almost all the energy of the photon. Suppose the incident photon has 50 kv. of energy. The photoelectron will acquire 49.5 Kv. of energy and the excited atom will have 0.5 Kv. of energy. When an electron fills the "hole" in the K shell a quantum of energy 0.5 Kv. will be radiated. This very soft radiation will be absorbed and changed into electronic motion almost within the same cell giving rise to a 0.5 Kv. electron. Thus although a small fraction has been radiated it is again absorbed so the net result has been a 50 Kv. photon changed into a 0.5 Kv. electron and a 49.5 Kv. photoelectron. *In tissue when a photon is absorbed by photoelectric absorption all the energy is transferred to the tissue giving rise to a photoelectron with most of the energy and a low energy (0.5 Kv.) electron.*

Mass photoelectric absorption coefficients are given in Table V for water and for lead. For water the coefficient falls rapidly from 39.7 cm.²/gm. at 5 Kv. to a negligible value at 200 Kv. It will be seen that doubling the energy causes a reduction in the photoelectric coefficient by a factor of approximately 8 (2³). It follows therefore that the coefficient τ/ρ depends on λ^3 or $1/E^3$.^{*} The same data is shown graphically on double logarithmic paper in Figures III-5 and III-6, where the mass coefficient ranging from 0.001 cm.²/gm. to 1000 cm.²/gm. is plotted against energy ranging from 1 Kv. to 100 Mev. On this graph the mass photoelectric coefficient plotted against energy yields a straight line of slope 3 indicating a dependence on λ^3 , or $1/E^3$. This mass absorption coefficient varies rapidly with the atomic number depending approximately on its 3rd power. Figures III-5 and III-6 illustrate this. At 100 Kv. τ/ρ for water equals 0.0042 while τ/ρ for lead equals 5.5. The ratio of these is about 1000 and the ratio of their atomic numbers is about 10 ($Z_{\text{lead}} = 82$, $Z_{\text{water}} = 7$). The photoelectric absorption shows sudden discontinuities. It will be seen (Fig. III-5) that as the energy decreases (λ increases) the absorption suddenly decreases at 88 Kv. Below this energy the photon has insufficient energy to eject the K electron from lead, so the absorption is smaller. As the energy is further decreased a value is reached when the photon has insufficient energy to eject the L₁ electron, then the L₂ and L₃.

^{*} $\lambda = 12.4/E$.

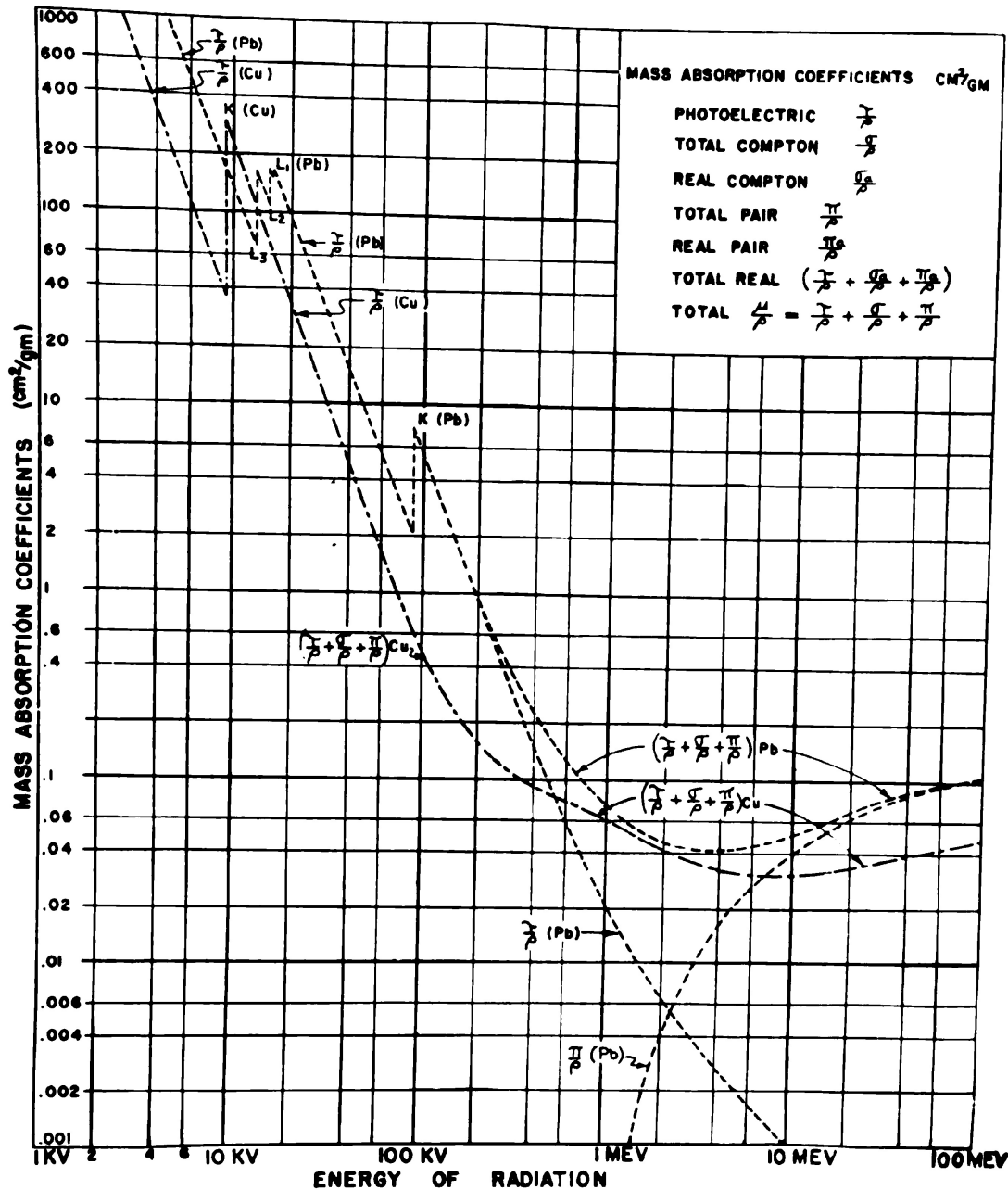


Figure III-5. Graph showing the variation of the total mass absorption coefficients with photon energy for copper and lead. For lead the photoelectric coefficient τ/ρ and the total pair π/ρ are also shown. Data taken from Table V.

If the curve were continued 5 "breaks" would occur for the M shell. These same "breaks" would occur for water but at energies of about 500 volts, and so are unimportant. The photoelectric absorption in lead is not negligible until energies of about 10 Mev. are reached. Examination of Figure III-5 will show that at energies above 1 Mev., the photoelectric absorption curve for lead gradually changes slope, finally attaining a value of 45° . In this region doubling the energy

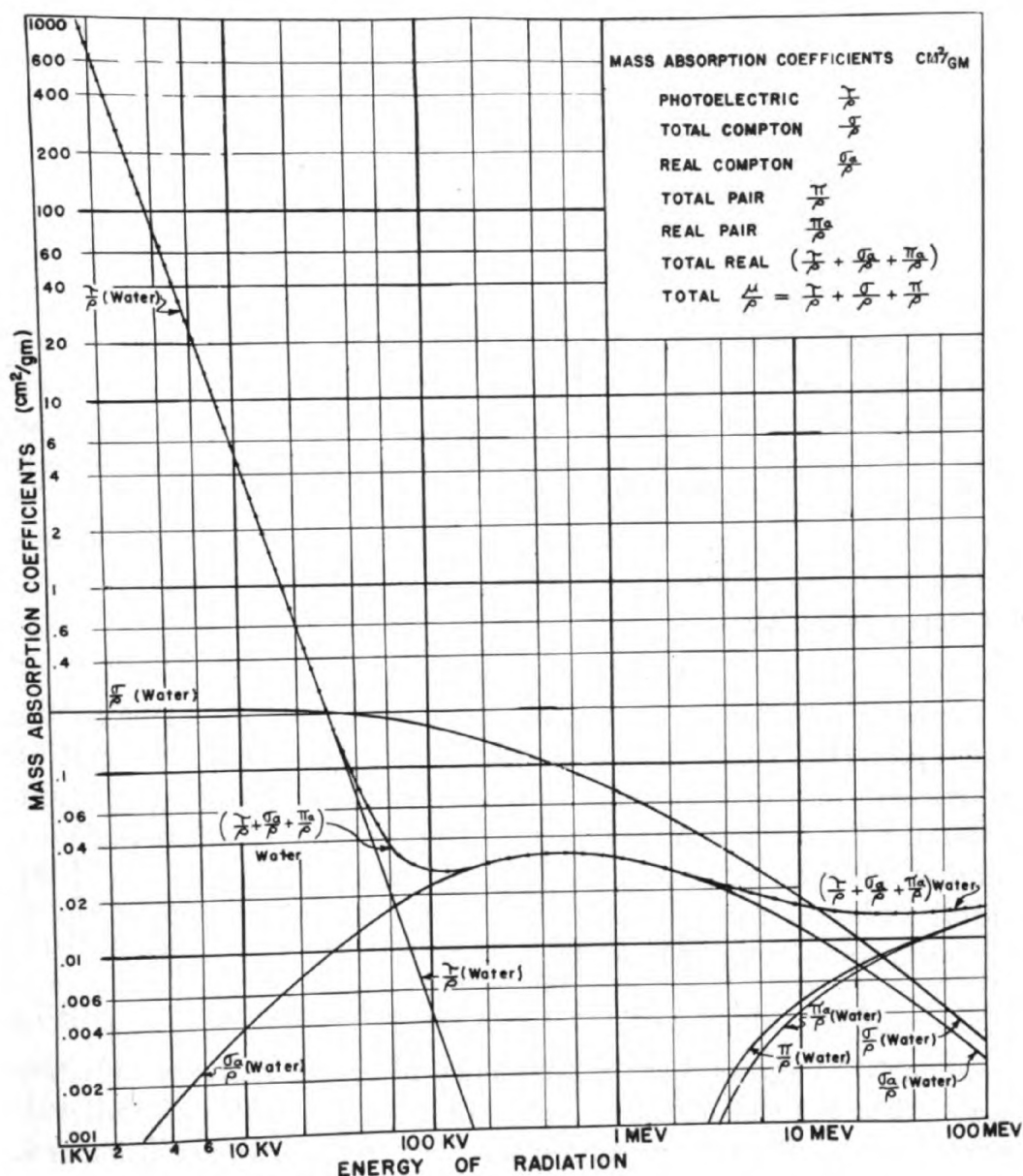


Figure III-6. Graph showing the variation of the mass absorption coefficient with photon energy for water. Curves are shown for the photoelectric coefficient τ/ρ , the total Compton σ/ρ , the real Compton σ_a/ρ , the total pair production coefficient π/ρ , the real pair production coefficient π_a/ρ , and the total real absorption coefficient $\tau/\rho + \sigma_a/\rho + \pi_a/\rho$. Data taken from Table V.

reduces the coefficient by a factor of about 2. In the last column of Table V is given the total absorption coefficient for copper. Up to energies of about 40 Kv. this total coefficient is essentially equal to the photoelectric coefficient. The curve (Fig. III-5) appears as a straight line of slope 3 as for water and lead, indicating the same variation with energy (λ^3). The K absorption "break" is shifted to a lower energy (9 Kv.) than the L "breaks" for lead. In a region around

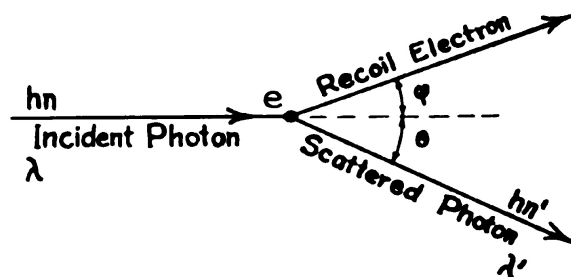


Figure III-7. Diagram illustrating the absorption of a photon by the Compton process.

10 Kv. it is seen that copper has a higher absorption coefficient than lead. The photoelectric curve for water (Fig. III-6) quite accurately parallels that for tissue. The curves for copper and lead are typical of a medium atomic number material and a heavy element respectively. *The photoelectric absorption decreases rapidly with increase in energy and depends on Z^3 .*

3.05 COMPTON ABSORPTION

In many cases when a photon with energy hn is incident on the atom (Fig. III-7) one of the loosely bound outer electrons will be ejected with part of the energy and another photon will emerge from the atom with the rest of the energy. Suppose the electron (called a Compton electron or recoil electron) emerges at an angle ϕ and the scattered photon at an angle θ with energy hn' . Since no energy is lost in the collision we may write

$$hn = hn' + (\text{Kinetic energy of recoil electron}) \quad (3-7)$$

Equation (3-7) shows that the frequency n' of the scattered radiation must be less than n , or the wavelength λ' of the scattered radiation greater than λ . Because momentum is conserved in the collision it is possible to show that the increase in wavelength $\Delta\lambda$ (expressed in Angstroms) is given by

$$\Delta\lambda = \lambda' - \lambda = 0.024 (1 - \cos \theta) \quad (3-8)$$

If the photon makes a direct hit on the electron, the electron will be projected straight forward ($\phi = 0^\circ$) and the scattered photon is directed backward ($\theta = 180^\circ$). The change in wavelength $\Delta\lambda = 0.048 \text{ \AA}$ ($\cos 180^\circ = -1$). If the photon makes a grazing hit the electron will emerge nearly at right angles ($\phi \approx 90^\circ$) and the scattered photon goes almost forward ($\theta \approx 0$). In this case $\Delta\lambda \approx 0$ ($\cos \theta = 1$) so that the scattered photon has the same wavelength and energy as the incident one and the recoil electron acquires no

energy. When the photon is scattered backward it suffers the greatest change in wavelength, and the recoil electron acquires its maximum energy.

If the incident photon energy is 12.4 Kv. ($\lambda = 12.4/12.4 = 1\text{A}$), the radiation scattered backward has wavelength 1.048A and that scattered forward 1.00A so the softening effect is unimportant and the recoil electron acquires little energy. However, when the incident photon has energy 1240 Kv. ($\lambda = 0.01\text{A}$) the radiation scattered backward has wavelength $(0.01 + 0.048) = 0.058\text{A}$ which means that the wavelength has been increased by a factor of nearly 6, and corresponds to a photon of energy $12.4/0.058 = 224$ Kv. The recoil electron has thus acquired an energy of $1240 - 224 = 1016$ Kv. In fact about 5/6 of the original photon energy has been converted into the energy of the recoil electron.

It is very important therefore that we distinguish between the energy which is scattered from the beam and the energy which is given to the recoil electrons and therefore truly absorbed. This is done by separating the Compton coefficient σ/ρ into two parts σ_s/ρ and σ_a/ρ to represent the fraction of the incident energy scattered and the fraction truly absorbed respectively. The total coefficient $\sigma/\rho = \sigma_s/\rho + \sigma_a/\rho$. Values for σ/ρ and σ_a/ρ for water are given in the third and fourth columns of Table V. σ_s/ρ can be found by taking the difference $\sigma/\rho - \sigma_a/\rho$. It is seen that at low energies σ_a/ρ is very small in agreement with the idea that at low energies the scattered photon gets nearly all the energy and the recoil electron very little. At very high energies σ_a/ρ reaches a value of about 80% of σ/ρ . The total coefficient σ/ρ falls continually as the energy is increased (Fig. III-6). This means the probability of a Compton interaction taking place gets smaller and smaller as the energy is increased. The real coefficient σ_a/ρ consequently rises to a flat maximum from 400 Kv. to 1 Mev. (Fig. III-6) and then falls to attain a value 80% of σ/ρ at 100 Mev. At low energies the Compton coefficients are small compared with the photoelectric coefficient. At medium energies, 100 Kv. to 1000 Kv., the photoelectric coefficient in water is negligible and the Compton process is the only way energy may be extracted from an x-ray beam.

Experiment and theory indicate that the Compton coefficients per electron σ , σ_s , σ_a are independent of Z so that an electron of any atom will absorb the same amount of radiation by the Compton process as an electron of any other atom. The Compton coefficients per gm. σ/ρ , σ_s/ρ , σ_a/ρ will therefore depend directly on the number of electrons

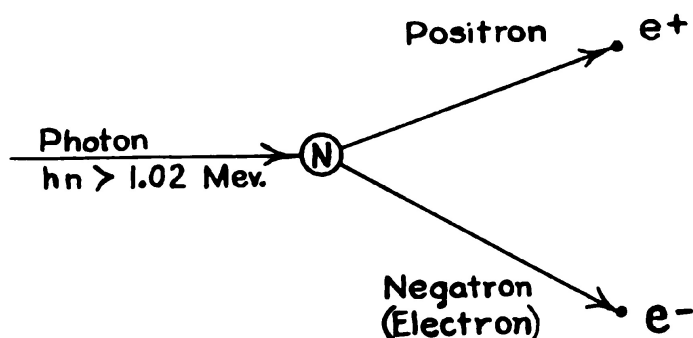


Figure III-8. Diagram illustrating the absorption of a photon by pair production.

per gm. (N_0) of the material (Table IV). Since all materials have essentially the same number of electrons per gm., all materials gm. for gm. will absorb the same amount of radiation by the Compton process. Slight variations in N_0 can easily be taken into account. For example, the value of σ/ρ for lead will be obtained from the value for water by multiplying the latter by $2.38 \times 10^{23}/3.34 \times 10^{23} = 0.712$. Values for lead given in column 9 of Table V were obtained this way. Values for other materials can be obtained in a similar way.

3.06

PAIR PRODUCTION

When the energy of the incident photon is greater than 1.02 Mev. it may be absorbed through the mechanism of pair production. When the photon comes near the strong field of the nucleus of an atom it may suddenly disappear as a photon and become a positive and negative electron pair (Fig. III-8). According to Einstein, mass and energy can be converted from one to the other by the relation

$$E = mc^2 \quad (3-9)$$

where m is the mass in gm., c is the velocity of light (3×10^{10} cm./sec.) and E is the energy in ergs. In Figure III-8 we see that a photon with energy has been converted into a pair of electrons with mass. Equation (3-9) may be used to calculate the minimum energy the photon must have in order to produce a stationary positron and negatron. The mass of an electron is 9.11×10^{-28} gm. so that its equivalent rest energy is $9.11 \times 10^{-28} (3 \times 10^{10})^2 = 82.0 \times 10^{-8}$ ergs. This can be converted to Mev. using equation (1-2) and yields $E = 0.511$ Mev. Therefore a photon of energy 0.511 Mev. could just produce an electron at rest. However, a photon could not produce one electron, for in this process one electronic charge would be created. If, however, the photon produces a positron and a negatron, then no net charge has been produced. Consequently the minimum energy for pair production is 2 (0.511) or 1.02 Mev. If pair production occurs with a

photon of energy 1.02 Mev. the positron and electron will be at rest, but if more energy is available this excess energy will be divided more or less equally between the two particles giving them kinetic energy. The probability of pair production occurring increases as the energy is increased beyond 1.02 Mev.

The converse of pair production, called annihilation, occurs when a positron and electron combine to form a quantum of energy (Fig. III-9). This process is unlikely unless the particles are nearly at rest. Under these circumstances the positron is captured by a free electron, the two charges cancel one another, the masses disappear and usually two photons each with 0.511 Mev. energy are projected in opposite directions from their point of origin. The positron was discovered many years after the electron because of its inability to exist in nature at rest. Since part of the photon's energy is reradiated from the tissue as annihilation radiation, we divide the absorption coefficient for pair production into two parts π_a/ρ and π_n/ρ such that $\pi_a/\rho + \pi_n/\rho = \pi/\rho$. π_a/ρ gives the fraction of the incident energy per gm. of absorber which appears as kinetic energy of the positron and negatron and is truly absorbed. π_n/ρ is the fraction of the incident energy per gm. of absorber which appears as annihilation radiation. Since annihilation of a pair is only likely to occur when the positron is at rest the total energy radiated from the tissue is 1.02 Mev. regardless of the energy of the incident photon. If a photon of energy E (Mev.) interacts with matter to form a pair, the fraction of its energy which appears as kinetic energy of moving particles and is truly absorbed is $(E-1.02)/E$. The relation between π/ρ and π_a/ρ is therefore

$$\frac{\pi_a}{\rho} = \frac{\pi}{\rho} \left(\frac{E - 1.02}{E} \right) = \frac{\pi}{\rho} \left(1 - \frac{1.02}{E} \right) \quad (3-10)$$

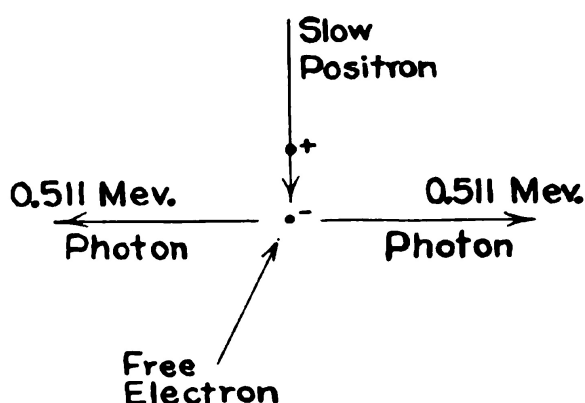


Figure III-9. Diagram illustrating the annihilation of a positron and electron to form two photons of radiation.

If E is 1.02 Mev. π_a/ρ is zero. For large values of E π_a/ρ is almost equal to π/ρ .

Values for π/ρ and π_a/ρ for water are given in columns 5 and 6 of Table V and shown graphically in Figure III-6. It is seen that the coefficients are very small at 2 to 4 Mev. but rise to values larger than the Compton coefficients at energies of 40 Mev. and greater. At 2 or 4 Mev. the value of π_a/ρ is considerably smaller than π/ρ but at the higher energies the two become sensibly equal. π/ρ for lead is shown in Table V and also in Figure III-5. The values at each energy are about nine times as great as the coefficients for water. Theory shows that the coefficient per electron $\epsilon\pi$ depends on the first power of Z . Hence $\epsilon\pi$ for lead should be about $82/7.4$ or 11 times as great as for water. However, there are fewer electrons per gm. in lead so that the ratio of the mass coefficients are about 9:1. Pair production in a heavy element at high energies is very much more important than the Compton process.

3.07 TOTAL APPARENT ABSORPTION COEFFICIENTS

In general when a photon interacts with matter electrons will be set in motion at low energies by the photoelectric process, at medium energies by the Compton process and at high energies by pair production. The total mass absorption coefficient is found by adding together the three effects $\mu/\rho = \tau/\rho + \sigma/\rho + \pi/\rho$. This has been done for lead and copper in columns 11 and 12 of Table V and shown graphically in Figure III-5. It is seen that the curve for lead follows the photoelectric curve to about 100 Kv. and then rises above it due to the Compton effect. It continues to fall with increasing energy until the increase in absorption due to pair production more than compensates for the reduction in the Compton process. The total absorption coefficient then rises as the energy is increased. At 100 Mev. the absorption in lead is almost all due to pair production. It is seen that a minimum absorption coefficient of $0.042 \text{ cm}^2/\text{gm.}$ is reached at an energy of 3 Mev. This means that in lead, radiation at 2 to 3 Mev. has the greatest penetrating power. Examination of Figure III-5 will show that radiation at 100 Mev. is easier to stop in lead than is radiation with 1 Mev. energy.

The results for copper closely parallel those for lead. The total mass absorption coefficient in copper is very nearly the same as for lead in the region where Compton absorption is predominant and all materials absorb about the same amount of radiation gm. for gm. At 100 Mev. the absorption in copper is considerably less than for lead because in this region pair production is important and depends on Z .

The total coefficient for copper is almost constant from 4 Mev. to 20 Mev. and reaches its minimum value about 8 Mev. Values of the total coefficient may be used to calculate the half value layer for these materials. For example, the total coefficient in lead at 1 Mev. is 0.0700 cm.²/gm. (Table V). Hence the half value layer is $0.693/0.0700 = 9.90$ gm./cm.².^{*} If the density is taken as 11.1 gm./cm.³ this "thickness" in gm./cm.² corresponds to 0.89 cm. That is, 0.89 cm. of lead is required to reduce the intensity of a 1.0 Mev. beam of radiation to half its intensity.

The total coefficient μ/ρ for water has not been tabulated but may be obtained by adding together τ/ρ , σ/ρ and π/ρ given in Table V. If this were done and plotted, a curve roughly parallel to that of copper but lower would be obtained.

3.08 TOTAL REAL ABSORPTION COEFFICIENTS

In discussing the absorption of radiation by biological material we are interested in the amount of energy which is given the electrons and hence truly absorbed and do not wish to include the energy which is scattered from the absorber. The total *real* absorption coefficient is $\tau/\rho + \sigma_a/\rho + \pi_a/\rho$. This is given in column 7, Table V, for water and shown graphically in Figure III-6. It is seen that it follows the photoelectric absorption of water up to 30 Kv., then rises above this curve because of the increasing effect of real Compton absorption. It reaches a minimum value at about 100 Kv. and then follows exactly the real Compton coefficient reaching a maximum at about 400 Kv. It begins to deviate from the Compton curve at 4 Mev. where pair production begins to take place and reaches another minimum at 30 Mev. At higher energies it rises, tending to approach the curve for π_a/ρ . The real absorption of energy by muscle closely follows this curve for water but deviations from it occur in bone and fat. These deviations will be discussed in detail in a later chapter.

3.09 THE RELATIVE IMPORTANCE OF DIFFERENT TYPES OF ABSORPTION

It will be seen from Figure III-1 that whenever an interaction occurs between the photon beam and the absorber, one photon is removed from the beam and an electron (photoelectron, Compton or pair) set in motion. For a given energy and thickness of absorber the total number of electrons set in motion will be proportional to $\tau + \sigma + \pi$ and the number of photoelectrons expressed as a percent

^{*}The equation $H. V. L. = 0.693/\mu$ may be used to find the "thickness" of the material measured in gm./cm.² required to reduce the intensity to one half if the coefficient μ is taken as the mass absorption coefficient.

of the total will be $100\tau/(\tau + \sigma + \pi)$. Similar expressions apply to Compton and electron pairs. These have been calculated using the data of Table V and are shown in Table VI. It is seen that at 28 Kv., half the electrons are photoelectrons and the rest Compton (σ/ρ curve for water crosses τ/ρ at 28 Kv., Fig. III-6). At 100 Kv., 97% of the electrons are Compton electrons and the rest photoelectrons. At 26 Mev., 50% of the electrons are Compton electrons, the rest electron pairs (25% positrons and 25% negatrons).

TABLE VI
RELATIVE IMPORTANCE OF THE DIFFERENT TYPES OF
ABSORPTION IN WATER

Energy	Relative Numbers of Electrons (%)			% Energy Carried by Electrons		
	Photo-electrons	Compton	Electron Pairs	Photo-electrons	Compton	Electron Pairs
	$\frac{\tau (100)}{\tau + \sigma + \pi}$	$\frac{\sigma (100)}{\tau + \sigma + \pi}$	$\frac{\pi (100)}{\tau + \sigma + \pi}$	$\frac{\tau (100)}{\tau + \sigma_a + \pi_a}$	$\frac{\sigma_a (100)}{\tau + \sigma_a + \pi_a}$	$\frac{\pi_a (100)}{\tau + \sigma_a + \pi_a}$
10 Kv.	96	4	0	100	0	0
20 Kv.	75	25	0	99	1	0
28 Kv.	50	50	0	95	5	0
62 Kv.	9	91	0	50	50	0
100 Kv.	3	97	0	15	85	0
400 Kv.	0	100	0	0	100	0
1 Mev.	0	100	0	0	100	0
4 Mev.	0	95	5	0	93	7
10 Mev.	0	78	22	0	73	27
26 Mev.	0	50	50	0	44	56
40 Mev.		38	62		32	68
100 Mev.		17	83		14	86

The relative numbers of each type of electron do not correspond to the energy given each type of electron for a photoelectron will have more energy on the average than a Compton electron. The total real coefficient $\tau + \sigma_a + \pi_a$ gives the fraction of the incident energy per cm. of absorber which is given to the electrons. The percent of this energy which is received by the photoelectron is given by $100\tau/(\tau + \sigma_a + \pi_a)$. Similar expressions apply to recoil electrons and electron pairs. These are shown in the last three columns of Table VI. It is seen that at 62 Kv., 9% of the electrons are photoelectrons yet they carry 50% of the energy which is truly absorbed by the water.

The results shown in Table VI may be summarized briefly as follows. Up to 50 Kv. photoelectric absorption is important; from 60 to 90 Kv. photoelectric and Compton absorption are equally important; from 200 Kv. to 2 Mev. Compton absorption alone is present; from 2 to 10 Mev. pair production begins to be important; at 20 Mev. Compton and pair production are equally important; from 50 to 100 Mev. pair production is the most important type of absorption. Since an x-ray tube operating at a given energy produces all radiations of energies less than the maximum, these figures can only be considered as a guide. These results apply to water, air and muscle. Variations appear when we consider the absorption in fat or bone.

When electrons are set in motion by either the Compton or pair process the electron may have any energy ranging from zero up to a maximum value which depends upon the energy of the photon. Since an x-ray beam contains photons of all energies up to a maximum value the electrons set in motion will have all energies up to a corresponding maximum value. The results of detailed calculations on the number of electrons in each energy interval will be found in Table B-1 of the Appendix. Results are presented for three types of radiation. It will be seen that the number of low energy electrons set in motion greatly exceeds the number of high energy ones.

3.10

SUMMARY

The mass photoelectric coefficient (τ/ρ) decreases rapidly with increase in energy and varies approximately as $1/E^3$. It changes rapidly with atomic number depending on Z^3 .

The total mass Compton coefficient σ/ρ falls continuously with increase in energy. It is independent of Z and depends only on the number of electrons per gm. In the region where only Compton absorption is important all materials gm. for gm. will absorb nearly the same amount of radiation. The real Compton coefficient σ_a/ρ rises from a small value at low energies to a maximum at 400 Kv. and then falls to a small value at high energies.

The total mass coefficient for pair production π/ρ increases rapidly as the energy is raised above 2 to 3 Mev. It depends approximately on the first power of Z . The real pair coefficient π_a/ρ is nearly equal to π/ρ except at energies near 1 Mev.

REFERENCES

1. Appleyard, R. K., and Allen-Williams, D. J.: *Brit. J. Radiol.*, 22:215, 1949.
2. Compton, A. H., and Allison, S. K.: *X-Rays in Theory and Experiment*. New York, Van Nostrand, 1946.
3. Davisson, C. M.: *Gamma Ray Absorption Coefficients*. Ph.D. Thesis, Massachusetts Institute of Technology, 1948.
4. Heitler, W.: *The Quantum Theory of Radiation*. Oxford, 1936.
5. Hulme, McDougall, Buckingham, and Fowler: *Proc. Roy. Soc.*, 149A: 131, 1935.
6. Lea, D. E.: *Actions of Radiation on Living Cells*. Cambridge Univ. Press, 1946.
7. Spiers, F. W.: *Brit. J. Radiol.*, 19:52, 1946.
8. Victoreen, J. A.: *J. App. Physics*, 20:1141, 1949.

Chapter IV

MEASUREMENT OF QUANTITY OF RADIATION

4.01 METHODS OF MEASURING QUANTITY

X-RAYS and gamma rays produce a number of effects on matter, and it is conceivable that several of these effects could be used to measure the quantity of radiation. X-rays cause certain materials to change colour. This was the basis of the Pastille method in which barium platinum cyanide was changed from pale green to brown as the dose progressed. The blackening of films by x-rays can be used to measure the quantity of radiation; however, this method is difficult because of the complicated nature of the laws of photographic blackening.* X-rays produce fluorescence in many materials and such an effect could be used for x-ray measurements. There are several biological units which have been used such as the threshold erythema dose but these are hard to reproduce.

From a theoretical point of view, the most satisfactory unit would be an energy unit — a unit which measures the radiation in terms of the energy in ergs absorbed per gm. of tissue. In practice, however, this amount of energy is very small and only refined physical equipment is capable of measuring the minute rise in temperature produced by the energy absorbed from an x-ray beam. X-rays produce ionization and this ionization is relatively easy to measure as delicate equipment of electronic nature has been developed. Consequently, today, x-radiation is measured in terms of the ionization produced by it under certain critical conditions. The unit of dose is called the “roentgen” and is defined in such a way that it can be reproduced without any reference to a biological subject. In certain cases we will find that it is proportional to the energy absorbed by biological material.

*Under certain controlled circumstances of exposure and development the density of a photographic film is directly proportional to the dose. However, because the response of a film varies rapidly with the quality of the radiation, it is difficult to use when a mixture of radiations is being measured. Nevertheless they have been used with considerable success as monitors for personnel protection and in certain research investigations.

4.02

THE ROENTGEN

This unit was defined by an international committee in 1937 (4) as follows. *The roentgen shall be the quantity of X or gamma radiation such that the associated corpuscular emission per 0.001293 grams of air produces, in air, ions carrying 1 e.s.u. of quantity of electricity of either sign.* The mass of 1 cm.³ of dry air at N.T.P. is 0.001293 gms. so that the definition can be considered as referring to the ionization per cm.³ of air. The corpuscles referred to in the definition are the recoil electrons and photoelectrons produced when the x-rays react with the air. To measure a dose in roentgens we must then segregate a known mass of air and measure the ionization produced in this mass of air. This can be done in a standard ionization chamber.

4.03

THE STANDARD IONIZATION CHAMBER

A standard ionization chamber is represented schematically in Figure IV-1. X-rays from the focal spot of an x-ray tube are limited by the circular diaphragm D of area A and enter the ionization chamber. Corpuscular radiation will originate everywhere within the cone FQR but will not be confined to this cone. Some of the corpuscles will be projected forward from their point of origin, and some at right angles to the beam. Thus ions will be produced in a much larger volume than that represented by the cone FQR. This region will extend from the volume FQR a distance R in all directions where R is the maximum range of the corpuscles at right angles to the beam. Typical tracks are shown in the insert to Figure IV-1.

We must now find a method to collect the ions produced in a given volume. This can be done by placing two metal plates parallel to the x-ray beam and at a distance greater than R from the cone FQR. The lower plate is made up of three sections with the outer

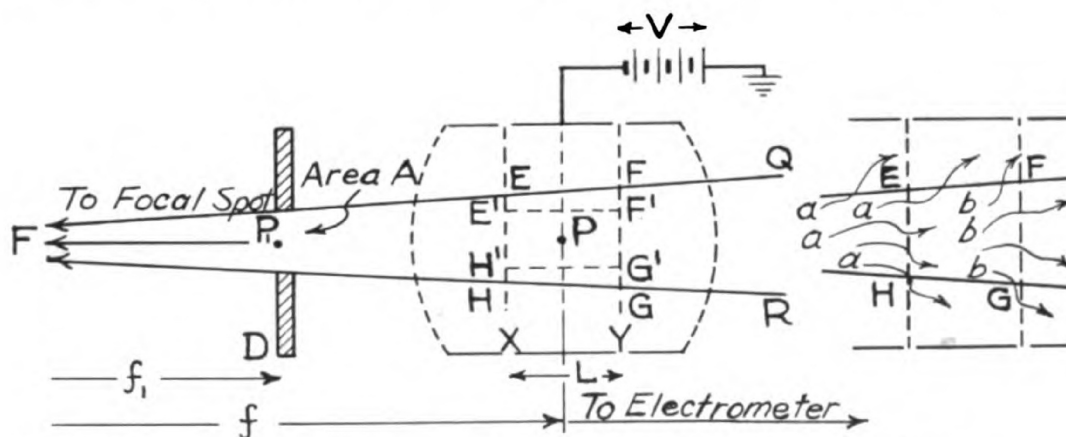


Figure IV-1. Schematic diagram of the "Standard Ionization Chamber."

two grounded and the middle one connected to a charge measuring electrometer. The upper plate is raised to a negative potential V . The upper plate will attract positive charges and negative charges will be driven on to the lower plates and the sensitive central plate. The directions in which the ions will move is represented by the dotted electric lines of force. In the central region the lines of force are straight lines so that all the negative ions produced between the planes X and Y will be collected by the electrometer.

However, all the ions produced between X and Y will not arise from corpuscular radiation originating in the volume $EFGH$. Some corpuscular radiation originating in front of X (tracks "a") will produce ions between X and Y , and similarly tracks "b" originating between X and Y will produce some of their ions beyond plane Y . In general, the number of ions which are lost through tracks "b" will equal the number which are gained through tracks "a." Because of this equilibrium we can consider that all the ions collected between the planes X and Y actually were produced by corpuscular radiation originating in the volume $EFGH$. We can thus segregate a known mass of air and measure the ionization produced by corpuscular radiation originating in it.

Since the x-ray beam always originates from a focal spot with finite area the edges of the cone FQR are diffuse in nature. Hence the accurate evaluation of the volume $EFGH$ is difficult to carry out. As a result the dose received at the point P cannot easily be obtained. In practice it is more convenient to determine the dose received by P_1 at the front surface of the limiting diaphragm. We take as the volume AL , where A is the area of the front diaphragm and L is the length of the sensitive plate (XY). This volume is illustrated schematically as $E_1F_1G_1H_1$. E_1H_1 is of course the diameter of the circular aperture of area A . The volume AL can be accurately obtained from the dimensions of the standard chamber. The ratio of the volume $EFGH$ to the volume of $E_1F_1G_1H_1$ is equal to f^2/f_1^2 where f and f_1 are the distances of P and P_1 from the focal spot. Since the dose in roentgens is found by taking the ratio of the charge collected to the volume in which it is collected, the dose determined using volume $E_1F_1G_1H_1$ will be greater by the ratio f^2/f_1^2 than the dose determined using volume $EFGH$. However, this is the dose which is received by P_1 which should be greater by exactly this ratio according to the inverse square law (see Section 4.06). This argument is based on the assumption that a negligible fraction of the radiation is absorbed by the air between P_1 and P . If this is the case, the same reading will

be obtained on the electrometer regardless of the distance of the parallel plate system behind the diaphragm D. Of course as the system is moved to larger values of "f" the volume from which ions are collected EFGH will increase but this volume does not enter into the calculation of the dose received by P₁. Below about 60 Kvp., absorption of the radiation by the air between P₁ and P will cause a slight reduction in the measured charge as the volume EFGH is moved to larger values of f. Under these circumstances the corrected charge can be determined by measuring the charge at a number of distances and then extrapolating to the case where the volume EFGH is right at the front surface of the limiting diaphragm.

4.04

PRECAUTIONS IN THE USE OF THE STANDARD AIR CHAMBER

A sufficiently high voltage V must be applied between the collector plates to ensure that all the ions produced are collected before they have a chance to recombine. In Figure IV-2 is shown the current in microamperes between the plates of an ionization chamber 1.0 cm. apart when the voltage between the plates is varied from 0 to 360 volts. Curves are shown for x-ray beams of three different intensities. For an intensity of 50 r/min. it is seen that practically all the ions are collected when 300 volts is applied between the plates.

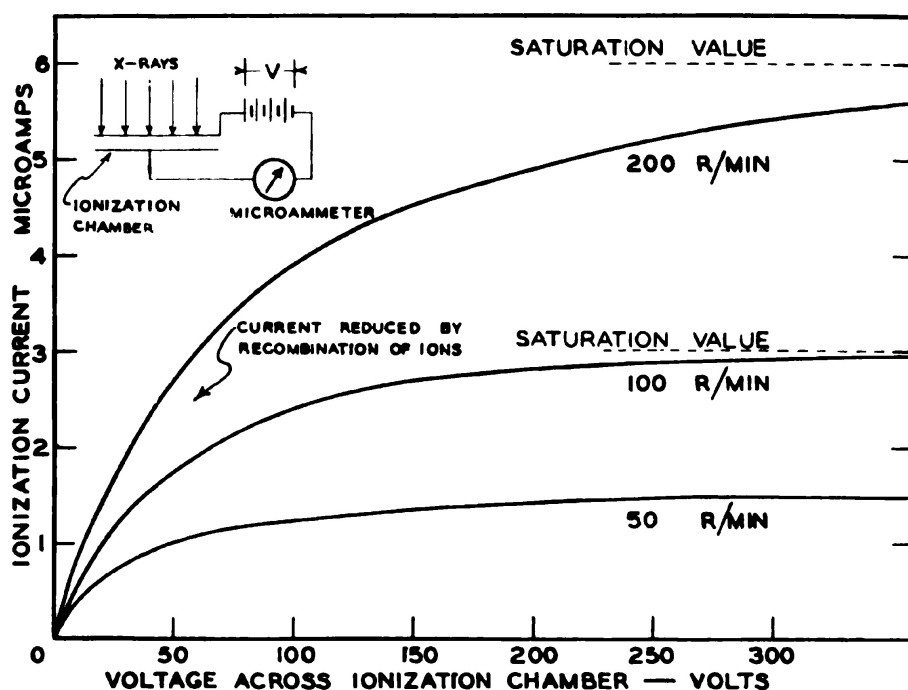


Figure IV-2. Graph showing the relation between the current through an ionization chamber and the voltage across it for three different intensities of radiation.

However, with a dosage rate of 200 r/min. there are four times as many ions formed in a given time and there is a greater chance for recombination. In this case the saturation current is not collected with 300 volts. It is obvious, then, that the voltage required will depend on the dosage rate. The voltage required will also depend on the distance between the plates. If this is reduced by a factor of 2 the electric field* will be doubled so that the velocity of the ions will be doubled. Since the distance they have to travel is reduced by a factor of 2 the time for collection of the ions will be $\frac{1}{4}$ the former value. In betatrons and synchrotrons the ions are all produced in bursts of very short duration and the ion density in the ionization chamber can be very high. Under these circumstances, rather high voltages with very small plate separations are required to obtain saturation. For most standard air chambers electric fields of about 150 volts per cm. are satisfactory.

If the plates of the chamber are closer to the volume EFGH than the maximum range R of the corpuscles, a corpuscle could strike the plate before it had expended all its energy and produced its full quota of ions. Under these circumstances the charge collected would be too small. By the same argument the sensitive volume EFGH must be placed so that P_1P is at least equal to the range of corpuscle in the forward direction. If this condition is not satisfied, more ions will be lost through tracks "b" than are gained through tracks "a." In Table VII are shown the maximum ranges of electrons in air and water for a variety of energies.

It will be seen that the dimensions of a standard chamber must be very large indeed when high energy radiations are to be measured. Since very few electrons acquire their maximum range it is usually unnecessary to satisfy completely the requirements of Table VII. In practice, plate separations of 12 cm., 30 cm. and 350 cm. are required for 180 Kv., 360 Kv. and for radium gamma rays respectively. The dimensions of a standard chamber may be reduced by placing the air under pressure. If the pressure is doubled the ranges of Table VII are halved and the dimensions may then be reduced by the factor 2. Measurements with standard ionization chambers have not been carried out for energies greater than 2 Mev. because of these difficulties. For further details concerning standard ionization chambers reference should be made to the following (1, 2, 3, 13, 14).

*Electric field is found by dividing the voltage between the plates by the plate separation and is measured in volts per cm.

TABLE VII
RANGE OF ELECTRONS IN AIR AND WATER

<i>Energy</i>	<i>Cm. of air at N.T.P.</i>	<i>Cm. of Water</i>
100 Kv.	16	0.015
500 Kv.	120	0.16
1 Mev.	310	0.4
2 Mev.	770	1.0
4 Mev.	1500	2.0
20 Mev.	7700	10.0

The definition of the roentgen requires that the charge liberated in 1 cm.³ of air at N.T.P. be measured. In practice a correction for temperature and pressure must be made according to Charles' and Boyle's Law. Suppose, in a standard ionization chamber, the area of the diaphragm is A cm.² and the length of the plate L cm. Suppose a charge of Q e.s.u. is collected in "t" seconds when the temperature and pressure are t°C and p mm. of Hg. The exposure rate at the front surface of the diaphragm will be

$$\left(\frac{Q}{t}\right) \cdot \frac{1}{A \cdot L} \cdot \left(\frac{273 + t^\circ}{273} \cdot \frac{760}{p}\right) \text{ r/sec.} \quad (4-1)$$

4.05

PRACTICAL IONIZATION CHAMBERS

The large standard chamber lacks mobility and could not be used for calibration purposes except in special circumstances or in a stand-

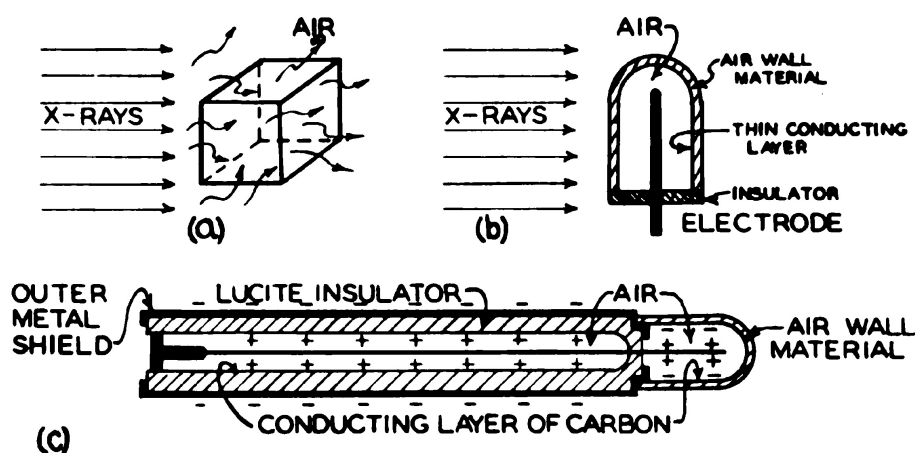


Figure IV-3. Schematic diagrams illustrating the nature of an "air wall" thimble ionization chamber.

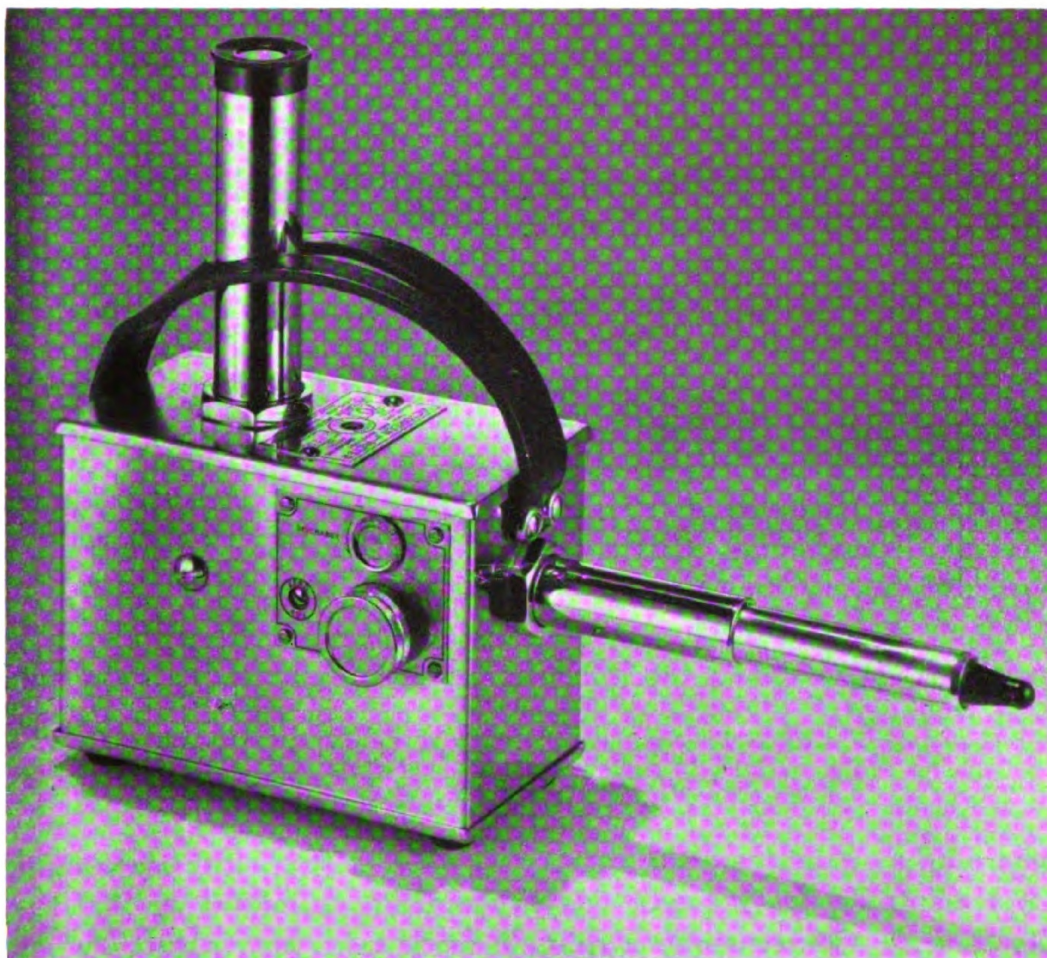


Figure IV-4a. Photograph of Victoreen Condenser r meter. (Courtesy of the Victoreen Instrument Co.)

ardization laboratory. This has led to the development of thimble chambers which although convenient must be standardized against a standard chamber at intervals. Suppose we consider a unit volume of air, completely surrounded by air and bathe the air with x-radiation (Fig. IV-3a). There will be some corpuscles entering this volume from outside and some leaving the volume. In general the number of ions produced outside the cube by corpuscles from inside the cube will be equal to the number of ions produced inside the cube by corpuscles originating outside. We may then consider that all the ions produced inside the cube were produced by corpuscles originating there and that they expended all their energy inside the cube. This would of course, be true only if the air around the cube extended to a distance equal to or greater than the maximum range of the corpuscles. If now all this "air" were condensed into a solid air wall we would not alter the state of affairs and we would have a

thimble chamber represented in Figure IV-3b. The inside of this chamber should be covered with a conducting layer and an electrode inserted. If the electrode is charged the ions produced can be collected. We have thus isolated a given volume of air and collected the charge liberated by the corpuscular radiation and so fulfilled the definition of the roentgen. The basis of the thimble chamber depends on an "air wall" and this may be difficult to achieve in practice. If the wall behaves in the same way as air as far as x-rays are concerned it will be referred to as an "air wall" chamber.

The behaviour of different materials to x-rays depends on the atomic number of the constituents and not on the chemical composition of these constituents. In the low voltage region where photoelectric absorption is important we know that the absorption per electron depends on Z^3 where Z is the atomic number. That is, each electron in an oxygen atom ($Z = 8$) should absorb $(8/6)^3 = 2.4$ times as much energy as each electron in a carbon atom ($Z = 6$). Mayneord (8) has defined the effective atomic number of a compound \bar{Z} as follows.*

$$\bar{Z} = \sqrt[2.94]{a_1 Z_1^{2.94} + a_2 Z_2^{2.94} + a_3 Z_3^{2.94}} \quad (4-2)$$

where a_1, a_2, a_3 etc. are the fractional contents of electrons belonging to elements Z_1, Z_2, Z_3 respectively. From this definition we find that $Z_{air} = 7.70$. Consequently a thimble made with any material whose Z is equal to 7.7 should be satisfactory. In practice the chamber is usually made of bakelite (C_6H_5OH) coated with carbon ($Z = 6$) and the electrode made of aluminum ($Z = 13$). By properly adjusting the size of the electrode and the amount of carbon it is possible to get a chamber that behaves like an "air wall" chamber.

In the standard ionization chamber it was necessary to provide a thickness of air on all sides of the sensitive volume equal to or greater than the range of the electrons. In the thimble chamber in an exactly analogous way the "air wall" material must be thicker than the maximum range of the corpuscles. In Figure IV-5, curve A, is shown the variation of the response of a carbon chamber, with wall thickness, (measured in cm. of carbon) as obtained by Mayneord and Roberts (9). The chamber was exposed to radium gamma rays. It is seen that as the chamber wall is increased the response rises to a maximum when the "equilibrium" wall is attained and then falls slowly.

*For low atomic number materials the photoelectric absorption depends more nearly on the 2.94th power than the third power, hence the use of 2.94 in equation 4-2 due to Mayneord.

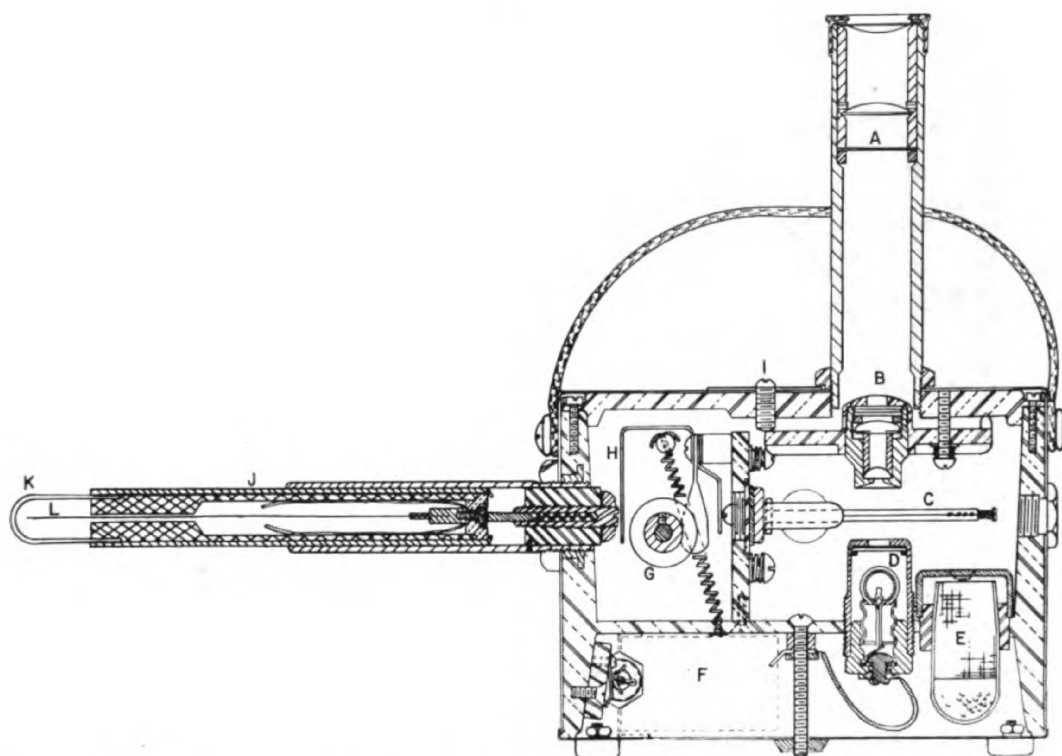


Figure IV-4b. Cross sectional diagram showing the details of the internal construction of a Victoreen Condenser meter. A calibrated scale to read the deflection of the string, B—objective of the microscope, C—platinum string, D—small light to illuminate the string, E—drying chamber, F—battery, G—charging disc made of amber, H—spring contact to make connections between the detachable condenser chamber and the string electrometer, I—focusing adjustment for the microscope, J—detachable condenser chamber, K—thimble chamber, L—collecting electrode for the thimble chamber. (Courtesy of the Victoreen Instrument Co.)

The reduction in response for thick chamber walls is due to the absorption in the walls themselves in exactly the same way as in the standard chamber when appreciable absorption occurred between the limiting diaphragm and the sensitive volume. As Mayneord has pointed out, there is no correct wall thickness but a corrected response which can be obtained by extrapolation of curve A to zero thickness (I_0). This corrected response for curve A is about 1.5% greater than the maximum response and can be obtained quite accurately. It is seen that for radium gamma rays the “equilibrium wall” is about 3 mm. of carbon. This corresponds to about 6 mm. of water or 460 cm. of air and is about what one would expect from Table VII for radium gamma rays with an “average” energy of about 1.6 Mev.

In Figure IV-5, curve B, is shown the variation of the response of a chamber exposed to 22 Mev. radiation from the University of

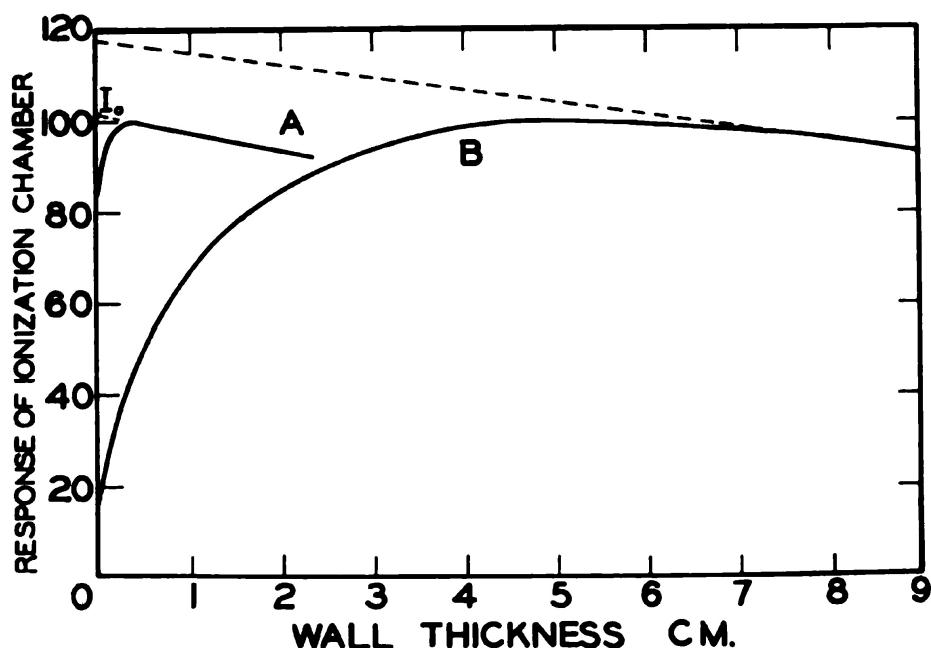


Figure IV-5. Graph showing the relation between the response of an ionization chamber and the wall thickness. Curve A—Data taken from Mayneord and Roberts⁽⁹⁾ for a carbon chamber exposed to radium gamma rays. Curve B—Unpublished data by author for 22 Mev. betatron radiation. Wall thickness expressed in cm. of water.

Saskatchewan betatron. The wall thickness in this case is expressed in cm. of water. It will be seen that the “equilibrium” wall thickness is now about 5 cm. of water. Because of this large distance, difficulty is experienced in extrapolating accurately the response curve to zero wall thickness. The value of I_0 in this case is about 18% greater than the maximum response but cannot be determined precisely. At these high energies the corpuscle has great range and does not liberate its energy near the point of its origin.

When all these precautions are taken with a thimble chamber the same results will be obtained with it as with the standard chamber. In practice, however, the thimbles are always calibrated against the standard and usually at several voltages. At higher voltages the effect of atomic number is not nearly as important since the Compton absorption is independent of Z . If a thimble is calibrated to be correct at 200 Kvp. but found to give too high a reading at 100 Kvp. it can be fixed by reducing Z . This can be done by shortening the aluminum electrode slightly, thus reducing the amount of material of Z greater than 7.7 in the thimble chamber. If the response at both voltages is too high then the volume of the thimble should be reduced. Experiment shows that in the low or very high energy region, the wall materials do have a very great effect on the ionization measured

by the thimble. This is due to the fact that for all practical purposes all the corpuscles which produce ionization in the air cavity originate in the walls and a negligible fraction originates in the air inside the cavity. The wall material thus supplies the corpuscles while the air supplies a medium in which these corpuscles may produce ionization. Gray (7) and others (5, 11) have worked out the theory for the ionization produced in an air cavity inside a medium. It can be shown that (J_v), the ionization produced per cm.³ of air cavity, is given by

$$J_v = \frac{E_v}{W\rho} \quad (4-3)$$

where E_v is the energy truly absorbed from the x-ray beam by 1 cm.³ of the wall material (expressed in ev./cm.³), W is the average energy expended to produce one ion pair ($W = 33$ ev. for air) and ρ is the stopping power of the medium relative to air for the secondary electrons. It is found that ρ does not vary greatly from one material to another so that the ionization produced (J_v) will depend on E_v . At high energies (above 10 Mev.) and low energies (below 400 Kv.) the total real absorption coefficient varies rapidly with the atomic number (see Fig. III-6) so that in these regions the wall material has a great effect on the reading of an ionization chamber.

It is wise to have a thimble chamber checked once a year against a standard chamber.

4.06 CALIBRATION OF AN X-RAY MACHINE

On the North American continent the instrument which is used almost universally for measuring the output of an x-ray machine is the Victoreen Condenser r meter (6, 15). It consists of a detachable condenser thimble chamber shown schematically in Figure IV-3c and a string electrometer, shown in Figure IV-4b. A photograph of the instrument is reproduced in Figure IV-4a and a cross sectional diagram giving the internal construction in Figure IV-4b. When the condenser chamber is inserted into the electrometer the central electrode is connected directly to the string electrometer. This electrometer may be charged by a friction drive and the motion of the string observed in a microscope. The electrometer is charged until the string reaches the zero mark of the scale, which actually corresponds to about 600 volts. The condenser chamber in a charged state is shown schematically in Figure IV-3c. Most of the charges are stored on the thin conducting layer facing the outer shield through the polystyrene insulator. The charged chamber is then removed, a protective cap placed over the sensitive central electrode and the thimble

part of the chamber placed in the x-ray beam for a measured period of time. The charged central electrode will collect negative ions formed in the air cavity of the thimble and this will reduce the charge on it and thus its voltage. (Let the resulting value be 400 volts.) X-rays passing through the stem of the chamber will produce ions in the air inside it but these ions find themselves in a region where there is no electric field and so will not be collected and will eventually recombine. The stem of the chamber is therefore insensitive to radiation.

The remaining charge on the electrode can be measured by reconnecting it to the electrometer. Before this is done the "r" meter should be checked to make sure no charge has leaked off it. If a charge has leaked off, the instrument will no longer read zero and it should be charged up to zero again. (Actually, the string of the electrometer should be charged to the place it occupied when the condenser chamber was first removed. This position may differ slightly from zero.) When the chamber is reconnected the voltage of the system will reach a value somewhere between 400 and 600 volts, say 450, and this reading will appear as a certain number of "r" units on the scale of the instrument. We know therefore that in the measured period of time, a certain dose in "r" units has been given the point occupied by the thimble chamber.

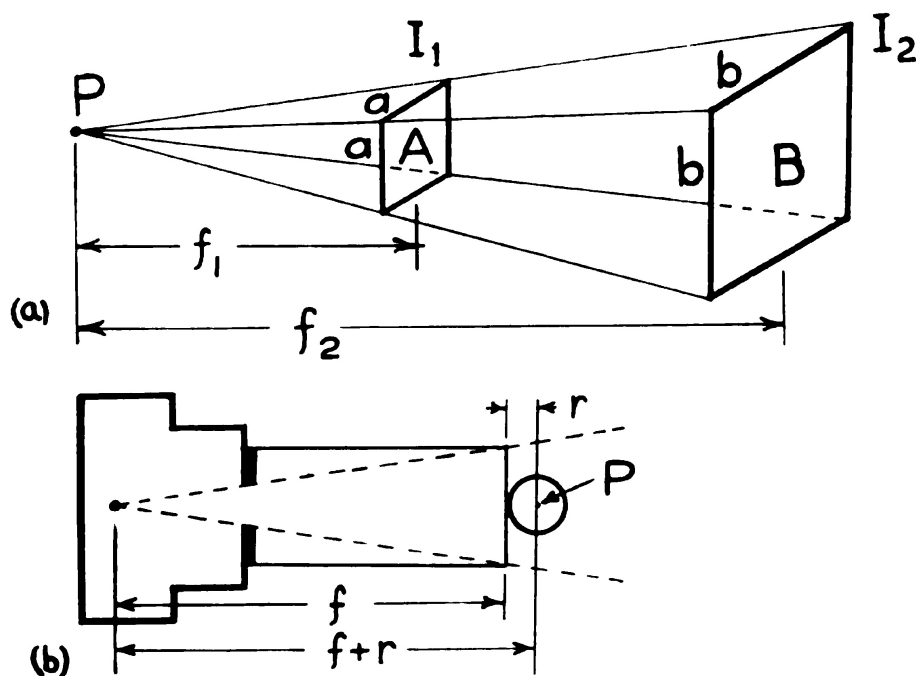


Figure IV-6. (a) Diagram to illustrate the inverse square law. (b) To illustrate the method for correcting the measured dosage rate at P to the dosage at the end of the treatment applicator.

Some of the precautions which should be taken in measuring the output of an x-ray machine without back scatter are as follows:

(a) The thimble chamber should be placed with the sensitive volume at the centre of the treatment field and in contact with the end of the treatment cone. The distance from the end of the treatment cone to the centre of the thimble chamber (r) should be measured carefully (Fig. IV-6b). The dose received by the thimble in a given time will be less than that received at the end of the cone because of the inverse square law. All the radiation which passes through A (Fig. IV-6a) must pass through B if there is negligible absorption of the radiation between A and B. If f_2 is exactly twice f_1 , then B will be 4 times as great as A, and thus the intensity (amount of radiation per unit area) at B will be $\frac{1}{4}$ of that at A. In general, it follows that

$$\frac{I_1}{I_2} = \frac{f_2^2}{f_1^2} \quad (4-4)$$

The thimble chamber measures the intensity at P, its centre, so that the intensity at the end of the cone will be greater than this by the factor $(f + r)^2/f^2$. For the Victoreen thimble ($r = 0.8$ cm.) this factor is 1.03 for a focal skin distance of 50 cm. or a correction of 3%. At the short focal skin distance of 15 cm. the factor is 1.11 and the percentage correction is 11%. This correction can therefore be very important at short focal skin distances.

(b) The machine should be built up to its correct operating point (tube kilo-voltage and current) before the shutter is opened. The time for the shutter to open and expose the centre of the treatment cone should be determined so that the true exposure time can be obtained. In some machines the shutter takes as much as 1.5 sec. to open. This time is a very important fraction of a 15 sec. exposure.

(c) While the exposure of the thimble chamber is being made, the current through the x-ray tube and the voltage applied it should be kept constant. Variations in voltage of 1% can alter the output by as much as 6%. Variations in the tube current of 1% will alter the output by about 1%. If the voltage cannot be kept constant a numerical correction should be made to the result to correct for this. The variation of output with voltage can be obtained by running the machine at a slightly lower voltage and measuring the output.

(d) A correction should be made for temperature and pressure. If the "r" meter is calibrated to be correct at 760 mm. pressure and 22°C, multiply the output by $\frac{760}{p} \frac{(273+t^\circ)}{295}$ At points well above sea

level this correction can be as high as 10%. Correction tables are usually supplied with the instrument but if not, see reference 15.

(e) At voltages below 80 Kvp. the "r" meter will read too low because of the absorption of the x-ray beam in the walls of the chamber.

(f) Scattered radiation from objects in the room back to the thimble chamber should be avoided by keeping objects out of the direct beam of the x-rays.

(g) The exposure time should be adjusted to yield a reading on the Victoreen of about 15r on the 25r scale or 60r on the 100r scale. The instrument has its greatest accuracy in this region.

(h) At least three readings of the output should be obtained and the average taken.

(i) The output without back scatter should be measured for each cone. It is not safe to assume that a group of treatment cones will give the same output in air, although the differences may be small.

To illustrate these corrections suppose an x-ray machine gives an average reading of 15.8r in 40 sec. Suppose the shutter requires 0.8 sec. to open and that the centre of the thimble chamber is 0.9 cm. from the end of a 50 cm. F.S.D. treatment cone. Suppose the temperature is 18°C. and the pressure 710 mm. of Hg. The corrected output is:

$$15.8 \times \left(\frac{60}{40 - .8} \right) \times \left(\frac{50.9}{50} \right)^2 \times \left(\frac{760}{710} \cdot \frac{291}{295} \right) = 26.4 \text{ r/min.}$$

4.07 OTHER TYPES OF RADIATION MEASURING DEVICES

(a) **Constancy Indicators.** In some x-ray machines a simple ionization chamber is placed in the x-ray beam just below the shutter. This chamber usually consists of a series of thin conducting plates of aluminum or lucite coated with carbon. This ionization chamber may be connected in series with a battery and microammeter as shown in the insert of Figure IV-2. This arrangement is very simple and dependable but requires a rather sensitive microammeter to give a suitable reading in most x-ray beams. For this reason, the small ionization current is often amplified and then measured with a more robust type of microammeter (10, 12, 15). The constancy meter is useful for detecting any changes in the output of the machine and of indicating whether the correct filter, tube voltage and current are being used. When a constancy meter indicates a change in output for the same tube current and voltage the machine should be

recalibrated with an "r" meter. If the ionization chamber is a sealed unit, its reading will be independent of changes in room temperature and pressure. This is of considerable value since the ionization chamber may become quite warm as the x-ray machine is operated. The plates of the chamber should have approximate "air wall" characteristics, otherwise the reading of the constancy indicator will not be proportional to the output of the machine in "r" units.

(b) **Integrating Meters.** If the output of an x-ray machine is held constant at a definite value for a given length of time, then a known dose is administered. Many machines are arranged to terminate the treatment automatically after a predetermined time. For these machines the accuracy of the treatment will therefore depend on keeping the output of the machine constant. This can be done only by continually adjusting to a constant value the tube current and voltage. The tube voltage will vary with line voltage fluctuations caused in part by the turning on and off of other x-ray machines in the department. Since the output of the machine varies rapidly with small changes in the tube voltage, it follows that it is difficult to keep the output of a machine constant. Under these circumstances an integrating type of meter which delivers a predetermined *dose* may be useful (15). The basic principles of such a device are shown in Figure IV-7. In this circuit the current through the ionization chamber is made to charge the capacity C. The quantity of electricity Q stored on C will be equal to the charge which has been liberated in the ionization chamber by the action of the x-rays and therefore proportional to the dose. As the condenser C charges up, the voltage across the ionization chamber falls but since this chamber is operated in the saturation region (Fig. IV-2) the small drop in voltage will not affect the ionization current. When C is charged to a certain voltage the vacuum tube will start to conduct. Conduction in this tube may be

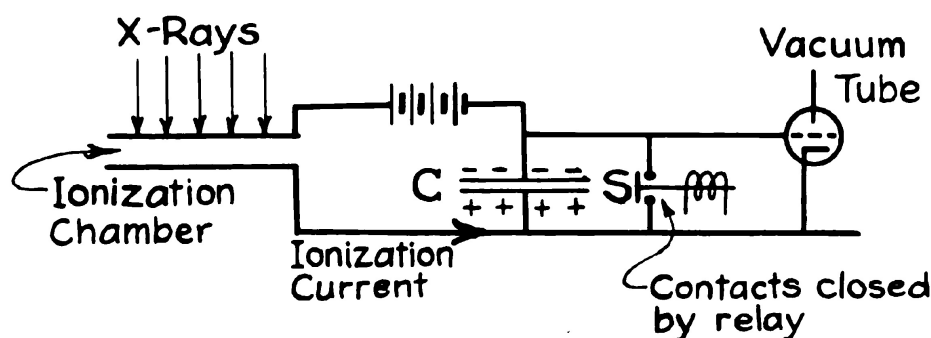


Figure IV-7. Schematic diagram of the integrating type of radiation measuring instrument.

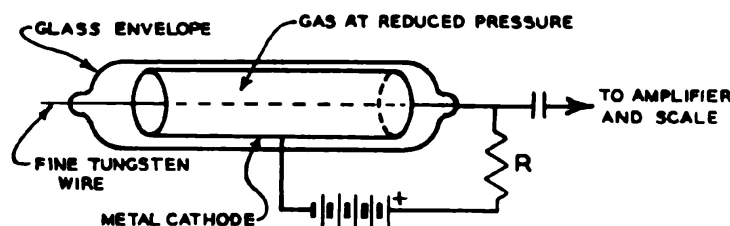


Figure IV-8. Schematic diagram of a Geiger counter.

made to operate a counter and actuate the relay which in turn momentarily closes the contact S shown in Figure IV-7. This will discharge the condenser C and the charging process from the ionization chamber will start again. Each time the counter operates a certain dose has been given. The actual dose delivered per count must be determined by means of an "r" meter. With such a device the machine is set to turn itself off after a predetermined number of "counts" have been given. In practice, it is found that most integrating devices of this type must be checked quite frequently with an "r" meter.

(c) **Protection Meters.** For measuring stray radiation several types of meters are available. One type is based on the principle of the Victoreen "r" meter (15), using a very large ionization chamber to increase the sensitivity of the instrument. Instruments which give a full scale deflection for a dose of 0.01 "r" units are available. Another useful type consists of an electrometer connected permanently to an ionization chamber and mounted in a container about the size of a pencil. The chamber is charged in an auxiliary device. It has the advantage that the wearer may examine it at any time and observe the radiation which has been received. For extreme sensitivity, use may be made of the "Geiger" counter illustrated in Figure IV-8. It consists essentially of fine tungsten wire placed along the axis of a metal cathode tube inside a vacuum tight glass envelope. The envelope is filled with a mixture of gases at a pressure of about 10 cm. of mercury. The central electrode is connected to a positive potential through a high resistance R. When a photon passes through the device it may eject an electron from the metal cathode (often made of copper). This high speed electron will produce ions in the gas. The negative ions will be attracted to the central electrode and may acquire velocities large enough to ionize by collision and produce a small discharge. This discharge current flowing through R will produce a voltage pulse which may be amplified and recorded on a counter. With this device it is possible to detect individual photons. Because of its great sensitivity it is useful in searching for lost radium

or for the detection of very small amounts of radiation. A correlation between the number of counts per minute recorded and the dosage rate in milliroentgens per minute is possible if the energy of the radiation and the efficiency of the Geiger counter are known.

REFERENCES

1. Behnken, H.: *Strahlentherapie*, 26:79, 1927.
2. Failla, G.: *Am. J. Roentgenol.*, 21:47, 1929.
3. Failla, G.: *Radiology*, 15:437, 1930.
4. Fifth International Congress of Radiology, Recommendations of International Committee for Radiological Units. *Radiology*, 29:634, 1937.
5. Fricke, H. and Glasser, O.: *Am. J. Roentgenol.*, 13:453, 1925.
6. Glasser, O., Portmann, U. V. and Seitz, V. B.: *Am. J. Roentgenol.*, 20:505, 1928.
7. Gray, L. H.: *Proc. Roy. Soc., London, S. A.*, 156:578, 1937.
8. Mayneord, W. V.: *Acta of the International Union Against Cancer*, 2:271, 1937.
9. Mayneord, W. V. and Roberts, J. E.: *Brit. J. Radiol.*, 10:365, 1937.
10. Roberts, J. E. and Farmer, F. T.: *Brit. J. Radiol.*, 16:353, 1943.
11. Sievert, R.: *Acta radiol.*, 21:189, 1940.
12. Taft, R. B.: *Am. J. Roentgenol.*, 60:260, 1948.
13. Taylor, L. S.: *Radiology*, 15:49, 1930.
14. Taylor, L. S. and Singer, G.: *Radiology*, 15:637, 1930.
15. Victoreen, J. A.: *Medical Physics*, Chicago, Yr. Bk. Pub., 1944, p. 1370.

Chapter V

THE QUALITY OF X-RAYS

5.01

HALF VALUE LAYER

THE quality of an x-ray beam can be specified completely only by determining the amount of energy in the x-ray beam at each wavelength, as in Figure II-8. This distribution of energy will depend on the inherent filtration, the filters used, the peak voltage applied, the wave form of the x-ray generator and the target material in the x-ray tube. Fortunately the biological effect of x-rays and their distribution in a scattering medium (see Chapter VI) does not vary rapidly with the quality of the radiation, so a cruder method of measuring quality is satisfactory. Today, quality is specified in terms of the thickness of some standard material which is required to reduce the intensity of a beam to one-half its original value. For voltages below 100 Kvp. the half value layer is usually expressed in mm. of aluminum, for voltages up to 400 Kv. in mm. of copper and for higher voltages in mm. of lead.

5.02

THE MEASUREMENT OF HALF VALUE LAYER

The half value layer of an x-ray beam can be obtained by measuring the output of an x-ray machine for a series of different filtrations. The thimble chamber of the measuring device should be arranged so that the sensitive volume may be returned to exactly the same point on the axis of the beam after each measurement has been made. If a Victoreen "r" meter is being used this may be done by holding the detachable cap of the Victoreen firmly in a clamp. A small area treatment cone should be used and radiation scattered from objects in the room should be avoided. For constant kilovoltage and milliamperage the output of the machine in r/min. should be determined for a number of different filtrations. The results of such an experiment on a 200 Kv. x-ray machine are shown in Figure V-1. In Chapter III we saw that a true exponential absorption curve should appear as a straight line when plotted on semi-log. paper. The curve of Figure V-1 is not linear because the beam of radiation from the x-ray machine is not monochromatic. However, under severe filtra-

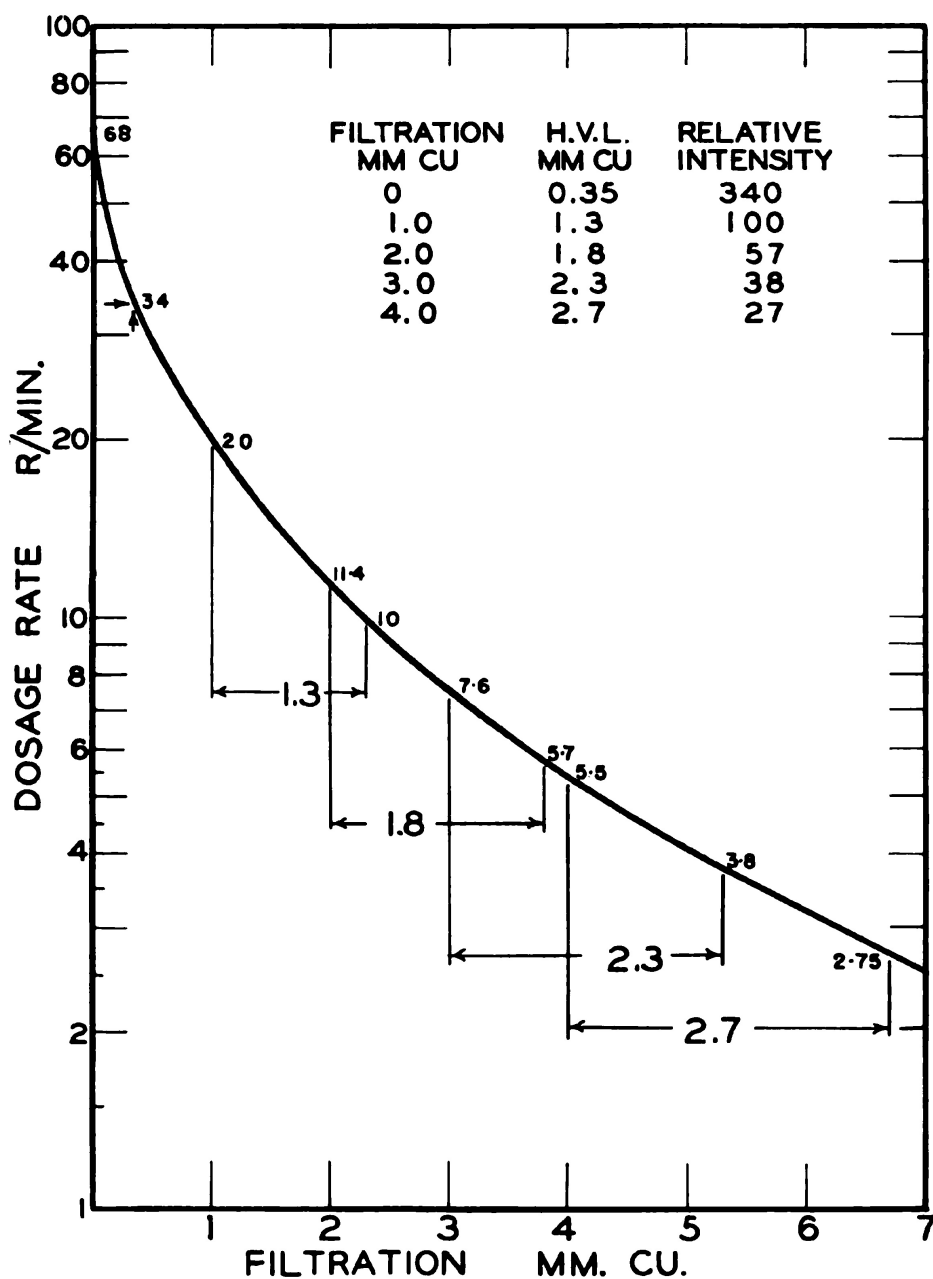


Figure V-1. Experimentally determined absorption curve for 200 Kv. radiation, showing how the half value layer may be determined for a number of filtrations.

tion the softer components are absorbed and the radiation which is transmitted is more nearly monochromatic and the absorption curve is more nearly linear.

Examination of Figure V-1 shows that the half value layer of the unfiltered beam is 0.35 mm. Cu. (0.35 mm. Cu. reduces the intensity from 68 r/min. to 34 r/min.). If 1.0 mm. of copper is used as the filter, then an extra 1.3 mm. is required to reduce the intensity to one-

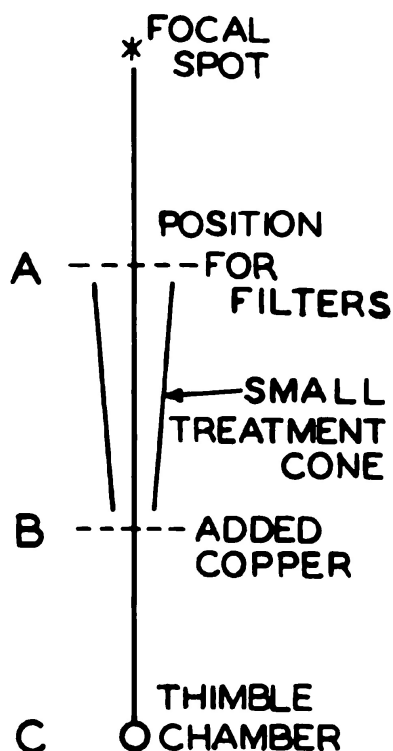


Figure V-2. Ideal arrangement for accurate measurement of half value layer.

half (20 r/min. to 10 r/min.), From this curve the half value layer for a number of filtrations can be obtained and are shown in the insert of Figure V-1. It is seen that with 4.0 mm. of copper filtration the half value layer can be increased to 2.7 mm. of copper. However, with this severe filtration the output is only 27% of that with 1.0 mm. of copper filtration.

It is customary to place an aluminum filter next the copper filter on the side remote from the tube to absorb the characteristic radiation from the copper. This aluminum filter can change the half value layer of the beam slightly. If a treatment cone with a bakelite end is used, this material can also change the quality of the beam. For these reasons, measurements of the half value layer should really be carried out on the beam which emerges from the treatment cone. This can be done readily by arranging the machine as in Figure V-2. The copper and aluminum filter should be placed at A, a small treatment cone should be used and added layers of copper should be placed at B. The thimble chamber should be some distance from B to avoid radiation scattered by the copper. It is not necessary to carry out a complete absorption experiment. Measurements should be made with no added copper filter, then with enough copper to reduce the in-

tensity to a little less than one half, and finally with enough to reduce it to a little more than one half. The half value layer can be obtained by interpolation. For the machine being discussed using 1.0 mm. Cu. and 0.5 mm. Al. filter the half value layer is 1.4 mm. Cu. as compared with 1.3 mm. Cu. obtained above.

5.03

FILTERS

The unfiltered x-ray beam from a thick target contains all wavelengths up to a minimum value which is determined by the voltage on the tube. The distribution of energy with wavelength was shown in Figure II-8 for several different kilovoltages and is repeated again in Figure V-8 for 200 Kv. (curve A). Radiation of wavelength greater than $0.3A^\circ$ can contribute no effect on a deep tumour and will merely increase the skin dose because such radiation is readily absorbed in the superficial layers of the body. This unwanted radiation may be removed from the beam by the use of appropriate filters. Using the known mass absorption coefficients for tin, copper and aluminum curves B, C and D were obtained from curve A. Curve B results when the beam is filtered by $\frac{1}{4}$ of a mm. of tin. It will be seen that this reduces the radiation intensity to practically zero in the

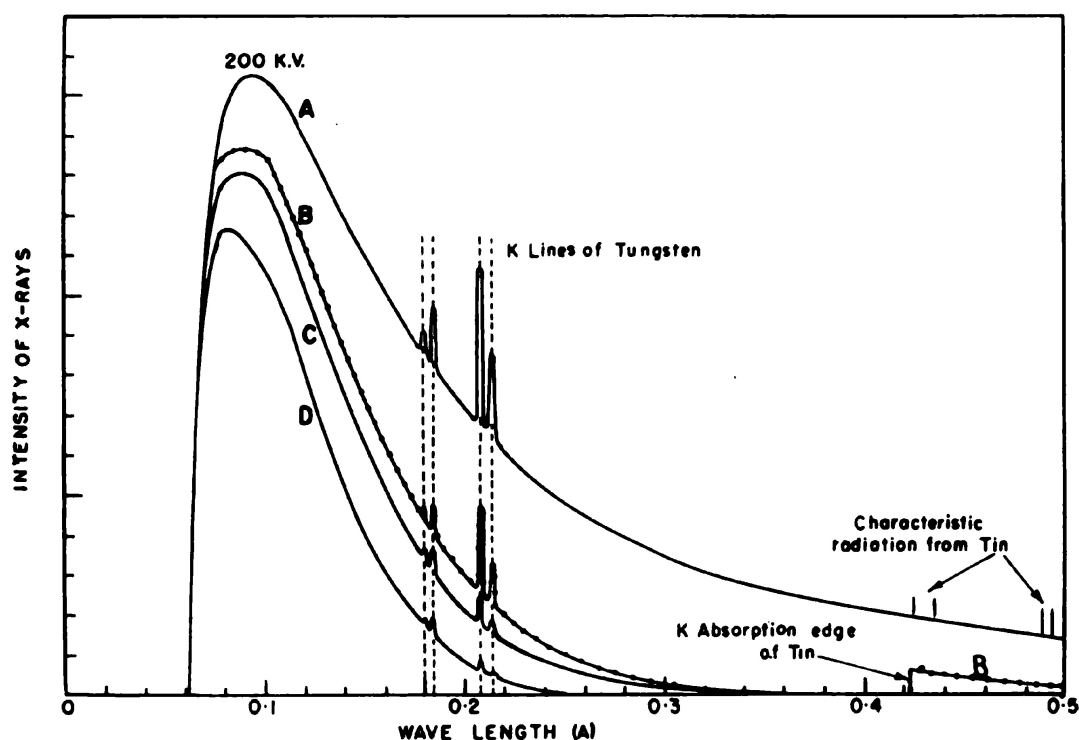


Figure V-3. To illustrate the effect of filtration on an unfiltered x-ray beam. Curve A—unfiltered 200 Kv. radiation from tungsten target; Curve B—filtered by $\frac{1}{4}$ mm. of tin and $\frac{1}{4}$ mm. copper; Curve D—filtered by $\frac{1}{2}$ mm. tin plus $\frac{1}{4}$ mm. copper plus $\frac{1}{2}$ mm. aluminum.

region from 0.3\AA to 0.424\AA . In this region the photoelectric absorption of tin is very large. However, for wavelengths greater than 0.424\AA the photons have insufficient energy to eject the K electrons from tin and the absorption coefficient suffers a sudden drop. In the region from 0.424\AA to 0.6\AA the tin transmits radiation. Curve B does not represent a satisfactory beam from a therapeutic point of view because of the soft radiation which passes through the tin filter at wavelengths greater than the K absorption edge. This situation may be rectified by placing a thin copper filter next the tin filter. With a $\frac{1}{4}$ mm. copper filter curve C is obtained. In the region from 0.424 to 1\AA the copper has a much higher mass absorption coefficient than tin* so the radiation in this energy range is reduced effectively to zero by the copper. The copper has another important purpose. In the region from 0.2 to 0.42\AA the tin absorbs strongly by the photoelectric process. K electrons are removed from the tin atoms and when the holes in the K shell are filled, characteristic radiation of wavelengths from 0.42 to 0.49\AA is emitted. This radiation is of just the right wavelength to pass readily through the tin. However, the thin copper will effectively stop this radiation. The copper thus absorbs the primary beam in the energy region where tin is a poor absorber and also serves to absorb the characteristic radiation from the tin. It is usual to place a thin layer of aluminum next the copper to stop the characteristic radiation from the copper. Composite filters of this kind are called Thoraeus filters (5). It is important that they be arranged in the proper order with the highest atomic number material nearest the x-ray tube. Curve D was obtained from A by filtration with $\frac{1}{2}$ mm. tin, $\frac{1}{4}$ mm. copper and $\frac{1}{2}$ mm. aluminum. Curve D is a satisfactory distribution from the point of view of therapy. Further filtration would yield a more penetrating beam with a higher half value layer but of course the intensity would be reduced. Beyond a certain point filtration becomes uneconomic because of the great reduction in intensity. If a higher half value layer is required the voltage across the x-ray tube should be increased. This will increase the intensity of the radiation in the short wavelength region.

The choice of the proper filter will depend on the voltage of the x-ray machine. A lead filter would not be useful with a 200 Kv. machine because it would very effectively reduce the radiation in the region from 0.06\AA to 0.141\AA and there would be no radiation transmitted. In the same way a tin filter would be of no value used

*This effect is illustrated in Figure III-5 where it is seen that copper has a higher absorption coefficient than lead in the energy region between their absorption edges.

with a 100 Kv. machine. With 100 to 140 Kv. machines it is usual to filter the radiation with aluminum and to use beams with half value layer from 1 to 3 mm. Al. With a 200 Kv. machine composite filters of copper and aluminum are used to produce beams with half value layers from 0.5 to 1.5 mm. of copper. In this energy region, Thoraues (5) filters made of tin, copper and aluminum are useful. Frequently a composite filter made of tin, copper and aluminum will give a beam of slightly greater intensity for the same half value layer than is obtained using copper and aluminum alone. For 400 Kv. radiation composite tin, copper and aluminum filters are useful and half value layers of about 4.0 mm. of copper can be obtained. In the 1 to 2 Mev. region composite filters of lead, tin, copper and aluminum are used. In the very high energy region produced by betatrons, with a continuous distribution of energies from 0 to 30 Mev., lead does not make a useful filter. Examination of Figure III-5 will show that the absorption coefficient for lead passes through a minimum value at 2 Mev. A lead filter will therefore discriminate against both the low and the high energy radiation and will transmit radiation at 2 Mev. energy. In the 0 to 30 Mev. energy region materials with low atomic numbers such as carbon reduce the low energy radiation slightly more than the hard radiation (1) although the effect is small. Filtration, in the usual sense, of betatron radiation does not serve a useful purpose. However, compensating filters of copper or carbon can be used to advantage to produce flat betatron fields (1, 3). These materials leave the spectral distribution of the radiation essentially unaltered.

It is possible for a heavily filtered beam from a 200 Kv. machine to have the same half value layer as a lightly filtered beam from a 400 Kv. machine. These beams are only the same to a crude first approximation for it is realized that the 400 Kv. beam has radiation from 200 Kv. to 400 Kv. which the 200 Kv. beam does not have. However, it is generally found that a statement of the half value layer and the peak kilovoltage yield sufficient information for the radio-therapist.

5.04 EQUIVALENT WAVELENGTH AND KILOVOLTAGE

In certain investigations it is convenient to express the quality of an x-ray beam in terms of the equivalent wavelength λ_e or equivalent kilovoltage V_e , both of which are derived from a knowledge of the half value layer. The type of x-ray beam used in radiology is always heterogenous, consisting of many wavelengths, but we can refer to it as having an equivalent wavelength λ_e if monochromatic radiation

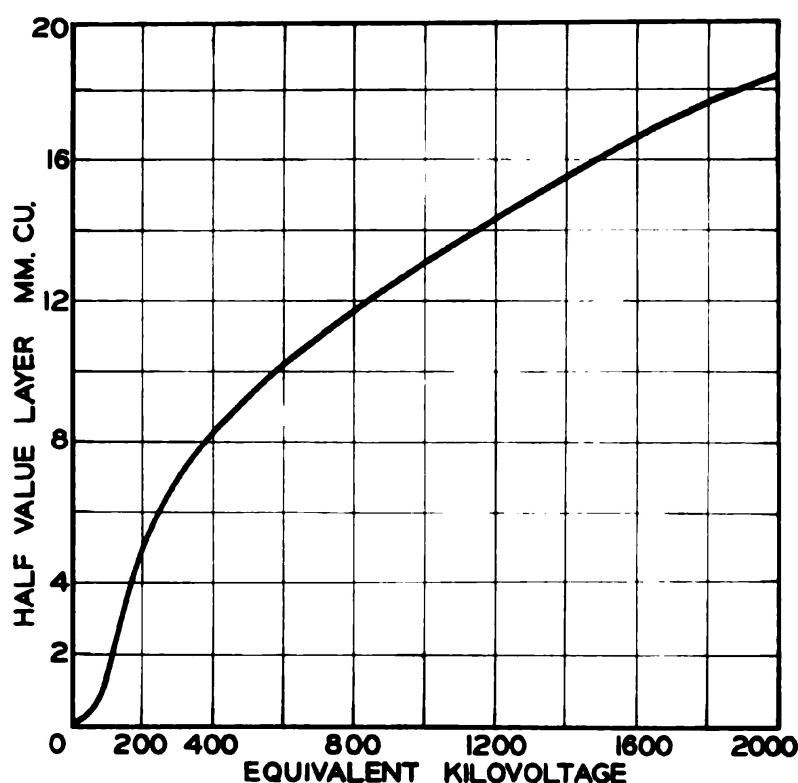


Figure V-4. Graph showing the relation between half value layer in mm. of copper and the equivalent kilovoltage, calculated from the total absorption coefficient data for copper given in Table V, Chapter III.

of wavelength λ_e has the same half value layer as the radiation in question. V_e is related to λ_e by the equation $\lambda_e V_e = 12.4$. (Equation 1-6.)

In the last column of Table V, Chapter III, the total mass absorption coefficient μ/ρ for copper is given for a number of photon energies. From the density of copper 8.93 gm./cm.³ (Table IV, Chapter III) the linear absorption coefficient may be obtained and then the half value layer ($\text{h.v.l.} = 0.693/\mu$). For example, μ/ρ for copper at 400 Kv. = 0.0920 cm.²/gm. Hence the linear absorption coefficient is 0.821 cm.⁻¹.^{*} The half value layer is $0.693/.821 = .845 \text{ cm.} = 8.45 \text{ mm.}$ of Cu. If, therefore, a heterogeneous beam of radiation has a half value layer of 8.45 mm. of copper it has an equivalent kilovoltage of 400 Kv. and an equivalent wavelength of $12.4/400 = 0.031 \text{ A.}$ Using the data of Table V the half value layers for a number of equivalent kilovoltages have been calculated and are shown graphically in Figure V-4. These results are in agreement with those due to Mayneord (4). Suppose the half value layer from a 400 Kv. machine is 4.0 mm. of

^{*} $\mu = (\text{Mass absorption coefficient}) \times (\rho) = .0920 \times 8.93 = 0.821 \text{ cm.}^{-1}.$

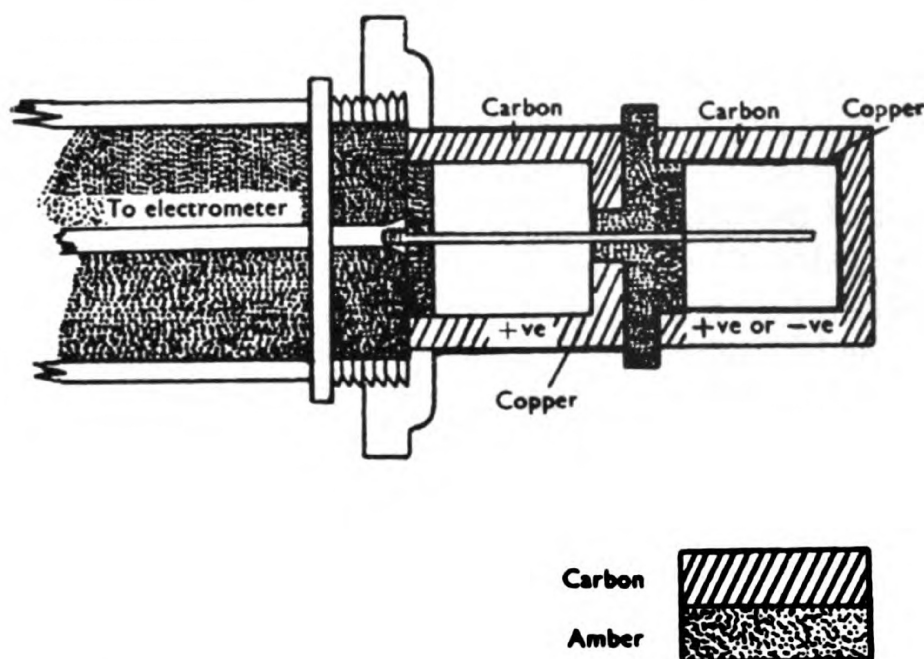


Figure V-5. Double ionization chamber due to Clarkson and Mayneord⁽²⁾.

copper. From Figure V-4 we see that $V_e = 165$ Kv. and $\lambda_e = 0.075$ A or 75 X.U. (1000 X.U. = 1A). It should be emphasized that both the equivalent kilovoltage and wavelength are determined from the half value layer and do not really yield any further information concerning the beam.

5.05

THE VARIATION OF QUALITY WITHIN A SCATTERING MEDIUM

When an x-ray beam strikes a scattering medium such as the human body, Compton scattering takes place so the average wavelength of the radiation will increase. To investigate this effect, Clarkson and Mayneord (2) directed an x-ray beam into a water phantom and measured the quality of the radiation within the medium using the ingenious double ionization chamber shown in Figure V-5.

One common electrode is placed through the centre of two coaxial cylindrical chambers made of carbon. The outer chamber is coated on the inside with a thin layer of copper equal to the maximum range of the photoelectrons and the other chamber is coated on the outside with the same thickness of copper. By a simple throw-over switch the potential on the outer chamber can be reversed so that in one case $I_1 + I_2$ is observed and in the other $I_1 - I_2$, where I_1 and I_2 are the ionization currents from the two chambers measured separate-

ly. Knowing $(I_1 - I_2)$ and $(I_1 + I_2)$ both I_1 and I_2 can be calculated. Very hard radiation will produce the same ionization in both chambers so that $I_1 = I_2$ but soft radiation will produce a much greater response in the chamber lined with copper, due to the copious emission of photoelectrons. By placing such a chamber in a beam of known quality, Clarkson and Mayneord were able to calibrate their double chamber. For example, they found that I_1/I_2 varied from 10 to 2.0 as the half value layer changed from 3.25 to 15 mm. of copper. Using such a chamber the quality of the radiation in the scattering material could be measured. Some of their results are shown in Figures V-6 and V-7 where a beam of radiation with $\lambda_e = 94$ X.U. is incident upon the scattering medium. In Figure V-6 the quality at points along the axis of the beam is shown as the depth below the surface is increased for three sizes of field. It is seen that as the depth increases the softening of the beam increases especially for the large fields where there is a large amount of scattered radiation. It is also seen that even on the surface of the phantom (depth 0) the radiation has been softened by the contribution of scattered radiation. This

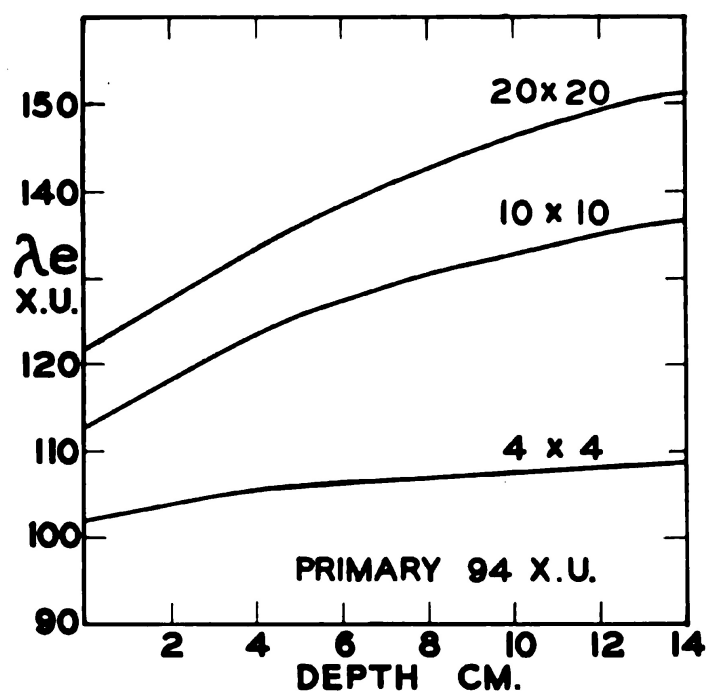


Figure V-6. Graph showing the variation of the equivalent wavelength λ_e as the depth below the surface of the phantom is increased for fields of 4 x 4, 10 x 10 and 20 x 20. Data taken from Clarkson and Mayneord⁽²⁾. Wavelengths are expressed in X.U. were 1000 X.U. = 1A.

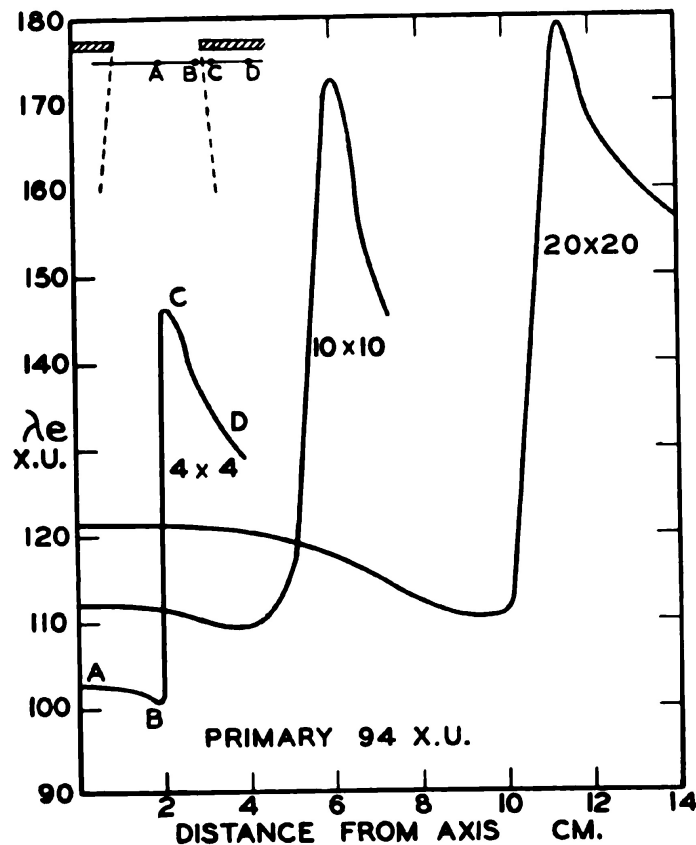


Figure V-7. Graph showing the variation of the equivalent wavelength on the surface of the phantom as one proceeds from the centre of the beam into the shadow of the limiting diaphragm (along line AD of insert) for four different sized fields. Data taken from Clarkson and Mayneord⁽²⁾. Wavelengths are expressed in X.U. where 1000 X.U. = 1Å. The points A, B, C and D on the graph correspond to the points A, B, C and D of the insert.

effect is most pronounced for the larger fields. In Figure V-7 are shown the results of measurements of quality at the surface of the phantom as one proceeds from the centre of the beam A (see insert Figure V-7) to the edge of the beam at B and into the shadow of the limiting diaphragm at C and D. At A there is more scattered radiation than at B so we observe softer radiation. At C all the radiation is scattered so we expect still softer radiation. At D all the radiation is scattered but it is filtered by the medium itself and so we observe a slight hardening of the beam. Fortunately the biological effect does not vary rapidly with the quality of the beam in the standard therapy region so that the effect of the variation of quality within the scattering medium is not too important clinically.

REFERENCES

1. Adams, G. D., Almy, G. M., Dancoff, S. M., Hanson, A. O., Kerst, D. W., Koch, H. W., Lanzl, E. F., Lanzl, L. H., Laughlin, J. S., Quastler, H., Riesen, D. E., Robinson, C. S. and Skaggs, L. S.: *Am. J. Roentgenol.*, 60:153, 1948.
2. Clarkson, J. R. and Mayneord, W. V.: *Brit. J. Radiol.*, 12:168, 1939.
3. Johns, H. E., Darby, E. K., Haslam, R. N. H., Katz, L., and Harrington, E. L.: *Am. J. Roentgenol.*, 62:257, 1949.
4. Mayneord, W. V. and Lamerton, L. F.: *Brit. J. Radiol.*, 14:255, 1941.
5. Thoraecus, R.: *Acta radiol.*, Supplement 15, 1932.

Chapter VI

THE INTERACTION OF X-RAYS WITH A SCATTERING MEDIUM

6.01

PHANTOMS

WHEN a patient is placed in an x-ray beam of known quality and intensity, the x-rays will be absorbed and scattered and both the quality of the beam and the intensity will be changed. To study such changes experiments have been carried out using phantoms to replace the patient. The phantom should be of such material that it will act on the x-rays in the same way as tissue. Water and wet tissue absorb x-rays in almost the same way and for this reason water has been used in many investigations. However, water offers some difficulties, since most thimble ionization chambers will leak electrically when wet. To avoid this difficulty different types of dry pressedwood phantoms have been used. These can be formed of the desired thickness by piling up layers of the material and the ionization chamber may be inserted into the phantom by providing a small cavity in one of the layers. However, pressedwood takes many different forms and often does not too closely parallel tissue in its absorption of x-rays. Spiers (25) has shown that the phantom material should have the same density as tissue and the same number of electrons per gm. He has found that a mixture of 60% rice flour and 40% sodium bicarbonate make an excellent dry phantom. However, for many purposes a water phantom is the most satisfactory. The ionization within a phantom or on its surface may be measured using an extrapolation chamber (2) or by means of a small thimble ionization chamber (3, 4, 5, 7, 13, 26). Devices have been developed for moving the detecting probe by remote control through a water phantom and of measuring the ionization at a number of points (8).

6.02

SURFACE BACKSCATTER

In section 4.06 the method by which the output of an x-ray machine could be measured was described. This output expressed in roentgens per minute and represented by D_a gives the dosage rate at the end of the treatment cone in air. If the beam of x-rays is directed against

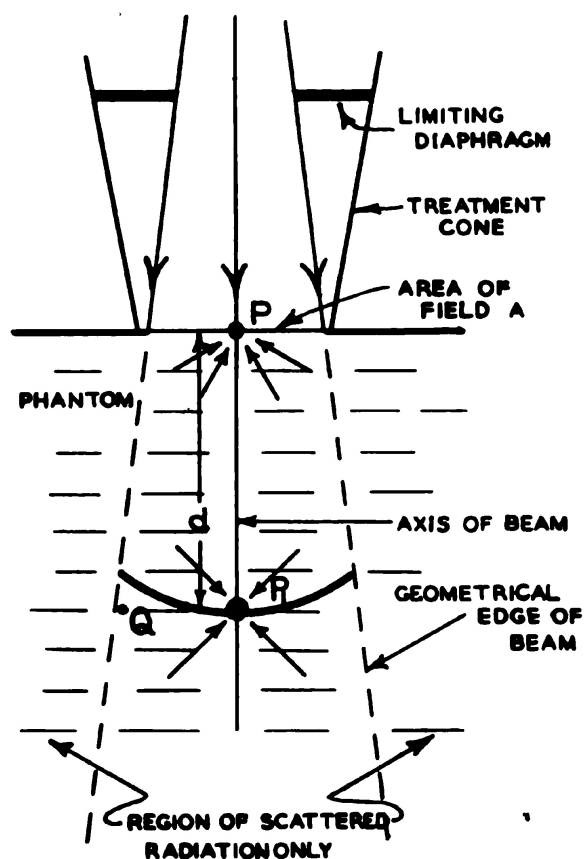


Figure VI-1. Sketch of treatment cone and phantom showing how the scattered radiation increases the dosage rate at the end of the treatment cone and at a depth "d" below the surface.

a patient the dosage rate at the skin will be increased by the x-rays which are scattered to the detector by the patient (Fig. VI-1). The output of the machine under these circumstances is referred to as the output with backscatter and will be represented by D_s . The percentage increase in the dosage rate, called the percentage backscatter P , is given by:

$$P = \frac{D_s - D_a}{D_a} \cdot 100 \quad (6-1)$$

It is usual to measure D_a , the output of a machine in air, and then calculate the dosage rate with backscatter D_s from a knowledge of the percentage backscatter. For example, suppose the output of an x-ray machine in air is 30 r/min. and the percentage backscatter is known to be 20%, then the output with backscatter or the dosage rate at the skin will be 36 r/min. Experiment shows that the percentage backscatter depends on the quality of the radiation, the area A of the

field, the depth of the scattering material, and to a small extent on the nature of the end of the treatment cone. It does not depend on the focal skin distance (F.S.D.). The percentage backscatter increases as the thickness of the material underlying P (Fig. VI-1) is increased but very nearly reaches its full value for layers of underlying material of the order of 10 cm. Since for most positions of treatment the patient supplies at least this thickness of scattering material the dependence on this factor usually need not be considered. Correction for the effect can be made by the use of Figure VI-2 which has been plotted from data due to Quimby (22). Here the percentage of the maximum surface backscatter is plotted against the thickness of the underlying tissue. The effect depends only slightly upon the area of the field so average values have been plotted in Figure VI-2. It will be seen that the same graph serves to show the variation for half value layers of 0.9 and 1.8 mm. Cu. The effect does not depend greatly on half value layer although it is seen that for soft radiation the maximum backscatter is attained for thinner layers of underlying tissue. The percentage backscatter for a 10×10 field at half value

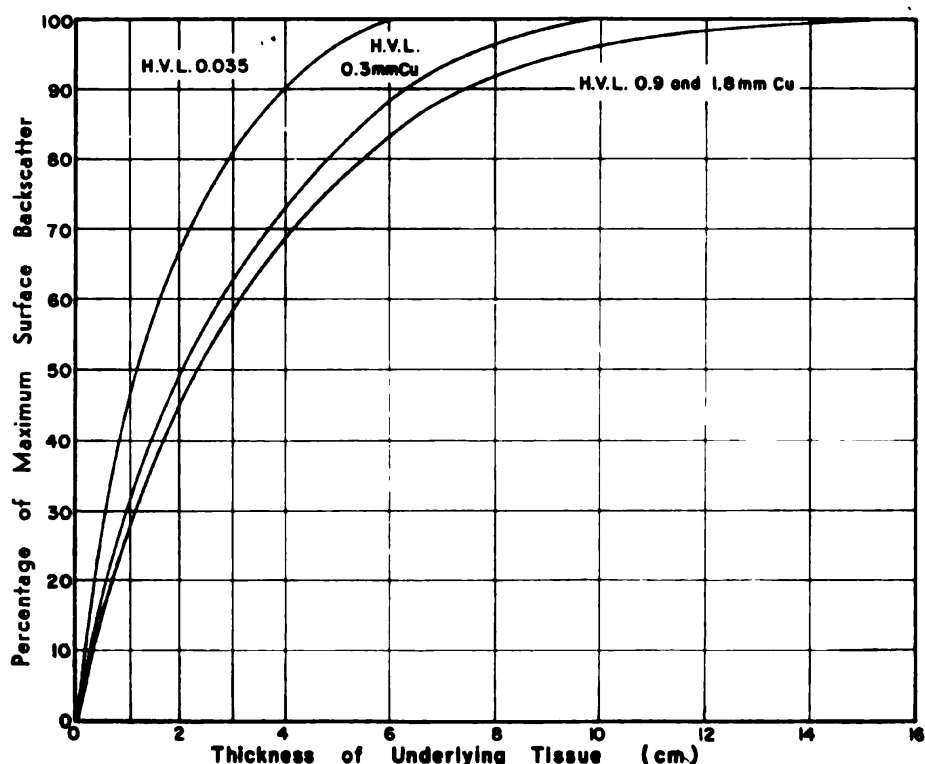


Figure VI-2. Graph showing the variation of the surface backscatter expressed as a percentage of its maximum value. The backscatter depends on the thickness of the underlying tissue. Graphs are presented for qualities of 0.035 mm. Cu., 3.0 mm. Cu. 0.9 mm. Cu. and 1.8 mm. Cu. Data taken from Quimby⁽²²⁾.

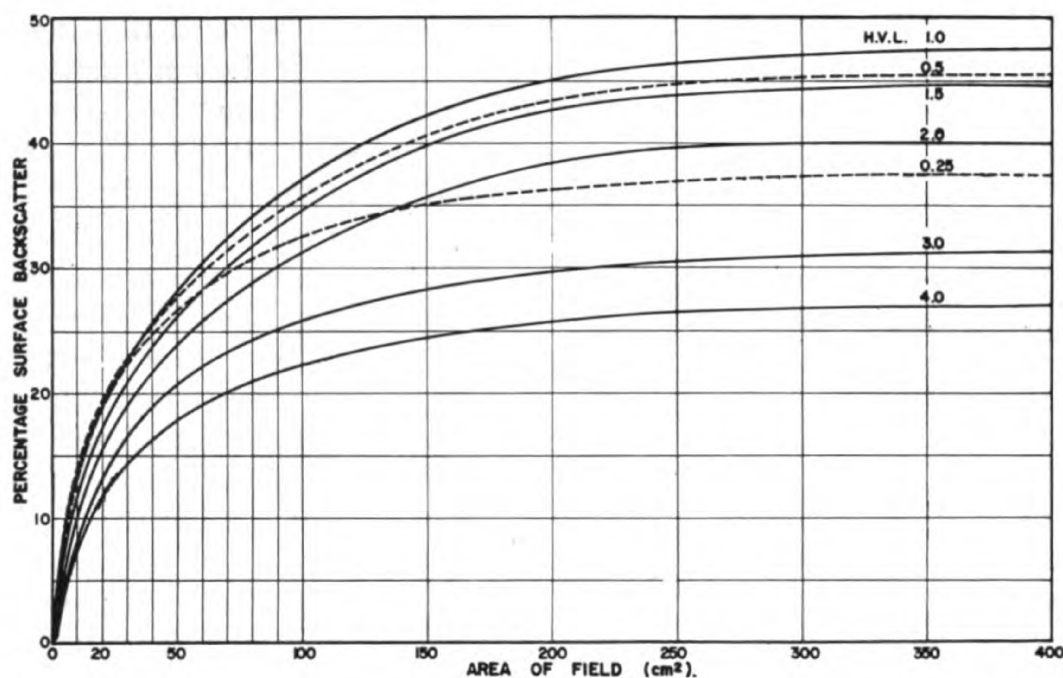


Figure VI-3. Variation of the percentage backscatter with area for half value layers of 0.25, 0.5, 1.0, 1.5, 2.0, 3.0 and 4.0 mm. of copper.

layer 1.0 mm. of copper is 37% (Fig. VI-3) when the tissue is thick enough to give full backscatter. If the underlying tissue is only 6 cm. thick the percentage backscatter is 83% of the maximum value (see Fig. VI-2), i.e., $0.83 (37) = 31\%$. This effect as well as the percentage backscatter depends upon the construction of the end of the treatment cone. This material should be made as thin as possible and be of low atomic number material. For many purposes it is advantageous to dispense with the end altogether. For the details of the effects of the end of the treatment cone reference should be made to Quimby (22). For most purposes the effect introduced by $\frac{1}{8}$ " of bakelite on the end of the cone may be neglected.

As the area of the "field" A is increased, the region around P (Fig. VI-1) which can scatter radiation to P is also increased and so the percentage backscatter increases with area. A typical curve showing the variation of percentage backscatter with area as obtained by the author (10) for a number of qualities of radiation is shown in Figure VI-3. It will be seen that the percentage backscatter increases rapidly with area for small areas but for large areas increases very slowly.

The variation of percentage backscatter with half value layer is much more complicated. At very small H.V.L. the backscatter is zero, it rises rapidly to a maximum at half value layers of about

1.0 mm. of copper and then falls slowly for very large values. This variation is shown graphically in Figure VI-4 for three different areas. Backscatter values for half value layers less than 4.0 mm. of copper

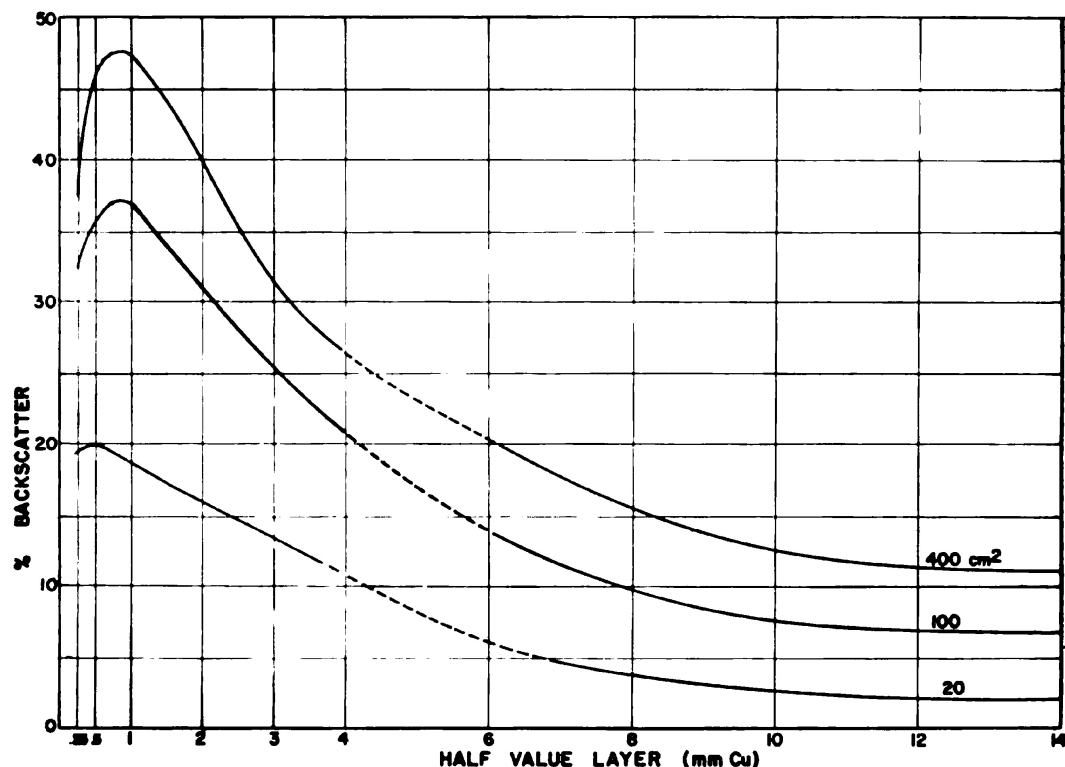


Figure VI-4. Graph showing the variation of the percentage backscatter with half value layer for areas of 20, 100 and 400 cm². (For qualities up to 4.0 mm. of copper⁽¹⁰⁾ for harder radiations Mayneord and Lamerton⁽¹⁶⁾.)

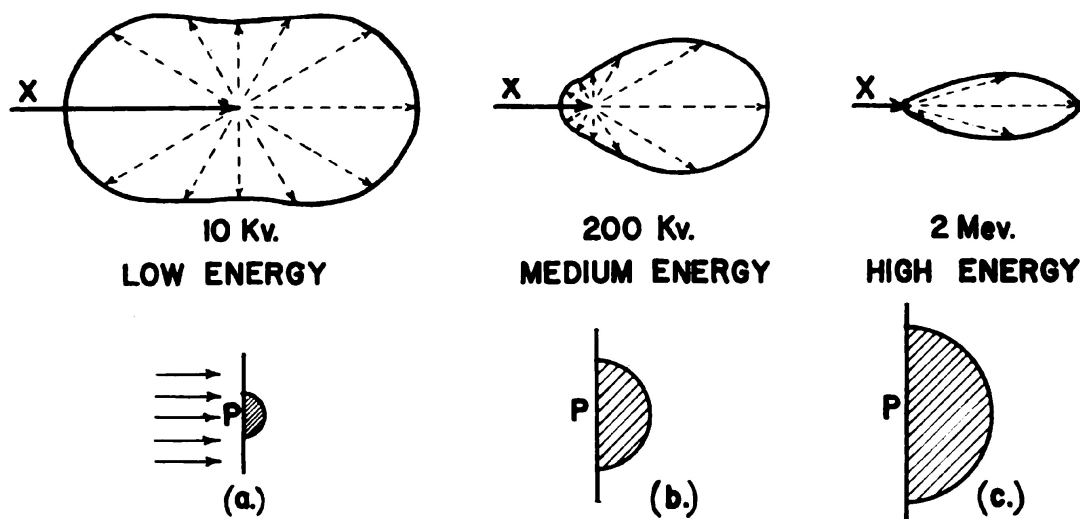


Figure VI-5. Polar diagrams giving the angular distribution of the scattered radiation for three different energies as calculated by the Klein Nishina formula. The shaded regions indicate the relative size of the hemisphere which can effectively scatter radiation back to P.

were obtained by measurement (10) while the values for harder radiation were taken from Mayneord and Lamerton (16). In the region between half value layers of 4 and 6 mm. of copper some difficulty was experienced in joining the two sets of data so in this region the graph has been dotted. This complicated variation of backscatter with quality can be understood by reference to Figure VI-5. At low energies an electron scatters as much energy forward as backward and exactly half as much at right angles. This type of scattering, called classical scattering, is represented in the polar diagram of Figure VI-5a. However, the region which can effectively scatter radiation to P is very small because the soft radiation is quickly absorbed in the medium. The backscatter for low energy x-rays will thus be small. At medium energies (Fig. VI-5b) more x-rays are scattered forward than backward but the effect is not too pronounced. The region which can effectively scatter to P is now much greater and maximum backscatter is obtained. At high energies (Fig. VI-5c) almost all the energy is scattered forward and even though a very large region is available for scatter to P the amount scattered back is relatively small.

The results of backscatter measurements as recorded by different experimenters do not agree too well (compare 10, 16, 12). The accurate measurement of backscatter requires considerable care. The thimble chamber must have the correct wavelength response and must fit snugly into the phantom surface. The stem of certain types of ionization chambers will cut off some of the scattered radiation to the chamber. Mabbs (15) has shown that as high as 30% of the scattered radiation may be cut off by this effect when the 100 r Victoreen chamber is used for measuring backscatter. He has also shown that the phantom material can have a large influence on measurements of backscatter. Most tables give the percentage backscatter as a function of the area of the field. It also depends on the shape of the field. An elongated rectangle will give a smaller backscatter than a square field of the same area. In an elongated rectangle much of the backscattering material is situated so far from the centre of the field as to scatter very little to the central point. Corrections for elongation have been determined by Jones (12). Some of his results are shown graphically in Figure VI-6. Here the corrections to be applied to the surface backscatter for rectangular areas are plotted for a number of elongation factors. For example, suppose the percentage backscatter from a 20×5 field is required at half value layer 1.5 mm. cu. In this case the area is 100 cm.² and the elongation factor

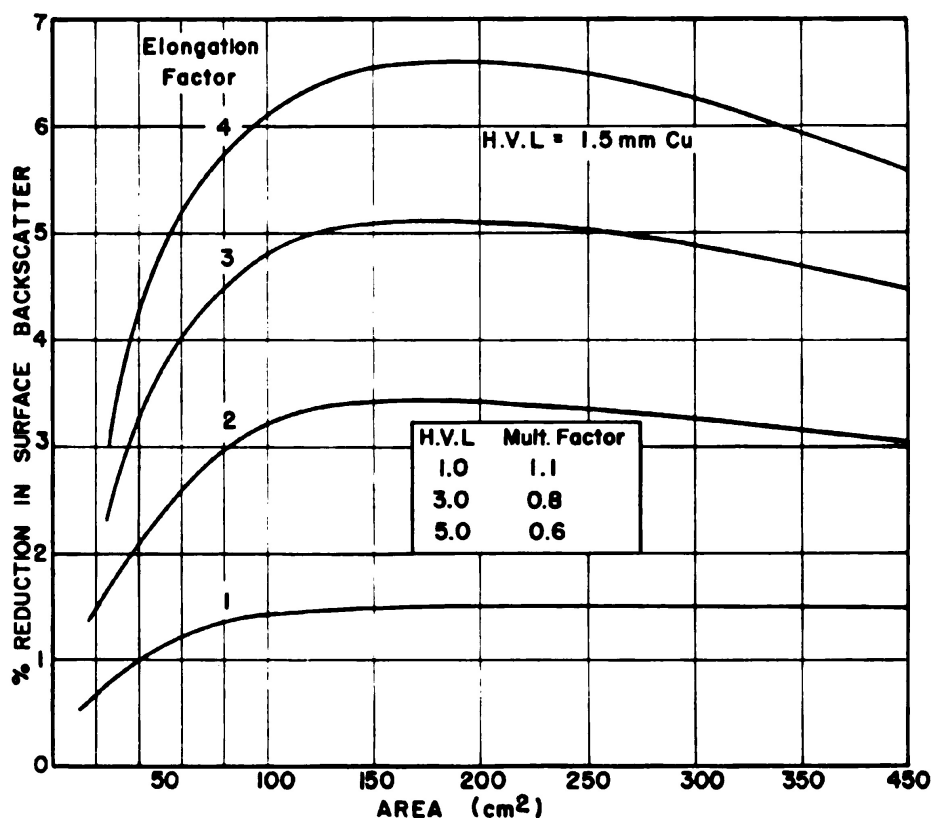


Figure VI-6. Graph showing corrections to the percentage backscatter for rectangular areas for elongation factors of 1, 2, 3, 4. The elongation factor is defined as the ratio of the longer axis to the shorter axis of the rectangle. The graph applies to a half value layer of 1.5 mm. of copper. The insert to the graph enables corrections to be made for other qualities of radiation. The graph is based on data by Jones ⁽¹²⁾.

4. The percentage backscatter of this rectangular field is 6% (Fig. VI-6) less than a square field of area 100 cm.². For radiation with half value layer 5.0 mm. of copper the reduction is 0.6 (6%) or 3.6%. Backscatter no doubt depends slightly on the particular arrangement of the treatment cone, the type of end to the treatment cone and other physical factors which are difficult to control.

Percentage surface backscatter values are given in Table A-1 of the Appendix.

6.03

PERCENTAGE DEPTH DOSE

If the dose D_d is measured at a distance "d" below the surface of the phantom (Fig. VI-1) it will, in general, be different from the dose on the surface. The percentage depth dose is defined as the ratio $(D_d/D_s) \cdot 100$ where D_s is the skin dose at P. Experiment shows that the depth dose depends upon the half value layer, the area of the field, the focal skin distance and the depth below the surface. In

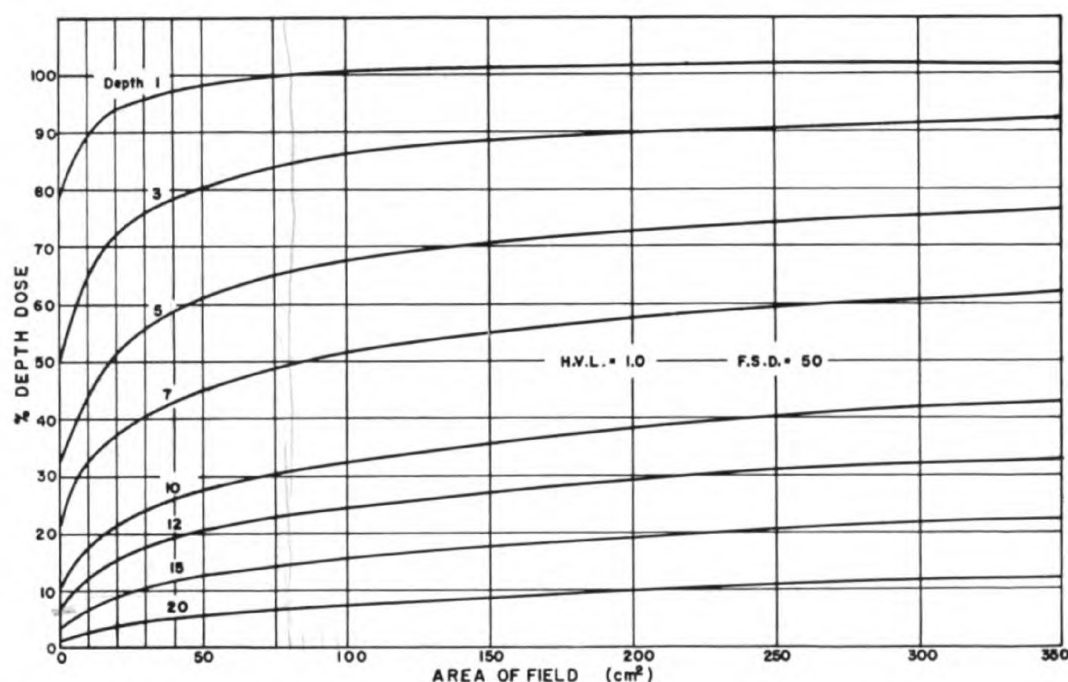


Figure VI-7. Graph showing the variation of the percentage depth dose with area for depths of 1, 3, 5, 7, 10, 12, 15, and 20 cm. H.V.L. 1.0 mm. Cu., F.S.D. 50 cm.⁽¹⁰⁾.

what follows, the symbol ${}^h(D_d)_A^f$ introduced originally by Mayneord (16) will be used to represent the depth dose at depth "d" when the area of the field is A, the focal skin distance f and the half value layer "h." In general there is considerable variation between the results obtained by different workers due to the use of a variety of phantom materials, and different types of ionization chambers. Much of the discussion here is based on an excellent paper on depth dose by Mayneord and Lamerton (16). However, there is some recent experimental evidence by Oliver (20) to indicate that Mayneord and Lamerton's values may be too high. For one standard quality of radiation Oliver obtains values lower than Mayneord and higher than those given by the extensive tables of Quimby (22). As in the case of backscatter factors there is little doubt but that the depth dose depends upon a number of different physical factors which are hard to control precisely. The depth dose data presented here and in the appendix are based on a comprehensive experimental survey by the author (10).

6.04 THE VARIATION OF PERCENTAGE DEPTH DOSE WITH AREA

When the area of the field is very small the dose D_d received at a point below the surface is due entirely to the primary radiation since

the volume which can scatter radiation to P_1 is very small (Fig. VI-1). As the area of the field is increased D_d will increase due to the radiation scattered from the increased volume. The percentage depth dose (D_d) increases rapidly with area at first and then much more slowly as the area is further increased. This variation as measured by the author (10) in a water phantom is shown in Figures VI-7, VI-8, and VI-9 for half value layer 1.0, 2.0 and 4.0 mm. of copper and 50 cm. F.S.D. Results are shown for depths of 1, 3, 5, 7, 10, 12, 15 and 20 cm. It will be seen that (D_d) increases much more as the area is increased from 0 to 100 cm.² than it does in going from 200 to 300 cm.².

The percentage depth dose also depends on the shape of the field. In an elongated field there will be a smaller contribution to the depth dose by scattered radiation. Jones (12) has shown that this can be corrected for by considering that the area of an elongated field is equivalent to a smaller square field. For example, the area of a 20×5 field (elongation 4) should be reduced by a factor 0.6 to 60 cm.² for purposes of depth dose calculation.

6.05 THE VARIATION OF PERCENTAGE DEPTH DOSE WITH DEPTH

In Figure VI-10 is shown the variation of the relative intensity of radiation as one proceeds to a depth of 16 mm. below the surface

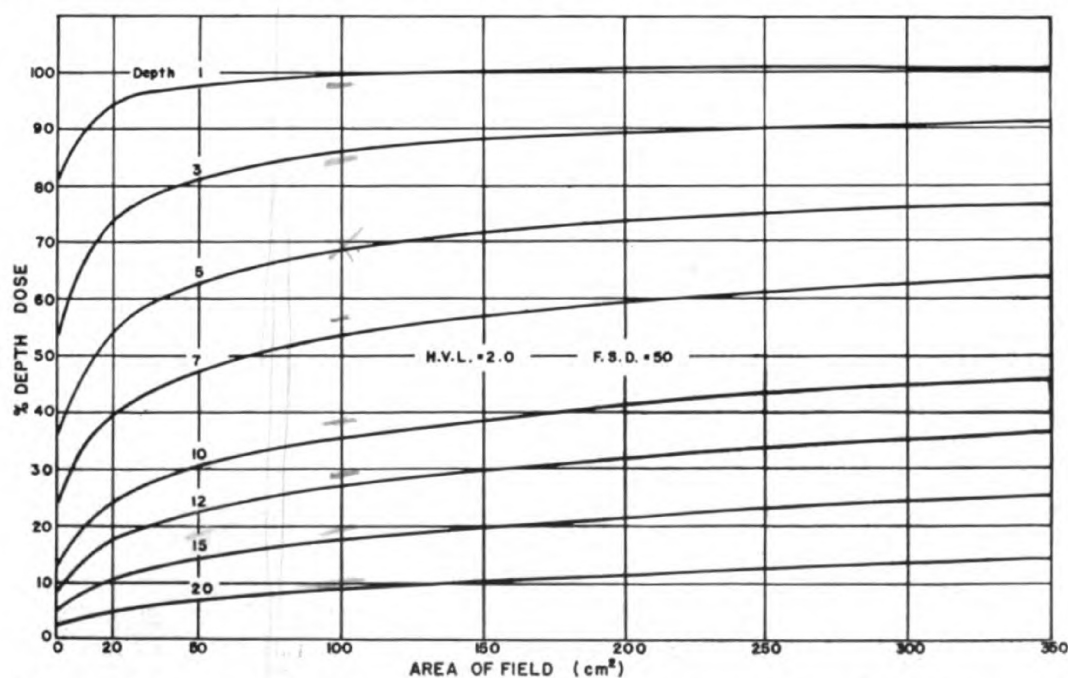


Figure VI-8. Graph showing the variation of the percentage depth dose with area for depths of 1, 3, 5, 7, 10, 12, 15 and 20 cm. H.V.L. 2.0 mm. Cu., F.S.D. 50 cm. (10).

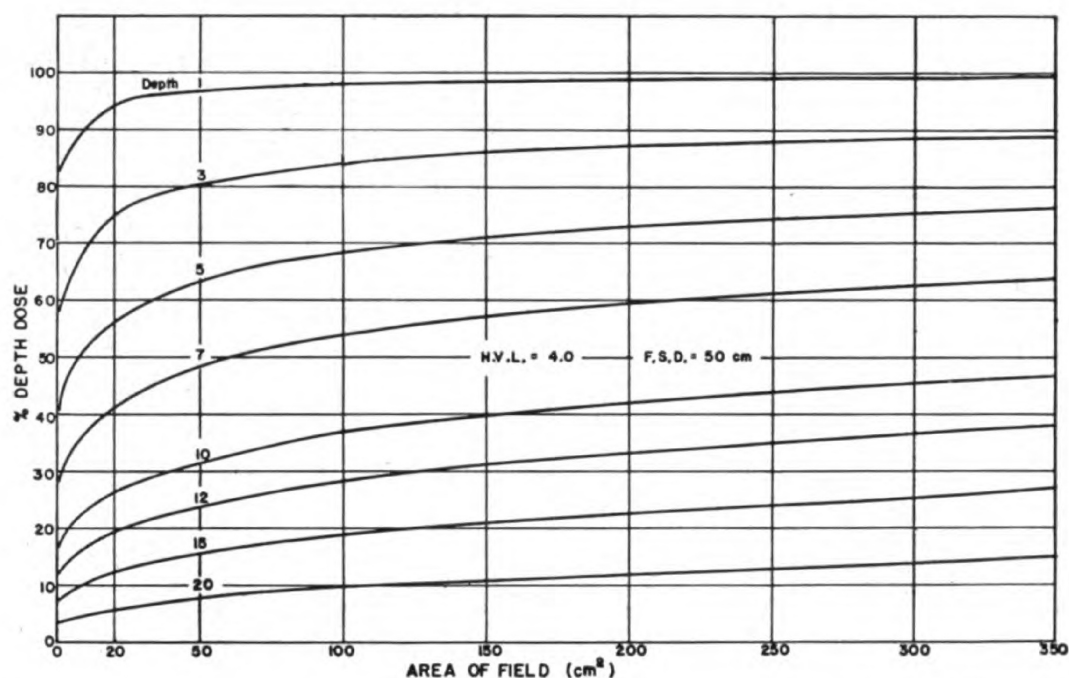


Figure VI-9. Graph showing the variation of the percentage depth dose with area for depths of 1, 3, 5, 7, 10, 12, 15 and 20 cm. H.V.L. 4.0 mm. Cu.; F.S.D. 50 cm.⁽¹⁰⁾.

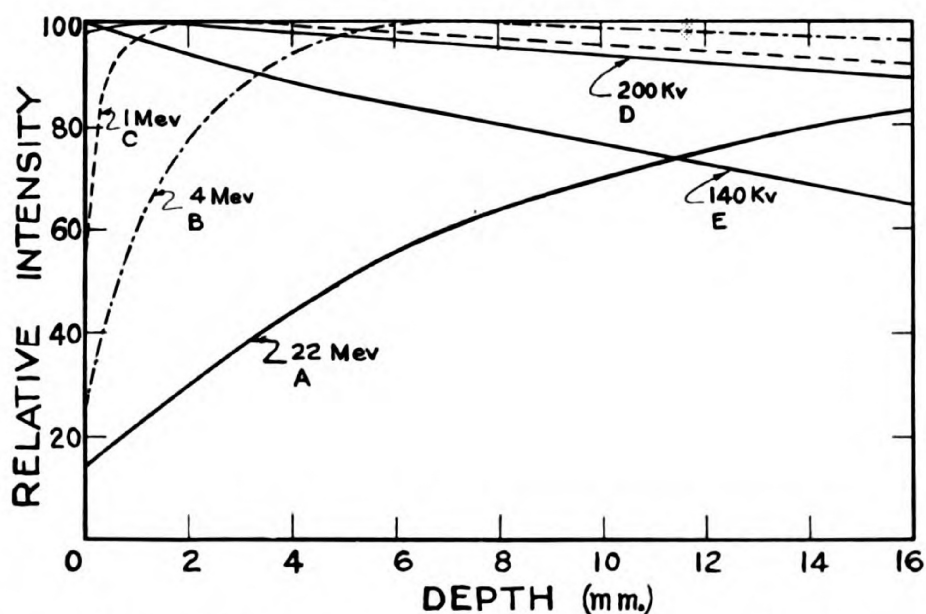


Figure VI-10. Graphs showing the variation of the relative intensity with depth for a number of radiations. A—22 Mev. radiation, 10 x 10, 70 cm. F.S.D., Johns⁽⁸⁾; B—4 Mev. radiation, 10 x 10, 70 cm. F.S.D., Trump⁽²⁷⁾; C—1 Mev. radiation, 10 x 10, 70 cm. F.S.D., Trump⁽²⁷⁾; D—200 Kv., 10 x 10, 70 cm. F.S.D., Trump⁽²⁷⁾; E—5 cm. circular field, F.S.D. — 15 cm., H.V.L. — 2.5 mm. Al.⁽¹⁰⁾.

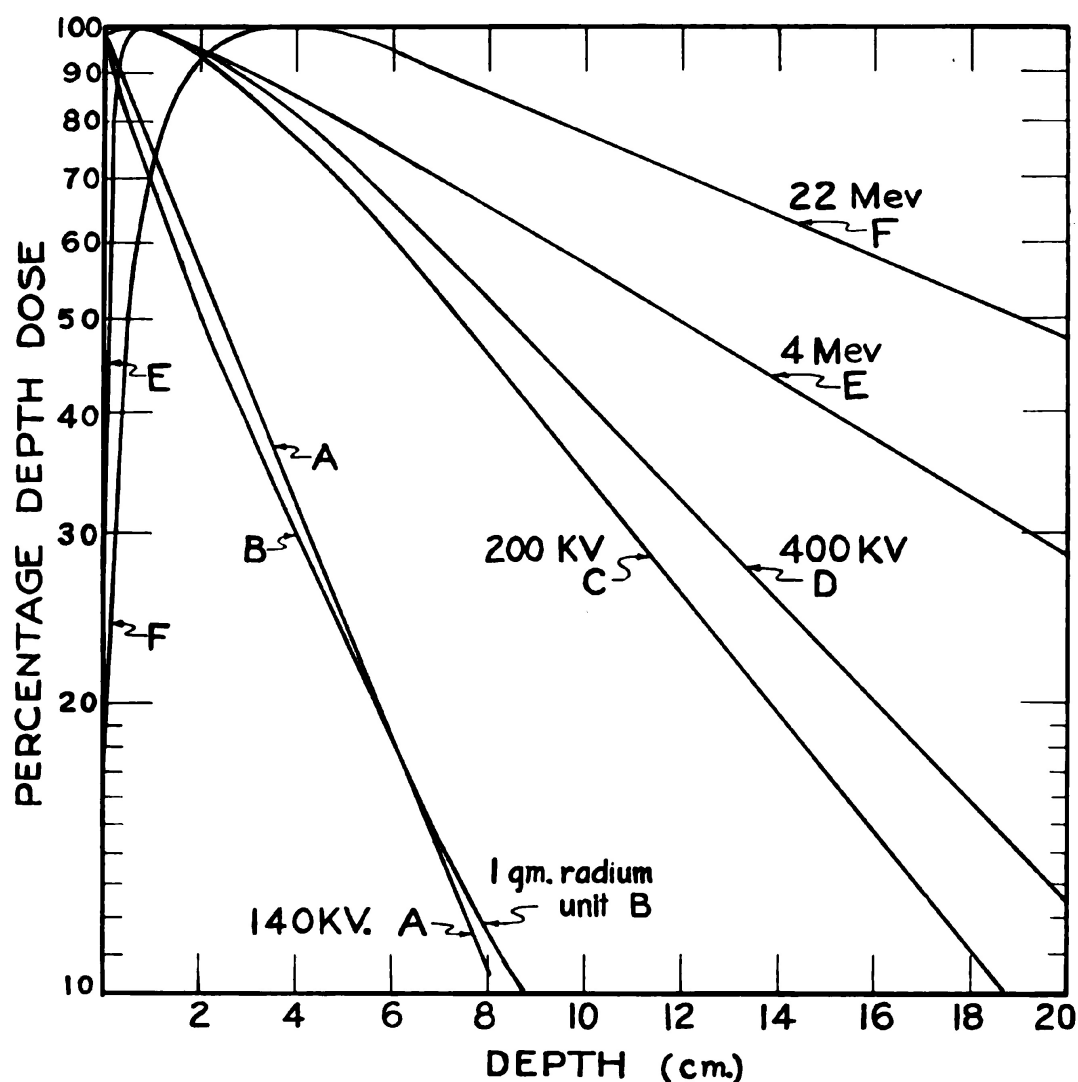


Figure VI-11. Graphs showing the variation of percentage depth dose with depth. A—H.V.L. 3.5 mm. Al., 5 cm. circular field, F.S.D. 15 cm.⁽¹⁰⁾; B—1 gm. radium unit Middlesex Hospital, 5 cm. circular field, F.S.D. 5 cm., Paterson⁽²¹⁾; C—200 Kv., H.V.L. 1.5 mm. Cu., 10 x 10 cm. field, F.S.D. 50 cm.⁽¹⁰⁾; D—400 Kv., H.V.L. 3.6 mm. Cu., 10 x 10 cm. field, F.S.D. 100 cm.⁽¹⁰⁾; E—4 Mev. radiation, filtration 20 mm. Pb. and 5 mm. Cu., 10 x 10 cm. field, F.S.D. 70 cm., Trump⁽²⁷⁾; F—22 Mev. radiation with copper compensating filter, 10 x 10 cm. field, F.S.D. 70 cm., Johns⁽⁸⁾.

of the phantom, for a number of radiations. For low energy radiation (H.V.L. = 2.5 mm. Al, curve E) the intensity falls continuously as one proceeds below the surface. At 200 Kv. the intensity rises slightly for the first millimeter and then falls slowly. For 1 Mev. radiation the intensity rises rapidly from 55% on the surface to a maximum value of 100 at a depth of 2.0 mm. At 4 Mev. this effect is more pronounced and at 22 Mev. the dose rises from a small value on the surface (8) to reach its maximum about 4 cm. below the surface.

Because the intensity at the surface varies very rapidly with depth (for high energy radiation) the dose on the surface which is recorded will depend to a great extent on the construction and the design of the ionization chamber. On the other hand the dose at the maximum does not vary rapidly with depth so that it can be measured easily. For high energy radiation it is convenient to express the dose at a depth "d" as a percentage of the maximum dose and not as a percentage of the skin dose. With this new definition of percentage depth dose, the results shown in Figure VI-10 can be considered as percentage depth dose curves. At 200 Kv. and 400 Kv. this need cause no ambiguity since the maximum dose occurs very near the surface and is the same as the skin dose within one or two percent. In the high energy region the small skin dose is sufficient to account in part at least for the decreased skin erythema (1). However, there is some evidence to indicate that the dose given 2 to 3 mm. below the surface of the skin has more effect on the skin reaction than the dose given the very superficial surface layers (14).

In Figure VI-11 is shown the percentage depth dose which has been obtained by a variety of workers using low, high and very high voltage radiations. The depth doses have been expressed as a percentage of the maximum dose in all cases. Curve A is typical of the depth dose which can be obtained from a reasonably well filtered beam at 140 Kv. The rapid fall in depth dose is due to the small field, the short focal skin distance and the lack of penetrating power of the low energy radiation. The depth dose which can be obtained from a 1 gm. radium unit (B) is very similar to that from the low voltage machine. In this case the small depth dose is not due to the lack of penetrating power of the gamma rays but to the very short focal skin distance. With a 1 gm. telerradium unit the intensity at 5 cm. F.S.D. is about 5 r/min. Because of this small intensity short focal skin distances must be used with their inherent small depth dose. At the present time very strong sources of radioactive cobalt 60 are available which enable one to use focal skin distances of about 80 cm. and thus to obtain a high percentage depth dose (see Chapter XII). Telerradium units have been used in the past because of the nature of energy absorption in tissue at these energies (see Chapter VIII) and not because of the depth dose.

Curves C and D are typical of the depth dose which can be obtained from standard therapy machines operating at 200 Kv. and 400 Kv. respectively. Both show a very slight rise in depth dose for the first few millimeters depth and then an exponential decrease. This

slight increase at a small depth is better illustrated in Figure VI-10. Some radiologists feel that an open ended treatment cone is advantageous at these energies because it brings the point of maximum dose slightly below the surface of the skin. The effect, however, is very slight and in general we can consider that in the standard therapy region the percentage depth dose decreases with depth.

Curves E and F (Fig. VI-11), show the depth dose obtainable using filtered radiation at 4 Mev. (Trump (27)) and compensated betatron radiation at 22 Mev., Johns (8). The maximum dose is now well below the surface and skin reactions can readily be avoided. At 22 Mev. the exit dose of the radiation is greater than the entrance dose. The reason for the rise of depth dose just under the surface of the skin can be seen from considerations of the fundamental processes involved. In Chapter IV it was seen that an ionization chamber required a certain minimum wall thickness to give the maximum response. The maximum dose in the phantom will occur at a depth corresponding to this wall thickness. When the x-ray beam enters the phantom, recoil electrons and electron pairs will be produced and projected primarily in the forward direction. The higher the energy of the beam the greater will be this effect. The average range R of these high speed electrons is considerable, being about 4 cm. at 20 Mev. Some electron tracks will originate at the surface of the phantom and some below the surface but the maximum ionization will occur at a depth R for this will be the place where there are the maximum number of electron tracks crossing each square centimeter. The maximum will be broad because in any x-ray beam there will be photons with all energies up to and including the maximum. When use is being made of this high energy effect, precautions should be taken to prevent the high energy x-ray beam from being contaminated by electrons which emerge from the donut and travel in the direction of the x-ray beam, for these will tend to raise the skin dose without altering the dose at the maximum.

6.06 THE VARIATION OF PERCENTAGE DEPTH DOSE WITH HALF VALUE LAYER

In the last section we saw that as the energy of the x-ray beam is increased, and with it the half value layer, the depth dose in general increases. However, the increase is not as great as one might hope. In Figure VI-12 is shown the variation of the percentage depth dose for the 10 cm. depth for four different areas as the half value layer is increased from 0.25 mm. Cu. to 16 mm. Cu. The graph is based on experimental values by the author (10) for qualities

ies with depth.
se just under the surface
pairs will be produced and
here there are the
the donut and travel in
ue layer is increased from

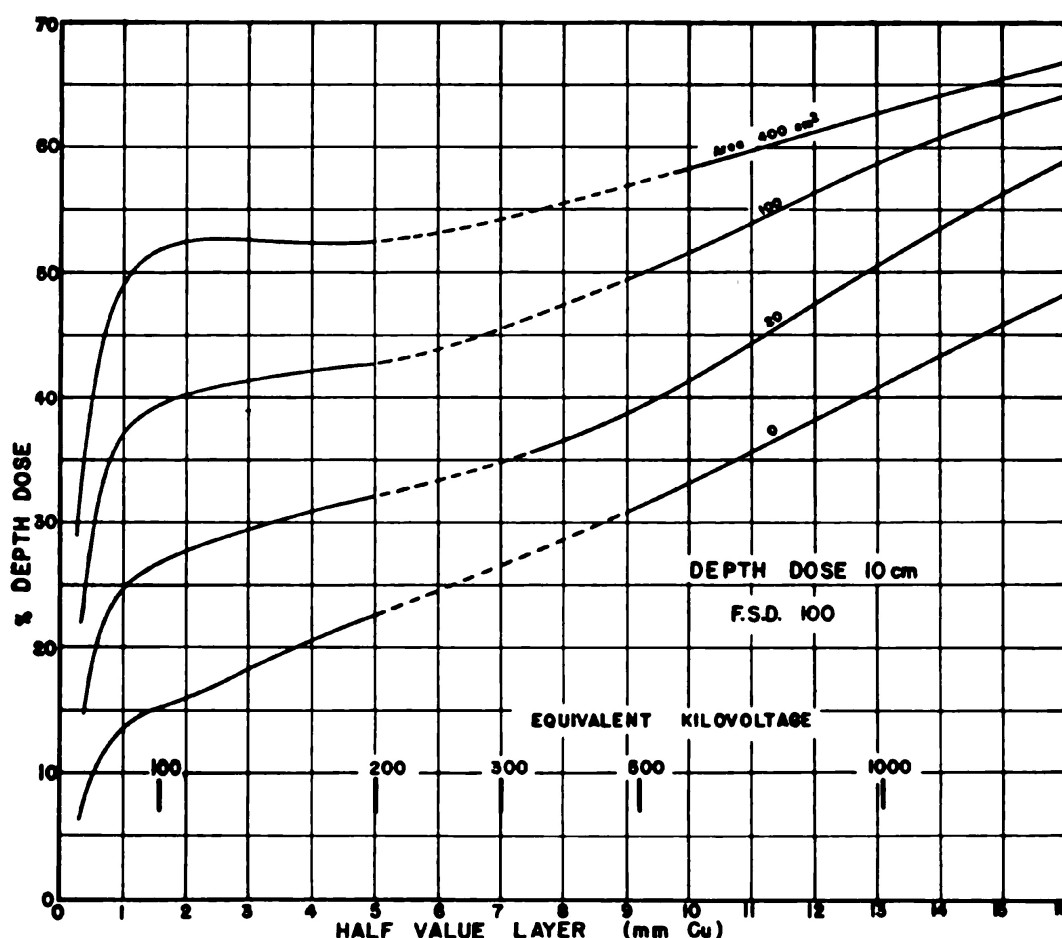


Figure VI-12. Graphs showing the variation of the percentage depth dose with quality for a depth of 10 cm. and F.S.D. 100 cm. Data by the author⁽¹⁰⁾ for qualities up to 4.0 mm. of copper and from Mayneord and Lamerton⁽¹⁶⁾ for the harder radiations.

up to 4.0 mm. Cu. and on Mayneord and Lamerton (16) for the harder radiations. This change in quality corresponds to an increase in equivalent kilovoltage from less than 100 Kv. to about 1500 Kv. (see auxiliary scale of Fig. VI-12). It is seen that the depth dose for the 400 cm.² field only increases from 48 to 67% for a change of quality from 1.0 mm. Cu. to 16 mm. Cu. The improvement of the depth dose for the 20 cm.² field is much better since it increases from 24.5% to 61%. When primary radiation alone is considered (i.e., a very small field) the improvement of depth dose with increase in half value layer is even better (14% to 48.5%). It follows then that the full advantage of a high voltage x-ray machine can be attained only with the use of small fields. There have been statements made to the effect that no advantage is to be gained in using a 400 Kv. machine over a 200 Kv. machine. This is very nearly true when large treatment fields are used because the depth doses are very similar,

but is not true when small fields are used. Examination of Figure VI-12 shows that as the energy is increased the depth dose curves for 0, 20, 100 and 400 cm.² tend to approach one another. If the energy is raised to 22 Mev. it is found that the depth doses obtainable from the three fields (20 cm.², 100 cm.² and 400 cm.²) approach a common value of 82.5% (8). At low energies a large field gives a higher depth dose than a small one but at high energies all sized fields tend to give nearly the same depth dose because the scattering now occurs only in the forward direction.

6.07 THE VARIATION OF PERCENTAGE DEPTH DOSE WITH FOCAL SKIN DISTANCE

The focal skin distance (F.S.D.) has a great effect on the percentage depth dose when the F.S.D. is about the same length as the depth d . In Figure VI-11 is shown the depth dose which is obtained from a 1 gm. radium unit working at an F.S.D. of 5 cm. If one considers a point 5 cm. below the surface of the phantom, then by the

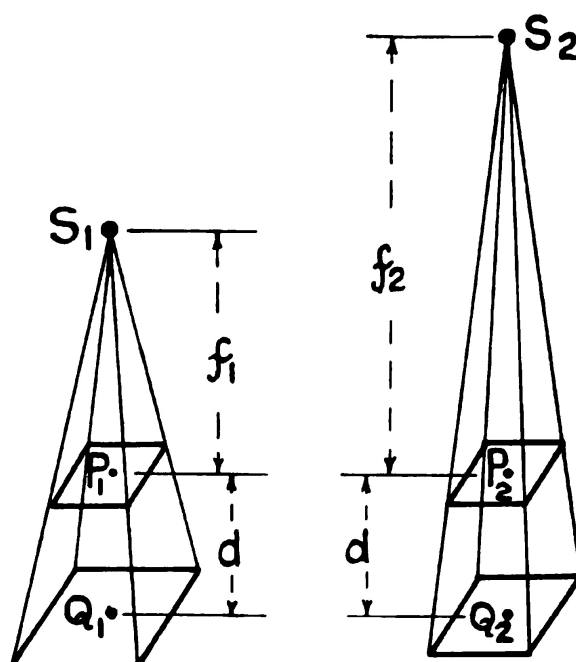


Figure VI-13. Diagram illustrating the dependence of the percentage depth dose on the focal skin distance.

inverse square law the dosage rate is only $\frac{1}{4}$ as great and the percentage depth dose should be 25%. Since the radium source is not a point source, the dosage rate would not decrease as rapidly as the inverse square law would indicate and the 5 cm. depth dose would be somewhat greater than 25%. From Figure VI-11, Curve B, we see

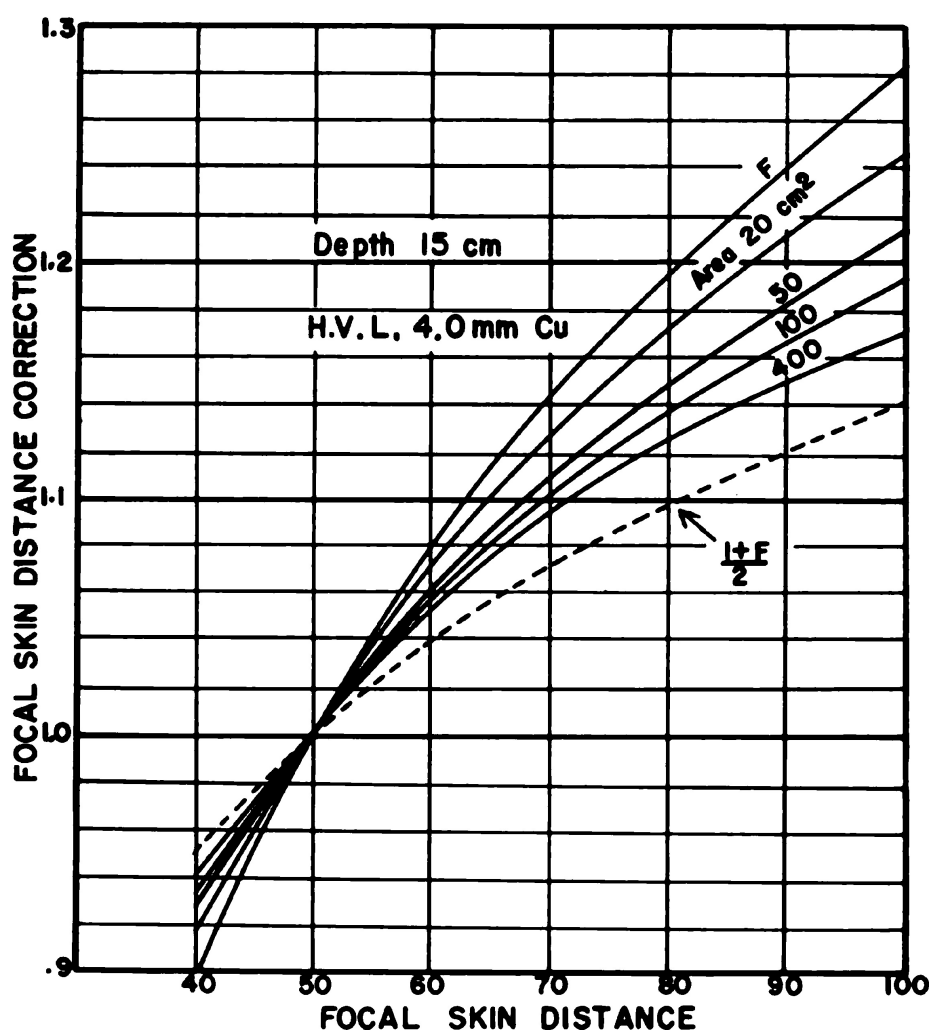


Figure VI-14. Graph showing the corrections to be used to obtain the depth dose at ~~one~~ focal skin distance when the depth dose at 50 cm. F.S.D. is known. The graphs are plotted for a depth of 15 cm. and for H.V.L. 4.0 mm. of Cu⁽¹⁰⁾. The correction depends upon the area of the field. For very small fields the correction is given by the F factor, for very large fields approximately by $\frac{1+F}{2}$.

the actual depth dose is 23%. The difference is due to the absorption of the gamma rays by the phantom. If the treatment distance were increased to 10 cm., then the 5 cm. depth dose would approach $(10/15)^2$ or 44%. However, the dosage rate at the patient's skin would now be $\frac{1}{4}$ its former value and the use of the unit in this way would be impractical. *If a high depth dose is required at a depth d , it is necessary that the F.S.D. be large compared with d .* In usual therapeutic ranges the F.S.D. is more important in determining depth dose than is the quality of the radiation.

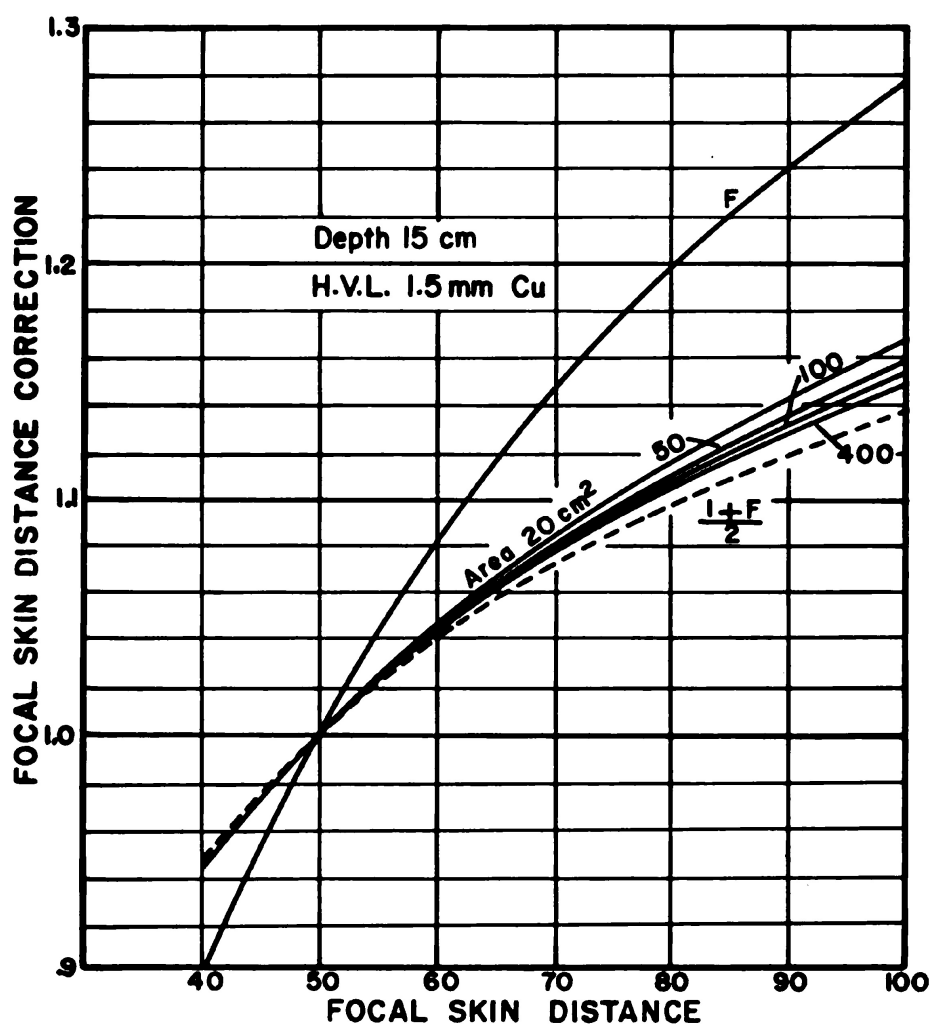


Figure VI-15. Graph showing the corrections to be used to obtain the depth dose at one focal skin distance when the depth dose at 50 cm. F.S.D. is known. The graphs are plotted for a depth of 15 cm. and for a H.V.L. of 1.5 mm. of Cu.⁽¹⁰⁾. The correction depends upon the area of the field. For areas from 20 to 400 cm² the correction is nearly given by the $\frac{1+F}{2}$ factor.

Under certain circumstances, it is important to know what improvement in depth dose can be obtained by increasing the focal skin distance from f_1 to f_2 keeping the depth "d" below the surface constant. Suppose S_1 and S_2 Figure VI-13 represent the focal spots of two tubes f_1 and f_2 cm. from the phantom surface. If there were no absorption of the x-rays in the phantom, the percentage depth doses $(D_d)^{f_1}$ and $(D_d)^{f_2}$ would be given by $(D_d)^{f_1} = \text{dose at } Q_1 / \text{dose at } P_1 = f_1^2 / (f_1 + d)^2$ and $(D_d)^{f_2} = \text{dose at } Q_2 / \text{dose at } P_2 = f_2^2 / (f_2 + d)^2$ respectively.

The ratio of the two depth doses has been called the F factor by Mayneord¹⁰ and is given by

$$F = \frac{(D_d)^{f_2}}{(D_d)^{f_1}} = \left(\frac{f_1 + d}{f_2 + d} \cdot \frac{f_2}{f_1} \right)^2 \quad (6-2)$$

For example, it might be required to know what improvement in percentage depth dose at 10 cm. depth could be expected by increasing the F.S.D. from 50 cm. to 70 cm. Using equation (6-2) we obtain

$$F = \left[\frac{(50 + 10)}{(70 + 10)} \cdot \frac{70}{50} \right]^2 = 1.10. \text{ This means we might expect a 10\%}$$

increase in depth dose. If the depth dose for $f = 50$ cm. were 30%, the depth dose for $f = 70$ cm. would be 33%. This theory is based on the assumption that the depth dose is due to primary radiation alone, whereas especially for low energy radiation and large areas, scattered radiation makes a very large contribution to the depth dose. Mayneord¹⁶ has found that the conversion from one F.S.D. to another is more accurately made by using the factor $(1 + F)/2$. In the above example this would mean the percentage depth dose would be increased by only 5% (from 30 to 31.5). Quimby,²³ on the other hand, feels that conversion from one F.S.D. to another can be carried out using the inverse square law (i.e., the F factor). The author has made measurements for several values of the F.S.D. using 200 Kv. and 400 Kv. equipment and finds that the correction from one F.S.D. to another is never as great as one would predict using the F factor except for very small fields. This is illustrated by Figure VI-14, where the measured conversion factor from one focal skin distance to another is plotted against the focal skin distance. This is done for H.V.L. 4.0 mm.Cu. and areas of 400, 100, 50, 20 and 0 cm.². The zero area corresponds exactly with the F factor since for this area primary radiation alone is present and the inverse square law must apply. On Figure VI-14 is shown the $(1 + F)/2$ factor and it will be seen that the corrections lie between the F and the $(1 + F)/2$ factor.

In Figure VI-15 is given the measured conversion factors for a depth of 15 cm. for radiation of half value layer 1.5 mm. of copper. Curves are given for areas of 20, 50, 100 and 400 cm.². It will be seen that the correction factors are much more nearly the same for all the areas considered than was the case for the harder radiation of Figure VI-14. The conversion factors as before lie between the F and the $(1 + F)/2$ factor, but they are now closer to the $(1 + F)/2$ curve.

It is evident from these two examples that the conversion factor depends in a complicated way on the area of the field and the quality

of the radiation. However, experiments show that the general trend is somewhat as follows. As the radiation is made harder the correction factors are found to depend more on the area of the field. For radiations with H.V.L. from 0.5 to 2.0 mm. of copper the corrections do not vary much, as the area of the field is changed from 20 to 400 cm.² Experiment has shown also that the variation with half value layer is not great in the range from 0.5 mm. Cu. to 2.0 mm. Cu. For these reasons average values for the correction factor have been determined and are given in Figure VI-16. These were obtained from the

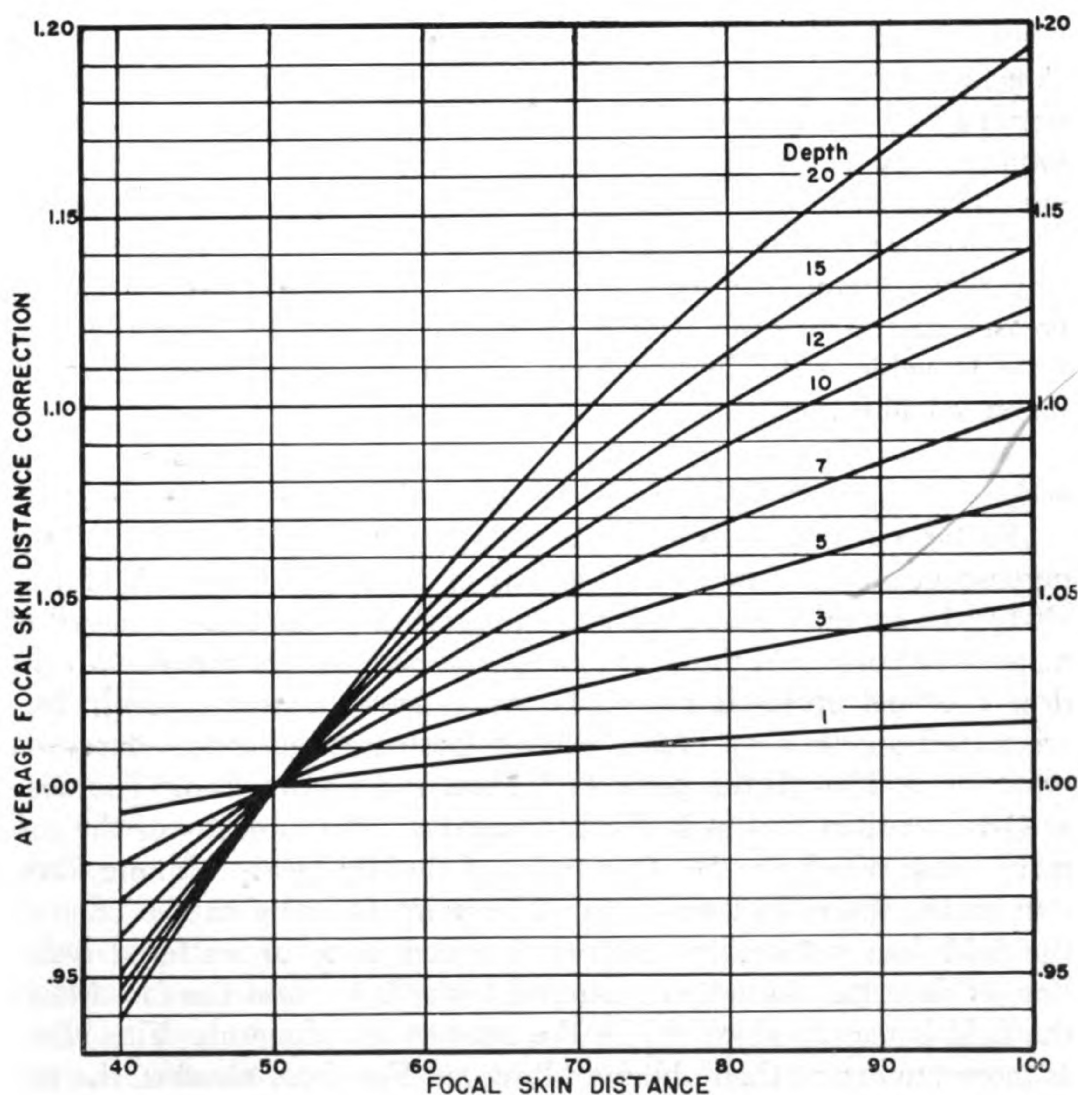


Figure VI-16. Average corrections to be used to convert from one F.S. D. to another for depths of 1, 3, 5, 7, 10, 12, 15 and 20 cm. The corrections are approximately correct for qualities from 0.5 to 2.0 mm. of Cu. and for areas in the range from 20 cm.² to 400 cm.². The actual corrections depend on area and quality as illustrated in Figures VI-14 and VI-15. The average corrections given in VI-16 are correct to about 1.5%.

measured values by averaging the corrections for areas of 20, 50, 100 and 400 cm.² and half value layers of 0.5, 1.0, 1.5 and 2.0 mm. of copper. These corrections should not in general be out more than 1.0 to 1.5% from the measured values given in the appendix. In all cases the corrections lie between the F factor and the $(1 + F)/2$ factor but closer to the $(1 + F)/2$ factor. Since the effect is complicated it is better to take depth dose data from tables rather than to correct from one F.S.D. to another. Depth dose data for focal skin distances of 40, 50, 60, 80 and 100 cm. are given in the Appendix.

The choice of a suitable F.S.D. is determined partially from economic considerations. For example, we see that the average conversion factor from 50 to 70 cm. F.S.D. as given in Figure VI-16 for a depth of 10 cm. is 1.066. This means the 10 cm. depth dose can be improved by 6.6% if the focal skin distance is increased from 50 to 70 cm. The dosage rate at the larger focal skin distance is reduced to $(50/70)^2$ or 0.5 of its original value. The radiotherapist may feel that this slight increase in depth dose does not justify the greatly increased treatment time. Under certain circumstances, it may be possible to achieve the higher depth dose more economically through increased filtration.

6.08 ISODOSE CURVES AND SURFACES

So far we have confined our attention to measurements of the percentage depth dose along the axis of the beam (i.e., PP₁ of Fig. VI-1). In actual treatment we are interested in the dose received at many other points in the phantom. These may be compared with the dose received at P. If all points which have the same depth dose are joined together we obtain what is known as an isodose curve. A typical one through the point P₁ is shown in Figure VI-1. The dose at Q is less than that at P₁ for two reasons. The intensity of the primary beam which reaches Q is reduced slightly by the oblique filtration of the filters and phantom. The point Q being at the edge of the field does not receive as great a contribution of scattered radiation as does P₁. Radiation scattered towards Q from the far side of the field is mainly absorbed by the intervening phantom. This effect is more important than oblique filtration. For these reasons, the isodose curve must be curved upwards as indicated in Figure VI-1.

For many years there was considerable discussion concerning the nature of the isodose distributions near the geometrical edge of the beam. Meredith and Neary (19) have devised a mathematical method for determining the isodose distributions from the published

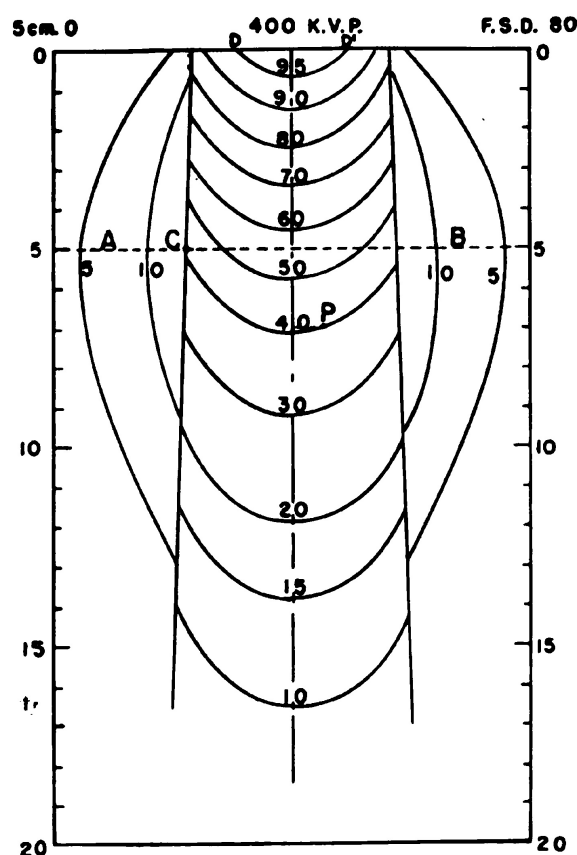


Figure VI-17. Isodose distribution for a 5 cm. circular field at F.S.D. 80 cm., 400 Kv., H.V.L. 4.0 mm. Cu.⁽¹⁰⁾.

data of the depth dose along the axis as determined by Mayneord and Lamerton (16). By this method one calculates the primary radiation reaching a point in the scattering medium and to it adds the scattered radiation. In the main beam both are present while outside the geometrical edge of the beam only scattered radiation is present. Distributions obtained by this method show a discontinuity at the edge of the beam. Jones (11) has obtained photographic evidence for this discontinuity, and the author (9) has shown it to exist by the use of a very small ionization chamber. The older distributions which show continuous lines reaching beyond the geometrical shadow are not strictly correct, although for practical radiotherapy the differences have no great significance. A typical distribution which was obtained by measurements using a small ionization chamber with inside diameter 3.1 mm. is shown in Figure VI-17. Such a distribution is obtained by moving the small ionization chamber across the beam at a number of levels and measuring the radiation at a number of points. Consider the motion of such a "probe" along

the line AB of Figure VI-17. When the centre of the chamber is at C half the probe is inside the beam and half outside so that an average reading somewhere between 15 and 43 would be obtained. When the centre of the chamber is 1.5 mm. inside the shadow a reading of 43 will be obtained while when placed 1.5 mm. outside the beam the reading would be greater than 10 and less than 15. It is obvious that the discontinuity will tend to disappear if measurements are made with a large chamber. If the focal spot of the x-ray tube were large and the limiting diaphragm (Fig. VI-1) some distance from the surface of the phantom, there will be no sharp demarkation between the two regions and the discontinuity will disappear.

From Figure VI-17 we see that there is not much scattered radiation using a 5 cm. circular field at 400 Kv. (H.V.L. — 4.0 mm. Cu.). In Figure VI-18 is shown a distribution obtained in the same way for the short axis of a 15×6 rectangular field (200 Kv., H.V.L. — 1.4 mm. Cu.). It is seen that radiation scattered outside the field is considerable. This is due in part to the softer radiation and also to the fact that a much larger field (area 80 cm.²) is being investigated. In Figure VI-19 is shown a typical distribution for 22 Mev. betatron

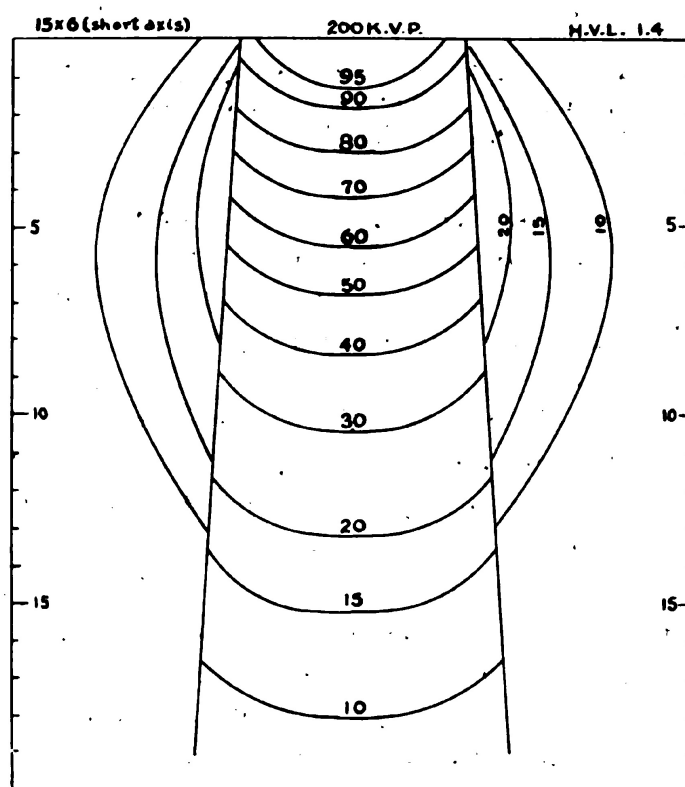


Figure VI-18. Isodose distribution for the short axis of a 15×6 rectangular field, 200 Kv., H.V.L. 1.4 mm. Cu.⁽¹⁰⁾.

radiation filtered by a copper compensating filter. It is seen that the maximum dose is about 4 cm. below the surface of the phantom. Measurements shown in Figure VI-19 were obtained using an ioniza-

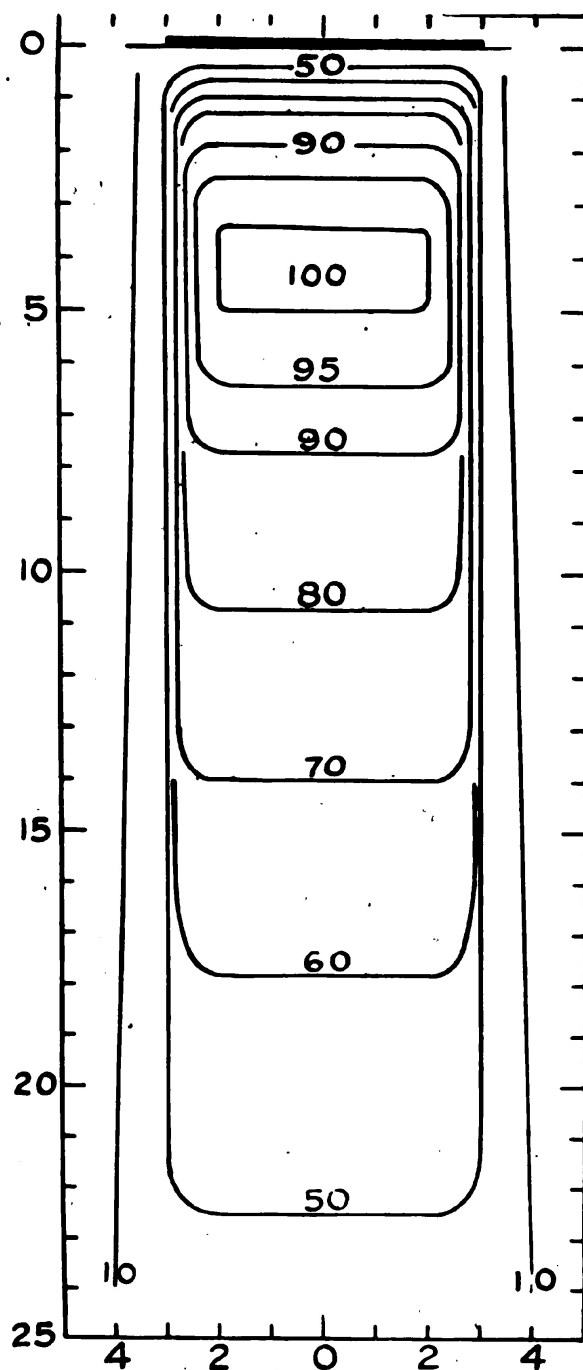


Figure VI-19. Isodose distributions for a 6 cm. circular field at F.S.D. 105 cm. using radiation from a 22 Mev. betatron with a copper compensating filter⁽⁸⁾.

tion chamber 6 mm. in diameter so that some inaccuracies are present at the edges of the beam.

The isodose curves shown in Figures VI-17, VI-18, and VI-19 give the distribution of radiation in a plane containing the axis of the beam. This plane is known as the principal plane. For circular fields, the distribution of radiation in any other plane through the axis will be identical with those shown. Rotation of Figures VI-17 and VI-19 about the axis of the beam will generate surfaces of equal dose known as isodose surfaces. When the field is rectangular (Fig. VI-18) the isodose surfaces are much more complicated. They are often represented by showing the distributions in two sections through the axis at right angles. Mayneord (17) and others have taken photographs of models to show the three dimensional nature of these isodose surfaces. The three dimensional aspects of these surfaces will be discussed in greater detail in the next chapter. Isodose curves for standard fields may be obtained through the Hospital Physicists' Association (6, 24). Distributions for a selected number of standard fields as determined by the author (10) are given in the appendix.

6.09

SUMMARY

Before accurately controlled radiotherapy can be carried out the following measurements and calculations should be made concerning the x-ray machines.

(a) Measure the half value layer of the x-ray beam with different filters and decide which filters should be used to get the half value layer desired.

(b) From this known half value layer obtain backscatter factors for a series of areas from the tables in the appendix or from some other source (6, 15, 16, 22, 23). Plot a graph of percentage backscatter against area and from this graph read off the percentage backscatter factors for the selection of treatment cones which are to be used.

(c) Measure the output of the machine without backscatter. This air dose should be checked for all fields. It will be found that the "air" dose is not the same for all the cones because of slight differences in F.S.D., thickness of the cone ends and the shapes and positions of the limiting diaphragms.

(d) From (b) and (c) calculate the output with backscatter for each of the treatment cones in use. The output with backscatter of course gives the dosage rate on the skin. It is not recommended to base treatments on "dosage in air."

(e) From the known half value layer, F.S.D. and field area obtain the appropriate isodose curves either from the appendix or from a central pool of such data (6) or measure these isodose curves for each of the fields. These isodose curves are the basis for accurately planned radiotherapy.

REFERENCES

1. Dresser, R., Rude, J. C. and Cosman, B. J.: *Radiology*, 34:12, 1940.
2. Failla, G.: *Radiology*, 29:202, 1937.
3. Farmer, F. T.: *Brit. J. Radiol.*, 19:27, 1946.
4. Happey, F.: *Brit. J. Radiol.*, 14:336, 1941.
5. Herbert, R. J.: *Brit. J. Radiol.*, 21:420, 1948.
6. Hospital Physicists Association. *Brit. J. Radiol.*, 23:139, 1950.
7. Johns, H. E., Darby, E. K. and Hamilton, J. J. S.: *Am. J. Roentgenol.*, 51:550, 1949.
8. Johns, H. E., Darby, E. K., Haslam, R. N. H., Katz, L. and Harrington, E. L.: *Am. J. Roentgenol.*, 62:257, 1949.
9. Johns, H. E. and Darby, E. K.: *Brit. J. Radiol.*, 23:193, 1950.
10. Johns, H. E.: Unpublished measurements, and *Brit. J. Radiol.*, 1952.
11. Jones, D. E. A.: *Brit. J. Radiol.*, 15:178, 1942.
12. Jones, D. E. A.: *Brit. J. Radiol.*, 22:342, 1949.
13. Kemp, L. A. W.: *Brit. J. Radiol.*, 18:107, 1945.
14. Klumpar, J.: *Acta Radiol.*, 31:223, 1949.
15. Mabbs, D. V.: *Brit. J. Radiol.*, 22:600, 1949.
16. Mayneord, W. V. and Lamerton, L. F.: *Brit. J. Radiol.*, 14:255, 1941.
17. Mayneord, W. V.: *Brit. J. Radiol.*, 16:291, 1943.
18. Mayneord, W. V.: *Brit. J. Radiol.*, 16:388, 1943.
19. Meredith, W. J. and Neary, G. J.: *Brit. J. Radiol.*, 17:75, 1944.
20. Oliver, R. and Kemp, L. A. W.: *Brit. J. Radiol.*, 22:33, 1949.
21. Paterson, R.: *The Treatment of Malignant Disease by Radium and X-Rays*. London, Arnold, 1948.
22. Quimby, E. H. and Laurence, G. C.: *Radiology*, 35:138, 1940.
23. Quimby, E. H.: *Am. J. Roentgenol.*, 36:343, 1936.
24. Read, J.: *Brit. J. Radiol.*, 18:116, 1945.
25. Spiers, F. W.: *Brit. J. Radiol.*, 16:90, 1943.
26. Spiers, F. W. and Hay, G. A.: *Brit. J. Radiol.*, 19:213, 1946.
27. Trump, J. G. and Cloud, R. W.: *Am. J. Roentgenol.*, 49:531, 1943.

Chapter VII

THE COMBINATION OF X-RAY FIELDS AND THEIR DISTRIBUTIONS IN SPACE

7.01

COPLANAR FIELDS

IN Figure VII-1 is shown the distribution obtained by combining two coplanar circular fields in opposition 12 cm. apart. The method by which this distribution is obtained is also indicated. The distributions of Figure VI-17 are shown in dotted form in Figure VII-1. By joining the points of intersection of appropriate isodose curves the resultant is obtained. For example, the 100% isodose curve is found by joining A (30, 70) B (30, 70) C (20, 80) etc. In the region of the discontinuity at the edge of the beam some difficulty is experienced but the general nature of the isodose curves can be obtained. When it is required to combine more than two coplanar distributions it is usually easier to lay the transparent isodose curves on a sheet of graph paper and read off and tabulate the dose received at lattice points 1 cm. apart. The second field is then laid over the graph page in its proper position and the contributions from this field tabulated. This process is carried out for all the fields and then the total dose for each of the lattice points obtained. These can be marked on the graph paper and by inspection, the position of the isodose curves may be sketched in. This method is more accurate and faster when the combination of several fields is required. Other methods for combining fields using tinted isodose curves have been developed (9). The resultant distributions of Figure VII-1 are shown as heavy lines. It is seen that the dose falls from 115 at the surface to 96 midway between the fields. Along the axis the dose is nearly constant (100 to 96) for more than 4.0 cm. The isodose curves of Figure VII-1 show the distribution in the one plane, whereas in reality we are dealing with a distribution in space. For this case the isodose *surfaces* are produced by rotation of Figure VII-1 about its axis. It will be seen that the dose falls from 96 on the axis to 90 at a point 1.3 cm. from the axis. Thus, although the dose is uniform for a considerable distance along the axis, this is not the case in a plane perpendicular to the axis. Rotation of Figure VII-1 will show that the 90% isodose surface

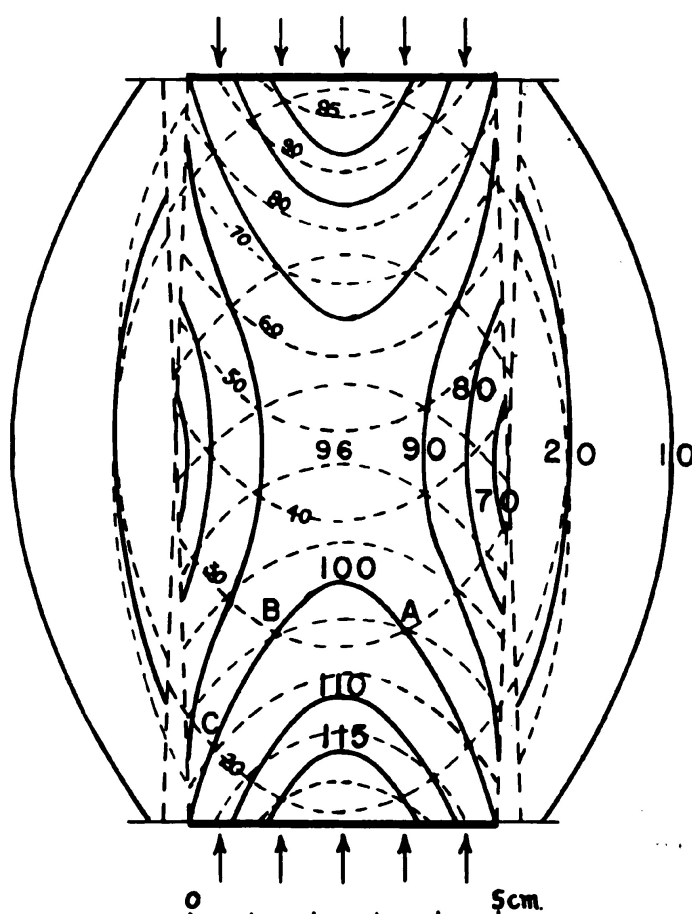


Figure VII-1. Distribution obtained by combining two coplanar 5 cm. circular fields in opposition 12 cm. apart, 400 Kv., H.V.L. 4.0 mm. Cu., F.S.D. 80 cm.

is a cylindrical-like surface whose height is very much greater than its diameter.

In Figure VII-2 is shown the resultant distribution when the same two fields are directed at 80° to one another towards a point P 7.2 cm. below the surface. It will be seen that the maximum dose of 100 does not occur where the axes of the fields intersect (point P) but much nearer the surface. This diagram illustrates the very important principle that when fields are directed through one side of a patient towards a tumor they should be aimed considerably below the tumor. It is seen that in the region where the beams intersect the resultant distribution (heavy lines) appears somewhat like a single field directed midway between the other two but starting below the skin surface. This has been called an internal field (4). From Figure VII-2 we can obtain no direct information concerning the distributions in space. In this case they cannot be obtained by rotation of the diagram about an axis. Methods for dealing with this problem will

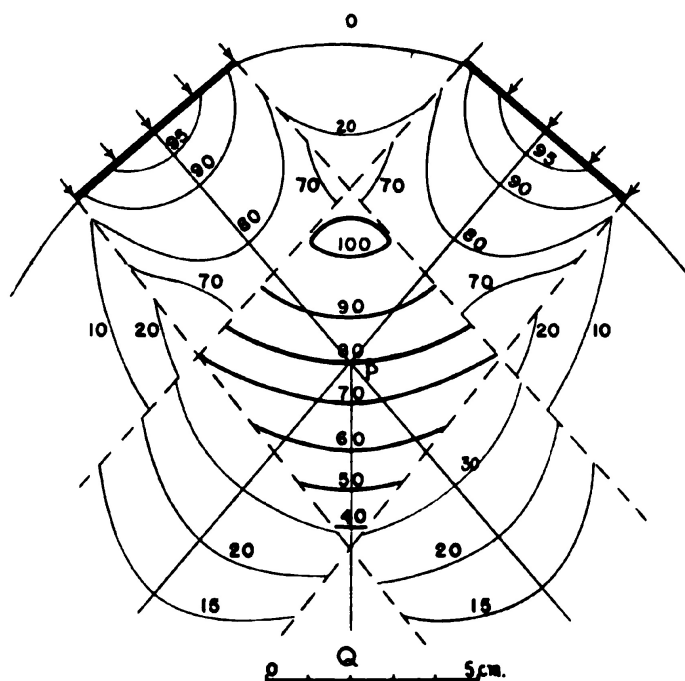


Figure VII-2. Distribution obtained by combining two 5 cm. circular fields making an angle of 80° with one another with their axes intersecting 7.2 cm. from the entrance point. 400 Kv., H.V.L. 4.0 mm. Cu., F.S.D. 80 cm.

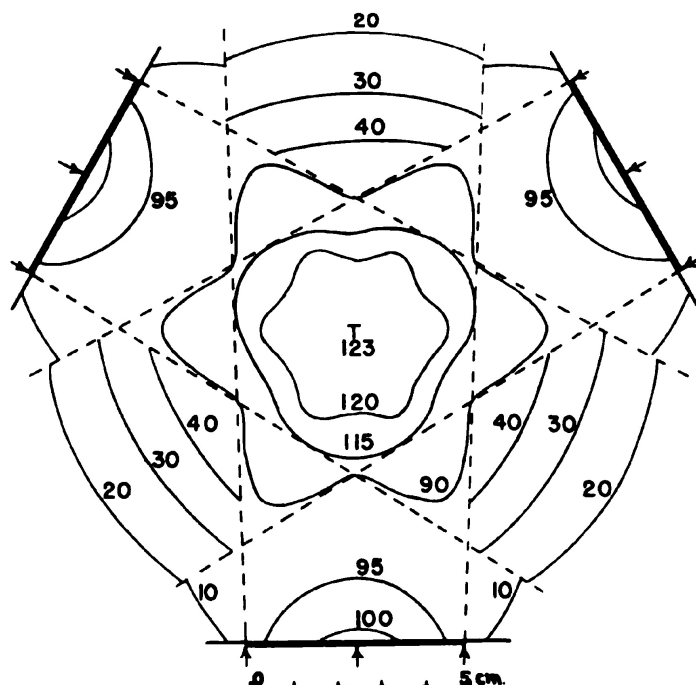


Figure VII-3. Distribution obtained by combining three 5 cm. circular fields distributed at 120° to one another around a circle of diameter 14 cm. 400 Kv., H.V.L. 4.0 mm. Cu., F.S.D. 80 cm.

be discussed later. The distribution of Figure VII-2 is not too bad for the treatment of a small tumor in the region of the 100% isodose surface but the falling off with depth introduces considerable inhomogeneity if the tumor is larger. If a field is directed from the other side of the patient along the line QP (Fig. VII-2) compensation for the falling "internal field" can be obtained. This is illustrated by the distribution of Figure VII-3 where three fields have been combined at an angle of 120° to one another around a circle of radius 7 cm. It is seen that the dose varies by less than 3% in a circular region of diameter about 4 cm. The distribution in planes other than the plane containing the axis of the three fields cannot be obtained easily; however, an estimate of the size of the 120 isodose surface can be made as follows. Directly above T (Fig. VII-3) the dose contributed by each of the three fields is the same, hence to get 120 each field must contribute 40. From Figure VI-17 at a depth of 7 cm. we see that dose 40 is obtained at P about 8 mm. from the axis. This means that the 120 isodose surface, which is about 4 cm. in diameter in Figure VII-3, disappears 8 mm. above or below the plane of Figure VII-3. The 115 surface extends about 1.5 cm. above and below the plane of Figure VII-3. This considerable falling off in a direction perpendicular to the plane of Figure VII-3 can be partially corrected by the use of rectangular fields. For this reason, rectangular fields are generally preferred to circular ones.

If the isodose curves of Figure VI-17 are superimposed over Figure VII-2 with the field directed in opposition to the internal field so that the entrance of the field is the same distance from P as the other two fields, it will be found that the dose still is not quite uniform. This is because the two fields of Figure VII-2 make an angle of 80° to one another whereas for homogeneity the angles should be 120° . However, by giving the third field a greater dose, homogeneity can be achieved. This is called biasing (4). In the case being discussed the third field should be given a dose of about 150 for 100 to the other two fields. The use of a "biased" field is convenient when anatomical considerations prevent the symmetry of Figure VII-3.

7.02

CANCER OF THE LARYNX

As an application of the combination of three coplanar fields one method for the treatment of cancer of the larynx will be discussed. In this method three small x-ray fields are directed towards the tumor. When small fields are used it is necessary to make sure the beam is accurately directed, otherwise the beam can miss the tumor.

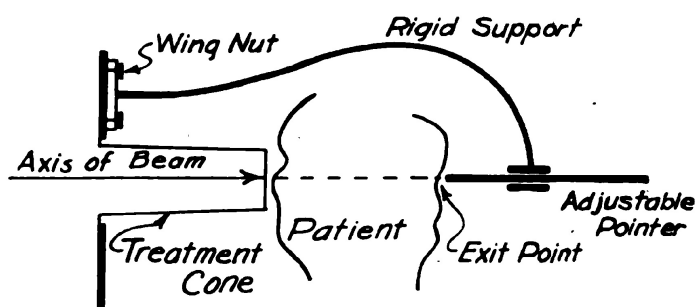


Figure VII-4. Schematic diagram showing one useful type of beam director.

Many devices have been designed to aid in the accurate direction of an x-ray beam (1). One very useful type is shown schematically in Figure VII-4. It consists of a rigid hook carrying a pointer which is constrained to move along the axis of the x-ray beam. Such a device can be arranged so that it may easily be fastened to the master cone of the x-ray machine when beam direction is required. If the point at which the beam enters the patient is determined as well as the exit point, then the path through the patient is known. The desired entrance and exit points may be marked on the skin, or, better still, on a plaster cast which the patient wears during treatment. It is a well known fact that skin markings are inaccurate because they can move considerably with respect to the underlying tissues. To illustrate the use of a plaster cast in beam direction the physical aspects of treatment of a larynx will be discussed in detail.

(a) A mould is made of the patient's neck using plaster of paris bandages. A photograph of a typical mould is shown in Figure VII-5. The mould should extend downwards to the shoulders of the patient and upward around the chin to immobilize the larynx with respect to the cast. The tumor can now be localized with respect to the cast. Lead markers should be placed along the anterior and posterior mid-lines.

(b) A lateral film is taken of the patient with the mould in place. This film will show the lead markers and the tumor. A line on this film can be drawn through the tumor and one of the lead markers. On this film the apparent diameter of the cast "a" and the distance from the front surface of the cast to the tumor "b" can be measured.

(c) The cast is removed, reassembled and a sharp bicycle spoke calibrated in cm. thrust through the cast in the exact position of the line drawn on the film. The antero-posterior diameter of the cast

m direction is required. If
to the underlying tissues. To
the anterior and posterior

"c" along this line can be measured by reading the divisions on the spoke. This is less than "a" because of the magnification of the x-ray image. The actual position of the tumor is then bc/a from the cast and can be located on the spoke. Many times the centre of the tumor is not in the midline as has been assumed here. If such is the case the antero-posterior spoke should be moved laterally.

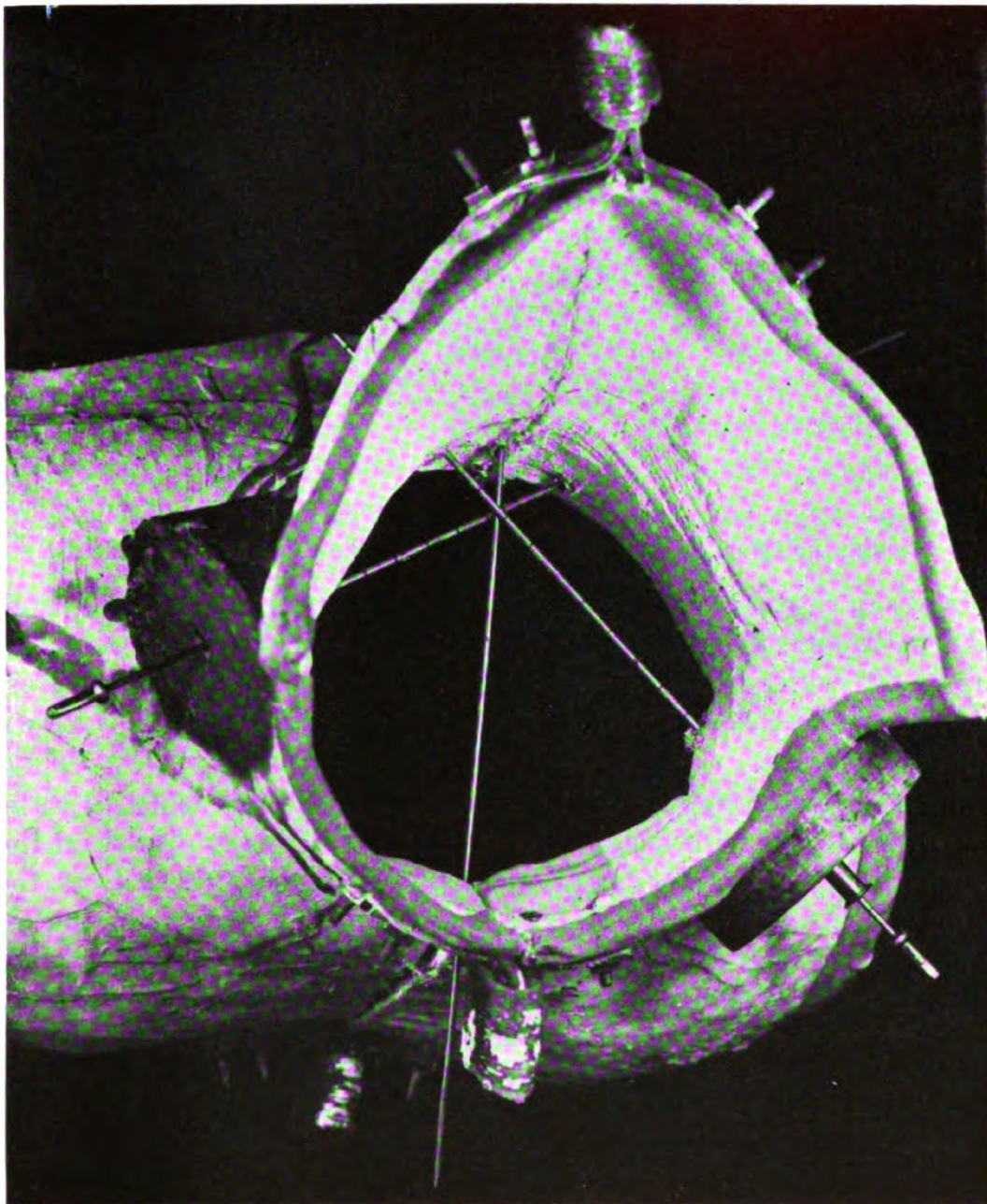


Figure VII-5. Photograph of typical plaster of paris cast for the treatment of cancer of the larynx.

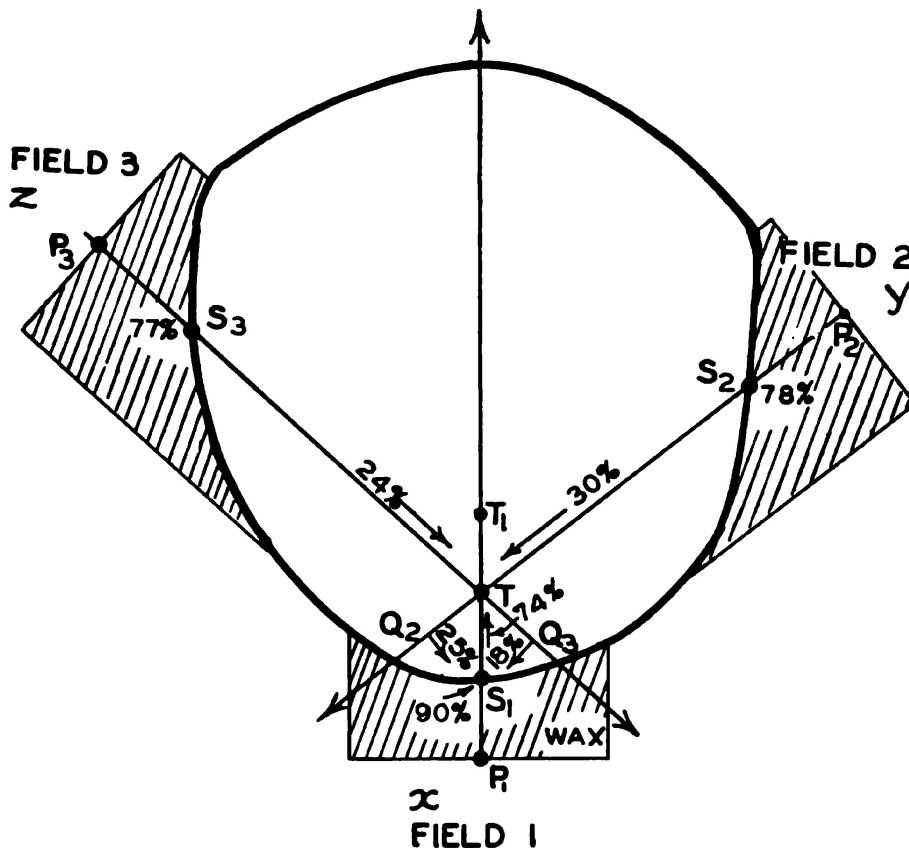


Figure VII-6. Diagram to scale of the cross section of cast and neck through the tumor and containing the axes of the three treatment fields.

(d) Two other spokes are then inserted through the mould from the posterior side and directed towards the tumor, at an angle of about 60° with respect to the midline. A diagram to scale of the cross section of the cast and neck in the plane of the three fields is shown in Figure VII-6.

(e) Wooden replicas of the end of the x-ray cone which is to be used are drilled with a hole in the centre and this is placed on the spoke in contact with the plaster cast. On a surface such as the neck it will make contact at only one point and the rest of the air gap is filled with soft wax. This wax mould provides a flat surface against which the treatment cone can be brought into contact and the exit point on the far side of the mould provides a point to which the back pointer (Fig. VII-4) is adjusted in setting up the patient for treatment.

(f) After the wax has been put in position the following measurements can be made with the calibrated spokes. The letters refer to Figure VII-6, and the depth dose data is obtained from Figure VI-17 for a 5 cm. circular field at H.V.L. 4.0 mm. Cu., F.S.D. 80 cm.

	<i>Depth Dose</i>		<i>Depth Dose</i>		<i>Depth Dose</i>
P ₁ S ₁ = 1.5	90%	P ₂ S ₂ = 2.6	78%	P ₃ S ₃ = 2.7	77%
P ₁ T = 3.0	74%	P ₂ T = 9.2	30%	P ₃ T = 10.5	24%
		*P ₂ Q ₂ = 10.0	25%	P ₃ Q ₃ = 12.0	18%
		Q ₂ S ₁ = 1.8		Q ₃ S ₁ = 1.5	

*S₁Q₂ is the perpendicular from S₁ onto the line P₂T.

(g) The maximum skin reaction will occur at the point S₁ since this point is being irradiated by all three fields. The exit points for fields two and three will receive a smaller dose than S₁. Suppose it is desired to give the tumor 5500r in five weeks. Since the tumor T is near the skin it is advisable to give S₁ the same dose. Under these circumstances the dose will be almost uniform from T to S₁. In order that the internal field produced by fields 2 and 3 be symmetrical with respect to the antero-posterior line, fields 2 and 3 should be made to contribute the same dose to the tumor T. This means that field 3 being farther away must be given a larger dose. These conditions may be put down mathematically as follows, where x, y and z are the doses to be given fields 1, 2, and 3 respectively.

$$\begin{aligned}
 5500 &= 0.74x + 0.30y + 0.24z \text{ (Tumor dose 5500)} \\
 5500 &= 0.90x + 0.25y + 0.18z \text{ (Skin dose at S}_1\text{ 5500)} \\
 0.30y &= 0.24z \text{ (contributions to tumor dose by fields 2 and 3 equal)} \\
 0.78y &= \text{dose to S}_2 \\
 0.77z &= \text{dose to S}_3
 \end{aligned}
 \tag{7-1}$$

From the third equation we see that $z = 1.25y$. Substituting this value in the first two we obtain

$$5500 = 0.74x + 0.60y \text{ and } 5500 = 0.90x + 0.475y$$

These two equations can be solved to yield

$$x = 3650 \qquad y = 4660 \qquad z = 5800$$

This arrangement of fields will give a homogeneous distribution about T but it remains to be seen whether any skin tolerances have been exceeded. The skin doses can be calculated from the last two equations of 7-1 yielding

$$S_1 = 5500 \qquad S_2 = 3640 \qquad S_3 = 4460$$

Since S₃ is not too large this arrangement is satisfactory. If S₃ came

out greater than 5500 it would be necessary to reduce S_3 to 5500 and increase S_2 by enough to give the 5500 tumor dose.

The arrangement described is symmetrical about the antero-posterior midline but it does not follow that the building up of the "internal field" produced by fields 2 and 3 exactly compensates the "falling off" of field 1. It may be that the dose at T_1 (a point 1.5 cm. from T) is considerably less than T or S_1 . In this case the contributions to T_1 are as follows: field 1 - 60%, field 2 - 32.5%, and field 3 - 27%. These give a dose of 5400r units at T_1 . It follows that the region from S_1 to T_1 (3.0 cm.) receives the same dose within 2%. Paterson (4) has introduced the idea of a "balanced" tumor dose in which equations are set down to give points T_1 and S_1 the same dose. From the calculations given here it is seen that essentially this result has been achieved. "Balancing" the tumor dose will always require a greater given dose from the field remote from the tumor and it may be that complete balancing is impossible because of limited skin tolerances. For a detailed discussion of possible field arrangements the reader should consult Paterson (4).

(h) So far we have not considered the falling off of the intensity above and below the plane of Figure VII-6. Examination of Figure VI-17 shows that along a line displaced 1.5 cm. from the axes the following percentage depth doses are received: 3 cm. depth - 70%; 9.2 cm. depth - 28.5%; 10.5 cm. depth - 23%. These are the percentage depth doses received at a point 1.5 cm. above T from fields 1, 2 and 3 respectively. In each case they are about 5% less than that received by T so that points 1.5 cm. above or below T (Fig. VII-6) will receive about 5200r when T receives 5500r. This falling off can be reduced by using rectangular fields which give flatter isodose curves than circular fields.

It might be argued that since the tumor is quite near the surface one single field applied directly towards the larynx would give a good distribution but examination of Figure VI-17 will show that the dose would fall from 5500 on the skin to 4100r at the remote part of the tumor (depth 3 cm.). Two lateral fields directed in opposition would give a better result but there would be a falling off of the dose in the plane of the fields in a direction at right angles to their common axis such as is illustrated in Figure VII-1. Three fields balanced in the way described will give a symmetrical distribution quite similar to Figure VII-3. The problem of inhomogeneity in the direction at right angles to their common plane can be improved by the use of rectangular fields but not solved. The technique illustrated in this ex-

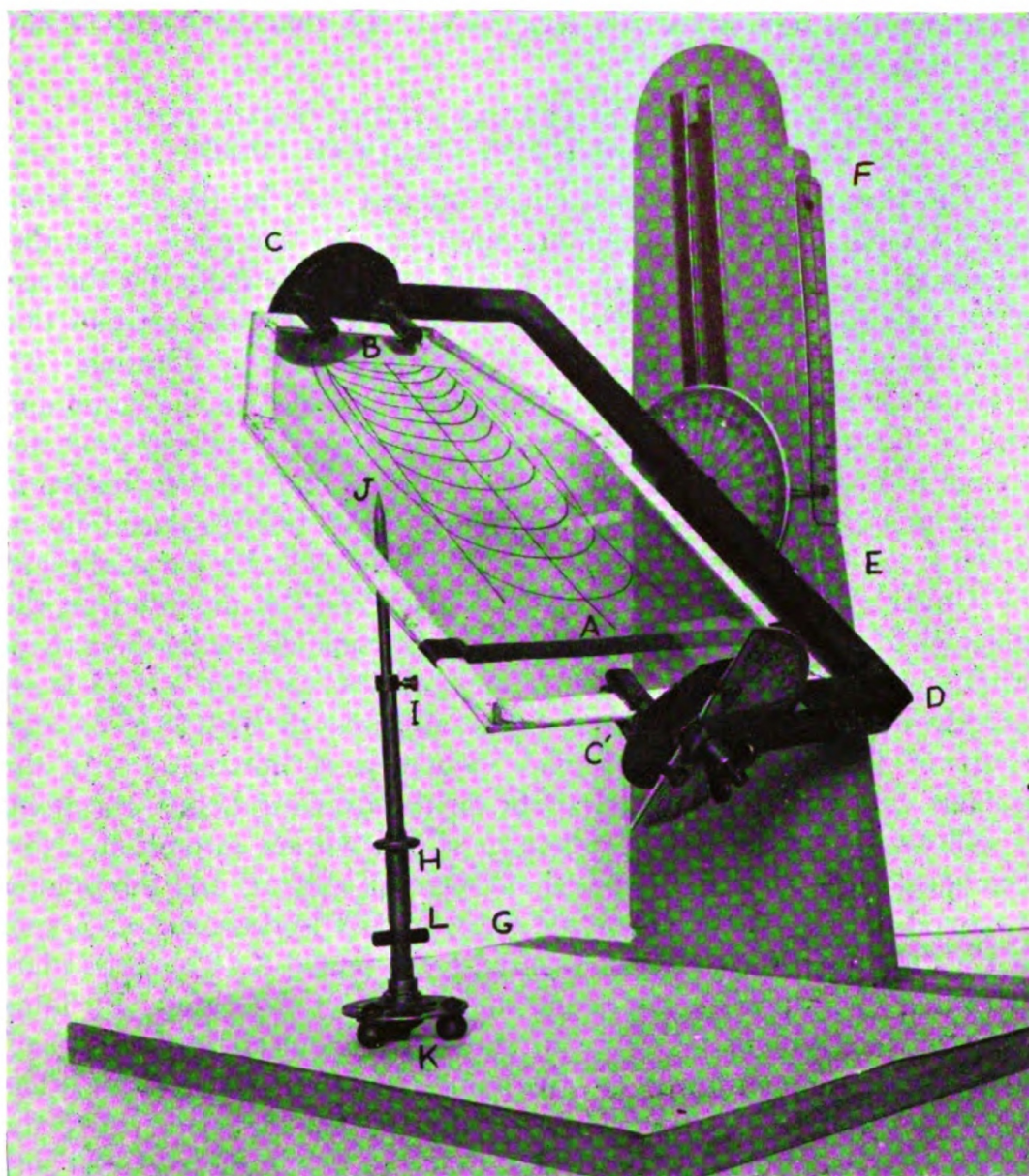


Figure VII-7. Photograph of a contour projector similar in design to that of Mayneord's⁽⁷⁾.

ample will work with 200 Kv. distributions although in this case slightly higher skin doses will be required. However, the preferential energy absorption by bone to be discussed in the next chapter indicates the fact that 400 Kv. should give slightly better clinical results for a larynx. The question arises as to whether the plaster of paris mould changes the depth dose or the tumor dose. Unpublished measurements by the author using a very small flat ionization chamber indicate that at 400 Kv. (H.V.L. 4.0 mm. Cu.) 3 mm. of plaster cast reduces the skin dose by 0.4% and the 10 cm. depth dose by 0.5%. The

corresponding figures for 200 Kv. (H.V.L. 1.5 mm. Cu.) are 1% and 1.3% respectively.

7.03 DISTRIBUTIONS IN PLANES OTHER THAN THE PRINCIPAL PLANE FOR CIRCULAR FIELDS

The plane of greatest anatomical interest may be displaced from the principal plane or may be at some angle to this plane. The distribution in such planes may be found for circular fields by the use of Mayneord's contour projector (7), by a geometrical method due to Wilson (11), or by an optical device developed by Flanders (2). However, regardless of the method the principles are the same and will be illustrated here by a discussion of Mayneord's contour projector shown in Figure VII-7. It will be used here to find the distribution in a plane parallel to the plane of Figure VI-17 but displaced up or down from it by 2 cm. Such a plane has been called a paraxial plane by Ungar (9). The distribution of Figure VI-17 is mounted on the glass plate of the projector so that its axis coincides with the axis of rotation of the glass plate. The framework C C'D (Fig. VII-7) is set exactly horizontal and the point J is adjusted so that it is 2.0 cm. short of reaching the glass plate when it is horizontal. As the pointer and stand are moved about on the drawing board, the point J will always remain in the plane in which we are interested. Now the glass plate is rotated about the horizontal axis AB and the pointer J moved until it comes in contact with the 90% isodose curve. A spot is then made on the drawing page with the pencil K. The glass plate is turned to a different angle and another point is located. In doing this it is convenient to trace out the geometrical edge of the beam first and then locate three or four points on each isodose curve. The result is shown in Figure VII-8. It will be seen that the size of the beam is considerably reduced and that the 90% isodose curve only barely reaches this plane. The depth dose at 8 cm. in this plane is 30% while in the principal plane (Fig. VI-17) it is 35%. The beam in this plane gives a smaller depth dose and covers a smaller region. The width of the beam in this plane for a rectangular field would be the same as in the principal plane and the depth dose would not be reduced as much.

By combining three of the fields shown in Figure VII-8 at 120° to one another around a circle of diameter 14 cm. we obtain the distribution of Figure VII-9. This is the distribution obtained in a plane 2 cm. above or below that shown in Figure VII-3. It is seen that in this plane the 120 and 115 isodose curves do not exist and that

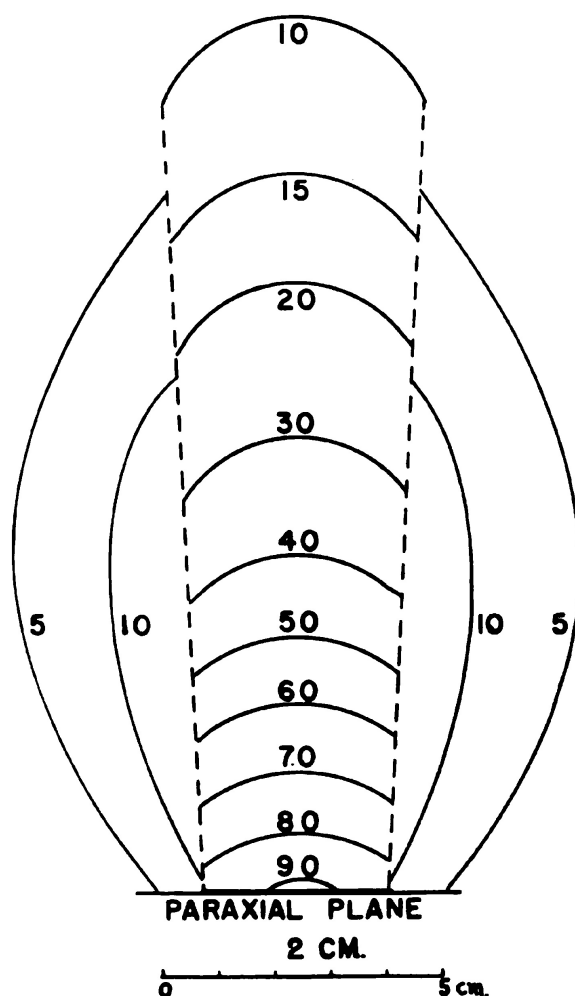


Figure VII-8. Distribution in a paraxial plane 2 cm. from the principal plane shown in Figure VI-17. 5 cm. circular field, 400 Kv., H.V.L. 4.0 mm. Cu., F.S.D. 80 cm.

the dose in the region where the beams intersect varies from 100 to 105. From examination of Figures VII-3 and VII-9 it should be possible to visualize the isodose surfaces in space.

It is sometimes required to determine the distribution of radiation on the patient's skin when the beam enters the skin surface at various angles. Distributions for angles of 90° , 60° and 30° are shown in Figure VII-10 for the 5 cm. circular field illustrated in Figure VI-17. The distribution for normal incidence shown in Figure VII-10a consists of a series of circles, whose diameters are obtained directly from Figure VI-17. For example, the diameter of the 95% circle is equal to DD' of Figure VI-17. It is seen that the dose varies from about 90% at the edge of the field to 100 at the centre. A circle of 5 cm. diameter marks the discontinuity at the edge of the beam.

Outside this circle the maximum dose is just a little greater than 5%. The distribution in the entrance plane for normal incidence of a rectangular field must be obtained either by measurement or from a knowledge of the distributions in several paraxial planes (section

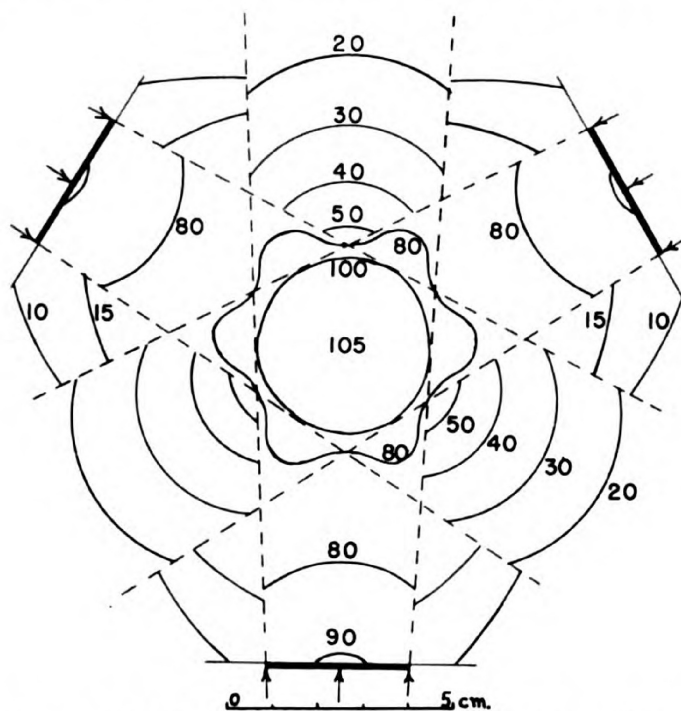


Figure VII-9. Distribution of radiation in a plane 2 cm. above that shown in Figure VII-3.

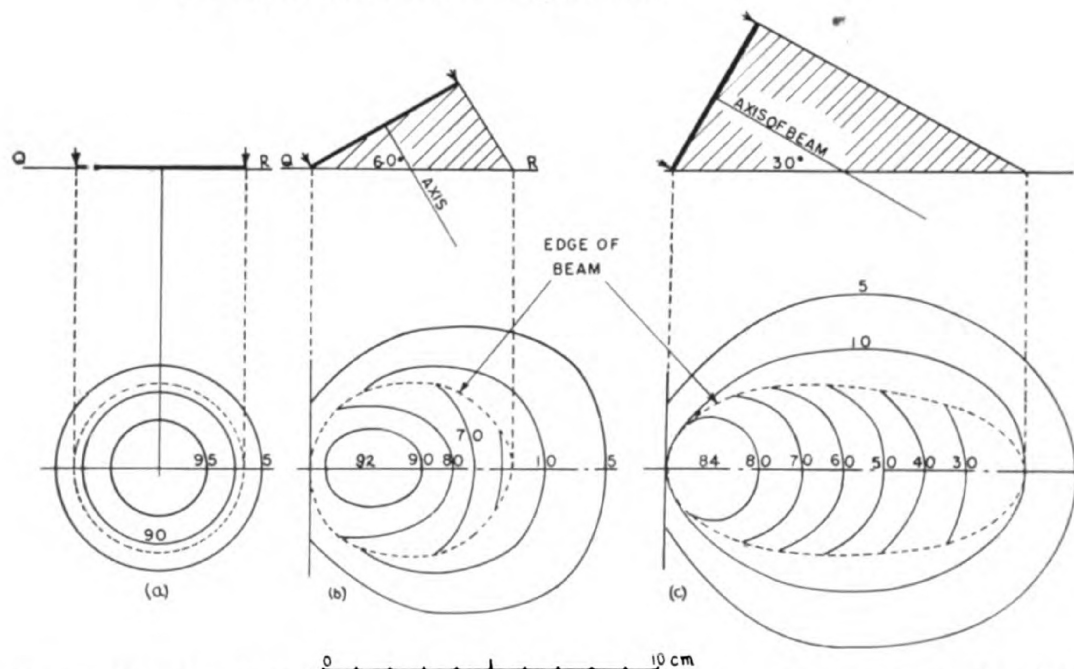


Figure VII-10. Distributions on the skin surface, when the 5 cm. circular field of Figure VI-17 is applied at angles of 90° , 60° and 30° to the skin surface.

7.04). However, their general nature is seen to be an elliptical type of distribution as illustrated schematically for a 6×8 field in Figure VII-11. The discontinuity at the edge of the beam will of course be rectangular in shape.

The contour projector may be used to find the distribution in a plane making any angle with the principal plane for a circular field. This method will be illustrated by determining the distribution on the skin when the 5 cm. circular field is applied obliquely at an angle of 60° with the skin surface as illustrated in Figure VII-10b. It is required to find the distribution in a plane perpendicular to the page through the line QR. The isodose curves of Figure VI-17 are mounted on the glass plate of the projector as above but now the whole framework is rotated through 60° . The height of the pointer is adjusted until it just reaches the edge of the beam when it is rotated to its lowest point. The procedure outlined above will then yield the results shown in Figure VII-10b. The highest dose reached on the skin is 92. The edge of the beam appears now as an elliptically shaped curve. In a similar manner the distributions of Figure VII-10c were obtained for an incident angle of 30° . The highest skin dose is now only 84 and the area of the entrance field is much larger. These distributions of course only result when bolus* material is placed between the end of the applicator and the skin surface. If bolus material is not used it is impossible to predict the distribution on the skin surface or the depth dose without recourse to experiment. The problems of radiotherapy become exceedingly complicated if the distributions for all the fields used in a radiotherapy department are required for a number of angles of incidence. It is doubtful if any great advantage is achieved by the use of oblique fields, without bolus material, except in the case of very high energy radiations when the maximum dose may be brought onto the skin surface by the use of such materials.

7.04

DISTRIBUTION IN SPACE FOR RECTANGULAR FIELDS

When rectangular fields are used the distributions in other planes cannot be obtained by any rotation technique. However, they may be obtained optically if a wire mesh model of the isodose surfaces is available (2) or by the method due to Ungar (9). In this latter method it is necessary to have the distribution in the principal plane, in a paraxial plane and the peripheral plane as indicated schematically in Figure VII-11. For very large fields it may be necessary to have

*A satisfactory bolus material is rice flour mixed with sodium bicarbonate held in a cotton bag. A variety of sizes of these bags is convenient.

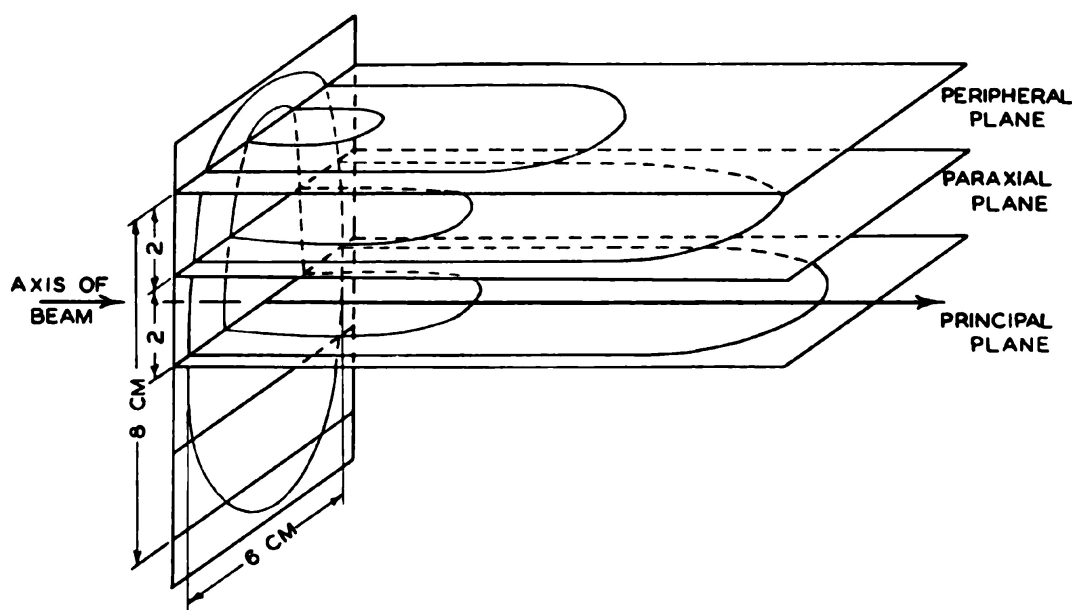


Figure VII-11. Schematic diagram showing distributions in the principal paraxial and peripheral planes for a 6 x 8 rectangular field.

more than one paraxial plane. Ungar has used this method for analysing the distributions obtainable when six or eight fields are directed towards a vertebra from the posterior surface of the patient. The fields are placed around a circle and directed towards a point below the tumor. The resultant distribution on the skin and in planes through the tumor may then be obtained. For further details concerning the method see Ungar (10) and Johns (5).

7.05

CANCER OF THE OESOPHAGUS

A particularly simple application of the method is found in the treatment of cancer of the oesophagus using six strip fields directed towards the tumor. The accurate beam direction can conveniently be carried out using a cast made of plaster of paris bandages which the patient wears during treatment. A photograph of a typical cast is shown in Figure VII-12. Lead markers are placed along the anterior and posterior midlines and a lateral x-ray picture is taken with the patient wearing the cast and with the oesophagus outlined with a barium paste. A line may be drawn on the film through the centre of the tumor and through one of the lead markers. The position of this line can be reproduced with a sharp bicycle spoke thrust through the cast and the position of the tumor located on it in the same way as in the treatment of the larynx. Two more spokes can be thrust through the cast to intersect at the tumor. Typical distributions for the principal plane are shown in Figure VII-13A due to

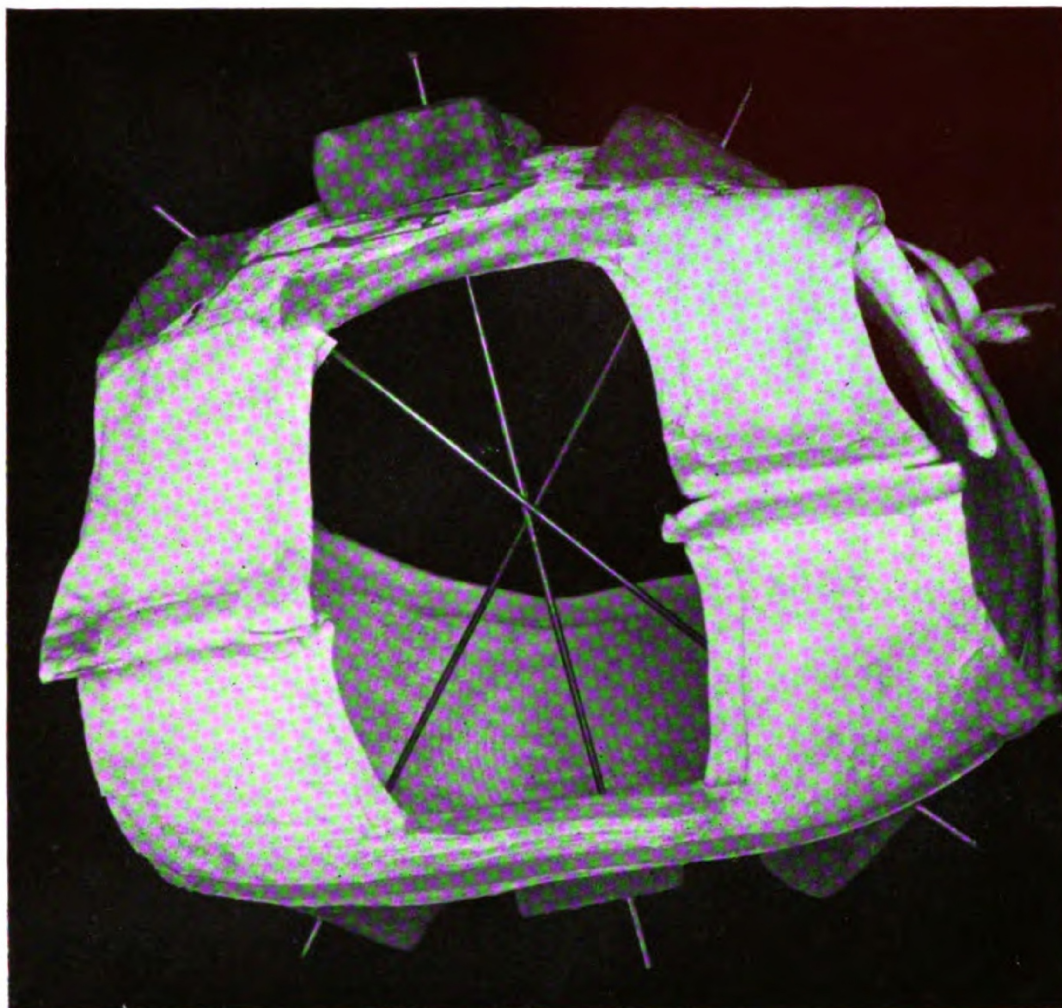


Figure VII-12. Photograph of a plaster of paris cast used in the treatment of cancer of the oesophagus.

Smithers (8). Some of the isodose lines have been left out for clarity in reproduction. Oesophageal tumors are usually quite long and it is important to obtain the distribution in planes above or below the principal plane. This can easily be done if the distribution in a peripheral plane 6 cm. from the principal plane is known. The results are shown in Figure VII-13B for two 6×15 fields and four 4×15 fields. Some radiotherapists prefer the use of six 6×15 strip fields as this gives a larger region around the tumor in which a high dose is given. The actual distribution, of course, depends greatly on the physical dimensions of the patient and when these become too great it is difficult to achieve a high enough tumor dose without high skin doses. For comparison, the distribution obtained by the author (6) using six betatron fields is shown in Figure VII-14. As in the case of 400 Kvp. radiation there is a tendency for unwanted

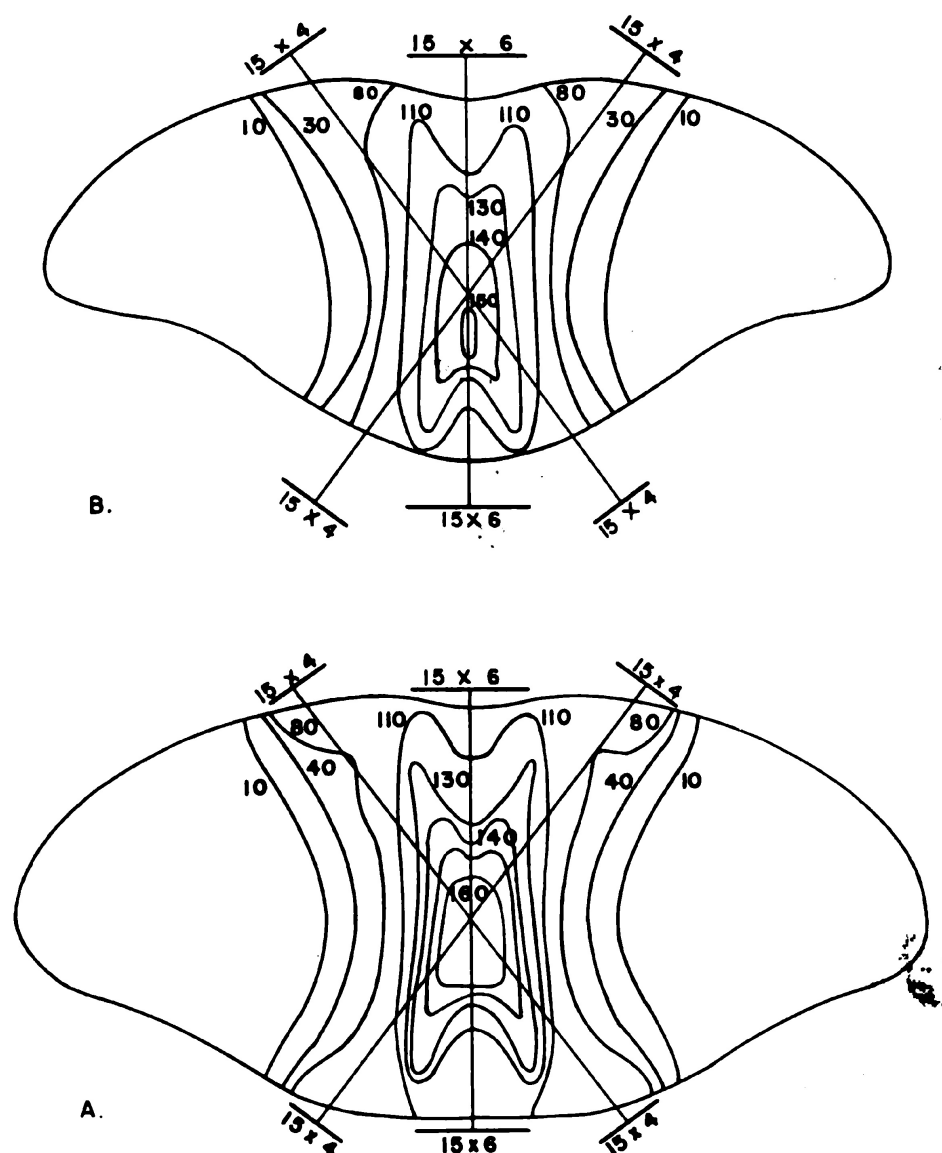


Figure VII-13. Distributions in the principal and peripheral planes obtained in treatment of cancer of the oesophagus by Smithers, Clarkson and Strong⁽⁸⁾. A—distribution in principal plane; B—distribution in plane displaced 6 cm. up from the principal plane.

“horns” to appear in the pinch spot region where the angled fields intersect the anterior posterior fields.

The few examples which have been discussed should serve to illustrate some of the physical principles involved in beam direction and the use of isodose distributions in radiotherapy. The particular techniques described are not necessarily the best techniques, as this is a matter of opinion, but they have given satisfactory results and illustrate many of the basic physical principles of radiotherapy.

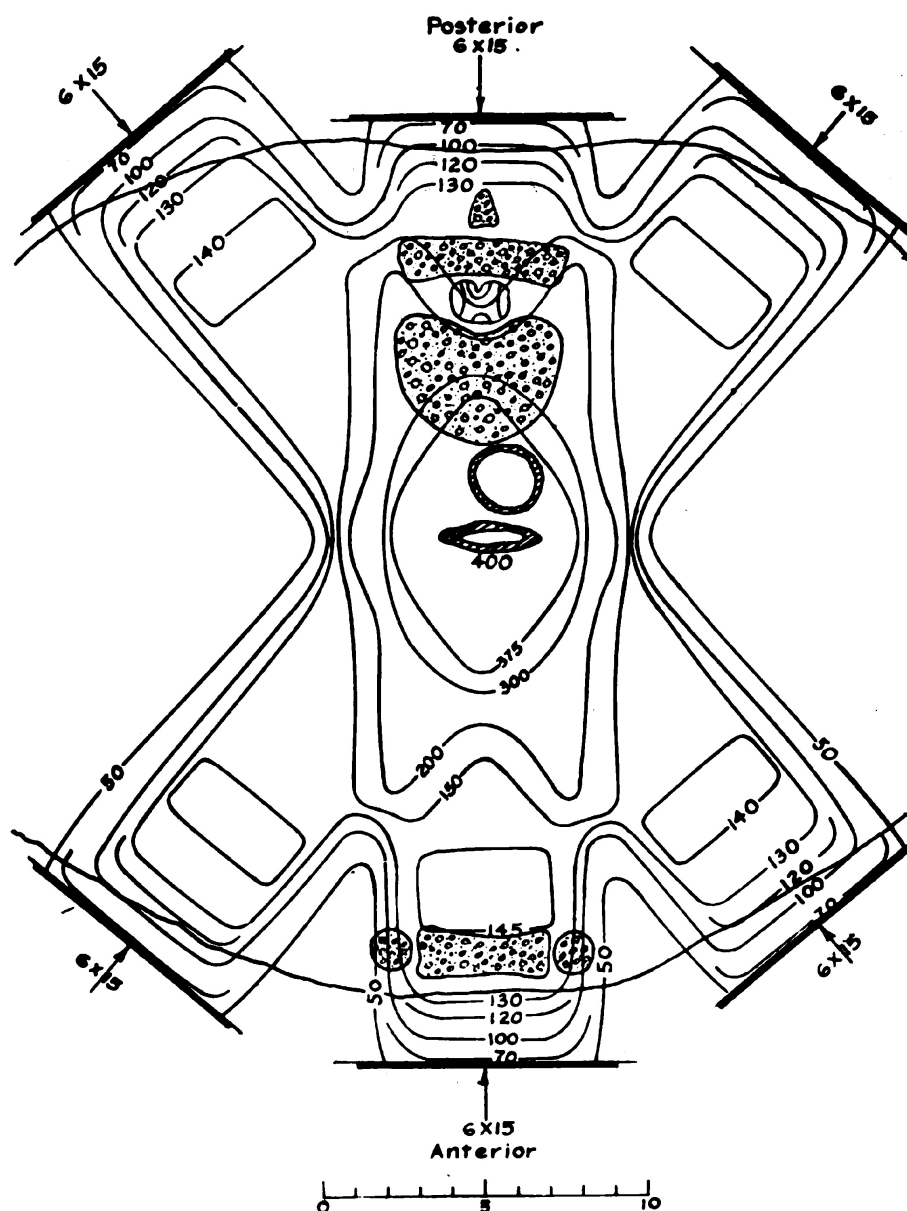


Figure VII-14. Isodose distributions for treatment of cancer of the oesophagus using 6 x 15 betatron fields with compensating filter at 22 Mev.⁽⁶⁾.

7.06 STATEMENT OF DOSAGE IN RADIOTHERAPY

Radiation fields should be arranged in number and direction so that the following fundamental principles are followed and so that the following statements concerning dosage may be made.

(a) A homogenous dose is given to the tumor including an adequate safety margin around it of at least 1 cm. Complete homogeneity can never be achieved so the maximum and minimum tumor dose should be evaluated and recorded.

(b) The skin dose with full backscatter including any dosage contributions by other fields should be given.

(c) The way the dose is administered is very important in determining the biological effect, hence the overall treatment time and the number of treatments should be recorded. It is generally agreed that fractionation of the total dose over a period of from three to five weeks gives better results than treatment by a single massive dose. For small superficial tumors there is no agreement on this point. Since the biological effect of a given amount of radiation depends on the fractionation, a statement that a tumor was given a dose of 5000r is meaningless unless the period over which this radiation was given, and the number of exposures, is definitely stated. It is generally agreed that for the range of dosage rates found in practice, the biological effect is independent of dosage rate. Hence dosage rate need not be specified.

(d) It is usual to state the focal skin distance, the half value layer and the kilovoltage of the radiation which is used. This is not absolutely necessary since tumor dose and skin dose are determined, in part at least, by these factors. However, there is still some doubt as to whether 1 roentgen of soft radiation produces the same biological effect on a tumor as 1 roentgen of hard radiation. Quimby has shown that 270 roentgens of 100 K.V. radiation is biologically equivalent to 1,000 roentgens of 1,000 K.V. radiation in the production of skin erythema. It does not follow, however, that about four times as much hard radiation as soft is required to produce tumor regression. In fact the differences if they do exist are much smaller than this. However, experience over many years has definitely demonstrated that a somewhat larger dose of radiations produced by radium gamma rays is required to produce tumor regression than of 200 K.V. radiation. For these reasons a statement of the half value layer of the radiations is of value.

(e) The number of fields, their size and arrangement should be stated.

(f) The normal tissue outside the tumor region should receive the minimum possible dose. An ideal never achieved in practice would be one in which only the tumor region receives any radiation. This necessitates accurate beam direction using a number of fields each of which is just large enough to cover the tumor region. The advantage of symmetrically arranged rectangular fields has been pointed out. It may be that two different techniques can yield the same tumor

dose over an adequate region. If this is the case, the technique which delivers the minimum radiation to the patient will be the best. This amount of radiation is determined by the *integral dose* to be discussed in Chapter VIII. A statement of integral dose is of some significance. The technique which gives a minimum integral dose for a given tumor dose should be used.

REFERENCES

1. Ellis, F., Wilson, C. W., Dobbie, J. L., Grimmett, L. G., Green, A.: Symposium on "Beam Direction in Radiotherapy," *Brit. J. Radiol.*, 16:31, 1943.
2. Flanders, P. H.: *Brit. J. Radiol.*, 16:314, 1943.
3. Honeyburne, J., Lamerton, L. F., Smithers, D. W., Mayneord, W. V.: Symposium on "Three Dimensional Radiation Distributions," *Brit. J. Radiol.*, 12:269, 1939.
4. Paterson, R.: *The Treatment of Malignant Disease by Radium and X-Rays*. London, Arnold, 1948.
5. Johns, H. E.: *Medical Physics*, Yr. Bk. Pub., 1950, Chicago.
6. Johns, H. E., Darby, E. K., Watson, T. A., Burkell, C. C.: *Brit. J. Radiol.*, 23:290, 1950.
7. Mayneord, W. V.: *Brit. J. Radiol.*, 12:262, 1939.
8. Smithers, D. W., Clarkson, J. R., Strong, J. A.: *Am. J. Roentgenol.*, 49:606, 1943.
9. Ungar, E. M.: *Brit. J. Radiol.*, 16:274, 1943.
10. Ungar, E. M.: *Brit. J. Radiol.*, 18:76, 1945.
11. Wilson, C. W.: *Brit. J. Radiol.*, 13:345, 1940.

Chapter VIII

ENERGY ABSORPTION

8.01

RELATION BETWEEN ENERGY ABSORPTION AND THE ROENTGEN

IN section 4.01, it was stated that under certain circumstances the energy absorbed by biological material is proportional to the dose in roentgens. We now inquire into the amount of energy which is absorbed and into the conditions under which the equivalence holds.

The results of a large number of experiments indicate that every time an ion pair (i.e., a positive and negative charge) is produced in air by a high speed corpuscle this corpuscle loses on the average 33 ev. of energy, or for each ion pair liberated in air 33 ev. of energy are absorbed. This figure appears to be independent of the wavelength of the radiation and the energy of the corpuscle. It is known to an accuracy of about 1%, values of 32.5 to 33.0 being given in the literature. Using this value we can calculate the energy absorbed when 1 roentgen is given to 1 gm. of air. One r unit is recorded when 1 e.s.u. of charge is liberated in 0.001293 gm. of air. Since the charge carried by an electron is 4.80×10^{-10} e.s.u., the number of ion pairs contained in 1 e.s.u. is given by

$$1 \text{ e.s.u.} = \frac{1}{4.80 \times 10^{-10}} \text{ ion pairs} = 2.08 \times 10^9 \text{ ion pairs} \quad (8-1)$$

Consequently the energy absorbed when 1 roentgen is given to 1 cm.³ of air at N.T.P. is $2.08 \times 10^9 \times 33$ ev. which can be converted to ergs using equation (1-1) to give $2.08 \times 10^9 \times 33 \times 1.60 \times 10^{-12}$ ergs = 0.110 ergs. Since 1 cm.³ of air at N.T.P. weighs 0.001293 gm. it follows that 1 gm. of air occupies 774 cm.³. Therefore when 1 roentgen is given to 1 gm. of air the energy absorbed is 774×0.110 ergs = 85 ergs. Mayneord (3) has called this unit of energy absorption the gram roentgen.

$$1 \text{ gm. roentgen} = 1 \text{ gm.r.} = 85 \text{ ergs} \quad (8-2)$$

A unit one million times as big has been found useful clinically and has been called the megagm. roentgen.

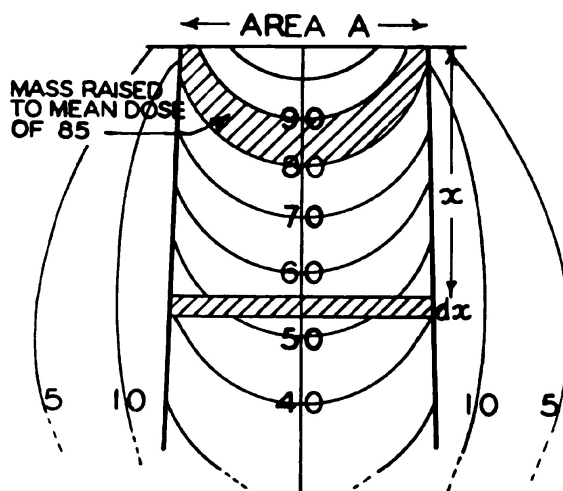


Figure VIII-1. Part of the isodose distributions for a 5 cm. circular field, area A, H.V.L. 4 mm. Cu., F.S.D. 80 cm., showing the meaning of integral dose.

$$1 \text{ megam.r.} = 85 \times 10^6 \text{ ergs} = 8.5 \text{ joules} \approx 2 \text{ calories}^* \quad (8-3)$$

It is seen that the megam.r. is about 2 calories. The energy absorption in a full course of x-ray treatment can reach values as high as 40 megam.r. when large fields are used. It cannot be stated that the biological effect depends only on the energy absorption but it is safe to say that energy absorption is a very important quantity in determining the biological effect. Because 1 gm. of air and 1 gm. of tissue absorb approximately the same amount of radiation for a wide range of energies, the gm.roentgen corresponds to a definite amount of energy absorption (85 ergs) in tissue. The close correspondence between energy absorption in tissue and the dose in roentgens indicates the suitability of the roentgen as a unit in which to measure radiation (4). Deviations from this simple correspondence (1 gm.r. = 85 ergs) will be discussed in section 8.06.

8.02

INTEGRAL DOSE

One of the fundamental principles of radiotherapy (7.06) is that the radiation should be absorbed and concentrated only in the tumor. This, of course, cannot be achieved in practice but one can try to keep the x-ray energy absorption by the patient to a minimum for a given tumor dose. The total energy absorption during an x-ray treatment has been called the "Integral Dose" by Mayneord (3). Consider Figure VIII-1 in which is shown a part of the isodose distributions of Figure VI-17. When 100r skin dose is given to the patient all the mass enclosed between the 100r isodose surface and the 95r surface

*4.18 joules = 1 calorie.

is raised to an average dose of 97.5r. The energy absorbed in gm. roentgens is consequently the product of 97.5 and the mass enclosed. The region between the 95% and 90% surfaces is raised to an average dose of 92.5r so the energy absorbed by this region will be the mass enclosed times 92.5. The total integral dose will be found by adding together the contributions between successive isodose surfaces. The evaluation of the integral dose by this method is not easy because of the difficulty of calculating the masses enclosed between the surfaces. This has been done by a mathematical method for the distribution of Figure VI-17 and the results are shown in Table VIII. It will be seen that integral dose contributed between successive isodose surfaces is nearly constant until the low dosage regions are reached. These contribute rather largely to the integral dose. The total integral dose is found by adding all the contributions as indicated in Table VIII. The integral dose received during treatment by a single field can be calculated approximately by a method due to Mayneord (3), if we assume that the isodose surfaces are flat from one edge of the beam to the other, that the dosage rate decreases with depth according to an exponential law, and that the size of the beam is of constant area A.

Table VIII

INTEGRAL DOSE FOR 5 CM. CIRCULAR FIELD (AREA 19.6 CM.²) AT F.S.D.
 80 CM., H.V.L. — 4.0 MM. CU., FOR SKIN DOSE OF 100r.

<i>Isodose Surfaces</i>	<i>Mass Enclosed</i>	<i>Mean Dose</i> <i>r</i>	<i>Integral Dose</i> <i>gm. r.</i>
100 — 90	13.1	95	1240
90 — 80	17.5	85	1490
80 — 70	20.0	75	1500
70 — 60	22.7	65	1480
60 — 50	26.6	55	1470
50 — 40	33.2	45	1490
40 — 30	46.6	35	1630
30 — 20	66.7	25	1670
20 — 10	122	15	1830
outside beam			
10 —	119	12.5	1490
5 — 10	388	7.5	2910
			18,200gm.r.

Under these simplifying assumptions the dose D_x at depth x can be written $D_x = D_0 e^{-\mu x}$ where D_0 is the dose on the surface. The integral dose received by the rectangular shaded volume of Figure VIII-1 is $D_x \cdot A \cdot dx$. The total integral dose to depth d is given by

$$^*\Sigma = \int_0^d D_x \cdot A \cdot dx = \int_0^d D_0 e^{-\mu x} \cdot A \cdot dx = \frac{D_0 A}{\mu} (1 - e^{-\mu d})$$

For large values of d this yields the simple expression $D_0 A / \mu$. If $d_{1/2}$ represents the depth of the 50% isodose surface then $d_{1/2}$ can be considered as the half value layer and is related to μ by the equation $\mu = 0.693/d_{1/2}$. Substituting this value for μ we obtain

$$\Sigma = \frac{D_0 A}{\mu} = 1.44 \cdot D_0 \cdot A d_{1/2} \quad (8-4)$$

This expression takes no account of the spread of the beam but can be corrected for this effect (3) to give as a first approximation

$$\Sigma = 1.44 D_0 A d_{1/2} \left\{ 1 + 2.88 \frac{d_{1/2}}{f} \right\} \quad (8-5)$$

where f is the focal skin distance. This expression gives the integral dose when the patient is thick enough to absorb all the radiation. Expression (8-5) can be used to calculate the integral dose for the 5 cm. circular field discussed in Table VIII. For this case $d_{1/2} = 5.8$ cm. (see Fig. VI-17), $A = \pi (2.5^2) = 19.6$ cm.², $D_0 = 100r$, $f = 80$ cm. Substitution of these values in (8-5) yields an integral dose of 19,800 gm.r. This value is larger than that obtained in Table VIII but the agreement is good when one considers the many approximations which have been made. We might expect the value calculated by (8-5) to be larger because it includes all the radiation absorbed up to great depths, while the results of Table VIII include values down to the 10% isodose surface in the main beam and out to the 5% surface in the shadow. For most cases the order of magnitude of the energy absorption is all that is required so that equation (8-5) is accurate enough.

* Σ is the Greek letter sigma which stands for "the sum of." Since integral dose is the sum of a large number of contributions Σ will be used to represent integral dose. \int is an integral sign which merely indicates that the summation is to be carried out for a very large number of very small terms. That is, the rectangular shaded region of Figure VIII-1 is to be made very small and the number of these increased proportionally.

From equation (8-5) we see that the integral dose depends directly on the area of the field. Some radiotherapists build up the depth dose by the use of a large field. This is a very bad practice because, in increasing the depth dose by a small percent, the integral dose may be increased by a large factor. For example, taking depth dose data from the Appendix for half value layer 2.0 mm. Cu. and F.S.D. 50 cm. we find that the 10 cm. depth dose can be increased from 24% to 47% by increasing the field size from an area of 20 cm.² to 400 cm.². In doubling the percentage depth dose (24% to 47%) the integral dose is increased by more than a factor of 20. (The area is increased by a factor of 20 and $d_{1/2}$ is also increased.) If a higher depth dose is needed, several small fields directed towards the tumor should be used rather than one or two very large fields. The smallest field which will adequately cover the tumor should be chosen and enough of them directed towards the tumor to give the desired tumor dose. In general, the smaller the area of the fields which can be used the smaller will be the integral dose for a given tumor dose. The actual ratio of the integral dose for a given tumor dose will depend on the type of radiation used. The author (1) has shown that betatron radiation used in similar techniques to that used with 200 Kv. radiation will yield an integral dose about $\frac{1}{2}$ as great for the same tumor dose.

Although the concept of integral dose is rather recent there is already sufficient evidence to show that there is some correlation between the white blood count and the integral dose. The sizes of the integral dose given in different x-ray techniques is also of interest. Smithers (10) has found that, in the treatment of cancer of the oesophagus using strip fields, the integral doses vary from about 10 to 26 megam.r. for 6000r units to the tumor, depending on the size of the patient. For cancer of the larynx the variations are from 4 to 10 megam.r. It is conceivable that two different techniques will enable one to deliver the same dose to the tumor with essentially the same skin dose. The technique which delivers the minimum integral dose for the given tumor dose will then be the better. Suppose for example that a patient with a carcinoma of the tonsil is treated with two directly opposing fields on either side of the neck, 11 cm. apart, and given a tumor dose of 6000r units. If the fields are 7 cm. circles the integral dose will be 3.3 megam.r. and with two 10 × 10 fields 8.5 megam.r. Provided that the minimum tumor dose is the same in each case there is little doubt that the patient will not only tolerate the treatment with the small fields

best, but that the tumor response will be more satisfactory. In general, the use of several small fields to obtain the required tumor dose will give a much smaller integral dose than the use of a smaller number of large fields.

8.03 WHOLE BODY IRRADIATION

In certain cases of blood disorders (leukemia, polycythemia, etc.) it may be advisable to treat the patient with whole body irradiation. Under such circumstances a statement of the skin dose has only limited meaning and what is required is a statement of the integral dose. Two different techniques yielding the same skin doses could produce widely different constitutional effects if the qualities of the radiation were very different. In order to calculate the integral dose in whole body irradiation it is necessary to determine the mean dose received by the patient. Mayneord and Clarkson (5, 6) have determined this mean dose experimentally by measuring the dose received at a large number of points within a model wax man. They found that the mean dose depended on the antero-posterior thickness of the patient, on the quality of the radiation used and, to some slight degree, on the focal skin distance. Some of their results are given in Table IX.

TABLE IX

MEAN DOSE RECEIVED DURING WHOLE BODY IRRADIATION FOR
FOCAL SKIN DISTANCE 200 CM.

Half Value Layer mm. Cu. —————→	<i>Mean Dose for 1 roentgen skin dose</i>			
	0.5	1.0	2.0	4.0
<u>A.P. Thickness of Patient</u>				
14	0.612	0.666	0.695	0.654
18	0.546	0.610	0.640	0.605
22	0.493	0.563	0.600	0.556
26	0.449	0.519	0.554	0.515
30	0.409	0.482	0.521	0.476

If the focal skin distance is 250 cm. the mean doses should be increased by 2% while for 150 cm. they should be decreased 2%. These focal skin distance corrections are only approximately correct since they

depend on the quality of the radiation, but for the range of qualities given in Table IX they are not in error more than 2%.

The integral dose is obtained by taking the product of the mass of the patient, the mean dose and the skin dose. An example will illustrate how the integral dose may be calculated. Suppose a patient 22 cm. thick weighing 65 kg. (1 Kg. = 2.2 lb.) is given a skin dose of 300r units in whole body radiation at F.S.D. 200 cm. with radiation of half value layer 2.0 mm. Cu. The integral dose is therefore

$$\Sigma = 65,000 \times 0.600 \times 300 \text{ gm.r.} = 11.7 \text{ megagm. r.}$$

In practice half the radiation would be given through the anterior surface and half through the posterior surface in order to give a more or less homogenous dose throughout the patient. This integral dose is very near the therapeutic body tolerance for whole body irradiation. It is, however, smaller than the integral dose which can easily be attained when limited volumes of the body are irradiated. It is obvious therefore that an exact correlation between integral dose and constitutional tolerance dose does not exist. It is possible that the explanation lies in the fact that during total body radiation all the bone marrow is irradiated whereas in more localized treatment some of the bone marrow is irradiated to a much higher level but the majority escapes irradiation altogether. From these facts it will be seen that the field of usefulness of integral dose in radiotherapy is limited.

In certain cases it is advisable to treat only the trunk with whole body irradiation. Under these circumstances the mean doses are less than those given in Table VIII by from 5% to 9% depending on the thickness of the patient. For most practical purposes, it is sufficiently accurate to multiply the values of Table VIII by 0.93 to obtain the mean dose for trunk radiation alone. To calculate the integral dose in this case it is necessary to determine the mass of the trunk which is radiated. By measuring the antero-posterior diameter "a" and the lateral dimensions "b" of the patient and the length "l" of trunk which is radiated, the mass may be determined as $\pi abl/4$.* Suppose in a certain trunk radiation $a = 24$ cm., $b = 35$ cm., and $l = 50$ cm. Then the mass irradiated is $\pi (24) (35) (50) / 4 = 33,000$ gm. For H.V.L. 2.0 mm. Cu. and F.S.D. 200 cm. the mean dose is $0.577(.93) = .537$ and the integral dose for 300r skin dose is

*The cross section of the trunk may be considered as an ellipse with major and minor axes "a" and "b." The area of the ellipse is $\pi ab/4$, and the volume treated $\pi abl/4$.

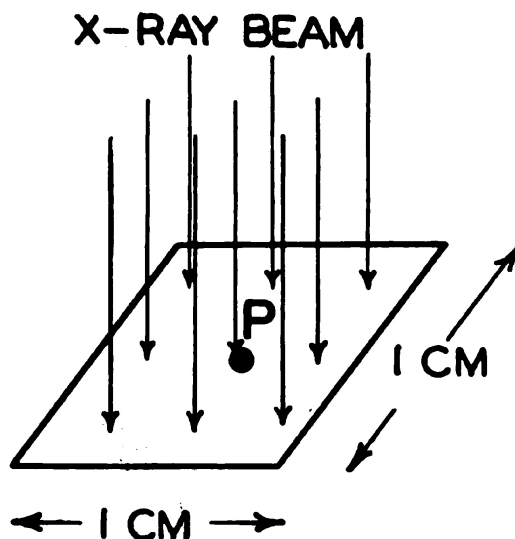


Figure VIII-2. Diagram to illustrate the energy flux required to record 1 roentgen.

$33,000 (.537) (300) = 5.31$ megam.r. For further details reference should be made to the original papers (5, 6).

8.04

ENERGY FLUX

In section 8.02 we found a method to calculate the energy absorbed within the direct beam, but we have no method of calculating the energy absorbed beyond the edge of the beam in the regions of very low dosage rates. However, it is possible to calculate the amount of energy which must pass through the surface of the medium in order to record 1 roentgen on the surface. The amount of energy which passes through a 1 cm.^2 surface is called the energy flux and may be measured in ergs/cm.^2 . Consider the parallel beam of radiation of Figure VIII-2 which is incident upon the surface of an extensive "air like" medium. We wish to calculate the amount of energy which must pass through each square cm. of area in order that a detecting device placed at P will record 1 roentgen. Let E be the required energy flux in ergs/cm.^2 in order to record one roentgen. One roentgen will be recorded when 85 ergs of energy are absorbed by one gm. of air. The fraction of the incident flux E which is absorbed by 1 gm. of air is $(\tau + \sigma_a + \pi_a)/\rho$ where τ/ρ , σ_a/ρ , π_a/ρ are the real mass absorption coefficients of air by the photoelectric, the Compton process and pair production respectively (see Chapter III, 3.08). Therefore we may write

$$85 = E \left(\frac{\tau + \sigma_a + \pi_a}{\rho} \right) \quad \text{or} \quad E = \frac{85}{\left(\frac{\tau + \sigma_a + \pi_a}{\rho} \right)} \quad (8-6)$$

The real mass absorption coefficients for air are known so that the energy flux E may be determined. In this analysis no account has been taken of the radiation which is scattered back to the detector by the medium. In certain energy regions for large fields, this yields an important contribution to the dose read by the detector so that the required energy flux to record a roentgen is reduced. Mayneord (7,8) has calculated the energy flux with and without backscatter and his results are plotted in Figure VIII-3. In order to include the large energy range from 0.01 Mev. to 100 Mev. a logarithmic scale has been used. This complicated curve is obtained because of the complicated variation of $(\tau + \sigma_a + \pi_a)/\rho$ with energy. The variation of this quantity for water was shown in Figure III-6. The variation for air will closely parallel that for water. The peaks in Figure VIII-3 will correspond to the minima of Figure III-6 since in Figure VIII-3 we

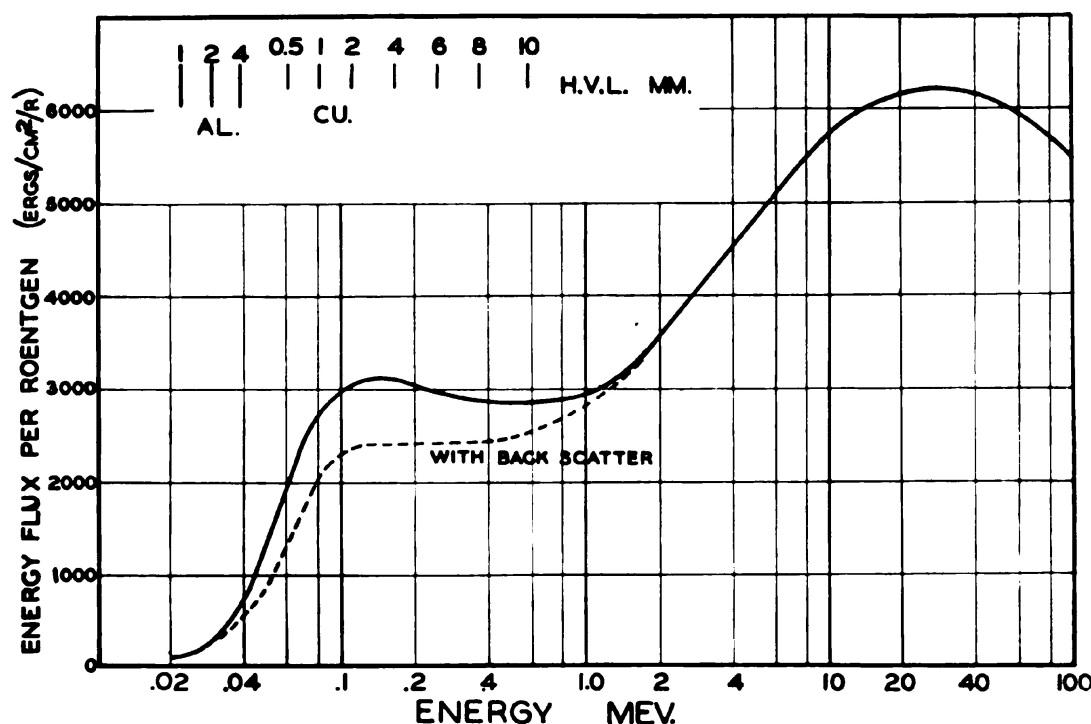


Figure VIII-3. Figure showing the variation of energy flux required to record 1 roentgen for energies from 10 Kv. to 100 Mev. Data taken from Mayneord (7, 8, 9). At low energies, the absorption coefficient of air is very large. Hence, a relatively small amount of radiation must pass through the detecting chamber before enough energy is absorbed to record a dose of 1 roentgen. Conversely, in the parts of the spectrum where the absorption coefficient of air is small, a large amount of radiation must pass through the chamber before enough energy is absorbed to record 1 roentgen. Thus when the real absorption coefficient is large the energy flux will be small and vice versa. Comparison of Figure VIII-3 with Figure III-6 will show that the energy flux reaches its peak values at energies corresponding to minimum values in the total real absorption coefficient.

have plotted a quantity proportional to the reciprocal of $(\tau + \sigma_a + \pi_a)/\rho$ (see equation 8-6). For example, Figure III-6 shows a sharp minimum at 100 Kv. while Figure VIII-3 shows a peak at this energy. We see that the energy which must pass through a cm.² to record a roentgen depends greatly on the energy of the radiation. At low energies, 40 Kv., the radiation is readily absorbed by the air and an incident flux of only 700 ergs/cm.² is required to yield a reading of 1 roentgen. At 100 Kv. the flux rises to about 3000 ergs/cm.². At 0.5 Mev. a slightly smaller energy flux is required to record a roentgen but the curve rises rapidly to reach a value of 6200 ergs/cm.² at 20 Mev. At very high energies (100 Mev.) the absorption coefficient of air increases because of pair production and thus the energy flux required to give a roentgen falls. In order to correlate the energy scale of Figure VIII-3 with the quality of the radiation a half value layer scale in mm. of aluminum and copper has been added. This scale was obtained from the relation between equivalent kilovoltage and half value layer shown in Figure V-4. For example, Figure V-4 shows that half value layer 4 mm. Cu. corresponds to an energy of 0.165 Mev.

These results may be used to investigate the integral dose for the 5 cm. circular field of section 8.02. The percentage backscatter for this field ($A = 19.6$ cm.² and H.V.L. 4.0 mm. Cu.) is 13% so that an air dose of 89r corresponds to a skin dose of 100r. From Figure VIII-3 we see that a flux of 3100 ergs/cm.² is required to give a skin dose of 1r. The energy flux into this field is therefore $3100 \times 19.6 \times 89 = 5.4 \times 10^6$ ergs. If all this were absorbed it would correspond to an integral dose of 64,000 gm.r. ($5.4 \times 10^6/85$). We saw, however, in section 8.02 that the integral dose down to the 10% isodose surface was 18,200 gm.r., a value less than one-third of this value. Mayneord (5, 6) has found that, in general, the integral dose to the 10% isodose curve is considerably less than the energy which enters the patient. This suggests that much of the energy which enters the patient is either absorbed beyond the 10% isodose surface or scattered from the patient.

8.05 PROTECTION CONSIDERATIONS

The tolerance dose is set at 0.05r per day in Canada. This must be interpreted as being the tolerance dose when all parts of the body receive this dose. Certainly a dose far greater than this could be given a small area of the skin every day of the year with no ill effect. We can calculate the integral dose received by a man in one year exposed to 0.05r/day. Suppose the radiation has a half value layer

of 2.0 mm. Cu. Then the energy flux per recorded roentgen measured with backscatter is 2400 ergs/cm.² (Fig. VIII-3). If we estimate the area of the anterior surface of the body as 30 cm × 70 cm. = 2100 cm.², we can calculate the total energy flux entering the body. The energy absorbed in 48, six-day weeks will be

$$2100 \times (2400) (.05) (6) \times 48 = 72.6 \times 10^6 \text{ ergs} = 0.85 \text{ megagm.r.}$$

If radiation at 2 mm. Al. were considered the integral dose would be about 1/5 this value (Fig. VIII-3). For high energy radiation the integral dose would be larger, although not as much greater as Figure VIII-3 indicates, because at high energies the person would not be thick enough to absorb all the incident radiation.

Since the integral dose determines constitutional changes, a person will not be able to tolerate as big a skin dose of high energy radiation, as low. It has been the policy in recent years to reduce continually the allowed tolerance dose. This is wise when one considers the larger integral dose which can result from the more recently produced high energy radiations. It might be advisable to state tolerances in terms of a maximum allowable skin dose for a small area and a maximum integral dose in gm.r. for whole body irradiation.

The integral dose of 0.85 megagm.r. determined above is of the same order of magnitude as may be given a patient in a course of x-ray treatments. In section 8.02 we obtained an integral dose of 0.018 megagm.r. from a 5 cm. circular field for a dose of 100r to the skin. The yearly tolerance dose would therefore correspond to a skin dose of 4700r [100(0.85)/0.018] on a single 5 cm. circular field. The difference in the biological effects of the two is of course partly to be found in the effects of fractionation.

8.06 ENERGY ABSORPTION IN BIOLOGICAL MATERIAL

In section 8.01 we saw that when a dose of 1 roentgen was given to 1 gm. of air the energy absorption was 85 ergs. We now enquire into the amount of energy absorbed when 1 roentgen is given to 1 gm. of typical biological material such as fat, muscle, and bone. Suppose 1 gm. of biological material and 1 gm. of air are placed in the same beam of radiation of energy flux E (ergs/cm.²). The energy absorbed by a gram of biological material will be $(\tau + \sigma_a + \pi_a)_b E / \rho$. This can be written in terms of the electronic absorption coefficients as $(e\tau + e\sigma_a + e\pi_a)_b \cdot (N_o)_b \cdot E$ where $(N_o)_b$ is the number of electrons per gm. of biological material and $(e\tau + e\sigma_a + e\pi_a)_b$ is the real absorption coefficient per electron for the biological material. A similar expression holds for the energy absorbed by the gm. of air. If the air

is given a dose of 1 roentgen then the energy absorbed is 85 ergs. Hence the energy absorbed by the biological material E_a will be given by

$$E_a = \frac{(e\tau + e\sigma_a + e\pi_a)_b}{(e\tau + e\sigma_a + e\pi_a)_{air}} \cdot \frac{(N_o)_b}{(N_o)_{air}} \cdot 85 \text{ ergs/gm. roentgen} \quad (8-7)$$

Biological material is in general complex in nature and is made up of materials of different Z . In the low energy region where the photoelectric effect is important and depends on $Z^{2.94}$, the effective atomic number \bar{Z}_L may be determined using equation (4-2). In the very high energy (pair production) region where the absorption per electron depends on Z , the effective atomic number \bar{Z}_h may be determined as follows

$$\bar{Z}_h = (a_1Z_1 + a_2Z_2 + a_3Z_3 \dots \dots) \quad (8-8)$$

where the quantities $a_1, a_2, a_3 \dots \dots$ are the fractional contents of electrons belonging to atoms of atomic number $Z_1, Z_2 \dots \dots$. In the region where Compton absorption alone is important the energy absorption is independent of Z . Fortunately at no energy (see Fig. III-6) are both pair production and photoelectric absorption possible. If this were the case an effective atomic number could not be defined. Values for Z_L and Z_h as well as the number of electrons per gm., (N_o) and ρ , are listed in Table X. Values for N_o and \bar{Z}_L have been taken directly from Spiers (11). Values for \bar{Z}_h have been calculated from the average chemical compositions of muscle, fat and bone (2).

TABLE X
DATA CONCERNING ATOMIC NUMBERS OF BIOLOGICAL MATERIAL

Material	Density ρ	Number electrons per gm. (N_o)	\bar{Z}_L	\bar{Z}_h
Air	0.001293	3.03×10^{23}	7.64	7.36
Water	1.00	3.34×10^{23}	7.42	6.60
Muscle	1.00	3.36×10^{23}	7.42	6.60
Subcutaneous				
fat	0.91	3.48×10^{23}	5.92	5.2
Bone	1.85	3.00×10^{23}	13.8	10.0

Using the tabulated values of Table X and the known real absorption coefficients (see Chapter III) Spiers (11) has calculated E_a (equation 8-7) for energies up to 830 Kv. The author has extended these calcu-

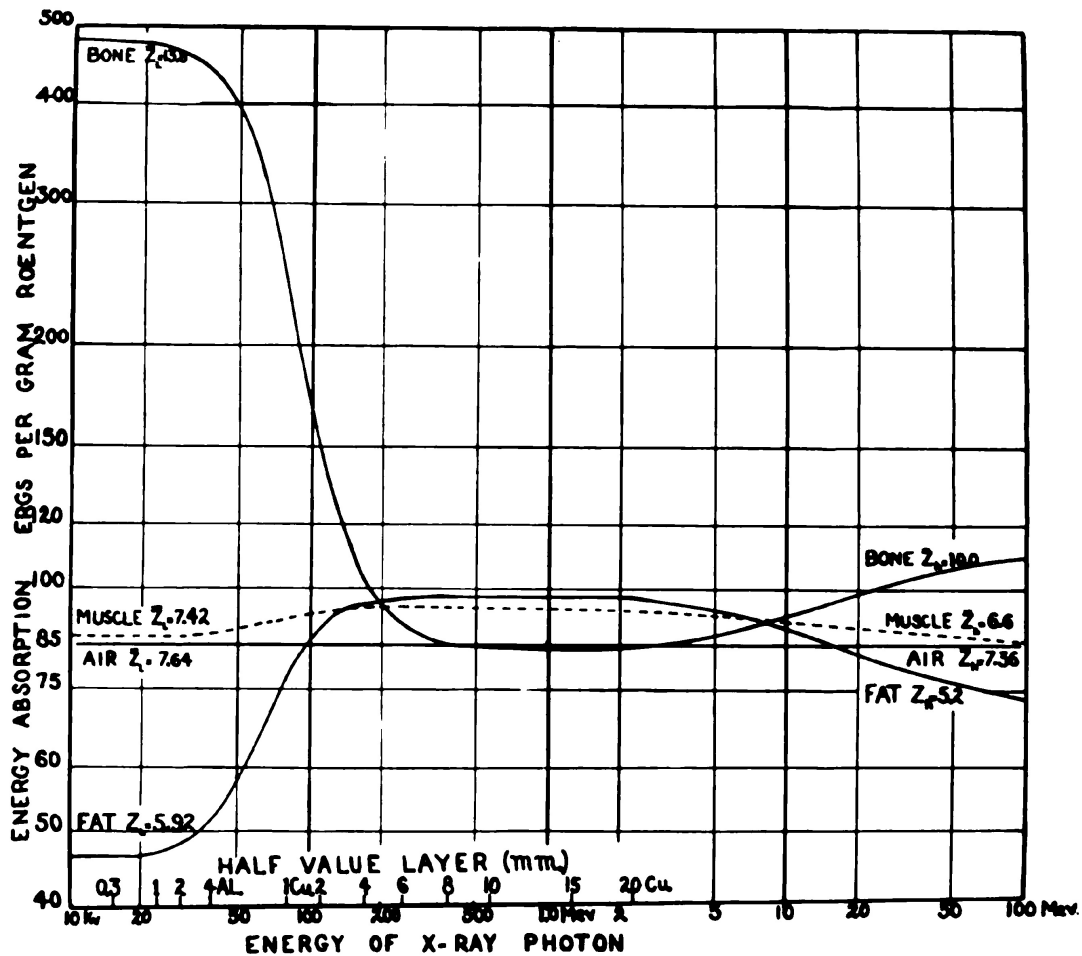


Figure VIII-4. Graph showing the variation of the energy absorption in biological material for energies ranging from 10 Kv. to 100 Mev. (2, 11).

lations to energies up to 100 Mev. (2) and all the results are shown graphically in Figure VIII-4. Here the energy absorbed per gm. roentgen is plotted against a logarithmic energy scale for air, muscle (or water), fat and bone. The energy scale has been correlated with a half value layer scale using Figure V-4. The rather complicated nature of these graphs may be understood by detailed examination of equation (8-7). In the very low energy region the photoelectric coefficient $\epsilon\tau$ is much greater than $\epsilon\sigma_a$ or $\epsilon\pi_a$ so that equation (8-7) reduces to

$$E_a = \frac{(\epsilon\tau)_b}{(\epsilon\tau)_{air}} \cdot \frac{(N_o)_b}{(N_o)_{air}} \cdot 85 \text{ ergs/gm.r.}$$

Since the photoelectric coefficient depends on $\bar{Z}_L^{2.94}$ this may be written

$$E_a = \frac{(\bar{Z}_L^{2.94})_b}{(\bar{Z}_L^{2.94})_{air}} \cdot \frac{(N_o)_b}{(N_o)_{air}} \cdot 85 \text{ ergs/gm.r.} \quad (8-9)$$

Since the number of electrons per gm. of all the materials listed in Table X have about the same value, equation (8-9) shows that 1 gm. of bone ($\bar{Z}_L = 13.8$) should absorb about $13.8^{2.94}/7.64^{2.94} = 5.7$ times as much energy as 1 gm. of air ($\bar{Z}_L = 7.64$). This is well illustrated in Figure VIII-4 where we see that 1 gm. of bone, air and fat absorb 485 ergs, 85 ergs and 46 ergs respectively for a dose of 1 roentgen. This exceedingly large energy absorption by bone in the low energy region is of considerable clinical significance (see section 8.08).

In the energy region from 400 Kv. to about 5 Mev., $e\sigma_a$ is much greater than $e\tau$ or $e\pi_a$ so that equation (8-7) reduces to

$$E_a = \frac{(e\sigma_a)_b}{(e\sigma_a)_{air}} \cdot \frac{(N_o)_b}{(N_o)_{air}} \cdot 85 \text{ ergs/gm.r.}$$

Since the Compton electronic coefficients are independent of Z (i.e., $(e\sigma_a)_b = (e\sigma_a)_{air}$) this further reduces to

$$E_a = \frac{(N_o)_b}{(N_o)_{air}} \cdot 85 \text{ ergs/gm.r.} \quad (8-10)$$

In this region except for slight variations in the number of electrons per gm. all materials absorb 85 ergs per gm.r. In this region the curves of Figure VIII-4 run essentially parallel. It will be seen that 1 gm. of fat absorbs slightly more energy than 1 gm. of bone because of the larger number of electrons per gm. In the intermediate region from 30 Kv. to 400 Kv. no simplification of equation (8-7) is possible.

In the very high energy region $e\pi_a$ becomes much greater than $e\sigma_a$ and equation (8-7) reduces to

$$E_a = \frac{(e\pi_a)_b}{(e\pi_a)_{air}} \cdot \frac{(N_o)_b}{(N_o)_{air}} \cdot 85 \text{ ergs/gm.r.}$$

Since the electronic pair production coefficient depends directly on \bar{Z}_h this equation simplifies to give

$$E_a = \frac{(\bar{Z}_h)_b}{(\bar{Z}_h)_{air}} \cdot 85 \text{ ergs/gm.r.} \quad (8-11)$$

Equation (8-11) is reasonably accurate at 100 Mev. but in the transition region from 5 Mev. to 100 Mev. the exact expression of equation (8-7) must be used. At these very high energies we find that bone ($\bar{Z}_h = 10.0$) should absorb about twice as much energy per gm. as fat ($\bar{Z}_h = 5.2$). For betatron radiation with peak energy at 25 Mev. we would not expect a very great variation in the absorption per gm. from fat to bone.

From Figure VIII-4 we see that for half value layers from 0.3 mm. Al. to 0.5 mm. Cu. the preferential absorption by bone is very serious. This is the reason why regions involving cartilage should not be treated with soft radiation. Although soft x-rays and a teleradium unit (Fig. VI-11) may give the same formal depth dose the biological effect of the two radiations will be very different.

8.07 THE EFFECT OF BONE AND FAT ON DEPTH DOSE DATA

The published depth dose data are all based on measurements made with a water or water-like phantom. From Figure VIII-4 we would expect this would give accurately the depth dose in muscle. Spiers (11) has made an effort to correct for this, using his measured absorption coefficients for bone and fat. He has investigated the problem of a beam of radiation directed towards a tonsillar region

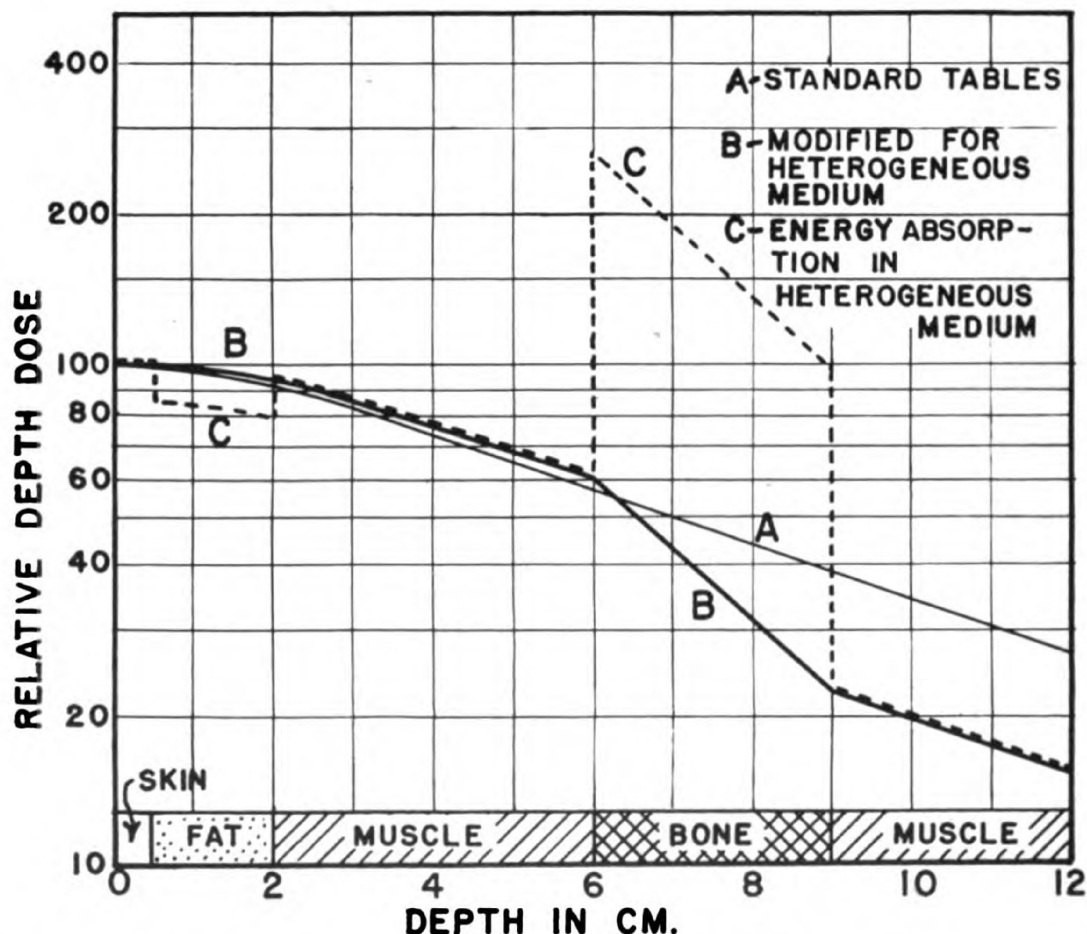


Figure VIII-5. Relative depth dose for a beam of radiation, H.V.L. 1.5 mm. Cu., F.S.D. 50 cm., area 100 sq. cm., directed into a composite phantom consisting of consecutive layers of skin, fat, muscle, bone and muscle. Data taken from Spiers⁽¹²⁾.

through layers of skin, fat, muscle, bone and muscle. His results are shown in Figure VIII-5 where the dimensions of the various layers are shown along the horizontal axis. Curve A represents the variation of depth dose in a water phantom for 100 cm.², F.S.D. 50, H.V.L. = 1.5 mm. Cu. taken from standard tables. In the heterogeneous medium the depth dose is given by curve B. The layer of bone reduces the depth dose for points beyond and layers of fat tend to increase it. Curve C on the same graph gives the relative energy absorption per cm.³ at different depths. It will be seen that the bone 6 cm. below the surface absorbs more energy per cm.³ than does the surface layer.

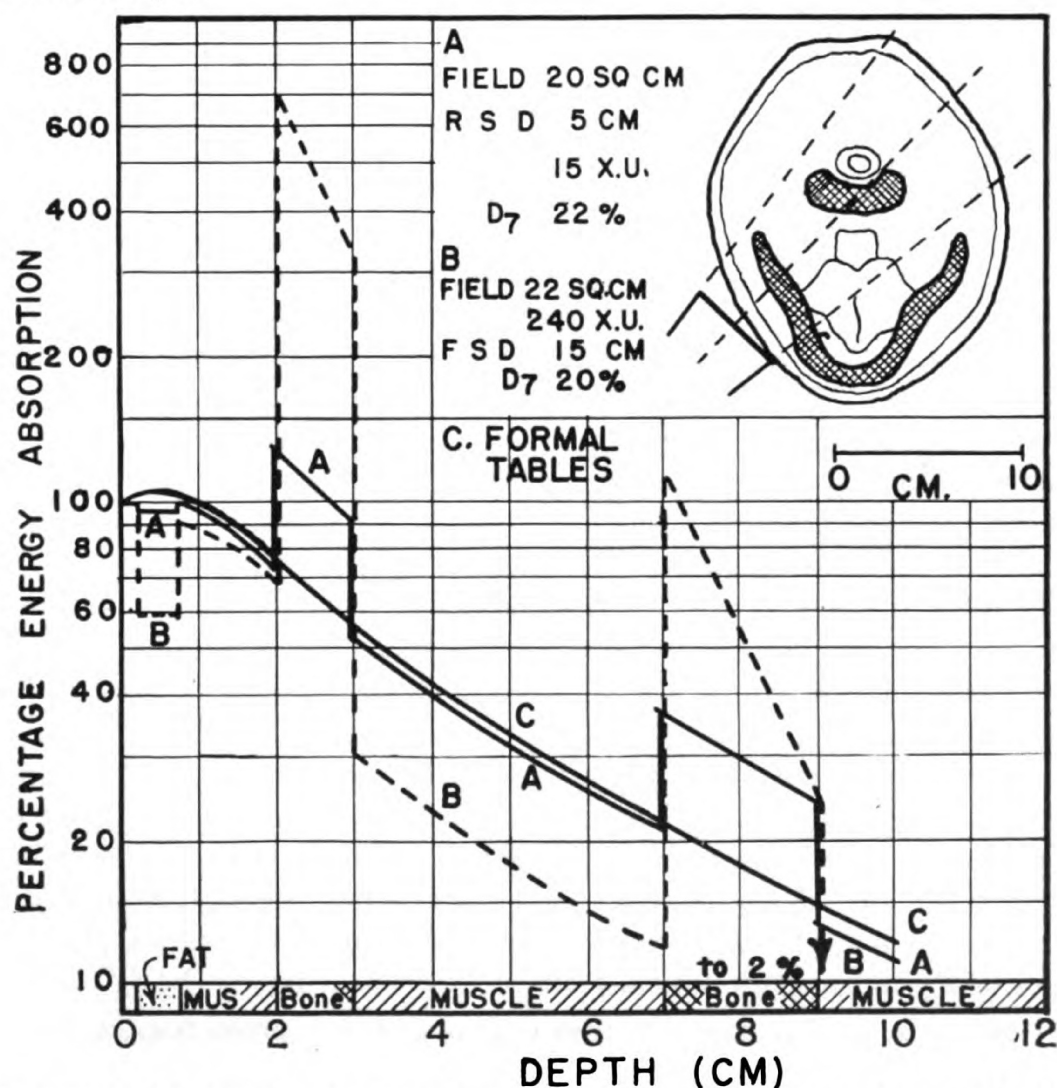


Figure VIII-6. Graph showing the percentage energy absorption for a field directed through the lower jaw into the tonsillar region, using techniques A, B and C. Technique A—Radium beam unit, F.S.D. 5 cm., $\lambda = 0.015A$, (D_7) = 22%. Technique B—140 Kv. X-rays, F.S.D. 15 cm., $\lambda = 0.240A$, (D_7) = 22%. Technique C—Formal depth dose tables. Data taken from Spiers⁽¹²⁾.

8.08 COMPARISON OF TECHNIQUES GIVING THE SAME FORMAL DEPTH DOSE

Using the same composite phantom discussed in section 8.07, Spiers (11) has compared two different techniques A and B which give the same formal depth dose. His results are shown in Figure VIII-6. The beams are applied in the direction of the tonsillar region through the lower jaw. The details of the two techniques are as follows.

Technique A Radium beam, 5 cm. F.S.D., $\lambda = 0.015A$ and $(D_7) = 22\%$

Technique B 140 Kv. x-rays, 15 cm. F.S.D., $\lambda = 0.240A$ and $(D_7) = 22\%$

Although technique A, using a teleradium unit, produces very penetrating radiation, the depth dose is small because of the short focal skin distance. Both techniques give 22% at 7 cm. depth. Curve C is the formal depth dose curve. Curve A gives the energy absorption per cm.³ when the gamma ray technique is used and curve B the corresponding curve for the x-ray technique. It will be seen that curve A does not differ too greatly from the formal depth dose curve while curve B is very different. In particular, in the muscular region behind the jaw, the energy absorption per cm.³ is much smaller for technique B because of the shielding effect of the bone for soft radiation. On the other hand, technique B delivers between four and five times as much energy to the jaw as does technique A. If, therefore, a tumor lay between 4 and 6 cm. from the skin, technique A would deliver almost twice the energy to it as technique B with only one quarter as much energy being given the bony structure of the jaw.

The dose received by bone situated below soft tissue is of considerable clinical importance. In some cases of skin lesions located on the back of the hand, or the forehead, the bony structures may be within 0.5 cm. of the surface. Spiers (11) has calculated the dose given such bone for a variety of techniques and his results replotted in slightly different graphical form are shown in Figure VIII-7.

Here the energy absorption in ergs per cm.³ is given for the bone at depths of 0.5, 1.0, 3.0 and 5.0 cm. below the surface when the surface is given a dose of 1 r. These results will, of course, depend on focal skin distance, so a field of 5 cm. diameter at F.S.D. 30 cm. has been assumed for all radiations. The half value layers of the different radiations are shown along the horizontal axis. It will be seen that

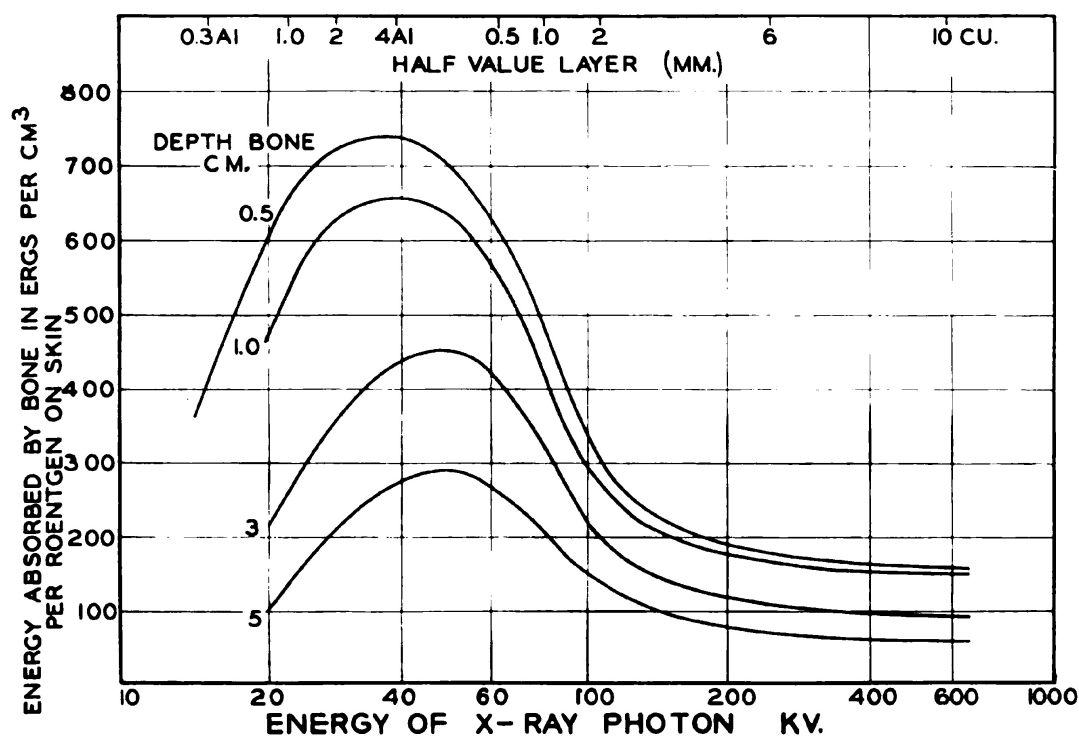


Figure VIII-7. Graph showing the variation of energy absorbed by bone (ergs/cm.³/roentgen on the skin) with the energy of the x-ray beam for the bony structure at depths of 0.5, 1.0, 3 and 5 cm. below the skin. Data taken from Spiers⁽¹²⁾.

all the curves show a maximum at half value layers of about 4 mm. of aluminum. At very short wavelengths the depth dose is high but the energy absorption per cm.³ of bone is small, hence the energy absorbed is small. At long wavelengths the depth dose is very small and even though the energy absorption per cm.³ of bone at this wavelength is large for a given dose, the net result is small. At medium wavelengths we find the maximum effect. These graphs indicate that such lesions should be treated either with very soft x-rays or with hard gamma rays if bone damage is to be avoided.

There is no doubt that more work along these lines will be carried out. Recently Spiers (12) and Wilson (13) have carried out investigations of the ionization produced in small cavities within bone such as in the Haversian canals. These discussions point to the use of hard radiation whenever bony structures are involved. Further work on actual depth dose data and energy absorption in real phantoms is required.

REFERENCES

1. Johns, H. E., Darby, E. K., Watson, T. A., Burkell, C. C.: *Brit. J. Radiol.*, 23:290, 1950.
2. Johns, H. E.: *Medical Physics*. Chicago, Yr. Bk. Pub., 1950.

3. Mayneord, W. V.: *Proc. Phys. Soc.*, 54:405, 1942.
4. Mayneord, W. V.: *Acta of the International Union against Cancer*. 11:271, 1937.
5. Mayneord, W. V. and Clarkson, J. R.: *Brit. J. Radiol.*, 17:151, 1944.
6. Mayneord, W. V.: *Brit. J. Radiol.*, 17:359, 1944.
7. Mayneord, W. V.: *Brit. J. Radiol.*, 13:235, 1940.
8. Mayneord, W. V.: Bulletin of the National Research Council CRM 315. Chalk River, Ont., July, 1946.
9. Quimby, E. H. and Lawrence, G. C.: *Radiology*, 35:138, 1940.
10. Smithers, D. W.: *Brit. J. Radiol.*, 15:50, 1942.
11. Spiers, F. W.: *Brit. J. Radiol.*, 10:52, 1946.
12. Spiers, F. W.: *Brit. J. Radiol.*, 22:521, 1949.
13. Wilson, C. W.: *Brit. J. of Radiol.*, 23:92, 1950.

Chapter IX

RADIUM AND ITS ACTIVE DEPOSITS

9.01

NATURAL RADIOACTIVITY

ALL of the heavier nuclei that contain more than 239 particles prove to be unstable and so eject particles to form new nuclei. This disintegration process will continue until a stable nucleus is formed. There are three main radioactive series which begin with uranium, actino-uranium, and thorium, and disintegrate through a long series until stable lead is produced. We can form a mental picture of this by imagining the protons and neutrons to be in motion inside the nucleus. Each nucleus will be characterized by a certain energy and if, by a series of chance encounters, one particle acquires more than its normal share of energy, it may have enough energy to escape from the nucleus. This ejection process is purely one of chance and there is no way to decide when a particular nucleus will disintegrate. We can say, however, that given a large enough number of nuclei a certain percentage will disintegrate in a given time. In this disintegration process three "particles" are ejected, called alpha, beta and gamma rays.

9.02

THE ALPHA PARTICLE

This particle is actually a helium nucleus consisting of two protons and two neutrons. It has a positive charge of 2 units and a mass of 4 units. The alpha particle, on striking a fluorescent screen, can produce enough light to be made visible to the human eye. A given alpha particle emitter will give alpha particles of very definite energies. For example, radon gives off one type of a particle with energy 5.49 Mev. Radium gives two alpha particles with energies 4.79 and 4.61 Mev. Sometimes the alpha particle "spectrum" is quite complicated, showing as many as 12 components.

The alpha particle, although its energy is great, is stopped in a few centimeters of air. In travelling through the air the large particle with its positive charge removes electrons from the atoms along its path and produces intense ionization. In general, the path of an alpha particle is straight because of its large mass but at times one will collide with a nucleus and be deflected. Figure IX-1a shows



Figure IX-1. Cloud chamber photograph of alpha, beta and gamma ray tracks. J. B. Hoag: *Electron and Nuclear Physics*, courtesy D. Van Nostrand Co.

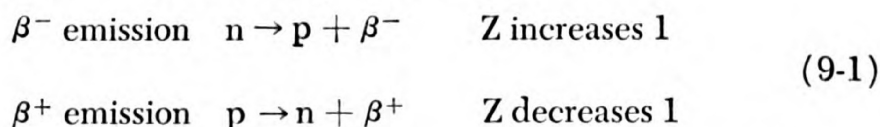
the track of an alpha particle made visible in a cloud chamber. Alpha tracks produce from 3000 to 7000 ion pairs per mm. of path in air. The cloud chamber track is, consequently, a very dense one. The ranges of alpha particles are from 2 to 10 cm. in air, depending on their origin. A common range is about 4 cm. of air. They are stopped completely by a thick sheet of paper. When an alpha particle is emitted the new nucleus formed has a mass number 4 less and atomic number 2 less than the parent.

9.03

BETA DECAY

Many radioactive disintegrations are accompanied by the ejection of a positive or a negative electron from the nucleus. The electrons under these circumstances are often called beta particles. The nucleus which emits the electrons is called a positron or negatron emitter. It might well be asked how an electron may be emitted from the nucleus when there are no electrons in the nucleus. If a β^- (negative electron) is emitted we consider that a neutron within the nucleus changes into a proton and a negative electron. Such a transformation will leave the mass number the same (the electron mass is negligible compared with the proton or neutron) but the atomic number Z will increase by one since there is now one more proton in the nucleus.

In a β^+ (positive electron) emission we consider that a proton changes into a neutron and a positive electron. In this case Z will decrease by one since there is now one fewer proton in the nucleus. Symbolically these reactions may be written



The beta particle which is ejected from a beta active nucleus may have any energy from zero up to a definite maximum value which is

characteristic of the parent nucleus. This is illustrated in Figure 9-2 which gives the distribution of β ray energies from radioactive phosphorus (P^{32}) (1). The most probable energy is considerably less than the maximum. In general, the average energy is about one-third the maximum. This means that one nucleus can disintegrate giving a beta ray of maximum energy 1.72 Mev. whereas the next nucleus to disintegrate may give a beta particle with only 0.5 Mev. energy. The question can well be asked, "Where has the rest of the energy gone?" Modern theory indicates that in a beta disintegration a neutrino is also ejected and this neutrino carries the rest of the energy. This means that each disintegration corresponds to the release of the maximum energy but this energy may be distributed in any way between the two particles. For example, if the beta particle has an energy of 1.0 Mev. then the corresponding neutrino will have an energy of 0.72 Mev. The neutrino is a neutral particle with a mass which is small when compared with the electron. Since it has no charge it can produce no ionization and hence cannot be made

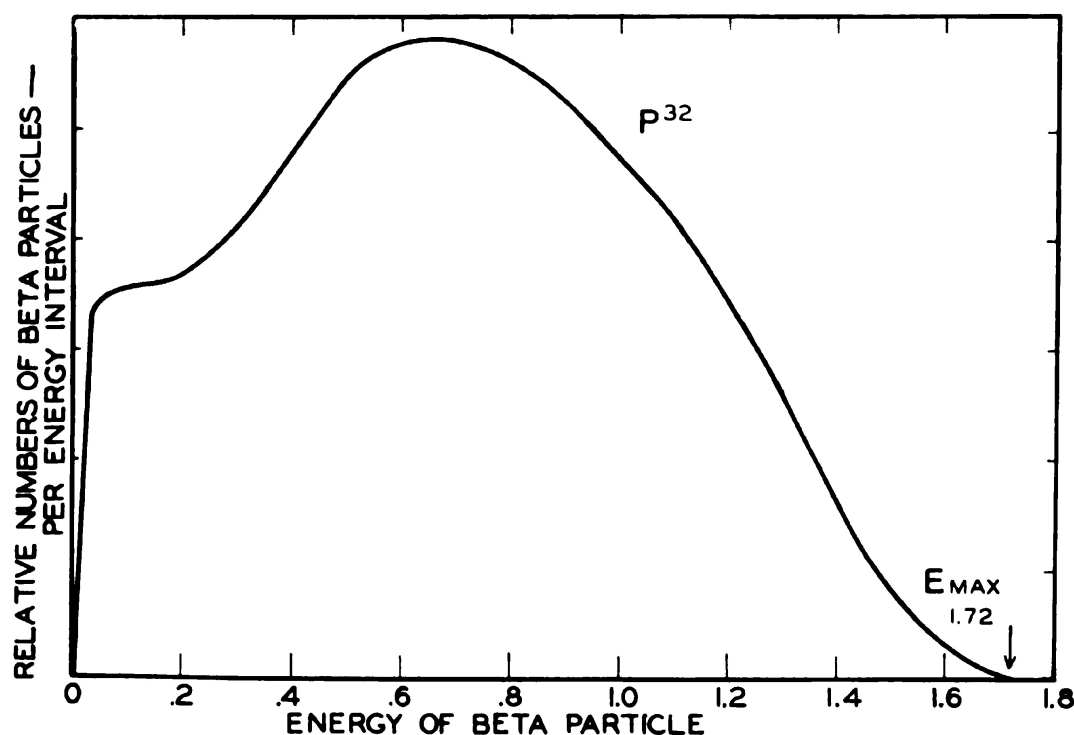


Figure IX-2. Beta decay graph showing the relative numbers of beta rays as a function of energy for radioactive phosphorous. In the decay of radioactive phosphorous a certain number of beta particles are ejected with each energy or in each small energy interval. The vertical scale gives the relative number which are emitted in each of the energy intervals up to the maximum of 1.72. For example, it is seen that there are about twice as many particles emitted with an energy of 0.6 Mev. as of 1.2 Mev.

visible in a cloud chamber. Neutrons also carry no charge and so cannot be observed in a cloud chamber except indirectly, by setting another particle such as a proton into motion through collision. The recoil proton leaves a dense track in the cloud chamber. The neutrino, however, has a mass which is much smaller than that of an electron so that it can set no particle in motion through collision. The neutrino has properties which make it very difficult to observe and, as a result, no one has yet detected it, although many have tried. However, there is considerable theoretical justification for the postulate that neutrinos do exist. Without this postulate it would be necessary to forego the much cherished physical principles of conservation of energy and momentum.

Although we cannot specify what energy a particular beta particle will have, we can state definitely that no beta particle from radioactive phosphorus will have an energy greater than 1.72 Mev. This maximum energy, called the end point of the spectrum, is characteristic of the emitter and is the value usually given in tables. Maximum beta ray energies ranging from 0.01 Mev. to 4 or 5 Mev. are common. When a beta ray emitter is injected into a patient the energy absorbed will correspond to the mean energy and not to the maximum energy of the beta particles. The energy carried away by the neutrino is not absorbed by the patient. The mean energy of a beta emitter can only be determined accurately if a curve such as given in Figure IX-2 is available. However, for many purposes, the mean energy may be taken as $\frac{1}{3}$ of the maximum energy. Although the energies of beta particles are often less than those of alpha particles their range is very much greater. Some ranges of electrons were given in Chapter IV, Table VII. The track of a beta particle in a cloud chamber is shown in Figure IX-1. It will be seen that the track is not dense, as in the case of the alpha ray, indicating that the ion density along its path is small. The number of ion pairs produced per cm. of path in air by a beta particle depends on its energy and varies from about 1000 for 10 Kv. electrons to about 45 for 1 Mev. electrons. Just before the electron is stopped the specific ionization reaches a value of over 8000 ion pairs per cm. producing a dense end to the track. Since the specific ionization is much smaller for a beta than for an alpha particle the ranges will be correspondingly greater. For example, the maximum range of the beta particle from RaC ($E_{\max.} = 3.15$ Mev.) is about 12 meters in air. Usually the electron tracks are very circuitous for a close approach to another electron or nucleus will change the direction of the beta particle materially because of its

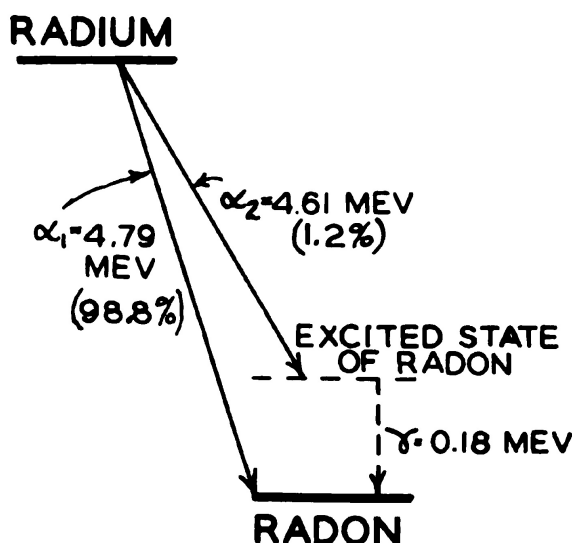


Figure IX-3. Energy level diagram for radium showing the two modes of disintegration into radon.

small mass. The beta ray spectrum from the decay products of radium is very complicated because there are superimposed the beta particles from Radium B ($E_{\max.} = 0.65$ Mev.); Radium C (3.15 Mev.); Radium D (0.025 Mev.); and Radium E (1.17 Mev.). Except in a relatively small number of applications, to be discussed in section 10.12 on beta ray applicators, the radium salt is always enclosed in a layer of platinum or gold of sufficient thickness to absorb all the beta particles. For most uses of radium, the gamma radiation alone need be considered.

9.04 THE GAMMA RAY

The third "particle" which can be emitted in a radioactive disintegration is not a particle at all but a photon carrying a certain amount of energy. The gamma rays from a given material have a very definite energy. A given disintegration may be accompanied by several gamma rays, but these will all have a very definite energy. When an alpha particle or beta particle is ejected the new nucleus formed may have an excess of energy and this energy will be radiated in the form of a gamma ray. A particularly simple case is that of the disintegration of radium into radon in which two different range alpha particles and a gamma ray are emitted. The mode of disintegration is shown in Figure IX-3; 98.8% of the time radium shoots out an alpha particle with energy 4.79 Mev. giving radon. However, 1.2% of the time an alpha particle with energy 4.61 Mev. is ejected. This leaves the radon in a state with an excess energy of $4.79 - 4.61 = 0.18$ Mev.

This excess energy is radiated in the form of a gamma ray of energy 0.18 Mev. The same sort of thing may happen in a beta ray disintegration. The new nucleus may find itself in an excited state and radiate the excess energy as a gamma ray. The gamma ray of 0.18 Mev. is, of course, in no way different from the maximum energy x-ray produced in an x-ray tube operating at 180 kilovolts.

The cloud chamber "track" of a gamma ray is shown in Figure IX-1c. Actually the gamma ray leaves no track except by setting electrons within the cloud chamber in motion. The many short tracks coming from the central region of Figure IX-1c are actually short electron tracks similar to those of Figure IX-1b. It will be seen that these tracks are projected slightly in the forward direction. For a higher energy gamma ray this effect would be more pronounced. Gamma ray energies from radioactive materials range from a fraction of an Mev. to several Mev.

9.05 RADIOACTIVE DISINTEGRATION

As indicated before, there is no way to determine when a given atom will disintegrate, for such disintegration is purely a matter of chance. Suppose there are N atoms present at zero time. The change in this number, ΔN , (i.e., the number which will disintegrate) which will occur in a short time Δt will be proportional to the number N which are present and to the interval of time Δt . If twice as many atoms were present we would expect twice the disintegrations. Also if twice the time were considered we would expect twice the number of disintegrations. Symbolically this fact may be written

$$\Delta N = -\lambda N \Delta t \quad (9-2)$$

where λ is the constant of proportionality called the transformation constant. The negative sign indicates that the number of atoms present is decreasing. If in equation (9-2) we consider an interval of time Δt equal to 1 second we see that *the number of disintegrations per second* is λN . λ is exactly analogous to the linear absorption coefficient μ and equation (9-2) is of exactly the same form as equation (3-2). The transformation constant of radon is $2.10 \times 10^{-6} \text{ sec.}^{-1}$. If we had a sample of radon containing 1 million atoms (10^6) we would expect on the average 2.10 disintegrations every second. However, after a few hours the number of atoms of radon left would be considerably less than the original number of 1 million so that the number which disintegrate per second would also be less. Equation (9-2) is only valid when a short enough interval of time is considered so that the number of atoms present has remained essentially constant. For

radon this would certainly be true for an hour or two. To find the number present at any later time "t" equation (9-2) must be integrated to yield

$$N = N_0 e^{-\lambda t} \quad (9.3)$$

In this expression N_0 is the number of atoms present at zero time and N is the number left at a later time t . This equation is of the same form as equation (3-3).

The time required for half the atoms to disintegrate is called the half life T_h . It is related to the transformation constant λ by the relation

$$\lambda T_h = 0.693 \quad (9-4)$$

which is of the same form as $\mu(\text{H.V.L.}) = 0.693$ given in equation (3-4). For the case discussed above $\lambda = 2.10 \times 10^{-6} \text{ sec.}^{-1}$ $T_h = 0.693 / 2.10 \times 10^{-6} = 3.30 \times 10^5 \text{ sec.} = 3.83 \text{ days}$. This means that in 3.83 days one-half the atoms of radon will disintegrate. In the next 3.83 days one-half of the atoms which are left will disintegrate leaving 25% of the original number. After another half life only 12.5% of the original atoms will remain. This decay is shown graphically in Figure IX-4. If the same data were plotted on a semi-logarithmic scale a

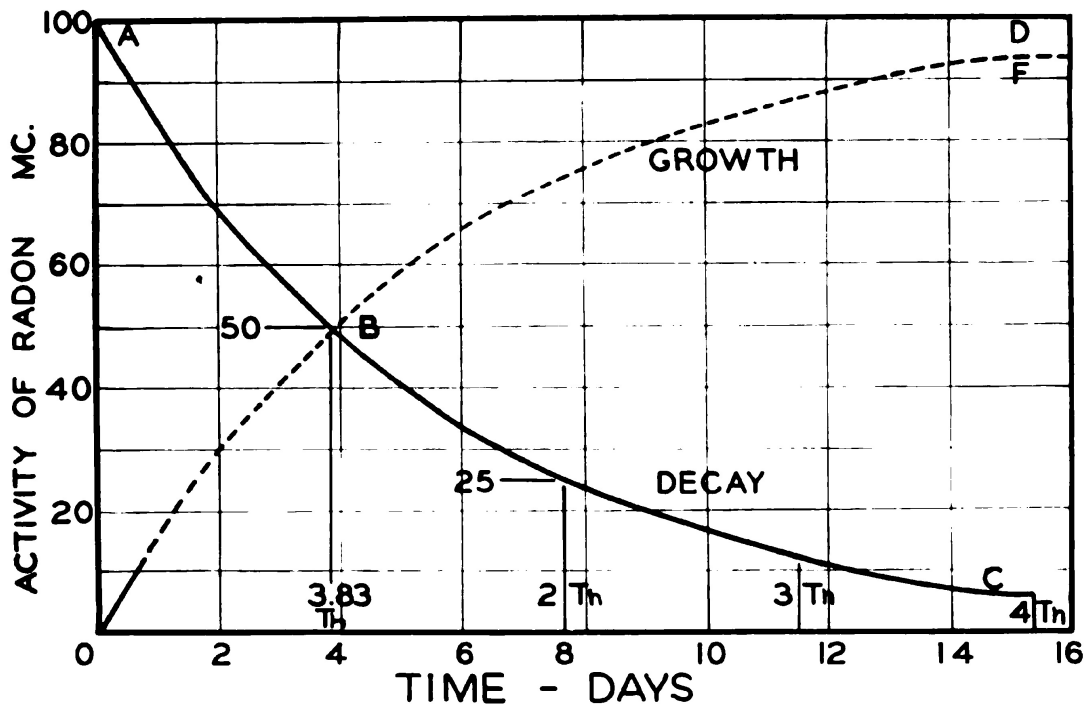


Figure IX-4. Graph showing the growth OBD and the decay ABC of radon.

straight line would result. Half lives ranging from a millionth of a second to millions of years are found occurring in nature. Each radioactive material has its own particular transformation constant and half life and it is impossible to change these constants by any physical methods.

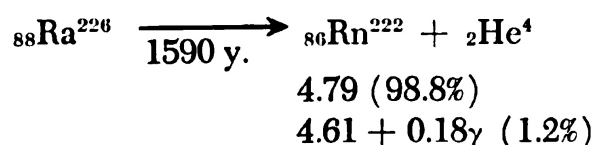
In calculating the emitted dose from a decaying source, use is made of the idea of average life (T_a). T_a is the average length of time that an atom exists. Half the atoms present decay in the first half life, T_h . In the next T_h fewer decay so that half the atoms live considerably longer than T_h . It follows that the average life T_a is greater than T_h . It can be shown mathematically that

$$\text{Average Life} = T_a = \frac{1}{\lambda} = \frac{T_h}{0.693} = 1.44 T_h \quad (9-5)$$

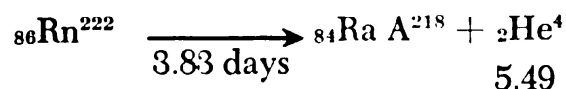
For radon the average life is $1.44(3.83) = 5.52$ days = 133 hours. This means that for radon the same dose is emitted if we consider the source to remain at constant strength for 133 hours and then fall to zero strength, as is actually emitted by the source decaying according to Figure IX-4.

9.06 RADIOACTIVE SERIES FROM RADIUM

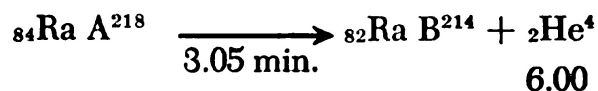
Radium is the 6th member of the Uranium Series and is produced by the disintegration of ionium. When radium is isolated from its parent it disintegrates with a half life of 1590 years to form radon. In this disintegration the radium ejects alpha particles to form the radon. The subsequent transformations are as follows: The half lives are given under the arrow and the numbers refer to the energies of the particles in Mev. For beta particles these energies are the maximum values.



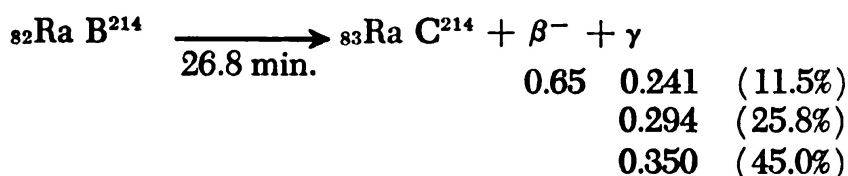
In 98.8% of the disintegrations one alpha particle is ejected with energy 4.79 Mev. In the rest of the disintegrations a lower energy alpha ray followed by a gamma ray is produced. Since the gamma ray energy is small and since it only occurs in 1.2% of the disintegrations, the gamma ray activity of radium can usually be neglected. The product nucleus radon (Rn) is a very heavy gas.



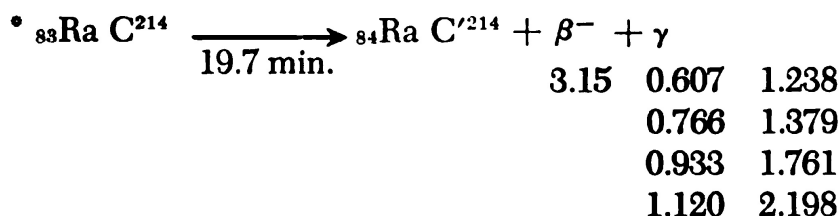
Radon shows only alpha ray activity.



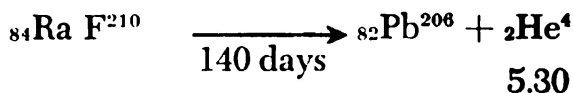
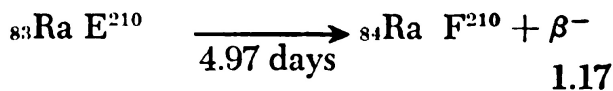
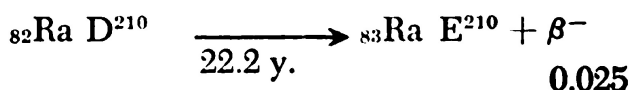
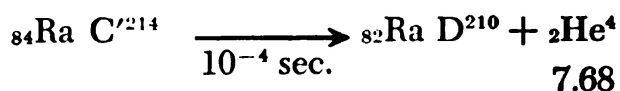
Radium A decays with a short half life by alpha ray disintegration.



Radium B produces beta rays of maximum energy 0.65 and three rather low energy gamma rays.



There are 8 main gamma ray lines with the energies shown. Actually many more have been observed. Because of the strong gamma lines with energies up to 2.2 Mev. the radiations from Ra C are very penetrating.



The final result of this chain is ${}_{82}\text{Pb}^{206}$, a stable isotope of lead.

*In 0.04% of its disintegration Ra C transforms into Ra C'' with the emission of an alpha particle, which in turn disintegrates by a beta emission into Ra D.

9.07

RADIOACTIVE EQUILIBRIUM

When a sample of radium is placed in a sealed container all of the products of the parent nucleus will be present after a short time. After a considerable time we will have radioactive equilibrium. This means that any element in the chain will be disintegrating at the same rate as it is being produced. If N_1 is the number of parent atoms present with decay constant λ_1 then the number disintegrating per second will be $N_1\lambda_1$. At equilibrium this will be equal to $N_2\lambda_2$, where the subscript 2 refers to the daughter element. At equilibrium $N_1\lambda_1 = N_2\lambda_2 = N_3\lambda_3$, etc. Since λ is inversely proportional to T_h (equation 9-4) this may be written

$$\frac{N_1}{T_{h1}} = \frac{N_2}{T_{h2}} = \frac{N_3}{T_{h3}} \quad (9-6)$$

where T_{h1} , T_{h2} stand for the half lives of the parent and daughter atoms respectively. Equation (9-6) shows that when an element has a small half life the number present will be small. For example, from the radioactive series, section 9.06, we see that after equilibrium has been established there will always be about 8 times 26.8/3.05 as many atoms of Ra B as Ra A present. The number of atoms of radium will decrease with a half life of 1590 yr. since there is no material present to replenish its supply. It follows that all the daughter products of radium present in the needle will decay with the half life of the radium. If at any time the needle sprung a leak some of the daughter radon would escape and the equilibrium conditions would be upset. Because of the long half life of radium we can consider that a radium needle which does not leak has a constant strength over many years.

9.08

**THE GAMMA RAY SPECTRUM OF RADIUM
 AND ITS ACTIVE DEPOSITS**

When either radium or radon is used for therapeutic purposes, the radon or radium is always placed in a container which will absorb all the alpha rays emitted and usually all the beta rays. Under such circumstances it is the gamma rays which produce the biological effect.

Radium and its equilibrium decay products emit an inhomogenous gamma ray spectrum containing 12 principal lines ranging from 0.18 Mev. to 2.198 Mev. Reference to section 9.06 will show that gamma rays are produced by the disintegration of radon, radium B and radium C. The 12 main lines are listed again in Table XI. In the

third column is shown the number of times on the average that the particular gamma ray is emitted for each 100 alpha ray disintegration of radium.

TABLE XI

PRINCIPAL GAMMA RAY LINES FROM RADIUM AND ITS ACTIVE DEPOSITS SHOWING THE RELATIVE NUMBERS OF GAMMA RAYS EJECTED FOR EACH 100 ALPHA RAY DISINTEGRATION OF RADIUM

<i>Transition</i>	<i>Energy of Gamma Ray (Mev.)</i>	<i>Relative Number</i>
Radium → Radon	0.18	1.2
Radium B → Radium C	0.241	11.5
	0.294	25.8
	0.350	45.0
Radium C → Radium C'	0.607	65.8
	0.766	6.5
	0.933	6.7
	1.120	20.6
	1.238	6.3
	1.379	6.4
	1.761	25.8
	2.198	7.4
		<hr/> 229.0

From Table XI we see that there is one line from radium, 3 lines from Ra B and 8 lines from Ra C. It will be observed that the penetrating gamma rays all arise from Ra C transitions. It is seen that on the average each alpha disintegration of radium is followed by 2.29 gamma rays.

The complicated spectrum can for many purposes be considered as equivalent to two lines of energy 0.55 and 1.65 Mev. Filtration of the radiations from radium will reduce the intensity of the low energy components thus producing a more penetrating beam. Protection problems are made difficult with radium because of the penetrating gamma ray of 2.2 Mev. energy. The complicated gamma ray spectrum from radium is of considerable disadvantage in teleradium units since filtration with its inherent reduction in intensity is required to

obtain a penetrating beam. At the same time the protection requirements must be designed to reduce the intensity of the 2.2 Mev. gamma line. A much more promising source for such units is Co^{60} which gives two gamma rays of 1.1 and 1.3 Mev. (see Chapter XII).

9.09 THE STRENGTH OF RADIOACTIVE SOURCES

The strength of a radium source is expressed in mg. or gm. of radium. The strength is not determined by weighing, however, but by comparison with certain standards. Madame Curie isolated the first chemically pure samples of radium salts and measured their activity. Any other radium source is compared with such a standard in terms of its activity. When radium is sealed into a tube it soon comes into equilibrium with its decay products. The activity which is measured is the gamma ray activity of radium B and radium C. If an unknown source shows the same gamma ray activity as a 1 mg. standard source then we say the unknown is a source of 1 mg.

Sometimes it is convenient to seal radon gas in a closed container and to use it instead of radium. The strength of such a source is measured in curies and millicuries. *The curie is that amount of radon in equilibrium with 1 gm. of radium.* Since the amount of Ra B, Ra C present depends on the amounts of radium or radon present, to say a seed has a strength of 1 mc. means that it has the same activity as 1 mg. of radium. The strength of a radon seed is measured by comparing its gamma ray activity with that of radium.

Early experiments with radon indicated that 1 curie of radon ejected 3.7×10^{10} alpha particles per second. Recently the term curie has been extended in meaning to include all natural and artificial radioactive materials. *Any material which disintegrates at the rate of 3.7×10^{10} disintegrations per second, regardless of the type of particle it ejects or the energy of these particles, is called a curie.* It must not be assumed that 1 curie of one material will produce the same effect as 1 curie of another material. *The curie is an activity unit only.* To find the dose given, other information concerning the energies of the particles, the arrangement of the source, etc. must be known. The terms, millicurie, mc., (10^{-3} curies) and microcurie, $\mu\text{c.}$, (10^{-6} curies) are also used extensively.

Some recent experiments indicate that 1 curie of radon (the amount of radon in equilibrium with 1 gm. of radium) may not disintegrate at exactly the value indicated above. However, regardless of the correct value of this constant, the curie for other materials should be taken as 3.7×10^{10} disintegration per second. It is un-

fortunate that the curie introduced originally to apply only to radium has been applied to all radioactive materials. An activity unit, the *rutherford*, has been suggested as an alternative unit. It is defined as an activity of 10^6 disintegrations per second.

9.10 THE DECAY OF RADON

Although 1 mg. of radium and 1 mc. of radon have the same initial activity, they will be very different sources of radiation after a few days. In the radium needle the radium continually replenishes the supply of radon which in turn keeps the supply of radium B and C constant. In the radon seed there is nothing to replenish the radon so the active deposits Ra B and C decay with the half life of the radon (3.83 days). Such a seed will decrease in activity by 8.7% in 12 hrs. or by 16.5% each day. The decay is shown graphically in Figure IX-4 and in tabular form in Table XII. Because of this rather rapid decay it is possible to leave a gold radon seed in tissue for ever. After a few weeks the seed loses its activity and becomes a small inert mass which will remain in the tissue without ill effects. This procedure may be more convenient than hospitalizing the patient while radium is being used.

TABLE XII
DECAY OF RADON AND EMITTED DOSE IN MILLICURIE HOURS

<i>Time (days)</i>	<i>Residue</i>	<i>Emitted Dose mc. hr.</i>	<i>Time (days)</i>	<i>Residue</i>	<i>Emitted Dose mc. hr.</i>
0	1.000	0	5.0	.404	79.1
0.50	.913	11.5	6.0	.337	88.0
1.00	.834	22.0	7.0	.281	95.5
1.5	.762	31.6	8.0	.235	101.7
2.0	.696	40.3	9.0	.196	106.9
2.5	.636	48.3	10.0	.163	111.3
3.0	.581	55.6	11.0	.136	114.9
3.5	.530	62.3	12.0	.114	119.9
4.0	.484	68.4	13.0	.095	111.3
4.5	.442	74.0	30 (∞)	0	133

For radium, the unit the mg. hour is a satisfactory unit of emitted dose. It is the dose emitted by 1 mg. of radium in one hour. It is not a satisfactory unit for measuring the dose received, for this will depend on factors such as distance, filtration, etc. For radon the corresponding unit is the mc. hour. One mc. hour gives exactly

the same emitted dose as 1 mc. hour. To calculate the emitted dose from a radon source, account must be taken of the decay of the radon.

This may be done as follows:

Since the average life of radon is 133 hours we know that 1 mc. allowed to decay completely will give the same emitted dose as if it remained at constant strength for 133 hours and then contributed no further effect. This is usually stated as follows:

$$1 \text{ mc. destroyed} = 133 \text{ mc.hr.} \quad (9-7)$$

Example 1: Suppose it is required to find the emitted dose from 2.5 mc. in three days. From Table XII we see that in three days a source with initial strength 1 mc. has decayed to 0.581 mc. Thus $1 - 0.581 = 0.419$ mc. have been destroyed. The emitted dose is $0.419 \times 133 = 55.6$ mc.hr. per initial mc. This value is given in the third column of Table XII. The total emitted dose from 2.5 mc. is $2.5 \times 55.6 = 139$ mc.hr. If 2.5 mg. of radium had been used for three days the emitted dose would have been $3 \times 24 \times 2.5 = 180$ mg.hr., a value greater than obtained above. The radon seed will contribute dosage at the same rate as the radium when it is first applied but the dosage rate will continually fall as the treatment progresses. The example shows how the emitted dose can be calculated for radon using the concept of mc. destroyed or by the use of the third column of Table XII.

Example 2: It is required to deliver an emitted dose of 260 mc. hrs. in eight days using radon. Find the required initial strength. From Table XII we see that 1 initial mc. will deliver 101.7 mc.hrs. in eight days. Hence the required seed strength is $260/101.7 = 2.56$ mc.

This type of problem and other more complicated ones involving the intermittent wearing of a radon mould may be done with ease on the radium dosage calculator designed by the author (3). A photograph of a commercial ruler based on this design is shown in Figure IX-5. For the solution of radon problems scales 9, 10, 11, 12 and 13 are used. The calculator has certain advantages over the tables when treatment periods other than whole days etc. are used. The other side of the calculator enables one to solve problems of radium dosage and is based on the Paterson Parker system to be discussed in the next chapter.

9.11 THE GROWTH OF THE ACTIVE DEPOSITS OF RADON

To obtain radon from radium, use is made of radon plants (2). In such plants a radium salt in solution is kept in a vacuum tight vessel in a safe. As the radium disintegrates the radon gas is liberated from the solution and collects above it. This radon gas may be pumped

off, purified and then forced into gold tubing or into a small glass bulb. Suppose a radon plant makes use of 100 mg. of radium. Then if the radon is allowed to collect until equilibrium occurs, 100 mc. of radon could be pumped off. The radon which has been removed will start to decay with half life 3.83 days (curve ABC, Fig. IX-4) and in the meantime the amount of radon in the plant produced by the radium will increase. The radon is thus in two portions, but we know that the activity of the two portions taken together must remain constant at 100 mc. (line AD, Fig. IX-4). This means that the radon in the plant will grow along the curve OBF such that the sum of the decay curve and the growth curve gives the line AD. Suppose a radon plant contains 500 mg. of radium. After one day's rest it should be possible to pump off $16.5 (500)/100 = 82.5$ mc.; after two days about 150 mc. etc. However, it is never possible to

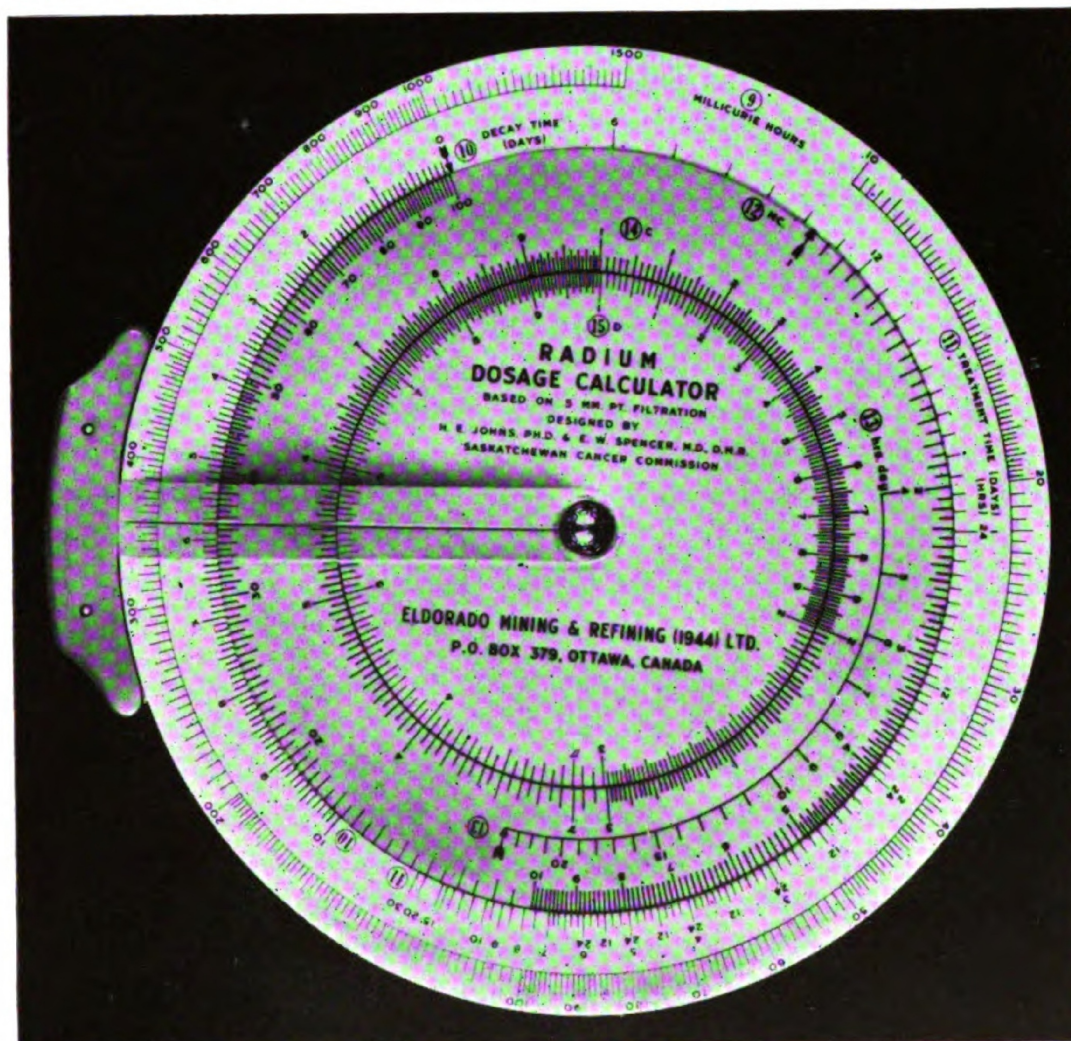


Figure IX-5. Photograph of radium dosage calculator, courtesy Eldorado Mining and Refining Co., Ottawa. See Figure X-2 for other face of the calculator.

collect all the radon from the radium solution so that the actual amounts which are obtained in a pumping are less than these. Efficiencies of about 80% are common. When radon is freshly prepared it has practically no gamma ray activity. This activity is due to radium B and C and freshly prepared radon has had no time to produce active deposits of these materials. However, these deposits grow quite rapidly so that after two hours, 88% of the maximum activity is reached and after four hours the maximum activity is attained. From this time on the activity will decay with the half life of radon. Since the strength of a radon source is measured by comparing its gamma ray activity with that of a standard radium source, radon seeds cannot be measured until three to four hours have elapsed after their preparation.

REFERENCES

1. Agnew, H. M.: *Physical Rev.*, 77:655, 1950.
2. Harrington, E. L.: *Medical Physics*. Chicago, Yr. Bk. Pub., 1944.
3. Spencer, E. W., and Johns, H. E.: *Am. J. Roentgenol.*, 57:711, 1947.

Chapter X

RADIUM DOSAGE

10.01

RADIUM DOSAGE

MANY clinics still state radium dosage in terms of mg. hours. Such a statement is meaningless since the actual effect on the patient will be determined by the size, shape and distance of the applicator as well as the filtration. Fortunately, it is possible to express radium dosage in terms of the r unit. From the information given in Table XI concerning the relative number and energy of the gamma rays emitted from radium it is possible to calculate the energy flux in ergs/cm.² at a point 1 cm. from a 1 mg. source of radium. Using the results of Figure VIII-3 dealing with the energy flux per roentgen it is then possible to calculate the reading of an r meter which will be produced by each of the gamma rays in turn. Because of the large number of gamma rays from radium the calculation is tedious, so the method will be illustrated in section 12.09 by a calculation on Co⁶⁰. The results of a number of calculations and experiments (3, 15, 17) on radium indicate the important result that *1 mg. of radium filtered by 0.5 mm. of platinum gives a dosage rate of 8.4 r/hour at 1 cm. distance.* The dosage rates at other distances may be calculated using the inverse square law. The linear absorption coefficient of tissue for gamma rays is about 0.028 cm.⁻¹, meaning that 1 cm. of tissue absorbs 3% of the radiation. Since in radium dosage we are not usually interested in points more than 1 cm. from the source this absorption is usually neglected.

The discussion which follows is based mainly on the rather widely accepted Manchester System of Radium Dosage (7). In this system the radiologist first decides how many 1000r units he desires to give in a certain time and then calculates how many mg. hours of radium is required to do this. This calculation is usually based on 0.5 mm. of platinum filtration. For other filtrations the number of mg. hrs. should be increased by 2% for each 0.1 mm. of Pt. filtration greater than 0.5 mm. For example, if radium with filtration 0.8 mm. Pt. is being used the number of mg. hrs. should be increased by 6%. A

number of the possible types of implants or distributions will be described in the following sections and illustrated with examples.

10.02 SURFACE APPLICATORS

In Figure X-1 the area A is to be treated by the distribution of radium on an equal area A' separated from A by a distance of "h." It is required to calculate the number of mg. hours, spread over the area A' to give 1000r on the surface A. This number will be referred to as R_A . When the radium is distributed over the area A' in such a way that a uniform dose will be received over A it can be shown that $R_A = F_A \cdot A$, where F_A is called the area factor and is a function of \sqrt{A}/h (14). This factor will apply to any shaped area A' provided it is not too elongated. The value of F_A may be obtained from the radium dosage calculator (Fig. X-2). To do this, set A on scale 3 opposite "h" on scale 2 and read off the value of F_A on scale 1 opposite the outpointing arrow. The value of R_A may also be found from the extensive tables and graphs of Paterson and Parker (9) or Meredith (7). In Table XIII a part of these tables have been reproduced through the kindness of J. W. Meredith.

This table shows, for example, that 795 mg.hrs. is required, distributed over an area of 30 cm.², to deliver 1000r to a like area 1.0 cm. away when the filtration is 0.5 mm. Pt. The values given in Table XIII are only correct when certain very definite rules (9) are followed concerning the arrangement of the radium over area A' (Fig. X-1). This distribution must be such as to yield a "uniform" dose over the treated area A.

10.03 DISTRIBUTION RULES FOR SURFACE APPLICATORS

(a) **Circular Arrangements.** In general a circular area and circular distributions will tend to give the most uniform dose. For small circles whose diameter is less than 3h all the radium should be placed around the periphery of the circle and there should be not less than 6 radioactive foci. The distance between active ends should

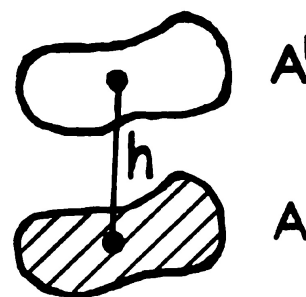


Figure X-1. Diagram showing how radium should be arranged on plane A' to treat a plane of equal area A separated by distance h.

TABLE XIII
SURFACE APPLICATORS AND PLANAR IMPLANTS
GIVING THE NUMBER OF MG. HRS. REQUIRED TO DELIVER 1000R (R_A)
FOR DIFFERENT AREAS AND TREATMENT DISTANCES
FILTRATION 0.5 MM. PT. DATA FOR PLANAR IMPLANTS ARE OBTAINED BY
USING A TREATMENT DISTANCE OF 0.5 CMS.

TREATMENT DISTANCE (cm.)										
Area cm. ²	0.5	1.0	1.5	2.0	2.5	3.0	3.5	4.0	4.5	5.0
0	30	119	268	476	744	1071	1458	1904	2412	2976
1	68	171								
2	97	213	375	598	865	1197	1595	2043	2545	3117
3	120	247								
4	141	278	462	698	970	1305	1713	2168	2665	3243
5	161	306								
6	177	333	536	782	1066	1405	1822	2286	2778	3360
7	192	359								
8	206	384	599	855	1155	1500	1924	2395	2883	3472
9	221	408								
10	235	433	655	923	1235	1590	2020	2500	2987	3580
12	261	480	710	990	1312	1673	2112	2603	3087	3682
14	286	524	764	1053	1386	1753	2200	2698	3185	3785
16	315	566	814	1113	1460	1830	2283	2790	3280	3883
18	342	605	863	1170	1525	1905	2363	2879	3370	3985
20	368	641	910	1225	1588	1979	2445	2965	3461	4080
22	393	674	960	1280	1650	2049	2522	3047	3550	4174
24	417	707	1008	1335	1712	2117	2598	3126	3639	4267
26	442	737	1056	1388	1768	2188	2670	3200	3724	4356
28	466	767	1100	1438	1826	2254	2742	3275	3804	4446
30	490	795	1142	1487	1880	2320	2817	3348	3883	4534
32	513	823	1185	1537	1936	2380	2888	3420	3966	4620
34	537	854	1226	1587	1992	2442	2956	3490	4047	4700
36	558	879	1268	1638	2048	2502	3022	3559	4125	4783
38	581	909	1308	1685	2100	2562	3088	3627	4198	4863
40	603	934	1346	1732	2152	2620	3150	3695	4273	4942
42	624	962	1384	1780	2203	2677	3215	3762	4348	5020
44	644	990	1420	1825	2255	2733	3275	3826	4423	5096
46	665	1015	1457	1870	2305	2788	3335	3890	4494	5174
48	685	1043	1490	1915	2354	2843	3395	3954	4565	5250
50	705	1072	1522	1958	2402	2897	3455	4018	4633	5327
60	800	1206	1682	2180	2646	3160	3735	4328	4970	5690
70	890	1340	1827	2380	2875	3410	4001	4618	5294	6033
80	981	1473	1966	2562	3103	3657	4260	4900	5600	6350
Filtration (mm. Pt.)			0.3	0.5	0.6	0.8		1.0		1.5
Correction to mg. hrs.			-4%	0	+2%	+6%		+10%		+20%

(Courtesy, J. W. Meredith and E. & S. Livingstone Ltd., Edinburgh.)

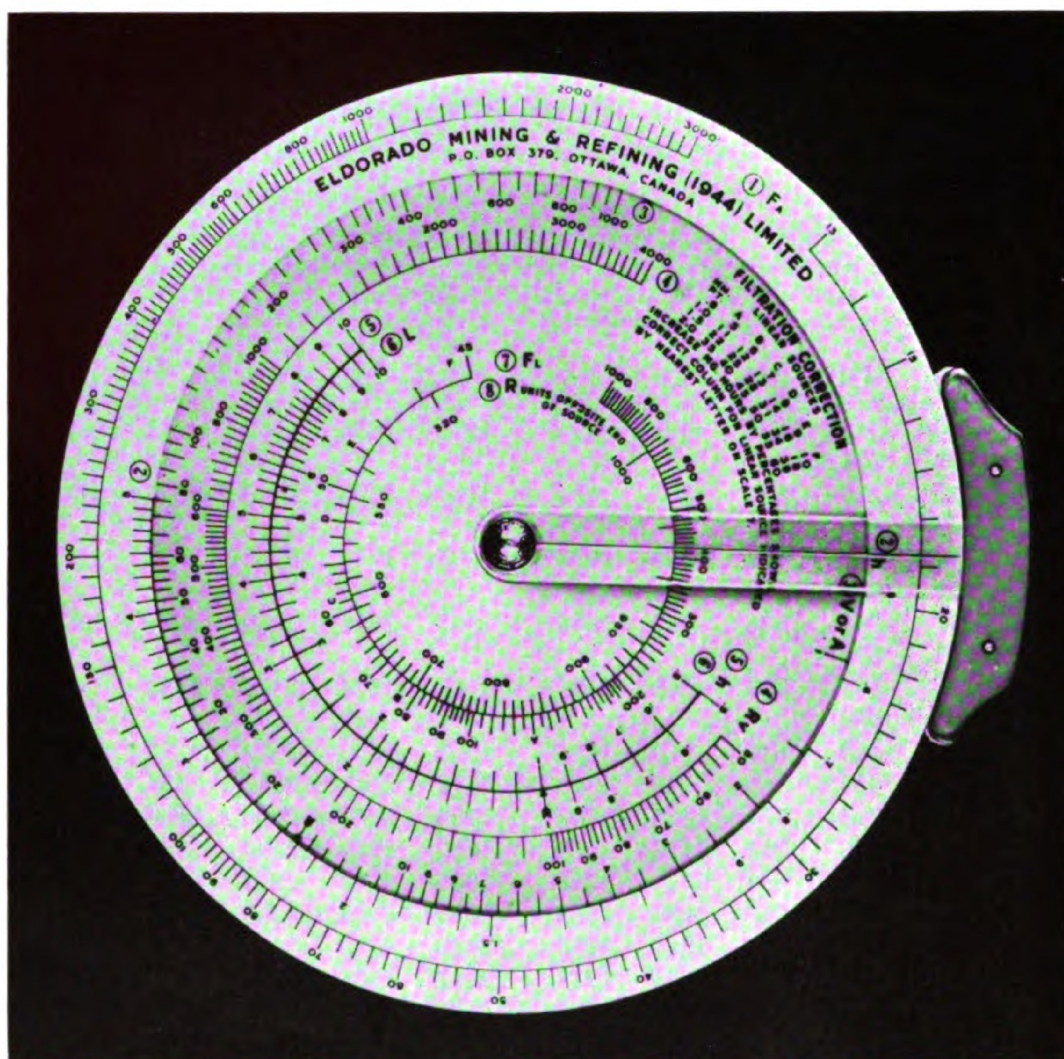


Figure X-2. Photograph of radium dosage calculator which may be used to calculate surface applicators, planar implants, 2 plane implants, sandwich moulds, volume implants and linear sources. Courtesy Eldorado Mining & Refining Co., Ottawa. See Figure IX-5 for the other face of the calculator.

not exceed h . For larger circles and small h the highest dose will appear near the periphery of the treated area under the ring of radium, and a low dosage region will occur at the centre of the circle. To correct for this some radium should be added in the centre. For very large circles and small h it will be necessary to place some radium on a circle of half the outer diameter as well as to place some in the centre. The distribution rules as worked out by Paterson and Parker (9) are given in Table XIV. For small circles even with all the radium on the periphery the dose at the centre will be greatest. For a circle whose diameter is equal to $2.83 h$ we get almost exact uniformity over the whole area, and this arrangement is referred to as *ideal*.

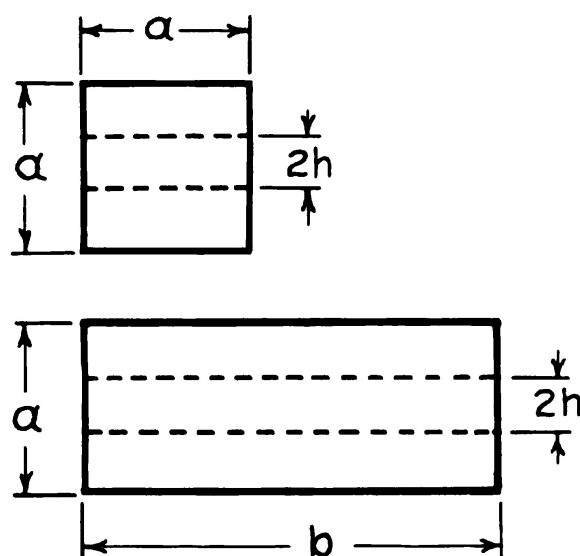


Figure X-3. Diagram illustrating the distribution rules for square and rectangular surface applicators or planar implants.

TABLE XIV

DISTRIBUTION RULES FOR CIRCULAR AREAS

<i>Diameter divided by h</i>	2.83 (ideal)	3 to 6	6	7.5	10
% radium in outer circle	100	95	80	75	70
% radium in inner circle	0	0	17	22	27
% radium in centre	0	5	3	3	3

In some cases it is not convenient to use an exact circle and under these circumstances ellipses of small eccentricity are quite satisfactory.

(b) **Rectangular Arrangements.** When it is not convenient to use a circular arrangement, squares and rectangles may be used. Referring to Figure X-3, if $a < 2h$ all the radium should be placed around the periphery. If $a > 2h$ lines spaced $2h$ should be added parallel to the longer side. If one line is added, its linear density should be one-half the linear density on the periphery. For two or more added lines, the linear density should be $2/3$. An elongated rectangular applicator will require slightly more radium to give the same dose. For $b/a = 2, 3$ and 4 (Fig. X-3) the mg. hours should be increased by 5, 9 and 12%.

The depth dose from a surface applicator may be determined from the values given in Table XIII. For example, an applicator designed to treat an area of 20 cm.^2 at a distance of 0.5 cm. requires 368 mg. hrs.

to deliver 1000r. To deliver the same dose to a plane 1.0 cm. away the number of mg. hrs. required is 641. Hence if 368 mg. hrs. is used the dose received on the plane 1.0 cm. away is $368 (1000)/641 = 574r$. The percentage depth dose is 57.4%. If the radium dosage calculator is used the percentage depth dose is the ratio of the two area factors F_A . If the depth dose of 57% is not high enough a larger value of h should be used. For example, if h is increased to 2.0 cm. then the depth dose on a plane 0.5 cm. farther away is $1225 (100)/1588 = 77\%$.

Sometimes the surface to be treated is curved, forming a part of a cylindrical or spherical surface. Under these circumstances the radium should be distributed over a parallel curved surface maintained at a constant distance h from the treated surface.

Paterson and Parker (9) have shown that for a convex surface the radium should be distributed over the corresponding larger convex surface but the amount of radium should be determined from the treated area. For a concave surface the radium is distributed over a smaller concave surface but the amount of radium is now determined from the area of the applicator. Curved areas can be used until the case of a semi-cylindrical or hemispherical surface is approached.

Rather than curve a plane area into a semi-cylinder it may be desirable to treat the whole cylindrical surface of diameter d and length L by placing radium on a larger coaxial cylinder of diameter D . The number of mg. hrs. required on the larger cylinder to deliver 1000r to the inner cylinder and the distribution rules may be obtained from the original paper (10).

10.04 INTERSTITIAL PLANAR IMPLANTS

Sometimes it is convenient to make a single plane implant below the surface of the skin. The dose in any plane parallel to this plane can be found from the information given in the last section on surface applicators (11). It is usual to evaluate the dose at $h = 0.5$ cm. since for this distance the dose in the plane of the implant is essentially the same as the dose at $h = 0.5$ except of course for the local "high" spots surrounding each needle. Such a planar implant is illustrated in Figure X-4. Under these circumstances we can consider that a block of tissue 1.0 cm. thick is radiated. *Example.* It is required to determine the amount of radon required to deliver a dose of 6500r by a non removable implant 0.5 cm. below the surface of the skin to a circular area of 4 cm.^2 (diameter 2.26 cm.). From Table XIII we find that 141 mg. hrs. are required to deliver 1000r. The required number of mg. hrs. to deliver 6500r is $6.5(141) = 915$ mg. hrs. 1 mc. of radon permanently implanted gives an emitted dose of 133 mc.

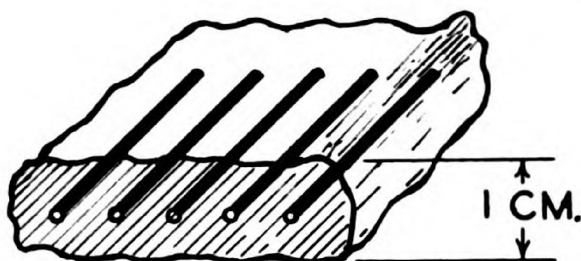


Figure X-4. Diagram illustrating the use of a single plane implant for the treatment of a block of tissue 1 cm. thick.

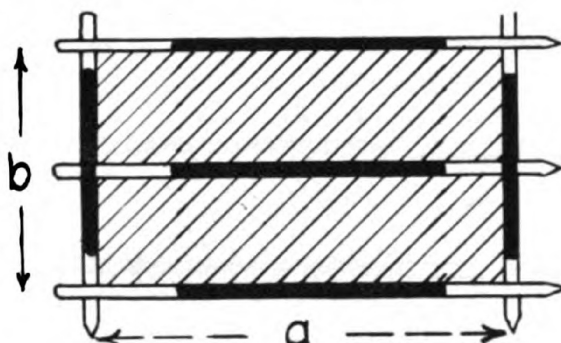


Figure X-5. Diagram illustrating the method of calculating the area treated for a rectangular implant.

hrs., hence $915/133$ or 6.88 initial millicuries are required. The ratio of the diameter of the circular implant to h is $2.26/0.5 = 4.5$ so that 95% of the radon should be placed around the periphery and 5% in the central spot (see Table XIV). This arrangement of radon will give 6500r to the block of tissue of area 4.0 cm.^2 and of thickness 1.0 cm.

In many cases of planar implants, especially where larger areas are involved, rectangular distributions are more convenient. Typical arrangements are shown in Figures X-5, X-6, and X-7. The active regions of the radium needles are shown by the heavily shaded part. Since for a planar implant $h = 0.5 \text{ cm.}$ the lines should be spaced $2h = 1.0 \text{ cm.}$ The area treated is the region enclosed by the active deposits and is given by $a \times b$ for Figure X-5. The quantity a is not the active length of the needles, but the distance between the crossing needles. The distance from the crossing needle to the active deposit should not exceed h (0.5 cm.). In certain cases it will be impossible to cross one end for technical reasons. The dose near the ends of the needles will fall and the area which is treated should be considered as 90% of the area bc , i.e., the shaded area in Figure X-6. c is the distance from the crossing needle to the end of the active deposit. If both ends are uncrossed (Fig. X-7) the area treated

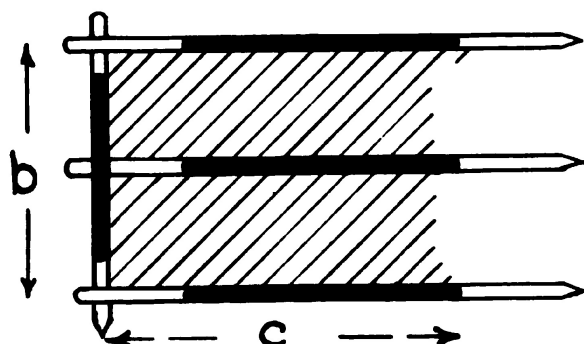


Figure X-6. Diagram illustrating the method of calculating the area of a single plane implant when one end is uncrossed.

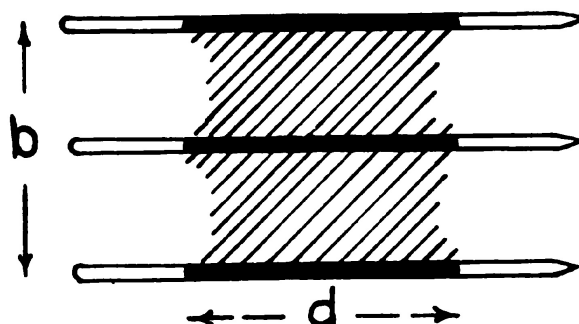


Figure X-7. Diagram illustrating the method of calculating the area of a single plane implant with both ends uncrossed.

should be considered as 20% less than the area bd where d is the active length. Of course care should be taken to insure that the shaded area amply includes the tumor.

10.05 TWO PLANE IMPLANTS

Often the tumor to be implanted is greater than 1 cm. thick, and under these circumstances more than one plane of radium is required. Two plane implants can be used for separations of 1.5 cm. up to 2.5 cm. but for the latter a low dose region will be obtained in the central plane. Suppose a region with area 40 cm.² and depth 2.0 cm. is to be treated with a two plane implant (Fig. X-8). The radium will be distributed on planes A and B. The number of mg. hrs. required to deliver 1000r to the central plane C can be found (using $A = 40$, $h = 1$) to be 934 mg. hrs. This amount of radium could all be placed on one plane as far as the dose in plane C is concerned, but for homogeneity it should be distributed with 467 mg. hrs. on each of planes A and B. Table XIII gives $R_A = 603$ for $A = 40$ and $h = 0.5$; and $R_A = 1346$ for $A = 40$ and $h = 1.5$. Hence the doses

received on planes D and E for 467 mg. hrs. of radium on plane A are $467(1000)/603 = 775r$ and $467(1000)/1346 = 347r$ respectively. The following table can be constructed.

	<i>Plane D</i>	<i>Plane C</i>	<i>Plane E</i>
Dose given by plane A	775r	500r	347r
Dose given by plane B	347r	500r	775r
Total dose received	1122r	1000r	1122r

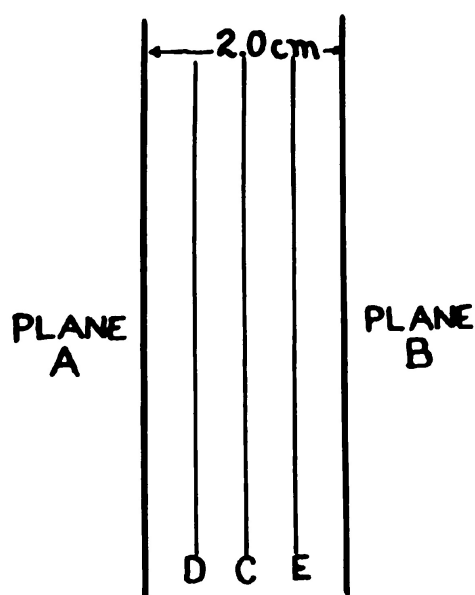


Figure X-8. Diagram illustrating the calculation of dosage on planes C, E and D between planes A and B of a two plane implant.

It will be seen that the dose at the centre is less than at the planes 0.5 cm. from either plane of radium. If the plane separations were 2.5 cm. this minimum would be even more pronounced, indicating that an implant of this kind is not too satisfactory. In the above example, we see that 934 mg. hrs. will deliver a dose of 1122r on planes D or E. Hence 830 mg. hrs. will deliver a dose of 1000r to planes D or E.

Paterson and Parker (11) calculate such an implant by placing $h = 0.5$ regardless of the plane separation and then

increase the mg. hrs. by 1.25, 1.41 and 1.52 for plane separations of 1.5, 2.0 and 2.5 cm. Such corrections are only approximate. Using this method, the number of mg. hrs. to give 1000 r to the "high" planes rather than to the central plane is determined. For this example, $R_A = 603$ and the corrected value is $603 \times 1.41 = 850$. This compares well with the value of 830 obtained above.

Problems with sandwich moulds can be solved with the information on surface applicators. An example will be discussed later.

10.06

VOLUME IMPLANTS

Where the region to be treated is more than 2.5 cm. thick the two plane implant is not satisfactory because of the low dosage region midway between the planes. A volume implant in the form of a sphere, cube or cylinder may then be useful. As in the case of all

implants there must be a region of high dose around each radium source. The number of mg. hrs. to deliver 1000r (R_v) can be read from Table XV or off the slide rule directly, using scales 3 and 4, Figure X-2. Scale 3 gives the volume to be implanted and scale 4 the value of R_v directly below it. For example, a volume of 30 cm.³ requires 329 mg. hrs. The values given in Table XV are correct only if certain distribution rules are followed to insure a uniform dose throughout the volume.

The volume to be implanted can be considered as being made up of a core and a surface. The surface should receive 75% of the radium

TABLE XV
VOLUME IMPLANTS
 R_v (MG. HR. TO GIVE 1000r) TO A VOLUME IMPLANT
FILTRATION 0.5 MM. Pt.

<i>Volume cm.³</i>	<i>R_v</i>
5	99.7
10	158.3
15	207
20	251
30	329
40	399
50	463
60	523
80	633
100	735
140	920
180	1087
220	1243
260	1390
300	1529
340	1662
380	1788

Increase R_v by 3, 6, 10 and 15% for elongation
factors of 1.5, 2.0, 2.5 and 3.0.

(Courtesy, J. W. Meredith and E. & S. Livingstone Ltd., Edinburgh.)

and the core 25%. By far the most important type of implant is the cylindrical one. With such a cylinder 50% should be placed on the belt and 12.5% on each end. The core should receive the remainder, distributed with a minimum of four needles. The belt should have a minimum of 8 needles. In many cases, one end of the cylinder cannot be given any radium and under these circumstances the volume should be reduced by 7.5%. When both ends cannot be closed the net reduction in volume should be 15%. The reduction in volume is necessary because of the region of low dose near the ends of the unclosed cylinder. For very long slender cylinders the mg. hrs. should be increased by 3, 6, 10 and 15% for elongation factors of 1.5, 2.0, 2.5 and 3.0. An example of a cylindrical volume implant will be discussed later. The distribution rules for other types of volume implants can be found in the original papers (5, 11).

10.07

LINEAR SOURCES

In certain cases, such as in the treatment of cancer of the uterus, the dosage rate near a linear source is required. Paterson and Parker (9) have calculated the number of mg. hrs. (R_L) in a source of active length L , required to deliver a dose of 1000r units to the point A (Fig. X-9) distance h from the source. The value of R_L can be obtained from Table XVI.

Table XVI-A is for a filtration of 1.0 mm. Pt. Values for other filtrations cannot be obtained by the simple filtration corrections discussed above. This is so because on a long needle the radiation from the ends to point A (Fig. X-9) passes through the platinum sheath at an angle and so increases the filtration. The amount of this in-

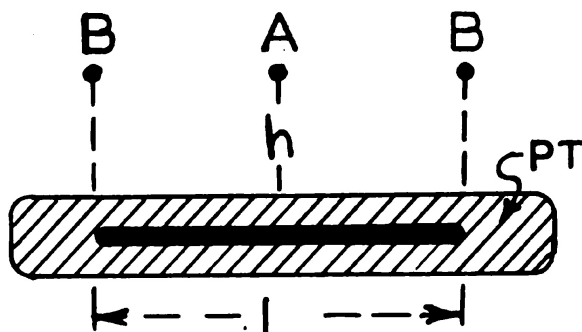


Figure X-9. Diagram of radium needle of active length L from which one desires to calculate the dose at a point A a distance h from the center of the needle.

TABLE XVI-A

LINEAR SOURCES

R_L (MG. HRS. TO DELIVER 1000r) TO A POINT h CM. FROM THE CENTRE
OF A LINEAR SOURCE OF ACTIVE LENGTH L (POINT A, FIG. X-9)
FILTRATION 1.0 mm. Pt.

Active Length L	Treatment Distance in cm.						
	0.5	.75	1.0	1.5	2.0	2.5	3.0
0.0	33	74	132	298	528	825	1188
0.5	39	78	135	302	533	829	1191
1.0	47	85	143	310	541	836	1200
1.5	55	97	156	320	554	849	1215
2.0	65	112	172	340	572	867	1234
2.5	75	128	190	361	595	893	1260
3.0	87	143	211	386	622	924	1290
3.5	100	161	232	415	654	958	1324
4.0	112	177	254	443	688	995	1363
5.0	137	213	300	504	763	1077	1452
6.0	162	249	347	570	844	1167	1552
7.0	187	286	395	638	930	1266	1662
8.0	213	325	444	709	1019	1371	1776
9.0	238	364	495	780	1110	1479	1894
10.0	265	402	546	853	1200	1589	2020
12.0	317	480	647	1001	1390	1816	2285
14.0	370	558	750	1151	1582	2050	2560
16.0	422	637	854	1302	1780	2289	2840
18.0	475	716	958	1456	1978	2530	3126
20.0	528	795	1060	1610	2178	2776	3415

scale 5 opposite $L = 10$ on
D. The corrections for

(Courtesy, J. W. Meredith and E. & S. Livingstone Ltd., Edinburgh.)

crease will depend on the relative values of L and h . Table XVI-B gives values of R_L for a filtration of 0.5 mm. of platinum.

The value of R_L , the dose at point B (Fig. X-9) opposite the end of the needle, and the proper filtration correction can be obtained directly from the radium dosage calculator using scales 5, 6, 7 and 8 of Figure X-2. It can be shown that $R_L = F_L \cdot L \cdot h$ where F_L is a function of L and h involving Sievert's integrals (13). Suppose $L = 10$ cm. and $h = 2.0$; set $h = 2$ on scale 5 opposite $L = 10$ on scale 6. The in-pointing arrow on scale 5 will locate the value of $F_L = 52$ on scale 7. The dose opposite the end of the needle is 560r units found on scale 8. $R_L = 10 \times 2 \times 52 = 1040$ mg. hrs. When the filtration is 0.5 mm. of Pt. 1040 mg. hrs. of radium will deliver a dose of 1000r units to A and 560r units to B (Fig. X-9). On the slide rule we find at $F_L = 52$ the letter D. The corrections for filtration can be found under letter D in

TABLE XVI-B

R_L (MG. HRS. TO DELIVER 1000_R) TO A POINT H CM. FROM THE CENTRE
OF A LINEAR SOURCE OF ACTIVE LENGTH L (POINT A, FIG. X-9)

Filtration 0.5 mm. Pt.

Active Length L.	Treatment Distance in cm.						
	0.5	.75	1.0	1.5	2.0	2.5	3.0
0.0	30	66	119	268	476	744	1071
0.5	33	70	121	272	478	747	1073
1.0	38	77	127	277	484	753	1082
1.5	47	86	138	287	497	764	1095
2.0	55	98	153	301	513	780	1114
2.5	64	112	168	320	535	800	1137
3.0	74	125	184	343	558	824	1163
3.5	84	140	203	368	583	853	1192
4.0	94	153	220	392	611	886	1222
5.0	116	183	259	443	675	957	1294
6.0	138	214	297	498	742	1035	1378
7.0	159	244	337	553	812	1118	1470
8.0	180	274	380	612	887	1204	1568
9.0	200	307	421	671	963	1292	1669
10.0	221	337	463	731	1042	1384	1774
12.0	263	401	546	853	1196	1573	1994
14.0	306	466	631	976	1355	1769	2220
16.0	349	532	715	1100	1518	1970	2452
18.0	394	596	802	1224	1683	2170	2687
20.0	437	662	887	1352	1849	2371	2930

(Courtesy, J. W. Meredith and E. & S. Livingstone, Ltd., Edinburgh.)

the table on the upper left hand corner of face A. For 1.5 mm. of Pt. the correction is 31% instead of the usual 20 to 22% where oblique filtration does not occur.

It is possible to arrange the radium as three collinear sources of equal length with a weaker central source (Fig. X-10) so that the doses at A and C are the same (2). Under these circumstances a greater value for R_L is required. The value of R_L and the percentage of radium which should be placed in the central source may be obtained from the following (2, 14). For the example above, 1000r is delivered along the line CAC (Fig. X-10) if 1180 mg. hrs. of radium are used with 23% of the radium placed in the central source.

10.08 RADIOGRAPHIC CONTROL OF RADIUM IMPLANTS

When surface applicators are constructed there is no difficulty in placing the radium accurately on felt or sponge rubber of the required thickness. (For details of mould construction see Paterson and Mac-

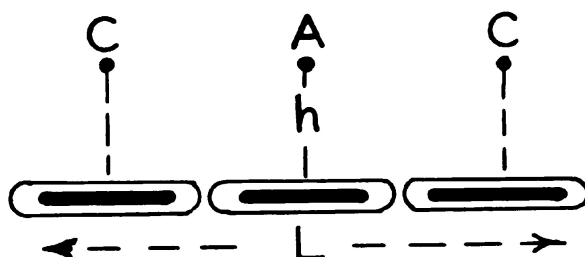


Figure X-10. Diagram illustrating 3 collinear sources arranged to give homogeneity at points C, A and C.

Vicar (12). If this is done with care the area "A" and the distance "h" can be controlled precisely and the dosage given the treated area accurately determined. The only difficulty may be in obtaining a proper distribution with the limited variety of radium needles which are available in the department. However, for planar implants, two plane implants, and volume implants, the radium can never be arranged exactly as the therapist plans so that some determination of the implant actually achieved is necessary (6). This can be done by taking antero-posterior and lateral x-ray plates of the implant and then making recalculation for the actual implant. A number of methods for doing this have been described, none of which are very simple. In this section a brief summary of the general principles is all that can be discussed.

Consider Figure X-11 in which the projections of a radium needle in two planes at right angles are shown. The apparent length of a needle of true length L on an A.P. film is a and on the lateral b . In this discussion we will assume no magnification of the x-ray image. It can easily be corrected for afterwards. From Figure X-11 it is apparent that a , c and L form sides of a right angle triangle so that $L^2 = a^2 + c^2$. The length c does not appear in the A.P. film because c is a line in the direction of the x-ray beam. It can be obtained from the lateral but it is *not* the apparent length of the needle in the lateral. On the lateral, the line EF should be drawn through E parallel to the direction of the x-ray beam for the antero-posterior film. There is no difficulty in doing this on an actual x-ray plate because one can orient oneself from anatomical markings. By drawing OF at right angles to EF a right angle triangle OEF is obtained. The dimension required is EF which is equal to c . The actual length L can now be determined from $L = \sqrt{a^2 + c^2}$. *The dimension which is required from the lateral is the one which is in the direction of the x-ray beam in the A.P.* If the needle were in the plane XOY then on the lateral EF would be zero.

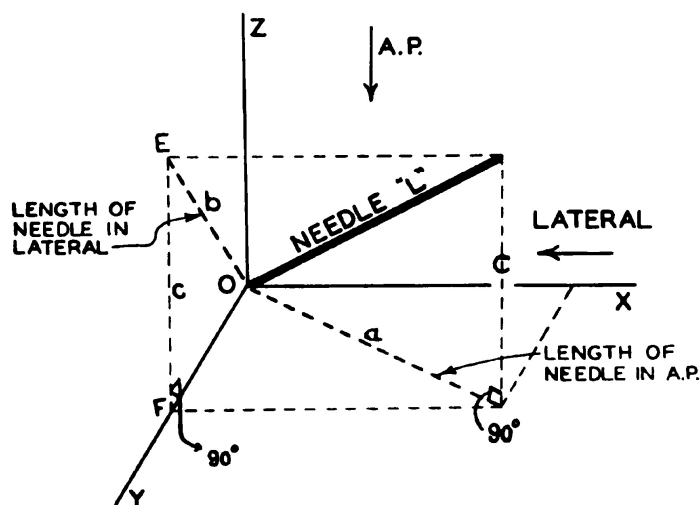


Figure X-11. Diagram illustrating the appearance of a radium needle as observed by an antero-posterior and a lateral x-ray film.

When x-ray pictures are taken it is necessary to determine the magnification. This can be done by placing a coin on the patient's skin the same distance from the film as the implant. If the maximum dimension of the coin in the x-ray picture is X and its actual dimension Y then the

magnification is X/Y . When radium needles are used in the implant the magnification can often be determined from the measurement of the apparent length of the needle and a knowledge of its actual length. For radon seed implants the coin or ring method is necessary. The problem of calculation is greatly simplified if the A.P. film is taken with the plane of the implant parallel to the film. Under these circumstances the lateral picture will appear as a line and is only of value in showing that the A.P. film was taken perpendicular to the plane of the implant. For further details concerning methods of dosage control the readers should consult (6, 18).

10.09

EXAMPLES

In order to illustrate the methods described in this chapter a number of typical examples will be discussed. It will be assumed that the department has available an unlimited number of radium needles of the following specifications.

Strength	Active Length	Length	Filtration
3 mg.	4.5 cm.	6.0 cm.	0.5 mm. Pt.
2	4.5	6.0	"
2	3.0	4.5	"
1.3	3.0	4.5	"
1.0	3.0	4.5	"
1.0	1.5	2.5	"
0.5	1.0	2.0	"
13.3	1.5	2.0	1.0 mm. Pt
10	1.5	2.0	1.0 mm. Pt.
3	1.5	2.0	1.0 mm. Pt.

(a) It is desired to treat an epithelioma of the dorsum of the hand with a surface applicator at a distance $h = 2$ cm. The tumor covers a circle of radius about 2.0 cm. and is to receive 6000r in eight days with a treatment time of about eight hours per day.

Treat a circle of diameter 3 cm. $A = \pi r^2 = 7.06$ cm.². $h = 2$, therefore $R_A = 819$ mg. hrs. per 1000r (Table XIII). 6000r requires 4910 mg. hrs. Distri-

bution should be a circle with radium around the periphery only. Approximate treatment time, 64 hours, therefore 77 mg. is required. Use six 13.3 mg tubes of active length 1.5 cm. and 1.0 mm. filtration arranged as in Figure X-12. More than six cannot be placed around this small circle. Actual radium is 80 mg., therefore actual treatment time $= 4910/80 = 61.4$ hours. Correction for filtration is 10% so the treatment time must be increased to 67.5 hours. Treatment time per day $= 67.5/8 = 8.45$ hours. To find the depth dose at 0.5 cm., obtain $R_A = 1110$ for $h = 2.5$ cm. Therefore dose on plane 0.5 cm. below surface is $819(6000)/1110 = 4430$ r.

It is difficult to arrange six radium tubes around the circle of diameter 3 cm. because of the inactive ends of the tubes. The problem could be solved neatly using eight radon bulbs each of strength 15 mc. The total radon is 120 mc. so that each initial millicurie must contribute $4910/120 = 40.9$ mc. hrs. In eight days this will be the emitted dose if the mould is worn 9.2 hrs. per day.

(b) It is desired to treat a superficial basal cell carcinoma of the forehead to 6000r in eight days with a superficial applicator at $h = 1.5$ cm. The tumor covers an area of 3.5×5.5 cm.². An applicator 6×8 cm. will adequately cover this area. $A = 48$ cm.², $h = 1.5$, therefore $R_A = 1490$ mg. hrs (Table XIII). 6000r will require $1490 \times 6 = 8940$ mg. hrs. The applicator is to be worn about eight hours per day so the treatment time is about 64 hours and therefore approximately 140 mg. of radium is required.

Distribution: Since $a > 2h$, lines should be spaced $2h$, that is, 3.0 cm. Therefore one central line is required with linear density one half. Use 10 mg. tubes of length 2.0 cm. Place 4 along sides and 3

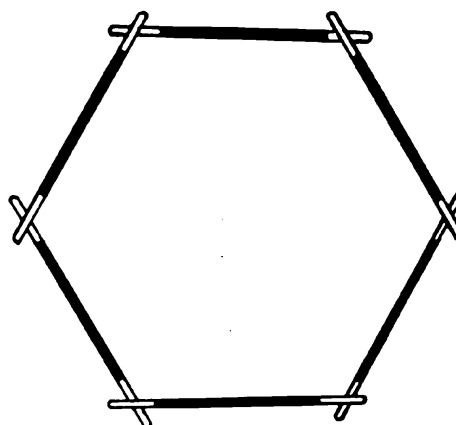


Figure X-12. Diagram illustrating the arrangement of radium to treat an epithelioma of the dorsum of the hand.

along ends and 2 along central line. Total amount of radium used is 16 tubes — 160 mg. Arrange this radium as in Fig. X-13. Total treatment time required = $8940/160 = 55.8$ hours. Correction for filtration is 10% giving 61.4 hours. Treatment time per day = $61.4/8 = 7.68$ hours or 7 hours 41 min. If the treatment distance had been 2 cm. the central line would hardly be required and satisfactory results would have been obtained with only one tube on the central line.

(c) It is desired to treat a rodent ulcer of the inner canthus to 6500r with a permanent gold seed implant. The tumor measures 1 cm. in diameter and it is decided to attempt an implant 2.0 cm. in diameter. $A = \pi r^2 = 3.14 \text{ cm.}^2$, $h = 0.5$, $R_A = 123 \text{ mg hrs.}$ to give 1000r (Table

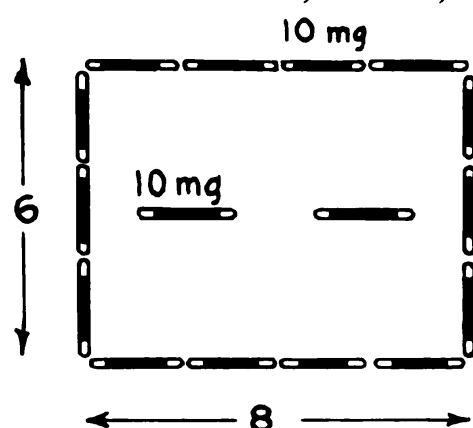


Figure X-13. Diagram illustrating the distribution of radium on a superficial applicator for the treatment of a basal cell carcinoma of the forehead.

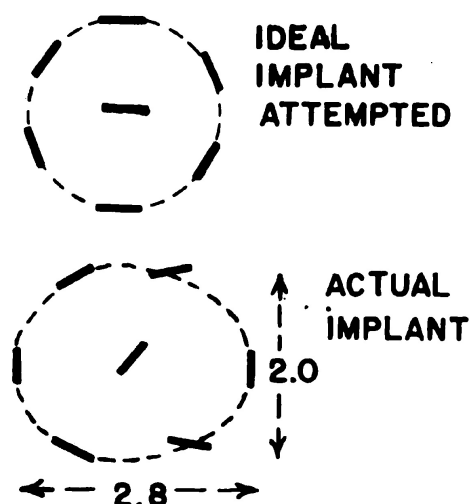


Figure X-14. Diagram illustrating the initial radon implant attempted and the actual implant achieved in the treatment of a rodent ulcer of the inner canthus.

XIII), 6500r requires 800 mg. hours. No correction for filtration. The distribution attempted is shown in Figure X-14. It consists of radon around the periphery with a 5% central spot. Initial radon strength required = $800/133 = 6.0 \text{ mc.}$ Use six 0.95 mc. seeds around the periphery and a 0.30 mc. seed in the centre. After the implant had been made two x-ray pictures taken at right angles and corrected for magnification revealed that the actual implant was elliptical with axes 2.8 cm. and 2.0 cm. (Fig. X-14). This means that an area $\pi ab = \pi(1.0)(1.4) = 4.40$ was treated. Therefore $R_A = 150 \text{ mg. hrs.}$ to give 1000r. Actual dose given by radon = $123(6500)/150 = 5340\text{r.}$ If it was felt that this dose was not sufficient to kill the tumor a small x-ray dose could be superimposed. A single x-ray dose of 2000r units would be considered a lethal tumor dose.

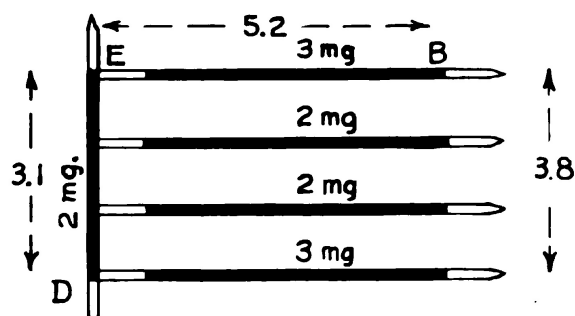


Figure X-15. Diagram illustrating the arrangement of radium to treat an epithelioma of the mucosa of the cheek.

Therefore single x-ray dose required = $(6500 - 5340) (2000) / 6500 = 356r$ units. In most cases the actual implant would correspond much more closely to the attempted implant and no extra x-ray dose would be required.

(d) It is desired to treat an infiltrating epithelioma of the mucosa of the cheek by a single plane implant to 6000r in about eight days. The lesion measures 2×4 cm. The implant is to be made using the 6.0 cm. length needles (active length 4.5 cm.) with the posterior ends uncrossed. The added lines should be $2h = 1.0$ cm. apart and four parallel needles (Fig. X-15), are required to cover the lesion adequately. The area to be attempted is $EB \times ED$. ($EB = 1.5/2 + 4.5 = 5.25$ cm., and $ED = 3.0$ cm.). Therefore $A = 5.25 \times 3.0 = 15.8$ cm.². This must be reduced by 10% for the uncrossed end to give 14.2 cm.². Therefore $A = 14.2$, $h = 0.5$ and $R_A = 290$ mg. hrs. (Table XIII), 6000r requires 1740 mg. hrs. Approximate radium required $1740 / (8 \times 24) = 9.0$ mg. The distribution shown in Figure X-15 should be attempted. This consists of two 3 mg. needles on the outside and two 2 mg. needles on the inner lines with one 2 mg. needle to cross the end. Total radium used = 12 mg. After the implant had been made x-ray pictures were taken and after corrections were made for magnification the measurements shown on Figure X-15 were obtained. Area = $5.2 (3.1 + 3.8) / 2 = 18.0$ cm.². Corrected area (for uncrossed end) = 16.2 cm.². $R_A = 318$ mg. hrs. 6000r requires 1910 mg. hrs. No correction for filtration. Treatment time = $1910 / 12 = 159$ hours or six days 15 hours.

(e) It is desired to treat a cancer of the tongue to 6000r in about eight days with a cylindrical volume implant. The lower end of the cylinder must remain uncrossed. The cylinder is to be implanted with needles 4.5 cm. long. The area is elliptical 3.0×4.0 cm. The actual length of the cylinder is L (Fig. X-16) less 7.5% for the uncrossed end.

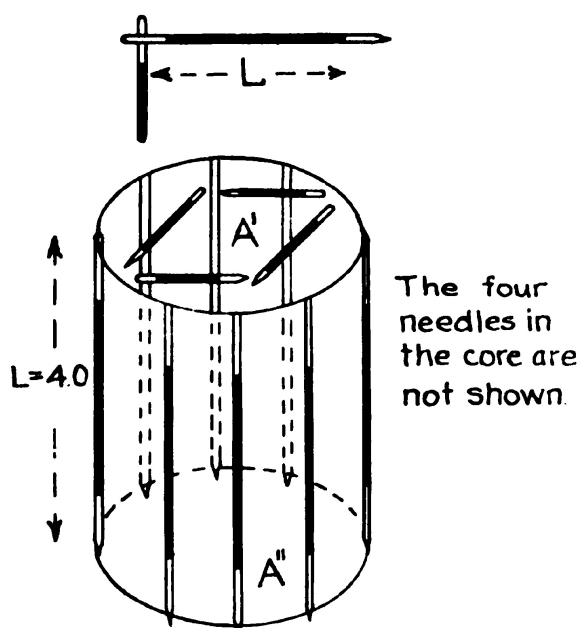


Figure X-16. Diagram illustrating the arrangement of radium needles in a cylindrical volume implant used in the treatment of cancer of the tongue.

The corrected value for L will be about 3.5 cm. Volume to be attempted $\pi(1.5)(2.0)(3.5) = 33 \text{ cm.}^3$ $R_v = 350 \text{ mg. hrs. for } 1000r$ (Table XV); 6000r requires 2100 mg. hrs. Approximate radium required $= 2100/(8 \times 24) = 11 \text{ mg.}$ Use eight 1.0 mg. needles on periphery, four 1.0 mg. needles in the core, four 0.5 mg. needles crossing the end. Total radium 14 mg. After the implant had been made it was found that $L = 4.0$ (Fig. X-16) and that A' and A'' were elliptical with dimensions $3.0 \times 4.0 \text{ cm.}$ and $3.5 \times 4.5 \text{ cm.}$ respectively. Therefore $A' = \pi(3.0/2)(4.0/2) = 9.4 \text{ cm.}^2$ and $A'' = \pi(3.5/2)(4.5/2) = 12.3 \text{ cm.}^2$. The corrected value for L is 4.0 less 7.5% which gives 3.7 cm. Corrected volume $= (3.7)(12.3 + 9.4)/2 = 40.2 \text{ cm.}^3$. $R_v = 400 \text{ mg. hrs. per } 1000r$ or 2400 mg. hours per 6000r. Therefore, the time required is $2400/14.0 = 171 \text{ hours}$ or 7 days 3 hours.

(f) It is desired to treat a carcinoma of the vagina which has spread for 6 cm. along the vagina. A sorbo applicator is to be used of diameter 4.0 cm. and the surface of the vagina is to receive 6000r in about eight days. If a uniform distribution of radium along the axis is to be used a length considerably more than 6 cm. will be necessary to prevent the dose from falling too badly at either end. Take $L = 10 \text{ cm.}$ and $h = 2 \text{ cm.}$ (Fig. X-17). $R_L = 1200 \text{ mg. hrs.}$ (Table XVI). To give 6000r on the surface of the mucosa, 7200 mg. hrs. are required. Approximate amount of radium required $= 7200/$

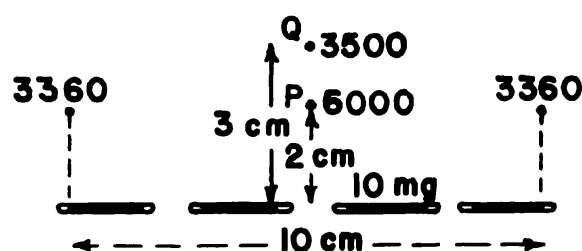


Figure X-17. Diagram showing the arrangement of radium for the treatment of carcinoma of the vagina.

$(8 \times 24) = 37$ mg. Use four 10 mg. tubes of active length 1.5 cm. and filtration 1.0 mm. Pt., arranged as shown. Hence treatment time = $7200/40 = 180$ hours or seven days 12 hrs. The dose opposite the end of the linear source can be obtained from the radium dosage calculator and is 3360r. The dose at Q, 3 cm. from the linear source is found from Table XVI to be $1200(6000)/2020 = 3560$ r.

A more homogeneous distribution will be obtained with three co-linear sources. With such a distribution the length to be treated can be reduced to 6.0 cm. The calculator (14, 2) indicates that 5940 mg. hrs. are required with 10.5% of the radium in the central source. This will give a homogeneous dose over about 5 cm. of the length.

(g) Carcinoma of the floor of the mouth invading the bone. It is decided to treat such a lesion with a sandwich mould. The floor of the mouth is at least 2.5 cm. thick so it will be impossible to deliver a homogeneous dose throughout this volume by this method. In order to obtain the maximum homogeneity the moulds should be made with large areas and arranged to work at large values of h . However, clinical considerations determine an upper limit to both of these factors. The inner mould (Fig. X-18) cannot be made larger than 10 cm.² and is arranged 0.5 cm. from the mucosa. There is not room for a larger area and no room for a greater treatment distance. The outer mould can be made 30 cm.² in area and can be arranged to treat at a distance of 2.0 cm. from the skin. The radium should not be placed nearer the skin of the neck than to the under surface of the chin, otherwise the skin of the neck may be damaged. This factor prevents the use of larger areas at greater values of h for the outer mould. From Table XIII, R_A , the number of mg. hrs. to deliver 1000r on the different planes may be set down as shown on the next page.

Since the upper limits of dosage to the mucosa and skin are 8000r and 6000r respectively, over a period of eight days at eight hours per day, the radium will be distributed on the two moulds to yield

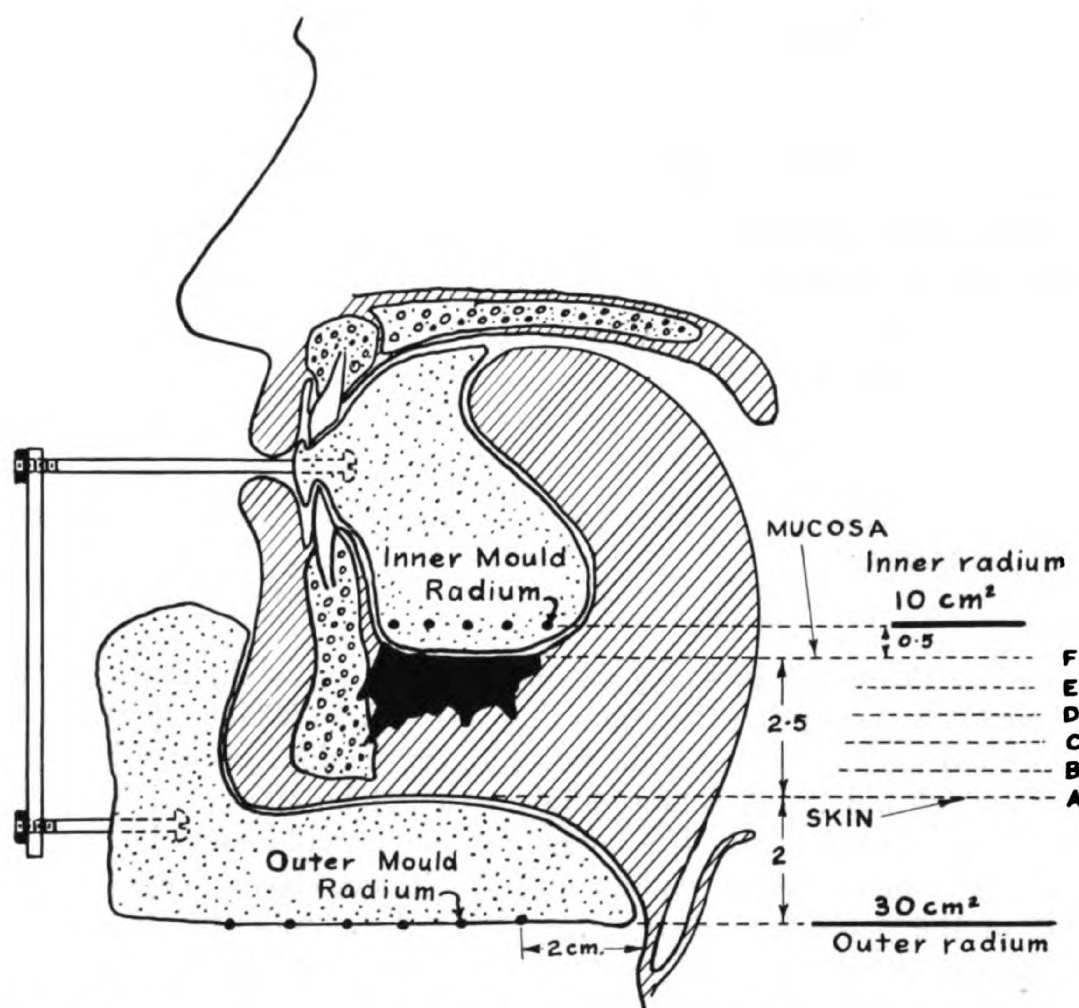


Figure X-18. Diagram illustrating the use of a sandwich mould in the treatment of a carcinoma of the floor of the mouth.

		A (skin)	B	C	D	E	F (mucosa)
From outer mould	}						
30 cm. ²							
x mg. hr.	R _A	1487	1880	2320	2817	3348	3883
From inner mould	}						
10 cm. ²							
y mg. hr.	R _A	1590	1235	923	655	433	235

this result. Let x and y be the number of mg. hr. required on the outer and inner mould respectively. Since the doses to be given plane A (skin) and plane F (mucosa) are 6000r and 8000r, the following equations may be set down. (See next page)

Solving these equations we obtain $x = 7590$ mg. hrs. and $y = 1422$ mg hrs. We see, as in the case of x-ray fields that the remote field

$$6000 = \frac{x}{1487} (1000) + \frac{y}{1590} (1000)$$

$$8000 = \frac{x}{3883} (1000) + \frac{y}{235} (1000)$$

must be given the greater dose. The dose received in the other planes can now be obtained.

	A (skin)	B	C	D	E	F (mucosa)
from outer mould 7590 mg. hrs.	5110	4040	3270	2700	2270	1950
From inner mould 1422 mg. hrs.	890	1150	1540	2170	3280	6050
	<u>6000</u>	<u>5190</u>	<u>4810</u>	<u>4870</u>	<u>5550</u>	<u>8000</u>

Since the tumor probably extends 1.5 cm. below the mucosa (to plane C) it is seen that the tumor dose varies from 8000 to 4810. This is not too satisfactory but is the best that can be done using radium in a sandwich mould. A volume implant cannot be attempted because of the presence of bone. If a larger area inner mould could be used a more homogenous dose would result. Experience shows that in about 50% of the patients, a double mould can be constructed in which homogeneity either equal to or better than that obtained in this example can be achieved.

10.10

RADIUM ISODOSE CURVES

Isodose curves can be constructed around any radium source by joining the points of a given dosage rate. This is illustrated in Figure X-19 where the isodose curves for a tube containing 13.3 mg. of radium are shown. Such curves can be obtained for any linear source by the use of Sievert's Integrals (13) although the calculations are tedious. The intensity of radiation along the axis of the tube is less than at right angles because of the increased effect of oblique filtration. Very near the needle in the region of the high dosage rates the isodose curves will tend to be almost parallel to the source over the central region and the isodose curves more or less elliptical. At great distances in the region at right angles to the needle, the isodose curves will be circles, for the source will behave as a point source. Along the axis the radiation will tend to be slightly more intense than along the line OB (Fig. X-19). Along OB the oblique filtration of the platinum is a maximum, while along the axis, part of the platinum filtration is

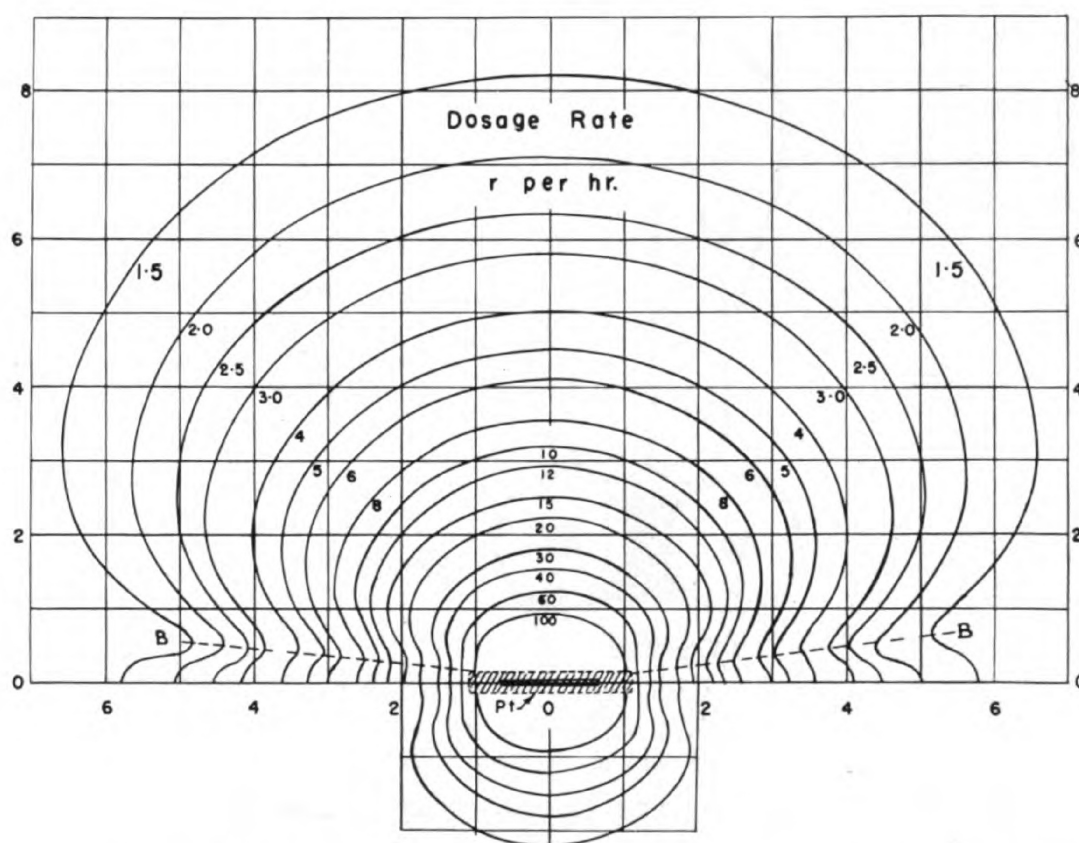


Figure X-19. Dosage rate in r/hour from a 13.3 m.gm. tube of radium of active length 1.35 cm., actual length 2.17 cm. and filtration 1 mm. of platinum.

replaced by the lesser filtration of the radium bromide. Consequently there is a small cone of more intense radiation along the axis. The distributions in space can be obtained by rotation of Figure X-19 about the axis of the tube. The distribution of radiation when radium is placed in the uterus or cervix can be obtained from such isodose curves.

10.11 CANCER OF THE CERVIX

One of the treatments of cancer of the cervix involves placing radium in ovoids in the vagina against the cervix and radium in the uterus itself. This is illustrated in Figure X-20. Tod and Meredith (16) have shown that the point of limiting tolerance is point A, 2 cm. from the uterine canal and 2 cm. above the lateral fornix. The obturator node is situated about 5 cm. from the uterine canal and at the same level as A. This is represented by point B. Many radiotherapists feel that stating the dose at points A and B is sufficient for treatment of cancer of the cervix. The dosage rates at points A and B can be found from the dimensions of the ovoids and the isodose curves for the radium which is being used.

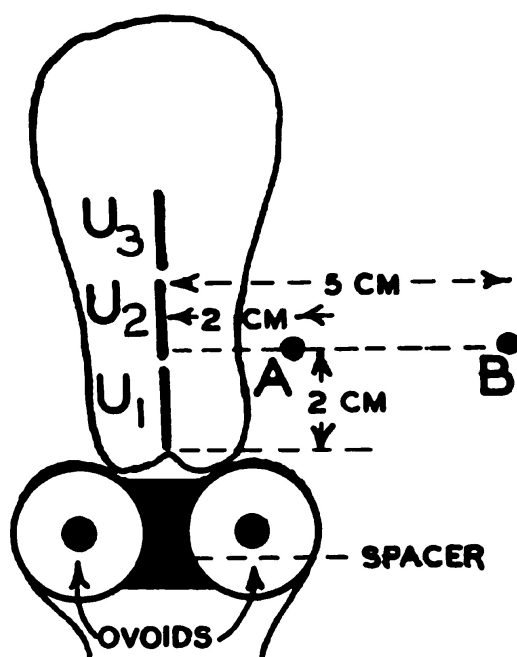


Figure X-20. Schematic diagram of the uterus showing the use of interuterine tubes and ovoids.

Table XVII applies to 13.3 mg. tubes of radium of active length 1.35 cm. and actual length 2.17 cm. with 1.0 mm. of platinum filtration. When these tubes are placed in the uterus end to end they occupy positions designated by U_1 , U_2 , U_3 (Fig. X-20).

Table XVII

THE DOSAGE RATE IN $r/24$ HRS. AT POINTS A AND B OF FIGURE X-20
WHEN RADIUM IS PLACED IN UTERINE POSITIONS U_1 , U_2 AND U_3 AND
IN SMALL, MEDIUM OR LARGE OVOIDS.
RADIUM USED 13.3 MG., ACTIVE LENGTH 1.35 CM., ACTUAL
LENGTH 2.17 CM. AND FILTRATION 1.0 MM. PT.

Position	Radium mg.	Dosage rate $r/24$ hrs.	
		A	B
U_1	13.3	480	96
U_2	13.3	396	92
U_3	13.3	112	62
2 small ovoids each with one 13.3 mg.		375	150
2 medium ovoids each with one 13.3 mg.		332	147
2 large ovoids each with one 13.3 mg.		291	143

From this table the dose given A and B can be calculated for any technique using this radium or submultiples of it.

Example: Suppose a patient is treated for five days altogether (three days treatment, one week rest followed by two days treatment) with two 13.3 mg. tubes in *each* ovoid (medium sized) and one 6.6 mg. tube in position U_1 and one 13.3 mg. in position U_2 .

<i>Position</i>	<i>A</i>	<i>B</i>
U_1	1200	240
U_2	1980	460
medium ovoids	3320	1470
Total Dose	6500r	2170r

In this technique point A receives 6500r and point B 2170r. It is possible to build up the dose at B by the use of a "split" 10×12 field whose isodose curves are shown in the Appendix. The field actually consists of two 10×4 fields with their edges separated 4 cm. When this special treatment cone is applied directly over the female pelvis the point A is shielded from further radiation while point B receives the largest dose. By applying two such fields in opposition it is possible to add to the radium dose an x-ray dose to point B of 2000 to 2500r. Roentgens of radium gamma rays may not be added directly to x-ray roentgens. If further radiation at B is required, two angled lateral fields may be directed towards each point B.

The integral dose received during radium treatment of cancer of the cervix can be calculated by a method due to Mayneord (4). The dosage rate 1 cm. from a 1 mg. source of radium filtered by 0.5 mm. of platinum is 8.4 r/hr. The dosage rate at any other distance r will be given by

$$D = \frac{8.4\epsilon^{-\mu r}}{r^2}$$

where $1/r^2$ corrects for the decrease due to inverse square law and $\epsilon^{-\mu r}$ corrects for the absorption by the tissues. For small thicknesses of tissue the last factor can be neglected but when a thick layer of tissue completely surrounds the radium as in a cervix treatment this factor is important. μ takes the value 0.028 cm.^{-1} for radium gamma rays. The integral dose received between spherical shells of radii r and $r + dr$ is given by $4\pi r^2 dr \cdot D$. This can be integrated for r going from 0 to ∞ to yield $\Sigma = 4\pi(8.4)/\mu = 3750 \text{ gm. r}$. This means the

integral dose received from 1 mg. of radium in 1 hr. is 3750 gm. r. or 1 mg. hr. = 3750 gm. r. This figure is based on the assumption that the patient is large enough to absorb all the radiation. A patient regarded as a sphere of radius 10 cm. will only absorb about one quarter of this — the rest being radiated from the patient. In a cervix case about 40% is absorbed. We see that the unit, the mg.-hr., is really a unit of energy absorption being proportional to the integral dose in gm.r. There is thus some justification for the statement of dosage in terms of mg. hr. when radium is placed in the cervix or uterus because the geometric factors are somewhat the same in all cases. However, it is much better to state dosage in terms of the r unit at certain particular points such as A and B (Fig. X-20).

10.12 BETA RAY APPLICATORS

Usually when radium is used in the treatment of cancer all the alpha and beta particles are stopped by the case surrounding the radium salt, and only the gamma rays contribute to the biological effect. In the very early days of radium therapy the containers often allowed some of the beta particles to escape in great enough quantities to give an excessive dose in the immediate neighborhood of the radium needle. The excess dose at the surface of the needle was attributed to the so called "caustic effect" of the beta particles. This "caustic effect" was not due to any specific property of the beta radiation but to the high local intensity. Today all radium needles are surrounded with 0.5 mm. Pt. which removes all the alpha and beta particles. Beta ray applicators are, however, useful for the treatment of certain very superficial lesions.

Modern beta ray plaques consist of a shallow metal box, the back and sides of which are thick enough to cut off the primary beta radiation (i.e., about 2 mm. of brass or monel metal). The front face of the box is made of monel foil about 0.1 mm. thick. The box is filled with radium salt and is made vacuum tight so that radon cannot escape. Plaques are loaded with from 1 to 10 mg. of radium per square cm. of surface. A common type has a strength of about 5 mg./cm.². The radioactive material is usually mixed with a filler and spread about 2 mm. deep in the shallow box. The uniform distribution of the radium may be checked by placing the radium plaque over a film to obtain an autoradiograph.

The beta particles which are of clinical importance are those from radium B (maximum energy 0.65 Mev.), radium C (3.15 Mev.) and radium E (1.17). The low energy particles from radium D (0.025) are absorbed within the radium salt itself. When a plaque is filled with

freshly prepared radium some time must elapse before the disintegration of the radium has produced equilibrium amounts of radium B, C, and E. Study of section 9.06 will show that after a few days equilibrium amounts of radium B and radium C will be present but that very long periods of time must elapse before much radium E will be present for it is produced from radium D with a half life of 22.2 years. For these reasons the activity of a beta ray applicator is likely to increase slowly with age. The radiations from such a plaque are a mixture of beta and gamma rays. Neary (8) has shown that at the surface of the plaque the ratio of beta to gamma ionization varies from 20 to 40 depending upon the construction of the plaque. In immediate contact with the plaque the main ionization is due to the beta particles while at depths of 5 mm. below the surface of a tissue-like absorbing medium the effects of beta and gamma rays are approximately equal. Blomfield and Spiers (1) and Neary (8) have measured the percentage depth dose in a water phantom and find about 50% depth dose at 1 mm. and about 30% at 2 mm. depth. The dosage rate at the surface of the applicator depends upon its construction but for the average plaque is about 1000 r/hr when it is loaded with 1 mg. of radium per cm.². Before such plaques are used, however, the dosage rate should be determined using a very thin walled flat ionization chamber.

The small depth dose indicates that such plaques should only be used on very thin superficial lesions such as Mooren's ulcer and some other non malignant conditions of the cornea and conjunctivae where a rapidly falling depth dose is essential to protect the near by lens.

Some use is also being made of nasopharyngeal applicators using a glass bulb of radon placed in a cylindrical brass holder with a thin window at one end. Such a device gives an indeterminant amount of both beta and gamma radiation because of uncertainties in the distance factor and the absorption of the beta particles by the glass walls of the radon container. It is impossible for a radon technician to reproduce glass bulbs of the same filtration, size and shape and uncertainties in these factors can easily alter the beta ray dose by a factor of 4 or more. If beta ray applicators are used they should be calibrated in terms of the dosage rate at the surface. It is likely that a number of the artificially produced beta ray emitters will prove to be convenient sources for this type of work.

10.13

SUMMARY

The author is aware that there are a number of satisfactory methods of treating the examples discussed in this chapter. However, these

examples do illustrate the fundamental physical principles involved. For example, in treating cancer of the cervix, a variety of techniques such as those developed in Stockholm, Paris, Manchester and elsewhere are in common use. They are all based on sound principles and the dosage received can be expressed in terms of the r unit. Many radiotherapists have achieved very fine clinical results through years of experience without the use of the physical approach discussed herein, but it is difficult for such skills to be passed on to others without placing the work on a physical basis. Many of the differences in techniques are based on the assumption that dosage rate is of great importance in determining clinical results. The author is not prepared to enter into such a discussion as further careful experimental work on this topic is required where depth dose and all other physical factors are carefully controlled.

REFERENCES

1. Blomfield, G. W. and Spiers, F. W.: *Brit. J. Radiol.*, 19:349, 1946.
2. Jones, D. E. A.: *Brit. J. Radiol.*, 17:46, 1944.
3. Mayneord, W. V. and Roberts, J. E.: *Brit. J. Radiol.*, 10:365, 1937.
4. Mayneord, W. V.: *Brit. J. Radiol.*, 13:235, 1940.
5. Meredith, J. W. and Stephenson, S. K.: *Brit. J. Radiol.*, 18:45, 1945.
6. Meredith, J. W. and Stephenson, S. K.: *Brit. J. Radiol.*, 18:86, 1945.
7. Meredith, W. J.: *Radium Dosage*. Edinburgh, Livingstone.
8. Neary, G. J.: *Brit. J. Radiol.*, 19:357, 1946.
9. Paterson, R. and Parker, H. M.: *Brit. J. Radiol.*, 7:592, 1934.
10. Paterson, R., Parker, H. M. and Spiers, F. W.: *Brit. J. Radiol.*, 9:487, 1936.
11. Paterson, R., and Parker, H. M.: *Brit. J. Radiol.*, 11:252, 1938.
12. Paterson, R. and MacVicar, W.: *Brit. J. Radiol.*, 11:452, 1938.
13. Sievert, R. M.: *Acta radiol.*, 11:249, 1930.
14. Spencer, E. W. and Johns, H. E.: *Am. J. Roentgenol.*, 57:711, 1947.
15. Taylor, L. S. and Singer, G.: *Am. J. Roentgenol.*, 44:428, 1940.
16. Tod, M. C. and Meredith, J. W.: *Brit. J. of Radiol.*, 11:809, 1938.
17. White, T. N., Marinelli, L. D. and Failla, G.: *Am. J. Roentgenol.*, 44:889, 1940.
18. Symposium: Dosage Control in Interstitial Radium Therapy. *Brit. J. Radiol.*, 19:133, 1946.

Chapter XI

HIGH ENERGY DEVICES

11.01

INTRODUCTION

In order to study the fundamental processes of nuclear physics, it is necessary to bombard the nucleus with a particle of sufficient energy to disrupt the enormous forces which hold protons and neutrons together within the nucleus. To do this the particles usually require an energy of a few million electron volts. Until a few years ago such disintegration experiments were, of necessity, confined to those which could be done using the alpha, beta and gamma rays emitted from natural radioactive materials. Recently, a number of high energy devices have been developed which are capable of producing much more energetic particles than those which occur in nature. These high energy particles are capable of inducing radioactivity in many new materials. New activities may be produced by the bombardment of stable nuclei with protons, neutrons, deuterons, alpha particles, electrons and gamma rays. Some of the devices developed for this work have been found useful in cancer therapy. In the following sections a few of these devices will be described briefly.

11.02

THE CYCLOTRON

In an x-ray tube the energy of the x-ray beam is determined by the voltage applied between filament and target. If this voltage is 100 Kv. the maximum energy of the accelerated electron and thus of the x-rays will be 100 Kv. If it were possible to make an electron fall through this same potential difference 1000 times then its final energy would be 100 Mev. In the cyclotron and betatron this is, essentially, what is done. The particle which is being accelerated is made to fall many times through a relatively small potential difference so that it acquires a large energy.

The cyclotron is shown diagrammatically in Figure XI-1. A and B are hollow semicircular pieces of metal with a short gap between them. These D's, as they are called, are placed between the poles of a large D.C. magnet (not shown). The D's are connected to a high frequency (10 million cycles per second) high voltage (20 Kv.) transmitter. A source of positive ions is arranged at the centre of the highly

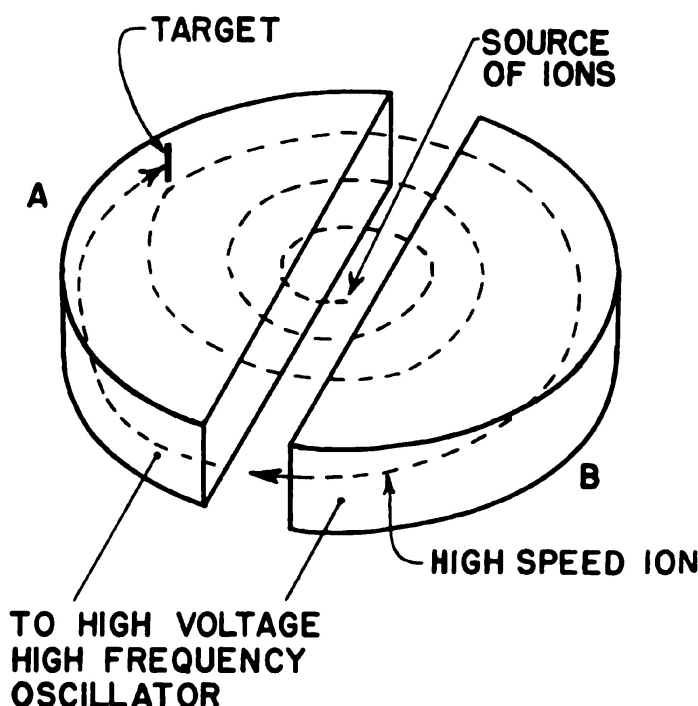


Figure XI-1. Diagram illustrating the operation of the cyclotron.

evacuated D's. If protons are to be accelerated a small amount of hydrogen is liberated at the centre and bombarded with electrons from a tungsten filament to produce a positive ion or proton. This positive ion finds itself in the electric field between the edges of the two D's and will be attracted by the negative one and repelled by the positive one. Once inside the negative D it would travel with uniform velocity were it not for the strong magnetic field. This magnetic field will cause the particle to move in the arc of a circle at constant speed until it again emerges between the D's. If it reaches the gap just as the direction of the electric field changes the particle will be accelerated and drawn into the other D. It is now travelling faster, but also on a larger circle, so that it will reach the next gap just as the electric field changes again, and so on. The basic principle of the cyclotron is the fact that a slow moving charge will take the same length of time to travel through the D as a higher speed particle for the latter will travel on a much larger circle.*

*A particle of mass m and charge e moving in a magnetic field H experiences a force Hev/c (H — gauss, e — c.s.u., v — cm./sec.) at right angles to its direction of motion. This bends the particle into a circle of radius R such that the centrifugal force is equal to the force exerted by the field, i.e., $Hev/c = mv^2/R$. This may be arranged to give $\pi R/v = \pi mc/He$. Now $\pi R/v$ is the time taken (distance/velocity) for the particle to traverse one D in a circle of radius R . This time is independent of velocity and so will be the same as long as m and H remain fixed. If m increases then the time required is longer and the particle will reach the gap between the D's behind time.

This condition for resonance is automatically satisfied for any particle whose mass remains constant with velocity. However, it is well known that the mass of a particle increases as its velocity approaches the velocity of light, according to Einstein's equation

$$m = \frac{m_0}{\sqrt{1 - v^2/c^2}} \quad (11-1)$$

In this equation, v is the velocity of the particle and c the velocity of light; m_0 is the mass of the particle when at rest and m the mass when the particle has a velocity v . A particle travelling with the large velocity of 18,600 miles per second ($1/10$ the velocity of light) has a mass $1.005 m_0$ ($m = m_0/\sqrt{1 - .01} = 1.005 m_0$). That is, the mass is increased by 5 parts in 1000. It is obvious that for velocities encountered in every day life the increase of mass with velocity is of no significance. However, for an electron the change in mass with velocity is quite large, even for a relatively low energy particle. A 100 Kv. electron has mass $1.197 m_0$; a 1000 Kv. electron has mass $2.29 m_0$; and a 10 million volt electron has a mass about 20 times its rest mass. *This means electrons cannot be accelerated in a cyclotron.* Although the change of mass of a heavy particle such as a proton, deuteron or alpha particle is not nearly so great, in the final analysis this change of mass does limit the energy of the particle which can be produced, for as the mass changes the particle gets out of step and reaches the gap between the D's at the wrong time. This can be partly overcome by increasing the field H near the periphery of the magnet to keep the particle in step or by means of the synchrocyclotron. In this device the frequency of the transmitter is reduced automatically as the particle acquires energy. The slight increase in time between oscillations can be made to compensate exactly for the longer time required for the particle to move through the D's. The large cyclotron at the University of California, which has pole pieces 184 inches in diameter, works on this principle and is capable of generating deuterons (heavy hydrogen) with an energy of 200 Mev. In this machine the particles acquire about 3000 e.v. of energy each time they cross the gap. The particle makes about 70,000 circuits around the pole in acquiring the 200 Mev. final energy.

A neutron beam from the cyclotron has been used by Stone, Lawrence and Aebersold (11) in the treatment of certain types of cancer. High speed alpha particles from the cyclotron were allowed to impinge on a beryllium target where they produced neutrons. These neutrons were then collimated by long slabs of paraffin to the size required for the treatment beam. The early results of such treat-

ments were reasonably satisfactory but the long term effects have not been good and such work has been discontinued (see Stone (12)).

There is a possibility that protons with energies of the order of 100 Mev., produced in the cyclotron, may be useful therapeutically. Wilson (16) has shown that 140 Mev. protons give a small ionization in tissue to a depth of about 12 cm., at which point the ionization rises sharply to a peak and then quickly falls to zero at a depth of 16 cm. The dose at the peak (depth 14.8 cm.) is about 10 times the surface dose. This distribution may be of use in the treatment of certain types of tumors.

To produce radioactive materials in the cyclotron the material is usually placed inside the vacuum chamber and bombarded with the high energy beam. For example, radioactive phosphorus and sodium may be produced by bombarding ordinary phosphorus or sodium with a beam of heavy hydrogen particles.

11.03

THE BETATRON

The betatron is a device for accelerating electrons. These high speed electrons may be removed from the machine and used as an electron beam or may be made to produce x-rays within the machine by bombardment of a target. When the betatron is used in the latter way it is merely a high energy x-ray machine. The depth dose achieved from machines operating from 20 Mev. to 50 Mev. indicate the fact that such machines may prove to be very useful tools in the treatment of cancer. The first betatron was produced by D. W. Kerst at the University of Illinois (5, 6). It was a 2 Mev. machine. He has recently constructed a 300 Mev. machine. The basic principles of the operation of a betatron are illustrated in Figure XI-2.

An evacuated doughnut-shaped porcelain envelope is placed between the poles of an A.C. magnet (Fig. XI-2a) with slightly tapered poles. The magnet is excited by an alternating voltage at 180 cycles per second. Electrons are liberated by the heated tungsten filament and injected into the doughnut by the injector. The electrons are bent into a circular path by the magnetic field and spiral slowly inwards until they reach the equilibrium orbit with radius r_0 (Fig. XI-2b). As the electrons travel around in this circle they are continuously accelerated. This will be understood by consideration of Figure XI-2c. It is well known that, when the flux through a closed loop is changed, an electric field is established around the loop and a reading will be obtained on a voltmeter V. If an electron were released at some point A (Fig. XI-2c) on this copper wire, it would travel around the loop

with increasing velocity were it not for the resistance of the copper which appears as friction. In the betatron a "frictionless" path is provided inside the evacuated doughnut and the electron is constrained to move in the circular path of constant radius r_0 by the magnetic field of the magnet. The changing magnetic field provides a changing flux and thus an electric field E (Fig. XI-2c) which soon gives the electron a high velocity. In order that the particle stay in the equilibrium orbit, a certain condition must be satisfied between the field at the orbit and the flux enclosed by the orbit. If this condition is not satisfied the electron will move away from the equilibrium orbit.

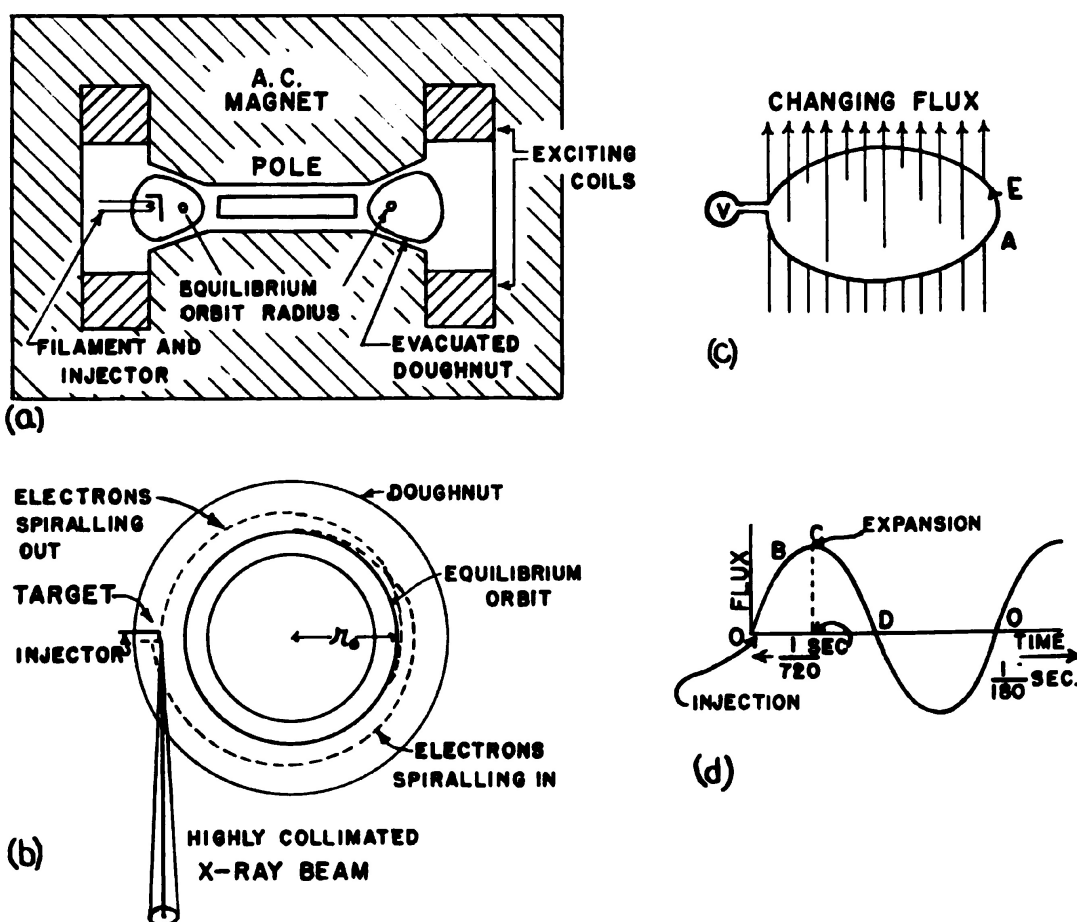


Figure XI-2. Diagrams illustrating the construction and operation of the betatron.

(a) Cross sectional diagram showing the A.C. magnet, the poles, the doughnut and injector.

(b) Illustrating the paths of the electrons within the doughnut and the method of production of the x-rays.

(c) Illustrating how an electric field is produced by a changing magnetic flux.

(d) Illustrating the cycle of operation of the betatron showing the time of injection and expansion.

As the magnetic field starts to increase from O (Fig. XI-2d) electrons are injected. At this instant the equilibrium conditions are not satisfied so the electrons spiral inward until they reach the orbit with radius r_0 . As the flux increases to C an electron acquires energy and at C will have its maximum energy. If it were left in the orbit it would be decelerated and brought to rest at D. However, if at C the equilibrium conditions are suddenly altered the electron will spiral outward to strike the back of the injector (Fig. XI-2b) where x-rays are produced.

In the Allis-Chalmers betatron installed at the University of Saskatchewan, the electrons acquire an energy of about 100 electron volts per turn. This energy corresponds to a large velocity so that the time for 1 transit will be small. In $1/720$ sec. the electron travels around the orbit about 250,000 times and acquires a total energy of 25 Mev. ($250,000 \times 100 = 25$ Mev.). It can be shown that after a very small fraction of the $1/720$ sec. has elapsed the particle has a speed very near the velocity of light. Further acceleration in the electric field merely increases the mass of the electron without appreciably changing its velocity. Of course, as the mass of the particle increases so does the energy of the particle. In the 25 Mev. betatron the mass of the electron just before it hits the target is about 50 times its rest mass.

If a lower energy x-ray beam is required the equilibrium conditions can be upset earlier in the cycle at some point, such as B (Fig. XI-2d), causing the electron to spiral out before its maximum energy is attained. The betatron is idle for the next $\frac{1}{4}$ cycle until the point O (Fig. XI-2d) is reached again at which time electrons are injected, then accelerated, and finally expanded to strike the target and produce x-rays at C. The radiation from the betatron thus comes off in pulses lasting about 1 microsecond and spaced $1/180$ sec. apart.

The efficiency of x-ray production is very high and no cooling mechanism is required. Evidently almost all the energy of the electrons is changed into x-rays. The x-ray beam is highly collimated (see Chapter II) in the forward direction. This effect becomes more pronounced as the energy is increased and offers a practical limit to the maximum energy which is useful for therapy. In order to give a useful distribution over a reasonable area of field, it is necessary either to reduce the intensity along the axis of the beam by means of a compensating filter (1, 4) or to use very great treatment distances. The latter tends to increase the exit dose which is already very much greater than the entrance dose. For these reasons the optimum energy for betatron therapy lies between 20 and 50 Mev. A photograph of

the Allis-Chalmers betatron in the Physics Department of the University of Saskatchewan, which is being used in cancer therapy, is shown in Figure XI-3. Typical isodose curves are shown in Figure VI-19.

Skaggs (10) has investigated the depth dose which may be obtained when the high speed electrons from the betatron are allowed to enter a water phantom. These electrons are removed from the doughnut by an ingenious "peeler" device (9). This electron "peeler" consists of a laminated iron channel placed tangentially to the equilibrium orbit just outside it. As the electron orbit is expanded the electrons will enter this channel where they are completely shielded from the magnetic field, and therefore, travel in a straight line until they emerge from the betatron through a thin window in the doughnut. The depth dose achieved with electrons is essentially constant to a depth corresponding to the range of the electrons in tissue, although there is a slight rise in depth dose near the end of the electron track. Depth dose data of this kind has also been obtained by Trump (13) using the Van de Graaff generator. Typical depth dose data for 1.5 Mev. electrons due to Trump (13) and 12.2 and 16.4 Mev. electrons from

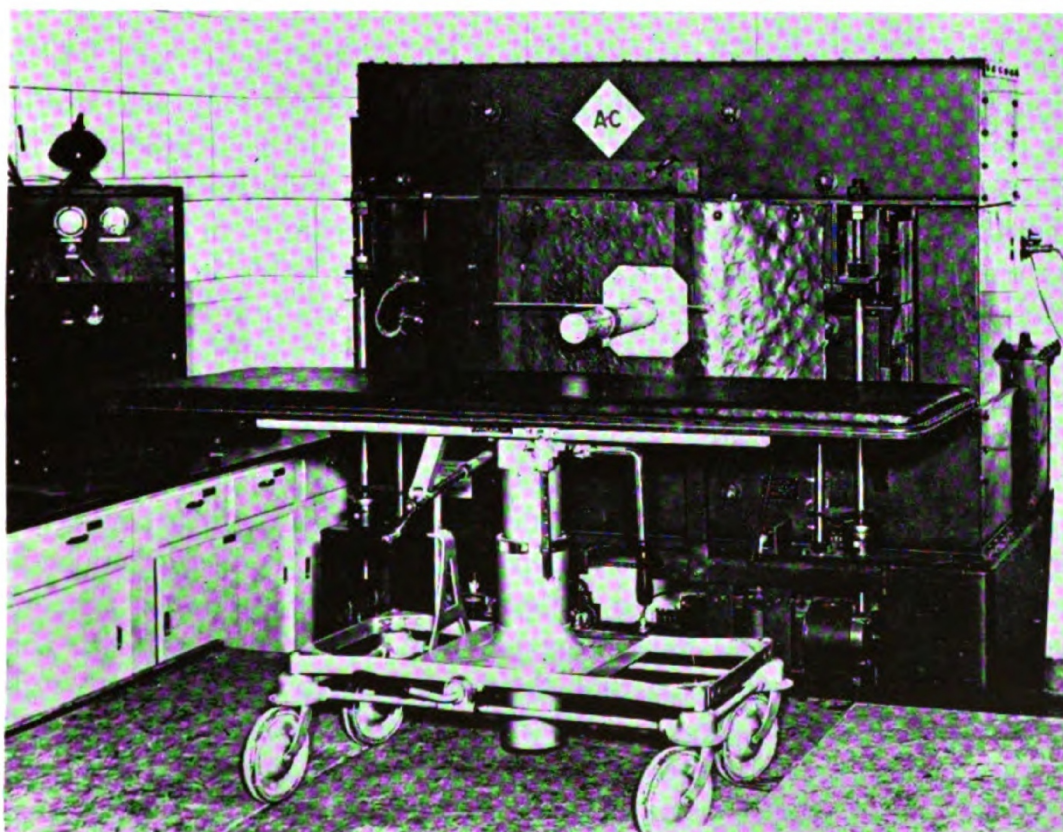


Figure XI-3. Photograph of the Allis-Chalmers betatron in the Physics Department of the University of Saskatchewan. Note the lead shield in front of the machine and the treatment cone in place.

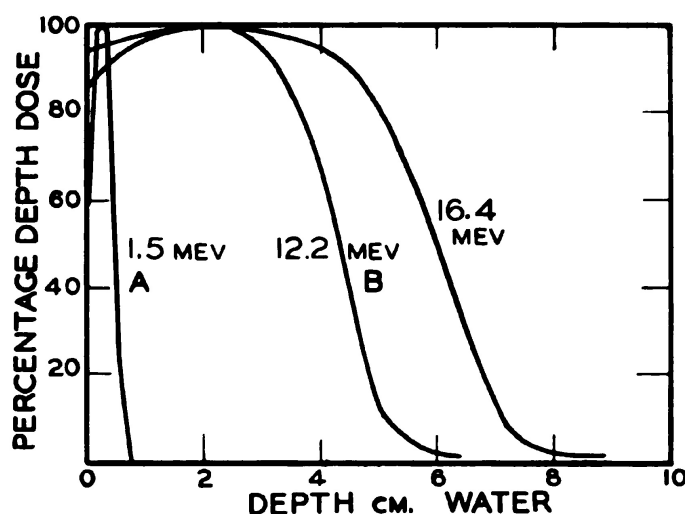


Figure XI-4. Graphs showing the percentage depth dose obtainable with electron beams at 1.5, 12.2 and 16.4 Mev. Data for 1.5 Mev. electrons were obtained by Trump⁽¹⁴⁾ using the Van de Graaff generator. Data for 12.2 and 16.4 Mev. were obtained by Skaggs⁽¹⁰⁾ using the electron beam from a 22 Mev. betatron.

the betatron due to Skaggs (10) are shown in Figure XI-4. It is doubtful if the distributions obtainable with electrons will be as useful as those obtained from x-rays except for very superficial lesions. The limited range is a definite advantage, but it is doubtful if as good a distribution can be obtained using an electron beam from the betatron as can be obtained with several betatron x-ray fields in a cross fire technique. There is no doubt that the electrons will produce the same biological effects as x-rays since the latter are only absorbed by setting electrons in motion. However, considerable caution will have to be exercised in using high speed electrons for therapy since the exposures required will have to be extremely short. In the conventional x-ray machine the energy of the electrons is first converted into x-rays in the machine and then the photons are converted back into electronic motion in the patient. Both these processes of conversion are inefficient. When the electron beam itself is used, the conversions are avoided so that the exposures to a beta beam will necessarily be short. Skaggs (10) has reported dosage rates of 1500 r/min. at a point 35 cm. from the window of the betatron doughnut and states that this dosage rate can likely be increased by a factor of 100. The beta particles from radium needles are usually suppressed because they are thought to have a very caustic effect. Actually this is not true, and if their energies and ranges were much

greater, they would be useful. Because of their small ranges they can produce an effect only near the needle, where the radiation intensity is highest. Beta particles of high energies have sufficient range in tissue to be useful medically.

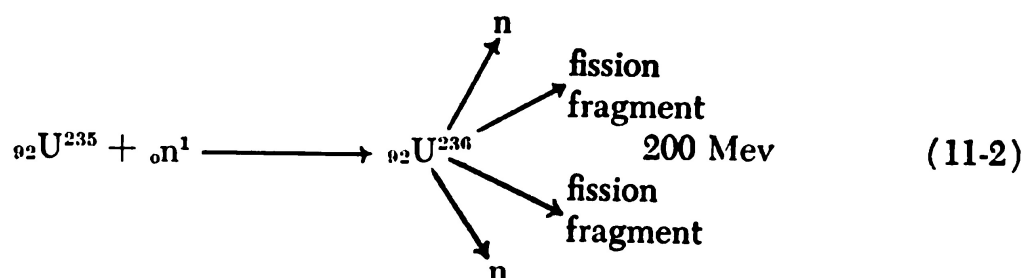
11.04 THE SYNCHROTRON

It is possible to increase the energy from a betatron by changing it into a synchrotron. In the betatron the accelerating electric field is supplied by the changing flux through the equilibrium orbit. In the synchrotron the electrons are accelerated by allowing them to pass through a small resonant cavity which is made an integral part of the electron doughnut. This resonant cavity is connected to a high frequency oscillator. The electrons are brought up nearly to the speed of light by means of the betatron principle and then power is automatically applied to the resonant cavity. This bunches the electrons and gives them energy every time they pass through the cavity. The increasing magnetic field continues to hold the electrons in their orbit as their energy increases. The synchrotron, because of its complexity, offers no advantages over the betatron for energies up to 25 Mev. However, for higher energies a saving in the size of the machine may be made. The synchrotron principle of operation is not limited to electron acceleration and plans are now under way to produce 10,000 Mev. protons at the Brookhaven Laboratory. Protons of high energy will be injected into the machine and accelerated by the resonant cavity. The orbit for this machine will have a diameter of 160 ft. and the protons will be held in this orbit as their energy is increased by a changing magnetic field which will be produced at the orbit by a ring type of magnet. With such machines it will be possible to produce energies comparable with those observed in cosmic rays.

11.05 FISSION

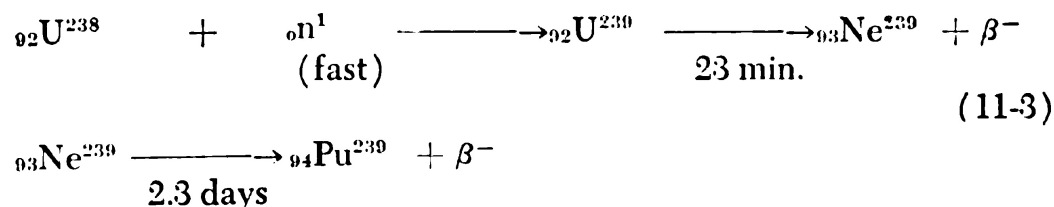
The uranium pile is today the most important source of radioactive materials. Most of these can be produced more easily in a pile than in a cyclotron or in any other high energy device. Such piles are all based on the fact that certain heavy elements undergo fission with the release of enormous amounts of energy. Previous to 1939 several experimenters came to the conclusion that elements with atomic numbers greater than 92 were being produced when uranium was bombarded with neutrons. These were called transuranic elements. In all such experiments β^- activity was observed and this was interpreted as being due to the conversion of neutrons into protons (equation 9-1), thus increasing the value of Z . The "new" elements

produced in minute quantities were fitted into the periodic table in the appropriate columns corresponding to their chemical properties. However, in 1939 Hahn and Strassmann obtained unquestionable evidence that, in reality, elements with Z less than 92 were being produced and that an isotope of uranium underwent fission into two fragments according to the equation



The release of 200 Mev. of energy by the fission of Uranium is enormous in comparison with the energy released by any other nuclear reaction. In this process two to three neutrons are also released so that if these neutrons are all used to initiate fission in other nuclei a chain reaction will be set up. All the elements near the centre of the periodic table can appear as fission fragments but in particular elements with mass numbers in the region of 140 and 90 appear most often. The uranium nucleus has 143 neutrons and 92 protons so that, when the nucleus splits up, the fragments will have a considerable excess of neutrons. These neutrons will change into protons with the emission of a β^- particle and the process will continue until a stable nucleus results. All fission fragments are β^- emitters.

Recent investigations have shown that at least four transuranic elements are produced: Neptunium (93), Plutonium (94), Curium (95) and Americium (96). The first two are produced thus:



There are at least three materials which are fissionable; these are ${}_{92}\text{U}^{235}$ by slow neutrons, ${}_{92}\text{U}^{238}$ by fast neutrons (although the probability of this reaction is small), and ${}_{94}\text{Pu}^{239}$ by slow neutrons. A small sample of either U^{235} or Pu^{239} is harmless, for too many neutrons escape and the chain reaction is impossible. If two particles, each less than a

certain critical size, are brought together to form one particle greater than the critical size, then an explosion will occur.

11.06 THE NUCLEAR REACTOR (PILE)

The first chain reacting pile was made using carbon and uranium. A large number of carbon blocks each bored with a hole in its centre were accurately stacked upon one another until they formed a large cube several yards to the side. Uranium rods were then inserted into the graphite blocks. The uranium used was natural uranium consisting of 140 parts of U^{238} to 1 part U^{235} . When an atom of U^{235} undergoes fission two to three fast neutrons are ejected. These may be captured by the U^{238} to form plutonium, or may bounce around in the carbon blocks until they are slowed down. After being reduced in speed they can initiate fission in other atoms of U^{235} . The carbon is known as the moderator and its sole purpose is to provide some material which will slow down neutrons. This material must be such that it will not capture neutrons.

To maintain a chain reaction at least one neutron per fission must be conserved to produce fission in another nucleus. In a small pile a large percentage of the neutrons will escape through the surface and thus tend to stop the reaction. In fact, a pile must exceed a certain critical size to operate at all. The level at which such a pile will operate can be controlled by the insertion of cadmium rods into the pile. Such rods will capture neutrons and thus tend to stop the reaction.

Neutrons carry no charge and therefore can only be slowed down by a collision with another nucleus. If the neutron collides with a particle exactly its own size it can lose all its energy but on colliding with a heavy nucleus it will lose only a small fraction of its energy. A much better moderator than carbon is heavy water. Using such as a moderator neutrons do not need to be conserved to the same extent, and the design of such a pile becomes less critical. Ordinary water will not do as a moderator because hydrogen will capture neutrons to form heavy hydrogen.

The Heavy Water pile consists of uranium rods placed in a vat filled with heavy water. High speed neutrons from the fission in the uranium rods travel out into the heavy water and by collision with the heavy hydrogen lose energy. When they are reduced to "thermal" velocities (slow neutrons) they can be captured by U^{235} to produce another fission. The uranium rods and the heavy water become hot and care must be taken to remove this energy. The uranium rods

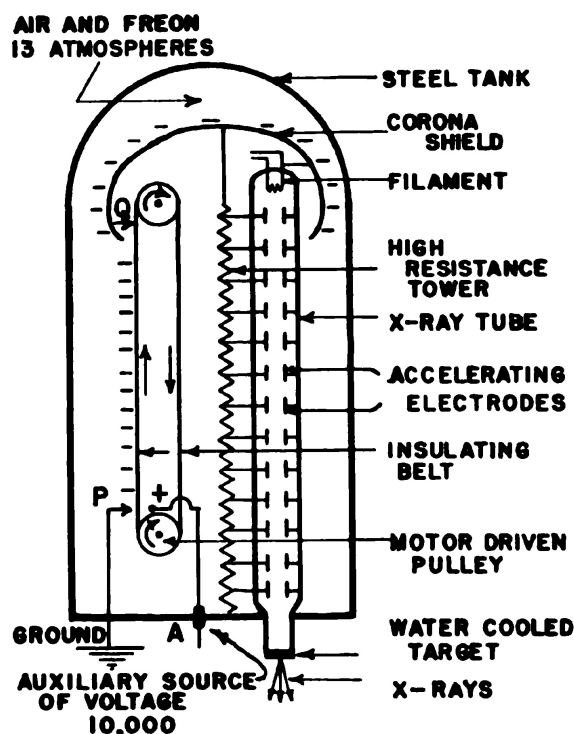


Figure XI-5. Schematic diagram of a pressure insulated Van de Graaff electrostatic generator.

also become poisoned by the fission fragments. The rods may be removed from time to time and the fission fragments and plutonium separated from the uranium. In the centre of a pile the neutron flux and gamma ray flux reach exceedingly high values equivalent in radiation effects to tons of radium. The neutron being uncharged suffers no repulsion on close approach to the positively charged nucleus and so, in general, can disrupt a stable nucleus more easily than the charged particles from the cyclotron. Almost all materials can be made intensely active by exposing them for a period of time to the high neutron flux near the centre of a pile.

11.07 THE VAN DE GRAAFF GENERATOR

This device, represented schematically in Figure XI-5 is really a large electrostatic machine. At the present time it is capable of developing up to 5 million volts in a relatively compact unit. The high voltage group at the Massachusetts Institute of Technology in Boston have been the ones chiefly concerned with its development (13, 14, 15). The basic principles are shown in Figure XI-5. An endless insulating belt is driven by a motor in the base of the instrument. An auxiliary source of voltage A at about +10,000 volts is used to spray

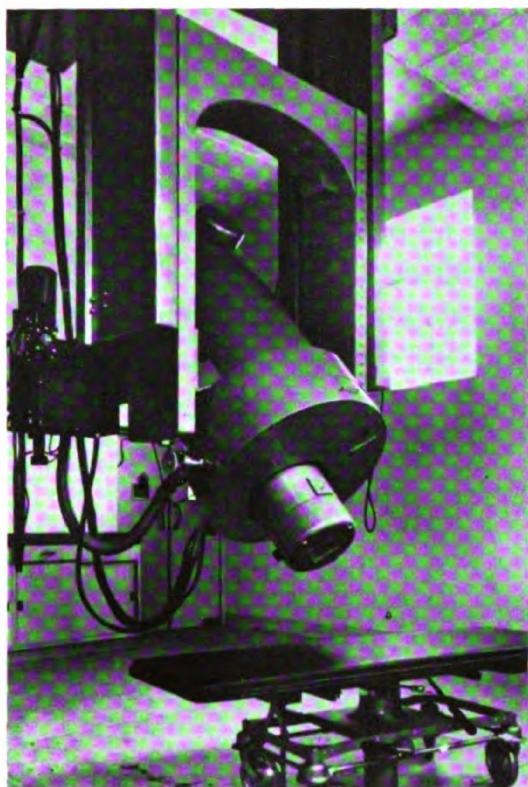


Figure XI-6. Photograph of a 2 million volt electrostatic x-ray generator for therapy. (Courtesy of High Voltage Engineering Corporation, Cambridge, Mass.)

negative charges by induction on this moving belt. A high electric field exists at the sharp point P and negative charges are attracted from P onto the belt by the positive potential of A. Near the top pulley these charges are removed by the collector Q which is connected to the spherical cap of the generator. The continuous motion of negative charges up to the upper sphere can lower its potential to 2 million volts below ground potential. The x-ray tube is placed parallel to the belt and to one side. It consists of a filament at the top, a large number of evenly spaced accelerating electrodes and a water cooled

target at the bottom. The upper spherical electrode at a high negative potential is joined by a series of high resistances to ground so that the potential falls uniformly from the bottom to the top. The accelerating electrodes of the x-ray tubes are joined to the appropriate points on this high resistance tower. A multi-section x-ray tube of this kind is required to avoid corona effects and to help focus the electrons during their transit to the target. The transmitted x-ray beam is used.

The whole of the generator proper is enclosed in a steel tank and is filled with a mixture of air and freon at a pressure of 13 atmospheres. Air at this pressure replaces, in insulating properties, several tons of transformer oil. The most recently produced generators are surprisingly compact, a 2 Mev. generator being about two feet in diameter and five feet high. The x-rays from such a generator are produced at constant potential and so give more penetrating radiation than other devices working at the same peak voltage. A photograph of a two million volt generator for therapy developed by the High Voltage Engineering Corporation is shown in Figure XI-6.

11.08 THE RESONANT TRANSFORMER

A low frequency resonant transformer has recently been developed by Charlton, (3) for the production of 1 and 2 million volt x-rays. The device is represented schematically in Figure XI-7. The transformer consists of a primary with a few turns (Fig. XI-7) and secondary consisting of a large number of turns chosen so that it will resonate with its own capacity at 180 cycles per second. There is no iron for the core so that the multi-section x-ray tube can be placed along the axis of the secondary. Suitable connections are made from the secondary to the sections of the x-ray tube so that a uniform potential gradient exists from one end to the other. Because the secondary is tuned to resonance, a small voltage in the primary produces very large oscillations in the secondary, thus developing a high voltage. Insulation is achieved using air and freon under pressure. The target of the x-ray tube is grounded and arranged so that the transmitted beam is used. The machine produces x-rays when the upper end of the secondary is negative. The machine does not deliver a constant potential. The device is slightly larger than the corresponding Van de Graaff type of generator. There is a real possibility that 250 to 400 Kv. machines may be built on this principle in the near future. Such units would be much smaller and more flexible in use than the present type of machine which is on the market. A photograph of a 2 Mev. G.E. Resonant Transformer type of x-ray unit is shown in Figure XI-8.

11.09 COBALT 60 TELECURIE UNITS

Teleradium units containing 10 gm. of radium must be used at short focal skin distances because of the low dosage rates obtained. This means that the percentage depth dose is of the same order as that achieved using 140 K.V. x-rays (see Figure VI-11). Larger radium sources are not feasible because of the cost of the radium and because, in a large source of radium, much of the radiation is absorbed by the radium itself. With the recent development of high neutron flux piles it is possible to produce specific activities of the order of 25 to 60 curies per gm. in cobalt in a reasonable time. One gram of cobalt with a specific activity of 50 curies per gram is equivalent in radiation to about 75 gm. of radium (see section 12.09). Sources of cobalt 75 to 100 times as powerful as those used in teleradium units are therefore feasible.

In the summer of 1951 two sources of cobalt, each with an effective strength of 1000 curies were made available by the Isotopes Pro-

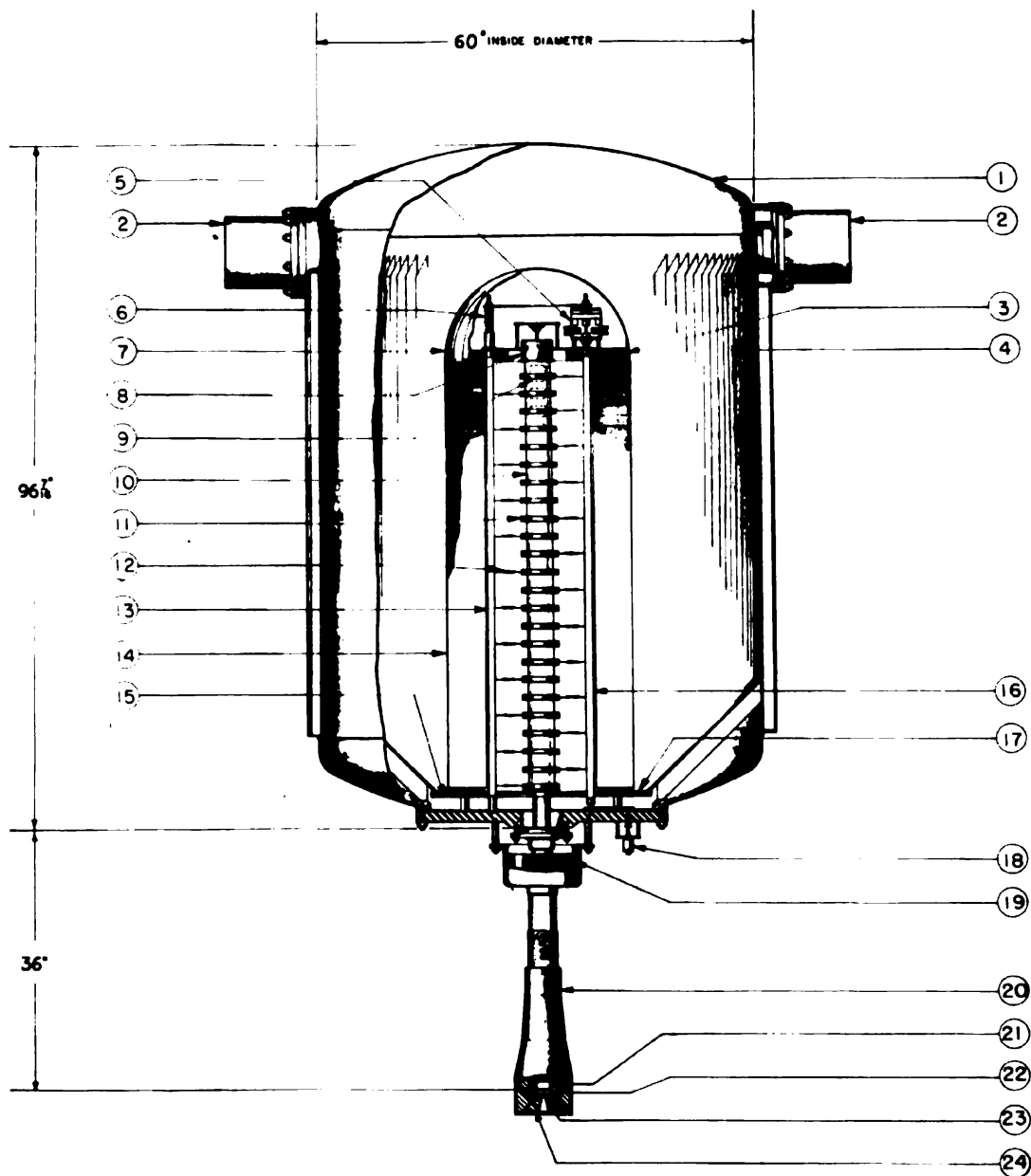


Figure XI-7. Sectional drawing of two-million-volt x-ray unit. Courtesy of General Electric.

- | | |
|---------------------------------|---------------------------------------|
| 1. Steel tank | 13. Glass tie rod |
| 2. Cooler | 14. Secondary coils |
| 3. End turn filament coil | 15. Primary winding |
| 4. Laminated shield | 16. Insulating filament-control shaft |
| 5. Variable reactor | 17. Laminated steel bottom |
| 6. Spring for tie rod | 18. Filament control motor |
| 7. Slotted brass shield | 19. Focusing coil |
| 8. Cathode assembly | 20. Lead shield |
| 9. First intermediate electrode | 21. Water jacket |
| 10. Glass envelope | 22. Extension chamber |
| 11. Shields around x-ray tube | 23. Tungsten target |
| 12. Tap lead | 24. Lead diaphragm |

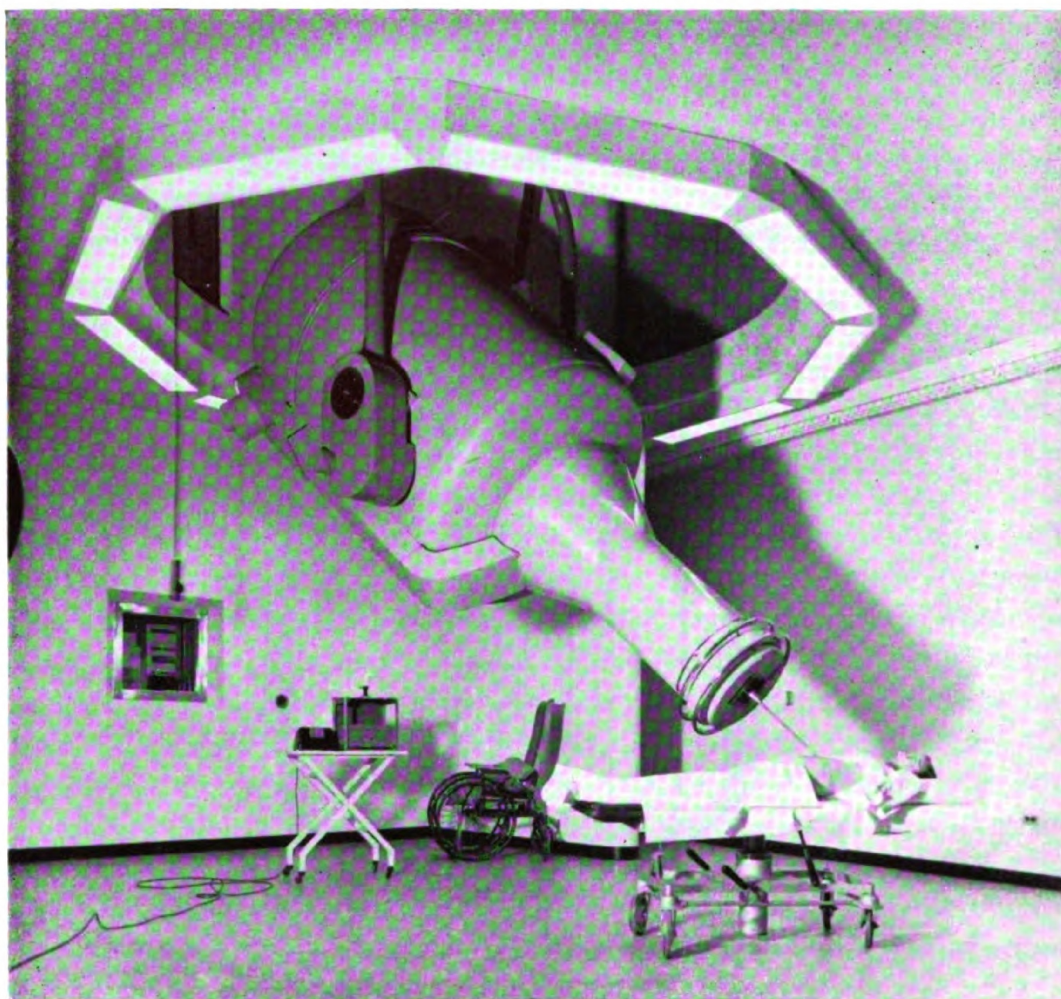


Figure XI-8. Photograph of General Electric two-million-volt resonant transformer x-ray machine which has been installed, at the Hospital for Joint Diseases in New York City. Photograph by Angelo Pinto.

duction Branch of the Canadian Atomic Energy Project at Chalk River for experimental and clinical purposes. The first unit was installed in the University Hospital, Saskatoon, and the second unit designed by Eldorado in the Victoria Hospital, London, Ontario. A diagram to scale of the treatment head designed by the author and built in Saskatoon is shown in Figure XI-9.

Cobalt metal in the form of discs 1 inch in diameter and 0.521 mm. thick were irradiated in the Canadian heavy water pile at Chalk River. These discs were spread over the available space in the pile in such a way as to minimize the shielding of one disc of cobalt by another. Cobalt has a high "capture cross-section" for neutrons, so that a beam of neutrons is rapidly attenuated in passing through cobalt. A layer of cobalt 2.3 mm. thick will stop 50% of the incident

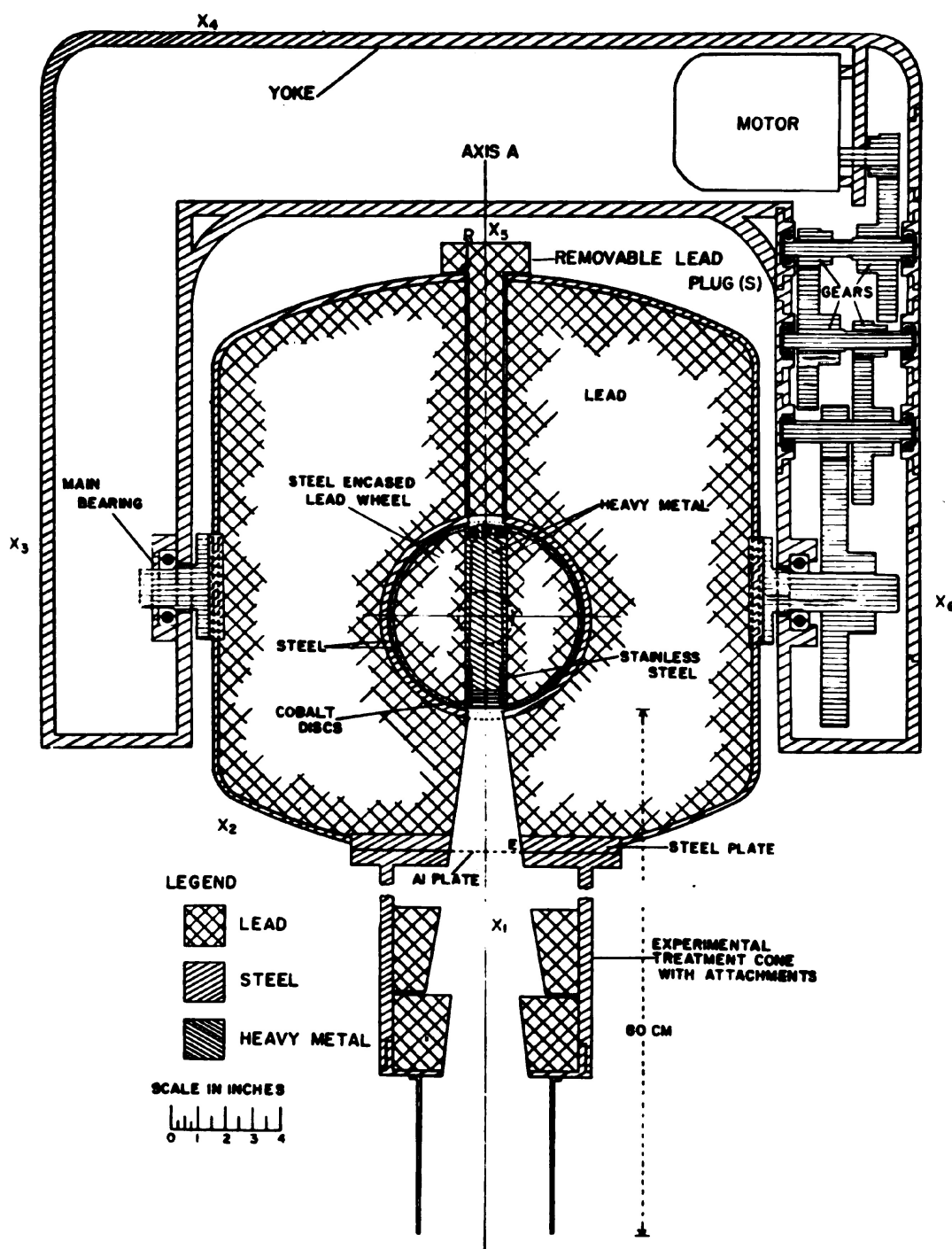


Figure XI-9. Diagram to scale of the treatment head showing the yoke which supports it, the rotating wheel which carries the source and an experimental treatment cone. The source unit consisting of a tapered cylinder of heavy metal, the stainless steel cup and the cobalt discs are shown near the centre of the head.

neutrons. After the cobalt discs were activated they were loaded by remote control into a stainless steel cup to form a source 1.30 cm. thick and 1 inch in diameter.

The cobalt discs were sealed into this cup by screwing into place a cylinder of heavy metal which appears in Figure XI-9 as a diameter of the wheel. The cobalt discs in the stainless steel cup are also shown. The source, consisting of the cobalt on the end of the heavy metal cylinder, was shipped to Saskatoon in a lead safe weighing over one ton. To load the unit, the lead plug S was removed from the head and the source pulled from the lead safe into the centre of the head, where it was firmly secured along a diameter of the wheel. The machine may be shut "off" by turning this wheel through 180°. In this position the source finds itself near the centre of a steel encased lead cylinder with 10 inches of lead on all sides and 7 inches of heavy metal between it and the opening of the head. To turn the machine "on" the wheel is rotated back through 180° to the position shown in Figure XI-9 where it is opposite the opening in the head. The motor which produces this rotation is not shown.

The machine makes no sound when it is "on" and this constitutes one of its dangers. Personnel are protected by a system of interlocking doors and lights. If the door to the treatment room is opened with the machine "on," the cobalt is immediately returned to the "off" position. With the cobalt in the "off" position, the dosage rate 1 foot from the head is less than 7 milliroentgens per hour or 50 milliroentgens per 7-hour day.

A photograph of the unit is shown in Figure XI-10. This shows the head supported between the arms of the inverted U-shaped yoke. The whole unit is supported from an overhead carriage by telescoping cylindrical steel sleeves. Motors for raising the unit, rotating it about a horizontal axis and moving the overhead carriage laterally, are controlled from the small panel shown in the photograph. The horizontal motion of the unit along the overhead track is necessary in positioning the unit for rotation therapy. In the floor of the room is a turntable 8 feet in diameter which can be rotated about a vertical axis. The rate of rotation of the turntable may be adjusted so that an integral number of turns takes place during the treatment time.

The dosage rate from the cobalt 60 unit is 33 roentgens per minute at 80 cm. or 84r/min. at 50 cm. The unit is used at a focal skin distance of 80 cm. One disadvantage of the cobalt unit lies in the relatively short half life of the source. Cobalt decays to half strength in 5.3 years so that periodically the source will have to be replaced by a new one. With the present source, useful outputs will be obtainable

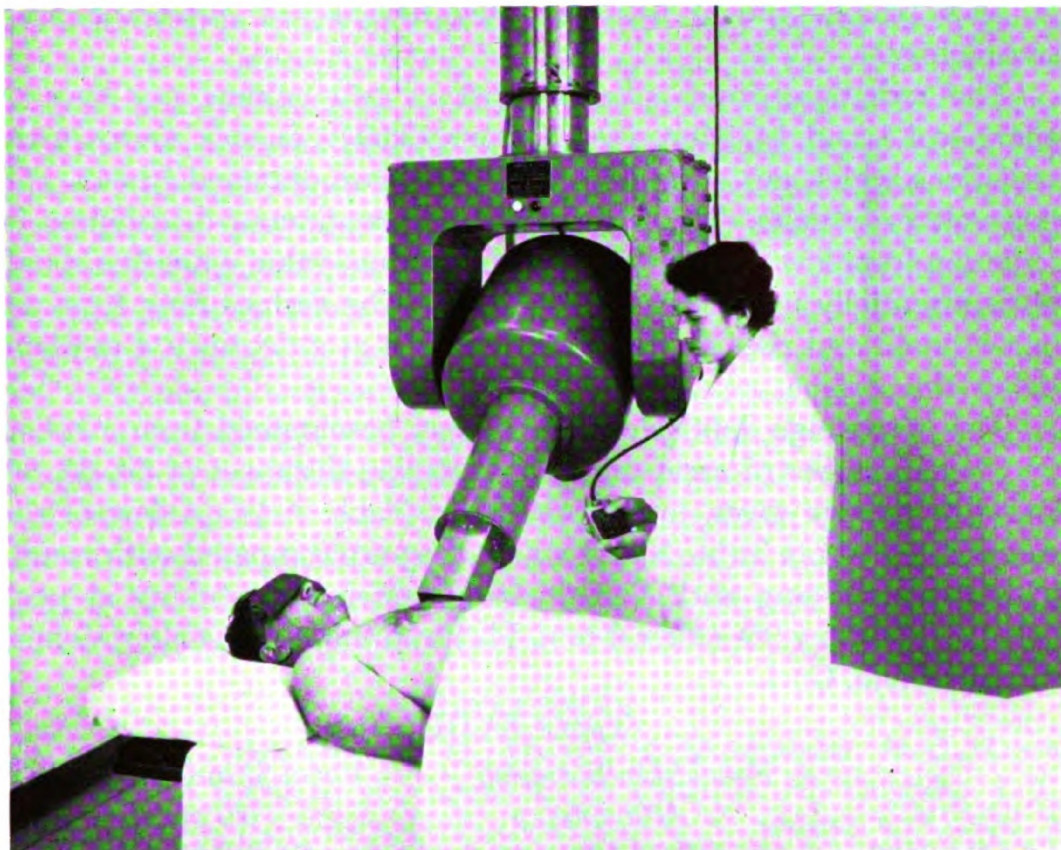


Figure XI-10. Photograph of the cobalt unit in operation in the University Hospital, Saskatoon. The unit was produced for the Saskatchewan Cancer Commission by the Acme Machine and Electric Company, Saskatoon.

for from 6 to 10 years. The problem of the design of treatment cones for such a unit is not easy. Because the source is rather large (1 inch in diameter), the diaphragm which limits the size of the field must be placed rather close to the surface of the skin, to prevent the penumbra region from being too large. If, on the other hand, the diaphragm is placed too close to the skin surface, scattered electrons and low energy photons from the diaphragm increase the skin dose and thus reduce the percentage depth dose. Experiments show that a diaphragm to skin distance of 15 to 25 cm. is a suitable compromise. The diaphragms must be made of lead 6 to 8 cm. thick and this constitutes a real problem, for the attachments become very heavy. However, it is possible to design the treatment cones so that none weigh more than 18 lbs. For details, reference should be made to the original papers (*British Journal of Radiology*, 1952). The unit designed by Eldorado uses a novel shutter arrangement to control the size of the field. The shutter is made of rectangular bars all moving in one plane in such a way that a continuous selection of rectangular fields is possible. It remains to

be seen which type of beam limiting device will prove the most satisfactory.

The radiations from cobalt consist of two gamma ray lines of energies 1.1 and 1.3 Mev. (see Section 12.09). Such a source gives radiations which are quite different from those obtained from 2 million volt x-ray units. The latter produce a continuous distribution of radiation from low energies up to the maximum value while the cobalt gives essentially monoenergetic radiation. The surface dose from cobalt is small and rises to its maximum value at a depth of 4 to 6mm. below the surface.

The percentage depth dose which may be obtained from a cobalt unit for a number of areas and source to skin distances of 50, 60, 80, and 100 cm. are given in the Appendix, Table A-13. A few of the values are given in Table XVIII where they are compared with results obtained by Trump with Van de Graff generators working at peak voltages of 2 Mev.⁽¹⁵⁾ (filter 9 mm. Pb.) and 3 Mev.⁽¹⁴⁾ (filter 10 mm. Pb. and 5 mm. Cu.).

TABLE XVIII

Depth	Focal Skin Distance 100 cm.		Focal Skin Distance 70 cm.	
	Field 100 cm. ²		Field 100 cm. ²	
	Co ⁶⁰	2 Mev. ⁽¹⁵⁾	Co ⁶⁰	3 Mev. ⁽¹⁴⁾
0.5	100	100	100	100
1.0	98	98	98	98
5.0	80	75	77	76
10.0	58	52	54	53
15.0	41	36	37	36
20.0	29	25	26	25

It is seen that the depth dose obtainable with the cobalt is slightly better than that obtained with a 3 Mev. x-ray machine. The unit is essentially much simpler than an x-ray machine and it is possible that such units will largely replace the more complicated types of x-ray generating equipment. The output of this first cobalt unit is smaller than that obtainable with present day 2 to 3 Mev. x-ray machines. This is certainly a disadvantage; however, future cobalt units can certainly be made with two to three times the activity of the one described here.

11.10

PROTECTION

In an x-ray department considerable care must be taken to assure that all personnel are protected against radiation hazards. This is

particularly true when one is dealing with high energy devices. It was shown in section 8.04 that the energy flux per recorded roentgen for high energy radiations is considerably greater than for low energy radiations so that the possible constitutional effects are greater. The so-called tolerance dose has been continually reduced and in Canada at the present time stands at 0.050 roentgens per day. Personnel must be protected against primary radiation and secondary radiation. The problem has been studied in a number of laboratories and it is now possible to design a radiotherapy department in such a way that the radiation is well below the weekly tolerance without wasting money in overdesign. For details concerning this problem the reader is referred to handbooks published by the National Bureau of Standards, Washington (7, 8). By judicious arrangement of the x-ray machines it may be possible to reduce the amount of lead protection required. For 2 Mev. installations the reader is referred to recent measurements by Braestrup and Wyckoff (2).

REFERENCES

1. Adams, G. D., Almy, G. M., Dancoff, S. M., Hanson, A. O., Kerst, D. W., Koch, H. W., Lanzl, E. F., Lanzl, L. H., Laughlin, J. S., Quastler, H., Riesen, D. E., Robinson, C. S., Skaggs, L. S.: *Am. J. Roentgenol.*, 60:153, 1948.
2. Braestrup, C. B., Wyckoff, H. O.: *Radiology*, 51:840, 1948.
3. Charlton, E. E., Westendorp, W. F. and Dempster, L. E.: *J. App. Physics*, 10:374, 1939.
4. Johns, H. E., Darby, E. K., Haslam, R. N. H., Katz, L. and Harrington, E. L.: *Am. J. Roentgenol.*, 62:257, 1949.
5. Kerst, D. W.: *Physical Rev.*, 60:47, 1941.
6. Kerst, D. W.: *Radiology*, 40:115, 1943.
7. National Bureau of Standards Handbook. HB 20. X-Ray Protection.
8. National Bureau of Standards Handbook. H 23. Radium Protection.
9. Skaggs, L. S., Almy, G. M., Kerst, D. W., Lanzl, L. H., and Uhlmann, E. M.: *Radiology*, 50:167, 1948.
10. Skaggs, L. S.: *Radiology*, 53:868, 1949.
11. Stone, R. S., Laurence, J. H. and Aebersold, P. C.: *Radiology*, 35:322, 1940.
12. Stone, R. S.: *Am. J. Roentgenol.*, 59:771, 1948.
13. Trump, J. G., Van de Graaff, R. J., and Cloud, R. W.: *Am. J. Roentgenol.*, 43:728, 1940.
14. Trump, J. G., and Cloud, R. W.: *Am. J. Roentgenol.*, 49:531, 1943.
15. Trump, J. G., Moster, C. R. and Cloud, R. W.: *Am. J. Roentgenol.*, 57:703, 1947.
16. Wilson, R. R.: *Radiology*, 47:487, 1946.

Chapter XII

ARTIFICIAL RADIOACTIVITY

12.01

TYPICAL NUCLEAR REACTIONS

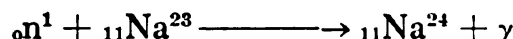
In the last few years a very large number of new radioactive isotopes have been produced by the bombardment of stable nuclei with high energy particles. A rather complete list of these new materials is included in a report by Seaborg (11) and a less complete list is given by Evans (1). In all cases they are produced by hurling a very large number of high energy particles at a stable material. A few of these projectiles will make a direct collision with the nucleus and will be absorbed, or eject some particle from the nucleus to form a new substance. The probability of such a collision is very small because the cross sectional area of the nucleus is only about 10^{-26} cm.². It follows that to produce any appreciable amount of radioactive material from stable nuclei the nucleus must be bombarded for long periods of time in an intense beam. If a copper coin is placed in the x-ray beam from the betatron for a few minutes some of the normal Cu⁶³ atoms are changed into Cu⁶² which in turn change into Ni⁶². Thus a few atoms of copper are changed into nickel and because of the radioactivity of Cu⁶² the process can easily be detected with a Geiger counter. However, it would be absolutely impossible to detect the Ni⁶² by a chemical separation, for the relative numbers of such nuclei is amazingly small.

When materials are exposed to intense beams for long periods of time, as in a pile, it is possible to produce enough new material to make a chemical separation feasible. In a 50,000 watt pile about 0.05 gm. of U²³⁵ are consumed per day. In a few months enough plutonium would be produced to enable one to separate it chemically. In general, however, the new isotopes can only be detected by their activity and not by any chemical separation process. A useful analogy is to think of the number of rifle shots required to hit a pin point at a range of several miles. It is convenient to represent a nuclear reaction symbolically by placing in brackets the bombarding particle and the "particle" which is ejected. For example an (n, γ) reaction is one in which a neutron is absorbed and a gamma ray ejected. A few typical

reactions which may be produced by neutrons, protons, deuterons, alpha particles and gamma rays are as follows:

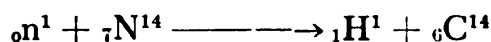
(a) *Induced by Neutrons*

The (n, γ) reaction in sodium is:

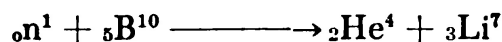


This reaction provides an easy way of producing Na^{24} . Na^{24} disintegrates to Mg^{24} with the ejection of a β^- particle and two gamma rays.

An example of an (n, p) reaction is:



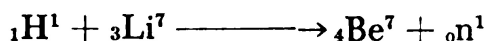
An (n, α) reaction is:



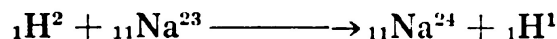
This reaction is used in the detection of neutrons. The inside of a Geiger counter is filled with boron trifluoride. The boron may capture a neutron and the ionization produced by the resulting alpha particles will trip the Geiger counter. Neutrons are very efficient particles for the production of a nuclear reaction, for they may approach the positively charged nucleus without experiencing a force of repulsion.

(b) *Induced by Protons*

An example of a (p, n) reaction is



(c) *Induced by Deuterons*



This reaction is called a (d, p) reaction since a deuteron is used to bombard the stable nucleus and a proton is ejected. This provides another method for the production of Na^{24} .

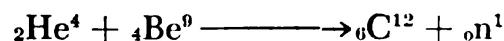
Another (d, p) reaction is



This reaction is the one used to produce P^{32} in a cyclotron. Phosphorus disintegrates with the emission of a beta particle to produce sulphur.

(d) *Induced by Alpha Particles*

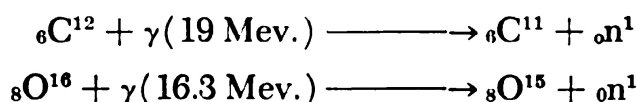
An example of an (α , n) reaction is:



This reaction is made use of in the production of a neutron source. Radium and beryllium are mixed together intimately. The alpha particles from the radium bombard the beryllium producing neutrons.

(e) *Induced by Gamma Rays*

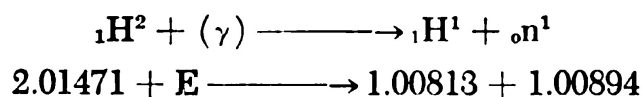
When high energy gamma rays are used to bombard stable materials photodisintegration can occur. Examples of (γ, n) reactions are as follows:



In many of these typical reactions the bombarding particle must have more than a certain minimum energy in order to bring about the reaction. This minimum energy may be calculated if the masses of the particles involved are known. In section 3.06 the energy required to create the mass of 1 electron was found to be about 0.5 Mev. Since the proton's mass is about 1800 times as great as that of the electron, the energy equivalent to 1 mass unit is about 1800 (0.5) = 900 Mev. Careful calculation shows that the relationship is

$$1 \text{ mass unit} = 931 \text{ Mev.} \quad (12-1)$$

Equation (12-1) relating mass to energy may be used to find the minimum gamma ray energy which will bring about the disintegration of the deuteron. The equation for this reaction and the masses involved are as follows:



$$\therefore E_{\min} = 0.00236 \text{ mass units} = 0.00236 \times 931 = 2.2 \text{ Mev.}$$

If the gamma ray has more than 2.2 Mev. energy the excess will be divided more or less equally between the proton and the neutron and appear as kinetic energy.

The lowest energy which will produce a (γ, n) reaction is called the threshold energy. The energies given in the equations above are the threshold energies for carbon and oxygen. For nitrogen the value is 11 Mev. When a 25 Mev. x-ray beam is used in therapy some energy will be absorbed by the production of isotopes of carbon, nitrogen, oxygen, etc., by means of the (γ, n) reaction. Experiments by Mayneord (6) indicate, however, that the energy absorbed from the x-ray beam by this process is of the order of 0.01 percent of the energy given recoil electrons and the electron pairs within the tissue. After a pa-

tient has been given a treatment on the betatron there is no difficulty in detecting the activity of the tissue, using a Geiger counter, but the ionization produced by the subsequent decay of the radioactive isotopes is very small compared with the ionization produced by the recoil and electron pairs set in motion by the x-rays during treatment. The possibility of biological changes resulting from the new isotopes produced in tissue cannot, as yet, be completely ruled out.

12.02

STABILITY OF NUCLEI

From what has been said it might be inferred that an infinite number of materials could be produced by bombarding stable elements. However, such is not the case, for many of the new materials are so unstable that they disintegrate as fast as they are produced. The question of nuclear stability can best be discussed by reference to Figure XII-1, where Z (the number of protons) is plotted against N , the number of neutrons in the nucleus ($N = A - Z$). Each type of nucleus appears as a square on the diagram. Stable nuclei are represented by solid squares and radioactive ones as a cross. The diagram shows only the first part of the periodic table from $Z = 1$ to $Z = 49$. Complete charts of this type giving most of the pertinent information

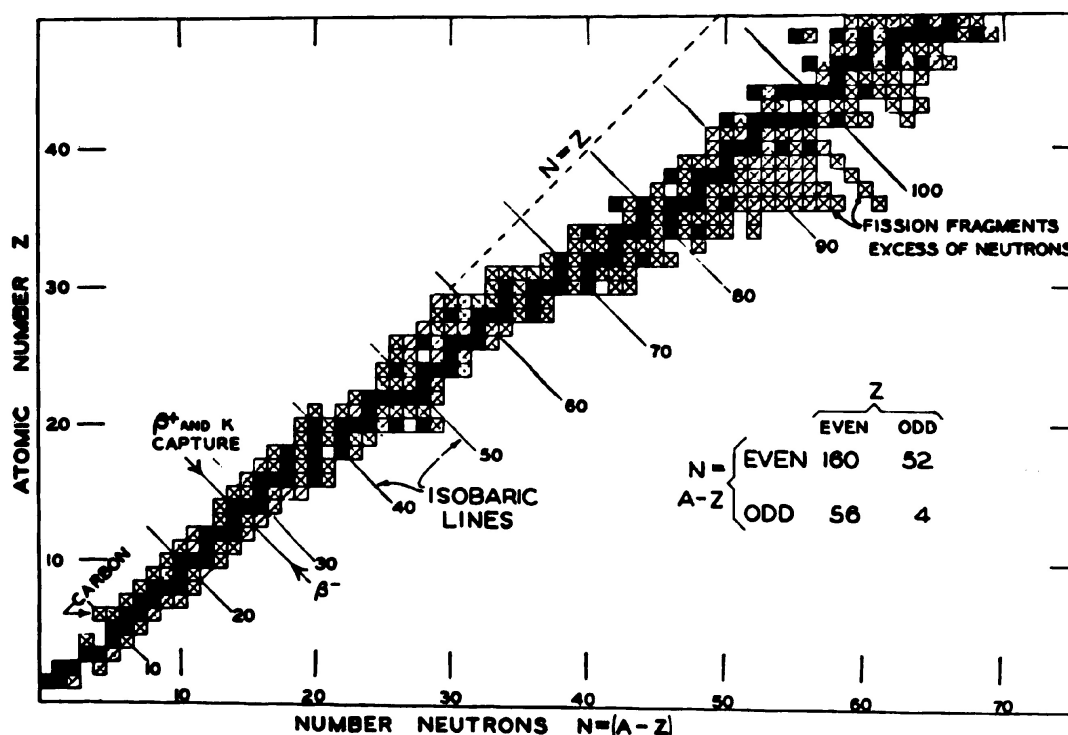


Figure XII-1. Chart showing the relative proportions of protons and neutrons in nuclei. Stable nuclei are represented by solid squares, radioactive nuclei by crosses. Nuclei with equal numbers of neutrons and protons lie along the line $N = Z$. Isotopes appear along horizontal lines and isobars along lines at 45° .

for each species of nucleus have been produced by Friedlander and Perlman (3) and may be obtained from the General Electric.

Examination of Figure XII-1 shows that all the stable and radioactive nuclei are found to cluster along a line which starts out at 45° for small values of Z and rises less steeply for the larger values of Z . For small values of Z the condition of stability is satisfied for a nucleus in which the numbers of protons and neutrons are equal or nearly equal. For large values of Z there tend to be more neutrons than protons (uranium contains 146 n and 92 p). This is due to the forces of repulsion exerted between protons so that less energy is required to add a neutron than a proton to a heavy nucleus.

In Figure XII-1 isotopes (nuclei with the same Z) lie along horizontal lines. It is immediately evident from Figure XII-1 that there are many more stable nuclei with even Z than with odd Z . Of the 272 stable isotopes existing in nature 216 have even values for Z . There is usually only one stable isotope with Z odd and never more than 2. When there are 2 they are always separated by a radioactive isotope. $^{63}_{29}\text{Cu}$ and $^{65}_{29}\text{Cu}$ are examples of two stable isotopes with odd Z . Nuclei with the same number of neutrons appear on the vertical lines of Figure XII-1. Again it is evident that there are many more stable nuclei with N even than with N odd. The relative numbers of stable nuclei are shown in the tabular insert of Figure XII-1. This table indicates the likelihood that nuclei are built up by using proton and neutron combinations as a unit.

Nuclear species with the same mass number A are called isobars and appear in Figure XII-1 along lines drawn at 45° called isobaric lines. It is found that a given isobaric line usually contains only one stable nucleus. When two appear along the line they are always separated by an unstable nucleus and occur for an even mass number.* For example, two stable isobars occur at mass number 36. These are $^{36}_{18}\text{A}$ and $^{36}_{16}\text{S}$, and they are separated by $^{36}_{17}\text{Cl}$ which is radioactive.

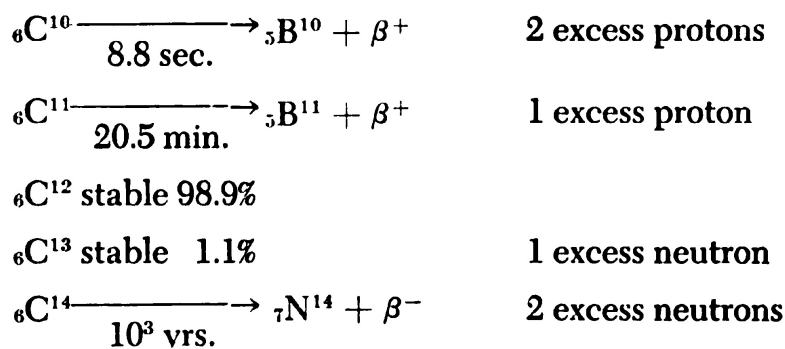
12.03

TYPES OF DISINTEGRATIONS IN ARTIFICIAL RADIOACTIVITY

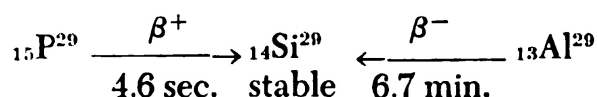
All the natural radioactive disintegrations occur by α , β^- or gamma ejections. In artificial radioactivity, α disintegrations never occur and β^+ and β^- occur about equally often. K-capture and isomeric transitions occur less frequently. There is no doubt that many more radioactive species will be produced and identified than are shown in

*There are three examples in which three stable isobars are known. These occur at $A = 40, 96, 176$.

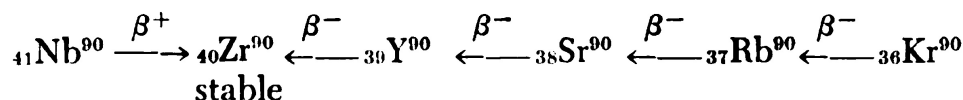
Figure XII-1. However, in general, the farther such isotopes are from stable species the shorter will be their half life and the harder it will be to detect them. Consider the case of carbon ($Z = 6$, see Fig. XII-1) for which 5 isotopes are known, two of which are stable.



${}^6\text{C}^{12}$ is the most stable form of carbon and is found in nature 98.9% of the time. ${}^6\text{C}^{11}$ has one excess proton and will disintegrate by changing a proton into a neutron and emitting a β^+ to form ${}^5\text{B}^{11}$. ${}^6\text{C}^{10}$ is still farther from satisfying the condition of equal numbers of protons and neutrons and so is more unstable and has a shorter half life. If a large number of cases are investigated it will be found that, in general, the heavier isotopes for a given Z are β^- active and the lighter ones β^+ active and that they will disintegrate, keeping their mass constant and ejecting either a β^+ or a β^- particle. Disintegrations will occur along an isobaric line until a stable isobar is reached. Species below the region of stability of Figure XII-1 show β^- activity and species above the region of stability β^+ activity. As an example of transitions along an isobaric line consider mass number 29.



Here radioactive phosphorus (P^{29})* disintegrates into stable silicon by β^+ emission and radioactive aluminum (Al^{29}) disintegrates into silicon with β^- emission. Sometimes a chain of radioactive disintegrations must occur along an isobaric line before a stable species is reached. Consider, for example, mass number 90.



${}^{36}\text{Kr}^{90}$ has a considerable excess of neutrons and achieves stability by changing a neutron into a proton and ejecting a β^- particle. This

*This isotope of phosphorus should not be confused with P^{32} which is used in tracer studies and therapeutically.

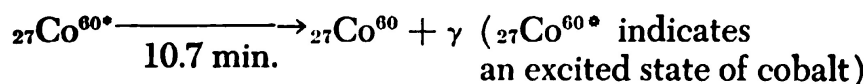
process takes place four times before stable zirconium (Zr^{90}) is produced. This chain of reactions is typical of those which take place within fission fragments. Fission fragments all have an excess of neutrons and appear on Figure XII-1 below the line of stability. They achieve stability by β^- emission.

In some cases an electron from the K shell of the atom is captured by the nucleus. This process, called K capture, will decrease its Z value by 1 and a proton will be changed into a neutron. An example of this type of disintegration is

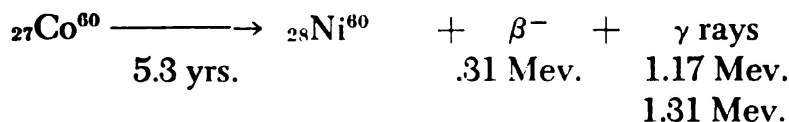


In this case Cu^{61} can disintegrate into Ni^{61} by β^+ emission as well.

Often a nuclei can be formed in an excited state. Such a nucleus will get rid of its excess energy in the form of a gamma ray. This will not change either Z or A. Co^{60} can exist in such a state and the disintegration is represented as follows:



The more stable form of cobalt then disintegrates with a β^- emission to form nickel as follows:



12.04 THE USE OF RADIOACTIVE MATERIAL TRACER STUDIES

When radioactive materials are prepared the relative number of active atoms is exceedingly small, so that, for example, a preparation of radio phosphorus P^{32} really consists of a mixture of P^{31} and P^{32} . These two kinds of phosphorus are identical chemically and so are absorbed in the body in the same way. However, the P^{32} serves to trace the absorption of the ordinary phosphorus, for it will render radioactive the organ in which it is deposited. If the tissue takes up a certain percentage of radio phosphorus, it will likewise take up the same percentage of ordinary phosphorus. Studies of metabolic processes and preferential uptake of different organs of radio material constitute tracer studies.

Radioactive materials have been used with some success as diagnostic aids. Smith and Quimby (13) have used radio sodium to study blood circulation in patients with peripheral vascular disease and

have thus been able to determine the site of amputation at which healing might be expected. The fact that radio phosphorus is preferentially taken up by rapidly growing neoplastic cells has been used by Low-Beer (5) in the diagnosis of breast tumors. Silverston (12) has inserted small Geiger counters at operation into brains with a view to localizing tumor extent.

Perhaps the greatest use which has and will be made of radio materials is in the study of the fundamental processes of metabolism. For example, use is being made of: radio-iodine in studies of the function of the normal and abnormal thyroid; radio-iron in hemoglobin studies; radio-phosphorus, calcium and strontium in the study of the metabolism of bone cells. There is no doubt that such studies will yield valuable information concerning metabolic processes.

12.05 RADIO ELEMENTS AS THERAPEUTIC AGENTS

When radioactive materials are used therapeutically, distinction should be made between those elements which give off beta rays and those which give gamma rays. For a beta ray emitter evenly distributed throughout the body, the dose at all points will be the same, except for a region around the outside surface of thickness equal to the range of the beta rays (a few millimeters). In this region the dose will be less. We will expect the same effect in a large biological subject, such as a man, as in a mouse, when the concentration per gm. is the same. For a gamma ray emitter this is not the case and the biological effect in a large object will be very different from that in a small object when the concentrations per gm. are the same. The reason for the difference is to be found in the great range of the gamma rays. Detailed calculations of the dose received from a uniformly distributed gamma ray emitter are difficult and will not be discussed here (see Mayneord (7)). Fortunately the most commonly used radiotherapeutic agents are beta emitters or emitters of very low energy gamma rays. Of course, very low energy gamma rays are readily absorbed in tissue and so behave somewhat similarly to beta ray emitters.

Of all the radio materials used therapeutically, P^{32} has shown considerable promise from the point of view of clinical results in the treatment of blood diseases. Its use has been carefully discussed, on the basis of results on over 300 patients, by Reinhard (10), and more recently, by Hall (4) on the basis of 214 patients. The radio phosphorus may be injected intravenously or taken orally. In the latter case about 25% is excreted in the first day. P^{32} appears to give about

equally good results as whole body x-radiation in the treatment of the chronic leukemias. It has been claimed, however, that radiation sickness is less with the use of P^{32} . It is now generally accepted that P^{32} shows considerable advantage over x-rays in the treatment of polycythemia vera.

12.06 UNITS FOR MEASURING IONIZING RADIATIONS

The roentgen was originally defined as a unit for the measurement of the dose received when an x- or gamma ray beam is absorbed in air. When ionization is produced in tissue by alpha rays, beta rays, protons, neutrons etc. the dosage cannot be expressed in roentgens. Parker (8) has suggested the roentgen equivalent physical (rep) as a unit for this purpose. *The "rep" is that dose of any ionizing radiation which produces an energy absorption of 85 ergs/cc. in tissue.** This unit may be applied to x-radiation, gamma radiation and all forms of corpuscular radiations. For certain energies and types of tissue the energy absorption per gm. roentgen is also 85 ergs (Chapter VIII). Under these circumstances the rep and gm. roentgen per gm. of tissue are equivalent if unit density material is considered. It is well known that equal energy absorption does not necessarily correspond to equal biological effect. This depends, amongst other things, on the ion density of the track produced by the particle. Alpha particles and protons produce much denser tracks than do beta particles. For these reasons Parker has introduced a biological unit, the "Roentgen Equivalent Man" (rem). One rem is that quantity of any radiation which produces a biological effect equal to that produced by one roentgen of high voltage x-radiation.

The relation between the rep and the rem for a given particle will depend on the biological indicator which is used in the comparison. Studies have been carried out using such things as shortening of life, acute mean lethal dose, mutation rate and others as the basis of comparison, and it is found that the conversion factor from rep to rem depends on the type of study which is made. However, approximate values due to Parker (9) are as follows: for beta rays, 1 rep = 1 rem; for protons and fast neutrons, 1 rep = 4 rem; for slow neutrons, 1 rep = 5 rem; and for alpha particles, 1 rep \approx 20 rem. When personnel is exposed to mixed radiations simultaneously, the dose received in rep may be determined from these factors.

*The figures 83, 84, 85 and 93 have appeared in this definition. The author has used the figure 85 in agreement with Chapter VIII. The "rep" has also been defined in terms of energy absorption per gm.

12.07 DOSE RECEIVED DURING TREATMENT WITH RADIOACTIVE ISOTOPE

Let the initial strength of the radioactive material which is administered the patient be I millicuries, the half life T_h (days), the average life T_a (days) and the *mean energy* of the beta particles emitted E (Mev.). Let the mass of the patient be M (Kg.) and let us assume that the average density is unity. The volume of the patient will be $1000 M \text{ cm}^3$.

The number of disintegrations per second is $(3.7 \times 10^7)I$ (section 9.09) so that if one assumes that all the beta particles expend their energy within the patient the energy absorbed per second is given by

$$(3.7 \times 10^7) I \times E \text{ Mev./sec.} = 3.7 \times 10^7 \times 1.6 \times 10^{-6} I E \text{ ergs/sec.} = 59.2 I E \text{ ergs/sec.}$$

The average energy absorbed per cm^3 of tissue per second = $59.2 I E / (1000) M \text{ ergs/sec./c.c.}$ The dosage rate is therefore $59.2 I E / M(1000)(85) = 0.696 I E / (1000) M \text{ rep/sec.}$ If we assume that the half life is long compared with one day, then we can consider that the disintegration rate of the radioactive material remains constant over 1 day and the dose received per day is given by

$$\frac{0.696 I E (24 \times 3600)}{1000 M} = \frac{60.1 I E}{M} \text{ rep per day } T_h \gg 1 \quad (12-2)$$

If T_h is not large compared with one day this expression should be multiplied by the factor $1.44 T_h (1 - e^{-.693/T_h})$. If we assume that all the radioactive material remains in the patient until it has completely decayed and that none is excreted, then the total dose is found by multiplying the dose received per day by the average life T_a ($T_a = 1.44 T_h$).

$$\text{Total dose} = \frac{60.1 I E}{M} \cdot T_a = \frac{86.5 I E}{M} \cdot T_h \text{ rep} \quad (12-3)$$

This relation is correct regardless of the length of T_h . In practice the dose will always be less than that given by equation (12-3) because of the amount which is excreted from the patient. If, however, this is measured the so-called biological half life may be determined. If the biological half life is used in equation (12-3) rather than the physical half life, correct results will be obtained.

An example will illustrate the calculation of dose using (12-3). Suppose 3.0 mc. of P^{32} are administered a patient of mass 70 Kg. For

P³² the average beta energy is 0.7 Mev. (max. 1.72 Mev., see Fig. IX-2) and $T_h = 14.3$ days.

$$\text{Dose} = \frac{86.5(3.0)(0.7)}{70} \cdot (14.3) = 37 \text{ rep.}$$

The dose per day at the beginning of the treatment can be obtained from equation (12-2) and is 1.8 rep. One would expect this patient to undergo the same constitutional changes as would be observed if the patient received a mean dose of whole body irradiation of 1.8 r per day and a total of 37 over the period of several half lives of the P³² (60 days). Since the use of P³² in this way is really a method of carrying out whole body irradiation, a statement of integral dose has perhaps more significance than the mean dose. The total integral dose expressed in gm. rep (or gm. roentgens) is obtained immediately from equation (12-3) by multiplying both sides of the equation by the mass M (expressed in grams) giving

$$\text{Integral dose} = 86,500 \text{ I.E.} T_h \text{ gm. roentgens} \quad (12-4)$$

In the above example the integral dose is 2.6 megagm.r. For pure gamma ray emitters of low energy equations 12-2, 12-3, and 12-4 will still apply except E will now represent the total gamma ray energy emitted per disintegration. For an element which gives both beta and low energy gamma rays E will be the total mean energy per disintegration. If the gamma rays have high energy the calculations become very complicated because much of the radiation will now escape from the patient without being absorbed.

The original basis for using P³² to treat blood disorders lay in the fact that phosphorus is preferentially taken up by the bones of the body. This effect does occur, but not to the extent that one might hope. It was also hoped at one time that P³² might prevent metastases by being absorbed in the rapidly growing tissue. There is little evidence that the concentration is sufficient to bring about this result. It follows that the use of P³² in the treatment of polycythemia is not fundamentally very different from the use of x-rays. However, the slight preferential absorption by the bone of the P³² must offer some advantage by tending to concentrate the dose at the site of the blood forming cells.

A number of experimenters have hoped to bring about intense tumor bombardment by injecting into the patient radioactive material which will subsequently be concentrated in the tumor and thus bring about its destruction. To date the concentration of energy in malignant

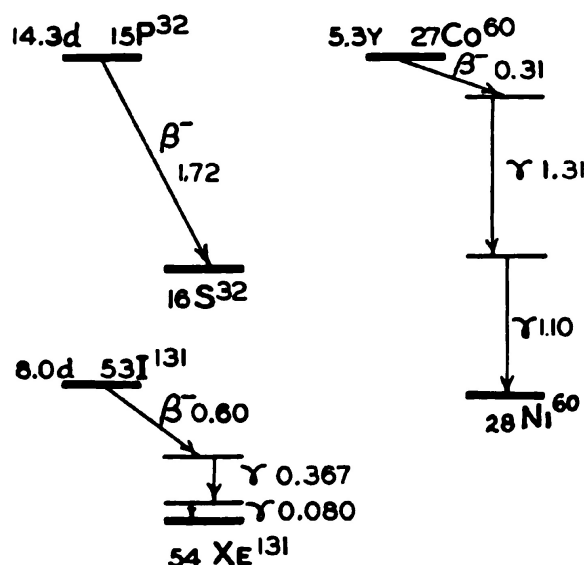


Figure XII-2. Disintegration schemes for phosphorus, cobalt and iodine. Vertical distances represent the energy difference between nuclear energy levels.

cells by this process has been disappointingly small. It begins to look as if no isotope will be of use in this way, with the possible exception of I^{131} in the treatment of thyroid tumors.

12.08 DISINTEGRATION SCHEMES OF RADIOACTIVE MATERIALS

Before the activity of radioactive material in millicuries may be determined, the disintegration scheme must be unravelled by detailed studies involving beta ray spectrometers, coincidence counters and other physical devices. Disintegration schemes for P^{32} , I^{131} , and Co^{60} are shown in Figure XII-2. The diagrams have been drawn approximately to scale so that the distance between the levels corresponds to the energy of transition from one level to the other.

P^{32} shows a simple spectrum. The difference in energy between the P^{32} nucleus and the S^{32} nucleus is 1.72 Mev., the maximum energy of the beta particle. However, when the disintegration occurs within the body only the mean energy (.7 Mev.) of the beta particle is absorbed.

I^{131} emits a beta particle (max. energy 0.60, mean energy $\sim .24$ Mev.) to yield an excited state of Xe^{131} . This excited state soon loses its energy by the emission of two gamma ray energies in cascade. There is no way to determine the order in which the gamma rays are emitted. If I^{131} were used in the example of section 12.07, the mean energy per disintegration would be given by $E = 0.24 + 0.367 +$

$0.080 = 0.69$ Mev. This value for E would be reasonably accurate because most of the 0.367 Mev. gamma ray energy will be absorbed within the patient.

The disintegration schemes for Co^{60} shows that 1 beta ray is emitted followed by two gamma rays in cascade of energy 1.1 and 1.3 Mev. Often the disintegration schemes are very complicated, involving several energy beta particles and gamma rays (Evans (2)). Under these circumstances, the measurement of an activity in millicuries becomes very difficult. For convenience, some of the radioactive isotopes which are commonly used in biological investigations are collected in Table XIX. Here are shown the half life, the maximum energy of the β particle, the energy of the γ rays, the product of the disintegration and the most convenient method for the production of the isotope.

TABLE XIX
LIST OF COMMONLY USED RADIOACTIVE ISOTOPES WITH
SOME OF THEIR PROPERTIES

<i>Isotope</i>	<i>Half life</i>	<i>Beta Particles</i> (Mev.)	<i>γ Rays</i> (Mev.)	<i>Product</i>	<i>Method of</i> <i>Production</i>
C^{14}	5100 y.	$\beta - 0.145$	None	N^{14}	Pile
Na^{22}	3.0 y.	$\beta + 0.58$	1.3	Ne^{22}	Cyclotron
Na^{24}	14.8 h.	$\beta - 1.4$	1.4, 2.8	Mg^{24}	Pile
P^{32}	14.3 d.	$\beta - 1.72$	None	S^{32}	Pile
S^{35}	87 d.	$\beta - 0.17$	None	Cl^{35}	Pile
Ca^{45}	152 d.	$\beta - 0.26$	None	Sc^{45}	Pile
Fe^{55}	4 y.	K capture	0.07	Mn^{55}	Cyclotron
Fe^{59}	47 d.	$\beta - 0.26, 0.46$	1.1, 1.3	Co^{59}	Cyclotron
Co^{60}	5.3 y.	$\beta - 0.31$	1.1, 1.3	Ni^{60}	Pile
Sr^{89}	55 d.	$\beta - 1.5$	None	Y^{89}	{ A mixture of Sr^{89} and Sr^{90} appear as fission fragments.
Sr^{90}	25 y.	$\beta - 0.6$	None	Y^{90}	
I^{130}	12.6 h.	$\beta - 0.61, 1.03$	{ 0.42, 0.54 0.67, 0.74	Xe^{130}	Cyclotron
I^{131}	8 d.	$\beta - 0.6$	0.37, 0.080	Xe^{131}	Fission product or by the bom- bardment of Tellurium in the pile.

From section 12.03, it is obvious that many of these isotopes may be produced in a number of ways. The actual method which is the most convenient will depend somewhat on the specific activity which is required.

From Table XIX it will be seen that in most cases the pile offers the simplest method of production. Some of the heavier isotopes appear as fission fragments and can be separated from the uranium rods. The lighter isotopes are usually produced by an (n, γ) reaction. For example, Na^{24} can readily be produced in the pile by irradiating stable Na^{23} with neutrons. This type of reaction is the most common one for the production of isotopes.

12.09 DOSAGE RATE FROM GAMMA RAY EMITTERS

The dosage rate 1 cm. from a 1 mc. gamma ray emitter can be calculated in r/hr. if the disintegration scheme is known. The method is illustrated in Table XX by a detailed calculation for Co^{60} . Use is made of Figure VIII-3 relating energy flux to the roentgen.

TABLE XX

CALCULATION OF DOSAGE RATE IN R/HR. AT 1 CM. FROM 1 MC. OF Co^{60}

		1.1 Mev.	1.3 Mev.
Number of gamma rays ejected per second	(A)	3.7×10^7	3.7×10^7
Number of gamma rays incident per second on an area of 1 cm ² at a distance of 1 cm.	(B)	2.94×10^6	2.94×10^6
$\frac{A}{4\pi(1)^2} = B$			
Energy flux through 1 cm. ² area in Mev./sec. (1.1 B and 1.3 B = C)	(C)	3.23×10^6	3.82×10^6
Energy flux through 1 cm. ² area in ergs/sec. (C $\times 1.6 \times 10^{-8}$ = D)	(D)	5.17	6.11
Energy flux through 1 cm. ² area in ergs/hr. 3600 D = E	(E)	1.86×10^4	2.20×10^4
Energy flux in ergs/cm. ² to record 1 roentgen (Fig. VIII-3)	(F)	3000	3100
Recorded dose in roentgens E/F		6.2	7.1
Total Dosage Rate in r/hr. = 6.2 + 7.1 = 13.3			

The method may be applied to other gamma ray emitters and yields the values given in Table XXI. In the case of radium the calculations illustrated in Table XX must be carried through for each of the 12

gamma ray energies listed in Table XI. Values for a number of other gamma ray emitters may be obtained from Evans (1).

TABLE XXI
DOSAGE RATE IN R/HR. AT A POINT 1 CM. FROM A 1 MC. SOURCE
OF GAMMA RAY EMITTERS

	<i>Half life</i>	<i>Energy of Gamma Rays (Mev.)</i>	<i>Dosage Rate (r/hr.)</i>
Na ²²	3.0 y.	1.3	13.0
Na ²⁴	14.8 h.	1.4, 2.8	19.2
Mn ⁵²	6.5 d.	0.73, 0.94, 1.5	19.3
Fe ⁵⁹	47 d.	1.1, 1.3	6.5
Co ⁶⁰	5.3 y.	1.1, 1.3	13.3
I ¹³⁰	12.6 h.	0.42, 0.54, 0.67, 0.74	12.5
Ra B+C	1590 y.	See Table XI	8.4

When the gamma ray emission is accompanied by betas, it is assumed that sufficient filtration is used to stop completely these electrons so that they do not contribute to the dosage rate. Cobalt is a very convenient type of gamma ray emitter because the accompanying beta particles of 0.3 Mev. are very easily stopped.

The dosage rate of 13.3 r/hr. 1 cm. from a 1 mc. source of cobalt may be used to calculate the output to be expected from a telecurie cobalt source. Suppose a source of 25 cobalt discs 1 inch in diameter and 0.5 mm. thick (2.31 gm./disc) is activated to 25 curies per gm. The total activity is then 1445 curies. If there were no absorption of the cobalt gamma rays by the cobalt itself the dosage rate at 80 cm. would be

$$\text{Dosage rate} = \frac{13.3 \times 1445 \times 1000}{(80)^2} = 3000 \text{ r/hr.} = 50 \text{ r/min.}$$

It can be shown that about 25% of the radiation is absorbed by the cobalt itself so that the actual dosage rate will be 36 r/min. It is certain that long lived gamma emitters, such as cobalt, will prove to be of great value in the field of therapy.

REFERENCES

1. Evans, R. D.: *Medical Physics*. Isotopes, p. 642. Chicago Yr. Bk. Pub., 1944.
2. Evans, R. D.: *Advances in Biological and Medical Physics*, 1:151, New York, Academic Press, 1948.

3. Friedlander, G. and Perlman, M. L., Chart of the Isotopes. General Electric, Dept. 6-235 A.
4. Hall, B. E.: *Isotopes in Biology and Medicine*. Madison, Univ. Wisconsin Press, 1949, p. 353.
5. Low-Beer, B. V. A., Bell, H. G., McCorkle, H. J. and Stone, R. S.: *Radiology*, 47:492, 1946.
6. Mayneord, W. V., Martin, J. H., and Layne, D. A.: *Nature*, 164:728, 1949.
7. Mayneord, W. V., CRM-315. National Research Council, Chalk River, Ont., Canada.
8. Parker, H. M.: *Advances in Biological and Medical Physics*, 1:223, New York, Academic Press, 1948.
9. Parker H. M.: *Radiology*, 54:257, 1950.
10. Reinhard, E. H., Moore, C. V., Bierbaum, O. S. and Moore, S.: *Lab. Clin. Med.*, 31:107, 1946.
11. Seaborg, G. T. and Perlman, I.: *Rev. of Mod. Phys.*, 20:585, 1948.
12. Silverston, B., Sweet, W. H., and Robinson, C. V.: *Ann. Surg.*, 130:643, 1949.
13. Smith, B. C. and Quimby, E. H.: *Radiology*, 45:335, 1945.

Appendix A

DEPTH DOSE DATA AND ISODOSE DISTRIBUTIONS

The fundamental principles of the physics of radiation therapy have been discussed in the body of the text. In this appendix will be found physical data which cover a wide range of energies and which should be of use clinically.

In Table A-1 appear percentage surface backscatter data for radiations with half value layers from 0.25 to 4.0 mm. of Cu. Values are given for circular areas of 20, 35, 50, 80, 100, 150, 200 and 400 cm.², and were obtained with open ended treatment cones.

In Tables A-2, -3, -4, -5, percentage depth dose data for radiations with half value layers of 1, 2, 3, and 4 mm. of Al. are given for circular areas and for focal skin distances of 15, 20 and 30 cm.

Tables A-6, -7, -8, -9, -10, -11, and -12 give depth dose data for radiations of half value layers of 0.5, 1.0, 1.5, 2.0, 3.0, 4.0 and 5.0 mm. of Cu. Values are presented for focal skin distances of 40, 50, 60, 80, and 100 cm. for circular areas of 0, 20, 35, 50, 80, 100, 150, 200 and 400 cm.². Although the data was obtained with circular fields, it should be quite accurate for rectangular fields of small elongation.

In Table A-13 are presented depth dose data obtained from a 1000 curie Cobalt 60 unit for source to skin distances of 50, 60, 80, and 100 cm., and for circular areas of 0, 20, 50, 100, 200 and 400 cm.².

In Table A-14 are given depth dose data obtained with a 22 Mev. betatron using a copper compensating filter. For these radiations the depth dose is independent of area. Values are given for focal skin distances of 70 and 100 cm.

Twenty isodose distributions shown in Figures A-1 to 20 for a variety of field sizes and for radiations with half value layers of 1.5 and 4 mm. of Cu. are given. These distributions are correct for treatment cones with open ends. The errors involved in using them for treatment cones with closed ends will usually be small.

All measurements recorded here were made by the author in collaboration with a number of graduate students in the Physics department of the University of Saskatchewan. They were obtained using small ionization chambers connected to a D.C. amplifier. The chamber could be moved at will in a water phantom by remote control.

For depth dose measurements along the axis of the field, flat circular chambers 1 to 2 mm. deep and 1 cm. or less in diameter were used. Thus the dimension of the chamber in the direction in which the dosage rate changes rapidly is small, so that measurements are effectively made at a "point." To obtain the isodose distributions, transits across the beam were made using a cylindrical ionization chamber about 3 mm. in diameter and 1 cm. long. With this type of chamber the radiation at a "point" is effectively measured and the distributions A-1 to A-20 show discontinuities at the geometrical edge of the beam.

For radiations from 100 K.V.P. to 400 K.V.P. depth doses have been expressed as a percentage of the surface dose. For these radiations the surface dose is usually greater than the dose at any depth. For large fields at large focal skin distances and half value layers of about 2.0 mm. of Cu. the dose at 1 cm. depth is 1% to 3% greater than the surface dose, giving a percentage depth dose greater than 100%. For more energetic radiations, the maximum dose occurs well below the surface and is much greater than the surface dose. For the radiations given in Tables A-13 and A-14 the depth dose has been expressed as a percentage of the maximum dose. This inconsistency in definition should cause no serious trouble.

One of the difficulties involved in making accurate depth dose measurements is the continual variation with time of the output of most x-ray machines. The output of the x-ray machines was continually monitored with a flat ionization chamber placed in the master collimator. The output from this chamber was recorded on a Leeds and Northrup self-balancing potentiometer. The output from the D.C. amplifier was recorded on another potentiometer. Simultaneous traces of the output of the machine and the dose received at a depth below the surface were thus obtained. With this arrangement it is possible to determine percentage depth doses very accurately even with a rapidly fluctuating source of x-rays. Data given in Tables A-6 to 13 were obtained in this way and are considered more reliable than the data given in Tables A-1 to 5 which were obtained without the use of the recorders. For the latter measurements the output of the machine was adjusted manually to a constant value.

The percentage depth dose for a field of small area (zero area) gives the dose below the surface due to primary radiation only. If this is known, the scatter contribution for the larger fields can be determined. The percentage depth dose for zero area was obtained using a new method. Attenuation of the x-ray beam by known thicknesses of water were determined in an experiment in which scattered

radiation was kept to a minimum. Zero area depth dose values were calculated from these measurements using the inverse square law.

Measurements given in Tables A-2 to 12 were made on 140 K.V.P., 200 K.V.P., and 400 K.V.P., x-ray machines. Measurements were carried out for a number of focal skin distances and it was found that the percentage depth dose depended, in a complicated way, on the focal skin distance. For very small area fields the percentage depth dose could be converted from one focal skin distance to another, using the inverse square law, but for larger fields, especially in the 200 Kv. region, the conversion factor from one focal skin distance to another is a complicated function of area and focal skin distance. Care was taken in the compilation of these tables to use measured values for the conversion factor rather than the inverse square law, which has been used by many investigators.

The data given in Tables A-2 to 5 is in fair agreement with that of Braestrup⁽¹⁾ especially for large depths. Depth dose data for small depths is, in general, somewhat higher than that recorded by Braestrup. Data given in Tables A-16 to 12 is not in close agreement with either Mayneord and Lamerton's⁽²⁾ tables or those due to Quimby,⁽³⁾ but in general is more nearly in agreement with the latter.

Much of this data has been published in the British Journal of Radiology (1952) and in the supplement to the British Journal of Radiology (1952). The author takes pleasure in acknowledging the assistance of Miss S. O. Fedoruk, now assistant physicist to the Saskatchewan Cancer Commission, Mr. R. O. Kornelson, now physicist at the Queen Elizabeth Hospital, Montreal, and Mr. E. R. Epp, graduate student at the University of Saskatchewan.

(1) Braestrup, C.: *Radiology*, 42:258, 1944.

(2) Mayneord, W. V. and Lamerton, L. F.: *Brit. J. Radiol.*, 14:255, 1941.

(3) Quimby, E. H.: *Medical Physics*. Yr. Bk. Publishers, Inc., Chicago, 1165, 1944.

TABLE A-1
Percentage Surface Backscatter

Half Value Layer (mm. Cu.)	Area of field in square centimeters							
	20	35	50	80	100	150	200	400
0.25	19.4	23.5	26.6	30.6	32.4	35.1	36.8	37.8
0.50	20.0	24.1	27.9	32.8	35.6	40.0	42.9	45.6
1.0	19.4	24.0	28.0	33.8	37.0	41.8	45.2	47.4
2.0	16.0	20.3	23.8	28.5	31.0	35.0	37.8	39.9
3.0	13.7	18.1	20.8	24.0	25.7	28.1	29.7	31.3
4.0	12.9	15.9	18.0	21.0	22.2	24.5	25.8	27.2

TABLE A-2

H.V.L. 1.0 mm. Al. (Approximately 70 K.V.P. Inherent filtration)

Area (cm. ²)	0	3.1	7.0	12.5	28.3	50	100
Diam. (cm.)	0	2	3	4	6	8	11.3
Depth (cm.)	Focal Skin Distance 15 cm.						
0	100	100	100	100	100	100	100
0.5	61	74	79	81	84	86	87
1	42	56	61	63	66	67	69
2	23	32	36	39	41	42	44
3	13	19	22	24	26	27	29
4	8	12	13	15	17	19	20
5	5	7	9	10	12	13	14
6	3	5	6	6	8	9	10
7	2	3	4	4	5	6	7
8	2	2	3	3	4	4	5

Focal Skin Distance 20 cm.

0	100	100	100	100	100	100	100
0.5	62	75	80	82	84	86	88
1	44	58	63	65	67	68	70
2	24	34	38	41	43	44	45
3	14	20	23	25	28	29	31
4	9	13	15	16	18	20	21
5	6	8	10	11	13	14	15
6	4	6	6	7	9	10	11
7	3	4	4	5	6	7	8
8	2	3	3	4	4	5	6

Focal Skin Distance 30 cm.

0	100	100	100	100	100	100	100
0.5	63	76	81	83	85	88	89
1	45	60	64	66	68	70	71
2	25	36	40	42	44	46	48
3	16	22	25	27	30	31	33
4	10	14	16	18	20	22	23
5	7	9	11	12	14	15	17
6	5	7	7	8	10	11	12
7	3	4	5	6	7	8	9
8	2	3	4	4	5	6	7

TABLE A-3
H.V.L. 2.0 mm. Al. (Approximately 120 K.V.P. Inherent filtration)

<i>Area (cm.²)</i>	0	3.1	7.0	12.5	28.3	50	100
<i>Diam. (cm.)</i>	0	2	3	4	6	8	11.3
<i>Depth (cm.)</i>	Focal Skin Distance 15 cm.						
0	100	100	100	100	100	100	100
0.5	71	82	85	87	88	89	90
1	52	65	69	72	74	76	77
2	31	42	47	49	53	55	56
3	20	28	32	34	38	40	42
4	14	19	22	24	27	30	32
5	9	13	15	17	20	22	24
6	6	9	11	13	15	17	19
7	4	7	8	9	11	13	14
8	3	5	6	7	9	10	11
9	2	4	4	5	6	8	9
10	2	3	3	4	5	6	7

Focal Skin Distance 20 cm.

0	100	100	100	100	100	100	100
0.5	72	83	86	88	89	90	91
1	54	66	71	73	76	77	78
2	33	44	49	51	55	57	58
3	22	30	34	36	40	42	44
4	15	21	24	26	30	32	34
5	10	15	17	19	22	24	26
6	7	11	12	14	17	19	20
7	5	8	9	10	13	15	16
8	4	6	7	8	10	11	13
9	3	4	5	6	7	9	10
10	2	3	4	5	6	7	8

Focal Skin Distance 30 cm.

0	100	100	100	100	100	100	100
0.5	73	84	87	88	89	91	92
1	55	68	73	74	77	79	80
2	35	47	51	54	57	60	61
3	24	33	37	39	43	45	47
4	17	23	27	29	32	35	37
5	12	17	19	21	25	27	29
6	9	12	14	16	19	21	23
7	6	9	11	12	15	17	19
8	5	7	8	9	11	13	15
9	4	5	6	7	9	10	12
10	3	4	5	5	7	8	10

TABLE A-4
H.V.L. 3.0 mm. Al. (Approximately 120 K.V.P. 1 mm. Al. filter)

<i>Area (cm.²)</i>	0	3.1	7.0	12.5	28.3	50	100
<i>Diam. (cm.)</i>	0	2	3	4	6	8	11.3
<i>Depth (cm.)</i>	Focal Skin Distance 15 cm.						
0	100	100	100	100	100	100	100
0.5	75	85	87	88	89	90	90
1	58	70	74	76	77	78	80
2	37	48	53	56	59	60	62
3	24	33	37	41	45	46	48
4	17	23	27	30	34	35	37
5	12	17	19	22	25	27	29
6	8	12	14	16	19	21	23
7	6	9	10	12	14	16	18
8	4	6	8	9	11	13	14
9	3	5	6	7	8	10	11
10	2	3	4	5	6	8	9

Focal Skin Distance 20 cm.

0	100	100	100	100	100	100	100
0.5	76	86	88	89	90	91	91
1	60	72	75	77	79	80	81
2	39	51	55	58	62	63	65
3	27	35	40	43	47	49	51
4	19	25	29	32	36	38	40
5	13	18	21	24	28	30	32
6	10	14	16	18	21	23	25
7	7	10	12	14	16	18	20
8	5	7	9	10	12	14	16
9	4	6	7	8	9	11	13
10	3	4	5	6	7	9	10

Focal Skin Distance 30 cm.

0	100	100	100	100	100	100	100
0.5	77	86	88	90	91	92	92
1	62	74	77	79	81	82	83
2	41	54	58	61	65	66	67
3	29	39	43	46	51	53	55
4	21	28	32	35	40	42	44
5	15	21	24	27	31	33	35
6	11	16	18	20	24	26	29
7	8	12	14	16	19	21	23
8	6	9	10	12	14	17	19
9	5	7	8	9	11	13	15
10	4	5	6	7	9	11	12

TABLE A-5

H.V.L. 4.0 mm. Al. (Approximately 140 K.V.P. 2.0 mm. Al. filter)

Area (cm. ²)	0	3.1	7.0	12.5	28.3	50	100
Diam. (cm.)	0	2	3	4	6	8	11.3
Depth (cm.)	Focal Skin Distance 15 cm.						
0	100	100	100	100	100	100	100
0.5	78	87	89	90	91	92	93
1	62	74	77	79	80	81	84
2	40	52	56	59	62	63	67
3	27	37	41	44	47	49	53
4	19	26	30	32	36	38	42
5	13	19	22	24	27	30	33
6	10	14	16	18	21	23	26
7	7	10	12	14	16	18	21
8	5	8	9	10	12	14	17
9	4	6	7	8	10	11	13
10	3	4	5	6	8	9	11

Focal Skin Distance 20 cm.

0	100	100	100	100	100	100	100
0.5	79	88	89	90	92	93	94
1	63	76	78	80	82	83	86
2	43	55	59	62	64	66	70
3	30	40	44	46	49	52	56
4	21	29	32	35	38	41	45
5	15	21	24	26	30	33	36
6	11	16	18	20	23	26	29
7	8	12	14	15	18	21	23
8	6	9	10	12	14	16	19
9	4	7	8	9	11	13	15
10	3	5	6	7	9	10	13

Focal Skin Distance 30 cm.

0	100	100	100	100	100	100	100
0.5	80	90	91	92	93	94	95
1	65	78	81	82	83	84	87
2	45	58	62	65	68	69	73
3	32	43	47	50	54	56	60
4	24	32	36	38	42	45	49
5	18	24	27	29	33	36	40
6	13	18	21	23	26	29	33
7	10	14	16	18	21	24	27
8	7	11	12	14	17	19	22
9	5	8	9	11	13	15	18
10	4	6	7	8	10	12	15

TABLE A-6
H.V.L. 0.5 mm. Cu. F.S.D.: 40 cm.

<i>Depth in cm.</i>	Area of field in square centimetres								
	0	20	35	50	80	100	150	200	400
0	100.0	100.0	100.0	100.0	100.0	100.0	100.0	100.0	100.0
1	74.6	91.7	93.6	94.7	96.4	97.0	98.0	98.6	99.3
2	56.5	78.1	81.5	83.4	86.0	86.9	88.8	89.9	91.9
3	43.2	64.8	68.9	71.6	74.6	76.0	78.4	80.0	83.4
4	33.3	52.9	57.7	60.5	64.2	65.6	68.1	69.7	73.9
5	25.8	43.3	47.8	50.9	54.6	56.2	59.0	61.0	65.1
6	20.0	35.4	39.3	42.4	46.0	47.5	50.5	52.8	57.0
7	15.5	28.9	32.6	35.6	38.8	40.1	43.2	45.4	49.8
8	12.1	23.7	27.1	29.5	32.5	34.0	36.8	39.0	43.5
9	9.4	19.4	22.3	24.7	27.3	28.7	31.4	33.4	37.5
10	7.4	16.1	18.4	20.5	23.0	24.3	26.6	28.5	32.7
11	5.8	13.2	15.3	17.0	19.3	20.5	22.5	24.3	28.2
12	4.6	10.8	12.8	14.3	16.3	17.4	19.2	20.8	24.5
13	3.7	8.8	10.7	12.0	13.7	14.7	16.3	17.6	21.1
14	2.9	7.3	8.9	10.0	11.5	12.3	13.9	15.3	18.3
15	2.4	6.0	7.4	8.3	9.7	10.4	11.8	13.0	15.7
16	1.9	4.9	6.1	6.9	8.2	8.8	10.1	11.1	13.6
17	1.5	4.1	5.1	5.8	6.9	7.4	8.6	9.6	11.7
18	1.2	3.4	4.2	4.8	5.8	6.3	7.3	8.2	10.1
19	1.0	2.8	3.5	4.0	4.9	5.3	6.2	7.0	8.7
20	.8	2.3	2.9	3.4	4.1	4.5	5.3	5.9	7.5

H.V.L. 0.5 mm. Cu. F.S.D.: 50 cm.

<i>Depth in cm.</i>	Area of field in square centimetres								
	0	20	35	50	80	100	150	200	400
0	100.0	100.0	100.0	100.0	100.0	100.0	100.0	100.0	100.0
1	75.3	92.3	94.3	95.4	97.1	97.7	98.7	99.3	100.0
2	57.7	79.0	82.5	84.4	87.0	87.0	89.9	91.0	93.0
3	44.5	66.0	70.2	72.9	76.0	77.4	79.8	81.5	84.9
4	34.5	54.3	59.2	62.1	65.9	67.3	69.9	71.6	75.9
5	27.0	44.7	49.3	52.5	56.3	58.0	60.9	62.9	67.2
6	21.1	36.7	40.8	44.0	47.7	49.3	52.4	54.8	59.1
7	16.5	30.1	34.0	37.1	40.4	41.8	45.0	47.3	51.9
8	13.0	24.8	28.3	30.8	34.0	35.5	38.5	40.8	45.2
9	10.1	20.4	23.4	25.9	28.6	30.1	32.9	35.0	39.4
10	8.0	16.9	19.4	21.6	24.2	25.6	28.0	30.0	34.4
11	6.3	13.9	16.2	18.0	20.4	21.6	23.8	25.7	29.8
12	5.1	11.4	13.5	15.1	17.2	18.4	20.3	22.0	25.9
13	4.1	9.4	11.3	12.7	14.5	15.6	17.3	18.7	22.4
14	3.3	7.7	9.4	10.6	12.2	13.1	14.8	16.2	19.4
15	2.6	6.4	7.8	8.8	10.3	11.1	12.6	13.8	16.7
16	2.1	5.3	6.5	7.4	8.7	9.4	10.8	11.8	14.5
17	1.7	4.3	5.4	6.2	7.3	7.9	9.2	10.2	12.5
18	1.4	3.6	4.5	5.2	6.2	6.7	7.8	8.7	10.8
19	1.1	3.0	3.8	4.3	5.2	5.7	6.6	7.5	9.3
20	.9	2.4	3.1	3.6	4.4	4.8	5.6	6.4	8.1

TABLE A-6
H.V.L. 0.5 mm. Cu. F.S.D.: 60 cm.

Depth in cm.	Area of field in square centimetres								
	0	20	35	50	80	100	150	200	400
0	100.0	100.0	100.0	100.0	100.0	100.0	100.0	100.0	100.0
1	75.8	92.9	94.9	96.0	97.7	98.3	99.3	99.9	100.6
2	58.4	79.9	83.4	85.3	88.0	89.0	90.9	92.0	94.0
3	45.3	67.1	71.4	74.1	77.3	78.7	81.2	82.9	86.3
4	35.3	55.4	60.4	63.3	67.2	68.6	71.3	73.0	77.4
5	27.8	45.8	50.5	53.8	57.7	59.5	62.4	64.5	68.9
6	21.9	37.7	41.9	45.2	49.0	50.7	53.9	56.3	60.8
7	17.2	31.0	35.1	38.3	41.7	43.1	46.4	48.8	53.5
8	13.6	25.6	29.2	31.8	35.1	36.7	39.8	42.1	46.7
9	10.7	21.1	24.2	26.8	29.6	31.2	34.1	36.3	40.8
10	8.4	17.5	20.1	22.4	25.1	26.6	29.1	31.1	35.7
11	6.7	14.5	16.8	18.7	21.2	22.5	24.8	26.7	31.0
12	5.4	11.9	14.1	15.7	17.9	19.2	21.1	22.9	27.0
13	4.3	9.8	11.8	13.2	15.1	16.3	18.0	19.5	23.4
14	3.5	8.0	9.8	11.1	12.7	13.7	15.5	16.9	20.3
15	2.9	6.6	8.2	9.2	10.8	11.6	13.2	14.4	17.5
16	2.3	5.5	6.8	7.7	9.1	9.8	11.3	12.4	15.2
17	1.9	4.6	5.7	6.5	7.7	8.3	9.6	10.7	13.1
18	1.5	3.8	4.8	5.4	6.5	7.0	8.2	9.2	11.4
19	1.2	3.1	4.0	4.5	5.5	6.0	7.0	7.8	9.8
20	1.0	2.6	3.3	3.8	4.6	5.1	5.9	6.7	8.5

H.V.L. 0.5 mm. Cu. F.S.D.: 80 cm.

Depth in cm.	Area of field in square centimetres								
	0	20	35	50	80	100	150	200	400
0	100.0	100.0	100.0	100.0	100.0	100.0	100.0	100.0	100.0
1	76.7	93.4	95.4	96.5	98.3	98.9	99.9	100.4	101.2
2	59.4	80.9	84.5	86.4	89.1	90.1	92.1	93.2	95.2
3	46.4	68.3	72.7	75.5	78.6	80.0	82.4	84.2	87.7
4	36.4	56.9	61.9	64.9	68.8	70.3	73.0	74.8	79.2
5	28.9	47.2	52.1	55.4	59.4	61.2	64.2	66.4	70.9
6	22.9	39.0	43.5	46.8	50.7	52.4	55.7	58.3	62.8
7	18.2	32.3	36.5	39.8	43.3	44.8	48.2	50.7	55.6
8	14.5	26.8	30.6	33.3	36.7	38.3	41.5	44.0	48.8
9	11.4	22.2	25.4	28.1	31.0	32.7	35.7	38.0	42.7
10	9.1	18.5	21.2	23.6	26.4	27.9	30.5	32.7	37.5
11	7.3	15.3	17.8	19.8	22.4	23.7	26.1	28.2	32.7
12	5.9	12.6	14.9	16.7	19.0	20.3	22.4	24.3	28.6
13	4.8	10.4	12.5	14.1	16.1	17.3	19.2	20.7	24.8
14	3.9	8.6	10.4	11.8	13.6	14.6	16.4	18.0	21.6
15	3.2	7.1	8.8	9.9	11.5	12.4	14.1	15.4	18.7
16	2.6	5.9	7.3	8.3	9.8	10.5	12.1	13.2	16.2
17	2.1	4.9	6.1	7.0	8.2	8.9	10.3	11.5	14.1
18	1.7	4.1	5.1	5.8	7.0	7.6	8.8	9.9	12.2
19	1.4	3.4	4.3	4.9	5.9	6.4	7.5	8.4	10.5
20	1.1	2.8	3.6	4.1	5.0	5.4	6.4	7.2	9.1

TABLE A-7
H.V.L. 1.0 mm. Cu. F.S.D.: 40 cm.

Depth in cm.	Area of field in square centimetres								
	0	20	35	50	80	100	150	200	400
0	100.0	100.0	100.0	100.0	100.0	100.0	100.0	100.0	100.0
1	78.3	93.5	96.2	97.5	99.2	100.1	101.3	101.9	102.3
2	61.7	82.1	87.2	89.0	92.0	93.0	94.7	95.6	97.1
3	49.0	71.1	75.9	79.0	83.1	84.7	87.1	88.9	91.4
4	39.0	60.5	65.5	68.8	73.2	75.2	78.2	80.3	84.2
5	31.1	50.9	55.8	59.3	63.9	65.6	69.1	71.3	75.5
6	25.0	42.8	47.4	50.7	55.1	57.1	60.3	62.6	67.4
7	20.0	35.8	40.1	43.2	47.4	49.3	52.7	55.1	59.9
8	16.1	29.8	33.7	36.5	40.5	42.6	45.7	48.1	53.1
9	13.0	24.9	28.5	31.0	34.7	36.7	39.9	41.9	46.9
10	10.4	20.8	24.9	26.4	29.6	31.4	34.4	36.4	41.5
11	8.4	17.4	20.3	22.4	25.3	27.0	29.6	31.6	36.4
12	6.7	14.6	17.1	19.0	21.5	23.1	25.6	27.5	31.8
13	5.4	12.2	14.4	16.0	18.4	19.7	22.0	23.9	27.8
14	4.4	10.2	12.2	13.6	15.7	16.9	19.0	20.7	24.3
15	3.5	8.5	10.2	11.5	13.5	14.5	16.3	17.8	21.3
16	2.8	7.1	8.6	9.7	11.5	12.4	14.0	15.4	18.6
17	2.3	6.0	7.2	8.3	9.8	10.6	12.1	13.3	16.3
18	1.9	5.0	6.1	7.0	8.3	9.0	10.4	11.5	14.3
19	1.5	4.2	5.2	5.9	7.1	7.8	8.9	9.9	12.5
20	1.2	3.5	4.4	5.0	6.1	6.7	7.7	8.5	10.9

H.V.L. 1.0 mm. Cu. F.S.D.: 50 cm.

Depth in cm.	Area of field in square centimetres								
	0	20	35	50	80	100	150	200	400
0	100.0	100.0	100.0	100.0	100.0	100.0	100.0	100.0	100.0
1	79.0	94.2	96.9	98.2	99.9	100.8	102.0	102.6	103.0
2	63.0	83.2	88.3	90.2	93.2	94.2	95.9	96.9	98.4
3	50.5	72.5	77.4	80.5	84.7	86.3	88.8	90.6	93.5
4	40.5	62.0	67.2	70.6	75.1	77.1	80.2	82.4	86.4
5	32.5	52.5	57.5	61.1	65.9	67.6	71.2	73.5	77.8
6	26.3	44.4	49.1	52.5	57.1	59.2	62.5	64.9	69.8
7	21.3	37.3	41.8	45.0	49.4	51.4	54.8	57.3	62.3
8	17.3	31.2	35.2	38.2	42.4	44.6	47.8	50.3	55.5
9	14.0	26.1	29.9	32.5	36.4	38.5	41.8	43.9	49.3
10	11.3	21.9	25.2	27.8	31.2	33.1	36.2	38.3	43.6
11	9.1	18.3	21.4	23.7	26.7	28.5	31.3	33.4	38.5
12	7.4	15.4	18.2	20.1	22.8	24.4	27.1	29.1	33.8
13	5.9	12.9	15.3	17.0	19.5	20.9	23.4	25.3	29.5
14	4.8	10.8	13.0	14.4	16.7	17.9	20.2	21.9	25.8
15	3.9	9.1	10.8	12.2	14.3	15.4	17.4	18.9	22.7
16	3.2	7.6	9.1	10.3	12.2	13.2	14.9	16.4	19.8
17	2.6	6.4	7.7	8.8	10.4	11.3	12.9	14.2	17.3
18	2.1	5.3	6.5	7.4	8.9	9.6	11.1	12.3	15.2
19	1.7	4.5	5.5	6.3	7.6	8.3	9.5	10.6	13.3
20	1.4	3.7	4.7	5.4	6.5	7.1	8.2	9.1	11.6

TABLE A-7
H.V.L. 1.0 mm. Cu. F.S.D.: 60 cm.

Depth in cm.	Area of field in square centimetres								
	0	20	35	50	80	100	150	200	400
0	100.0	100.0	100.0	100.0	100.0	100.0	100.0	100.0	100.0
1	79.6	94.8	97.5	98.8	100.5	101.4	102.6	103.2	103.6
2	63.8	84.2	89.4	91.3	94.3	95.3	97.1	98.1	99.6
3	51.5	73.8	78.8	81.9	86.2	87.9	90.4	92.2	95.2
4	41.5	63.4	68.7	72.2	76.8	78.9	82.0	84.3	88.4
5	33.5	54.0	59.0	62.7	67.6	69.4	73.0	75.3	79.7
6	27.4	45.6	50.5	54.0	58.7	60.9	64.3	66.7	71.8
7	22.2	38.5	43.0	46.4	50.9	53.0	56.5	59.1	64.2
8	18.1	32.2	36.4	39.5	43.8	46.1	49.5	52.0	57.3
9	14.6	27.0	30.9	33.6	37.7	39.8	43.2	45.4	51.0
10	11.8	22.7	26.2	28.8	32.4	34.3	37.5	39.7	45.2
11	9.7	19.0	22.2	24.6	27.7	29.6	32.5	34.7	40.0
12	7.8	16.0	18.8	20.8	23.7	25.4	28.2	30.3	35.2
13	6.4	13.4	15.9	17.7	20.3	21.8	24.4	26.4	30.8
14	5.2	11.3	13.5	15.0	17.4	18.7	21.0	22.9	27.0
15	4.2	9.5	11.3	12.7	15.0	16.1	18.1	19.8	23.7
16	3.4	8.0	9.6	10.7	12.8	13.8	15.6	17.2	20.8
17	2.8	6.7	8.1	9.2	10.9	11.9	13.5	14.9	18.2
18	2.3	5.6	6.9	7.8	9.3	10.1	11.7	12.8	15.9
19	1.9	4.7	5.8	6.6	8.0	8.7	10.0	11.2	14.0
20	1.6	3.9	4.9	5.6	6.8	7.5	8.6	9.6	12.2

H.V.L. 1.0 mm. Cu. F.S.D.: 80 cm.

Depth in cm.	Area of field in square centimetres								
	0	20	35	50	80	100	150	200	400
0	100.0	100.0	100.0	100.0	100.0	100.0	100.0	100.0	100.0
1	80.4	95.3	98.1	99.4	101.1	102.0	103.2	103.8	104.2
2	64.9	85.4	90.6	92.5	95.5	96.6	98.3	99.3	100.9
3	52.6	75.3	80.3	83.4	87.7	89.4	91.9	93.8	96.8
4	42.7	65.0	70.4	73.8	78.6	80.6	83.8	86.1	90.3
5	34.8	55.4	60.7	64.4	69.5	71.3	75.0	77.4	81.9
6	28.6	47.2	52.2	55.8	60.7	62.9	66.4	68.9	74.1
7	23.4	40.0	44.7	48.2	52.9	54.9	58.6	61.3	66.6
8	19.2	33.6	38.1	41.1	45.6	47.9	51.4	54.0	59.6
9	15.7	28.3	32.4	35.2	39.5	41.6	45.1	47.5	53.2
10	12.9	23.9	27.5	30.3	34.0	36.0	39.4	41.6	47.3
11	10.5	20.1	23.4	25.9	29.2	31.1	34.2	36.5	42.0
12	8.6	17.0	19.8	22.1	25.1	26.8	29.7	31.9	37.0
13	7.0	14.3	16.8	18.8	21.5	23.0	25.7	27.8	32.4
14	5.7	12.0	14.3	16.0	18.4	19.8	22.3	24.2	28.5
15	4.7	10.1	12.1	13.6	15.8	17.1	19.3	21.0	25.2
16	3.9	8.5	10.2	11.5	13.6	14.7	16.6	18.3	22.1
17	3.2	7.2	8.7	9.8	11.7	12.6	14.4	15.9	19.4
18	2.6	6.0	7.4	8.4	10.0	10.8	12.5	13.8	17.0
19	2.2	5.1	6.2	7.1	8.6	9.3	10.7	11.9	14.9
20	1.8	4.2	5.3	6.1	7.4	8.0	9.3	10.4	13.1

TABLE A-8
H.V.L. 1.5 mm. Cu. F.S.D.: 40 cm.

Depth in cm.	Area of field in square centimetres								
	0	20	35	50	80	100	150	200	400
0	100.0	100.0	100.0	100.0	100.0	100.0	100.0	100.0	100.0
1	80.1	94.3	96.3	98.0	98.9	99.7	100.7	101.5	102.0
2	63.9	83.8	87.4	89.3	92.0	93.0	94.8	95.9	98.0
3	51.2	72.4	76.9	79.8	83.3	85.1	87.6	89.2	92.3
4	41.5	61.7	66.5	69.6	74.0	76.0	78.9	80.8	84.7
5	33.5	52.3	57.0	60.4	64.8	66.7	70.0	72.1	76.6
6	27.0	44.3	48.6	52.0	56.4	58.9	62.1	64.4	69.2
7	21.8	37.4	41.8	44.7	49.1	51.3	54.4	56.9	62.3
8	17.6	31.5	35.4	38.2	42.7	44.4	47.6	50.0	55.8
9	14.2	26.4	30.0	32.6	36.8	38.3	41.7	44.0	49.6
10	11.4	22.2	25.5	27.9	31.5	33.2	36.4	38.3	44.0
11	9.3	18.7	21.6	23.7	27.1	28.5	31.5	33.4	38.7
12	7.5	15.8	18.4	20.3	23.3	24.6	27.4	29.2	34.1
13	6.1	13.2	15.6	17.3	20.0	21.3	23.8	25.4	30.1
14	5.0	11.1	13.2	14.8	17.2	18.4	20.7	22.3	26.3
15	4.1	9.4	11.2	12.6	14.8	15.8	17.9	19.5	23.2
16	3.3	7.9	9.6	10.8	12.7	13.6	15.6	17.0	20.3
17	2.7	6.7	8.1	9.2	11.0	11.8	13.6	14.9	17.9
18	2.2	5.6	6.9	7.9	9.5	10.2	11.9	13.1	15.7
19	1.8	4.8	5.9	6.8	8.1	8.8	10.3	11.5	13.8
20	1.5	4.0	5.0	5.8	7.0	7.6	8.9	10.1	12.1

H.V.L. 1.5 mm. Cu. F.S.D.: 50 cm.

Depth in cm.	Area of field in square centimetres								
	0	20	35	50	80	100	150	200	400
0	100.0	100.0	100.0	100.0	100.0	100.0	100.0	100.0	100.0
1	80.8	95.0	97.0	98.0	99.6	100.4	101.5	102.2	102.7
2	65.2	84.9	88.6	90.5	93.2	94.2	96.0	97.2	99.3
3	52.7	73.9	78.5	81.4	85.0	86.8	89.4	91.0	94.2
4	43.0	63.3	68.3	71.5	76.0	78.0	81.0	83.0	87.0
5	35.0	53.9	58.8	62.3	66.8	68.8	72.1	74.3	79.0
6	28.4	45.9	50.3	53.8	58.4	61.0	64.3	66.7	71.6
7	23.2	38.9	43.4	46.4	51.0	53.3	56.5	59.1	64.7
8	18.8	32.8	36.9	39.8	44.5	46.3	49.6	52.1	58.2
9	15.3	27.6	31.4	34.1	38.5	40.1	43.6	46.0	51.9
10	12.4	23.3	26.8	29.3	33.1	34.8	38.2	40.2	46.2
11	10.2	19.7	22.8	25.0	28.6	30.0	33.2	35.2	40.8
12	8.3	16.7	19.4	21.4	24.6	26.0	28.9	30.8	36.0
13	6.7	14.0	16.5	18.3	21.2	22.5	25.2	26.9	31.8
14	5.5	11.8	14.0	15.7	18.2	19.5	21.9	23.6	27.9
15	4.5	10.0	11.9	13.4	15.7	16.8	19.0	20.7	24.6
16	3.7	8.4	10.2	11.5	13.5	14.5	16.6	18.1	21.6
17	3.1	7.1	8.7	9.8	11.7	12.5	14.4	15.8	19.0
18	2.5	6.0	7.4	8.4	10.1	10.8	12.6	13.9	16.7
19	2.1	5.1	6.3	7.2	8.6	9.4	10.9	12.2	14.7
20	1.7	4.3	5.3	6.2	7.4	8.1	9.5	10.7	12.9

TABLE A-8

H.V.L. 1.5 mm. Cu. F.S.D.: 60 cm.

Depth in cm.	Area of field in square centimetres								
	0	20	35	50	80	100	150	200	400
0	100.0	100.0	100.0	100.0	100.0	100.0	100.0	100.0	100.0
1	81.4	95.6	97.6	98.6	100.2	101.0	102.1	102.8	103.3
2	66.0	85.8	89.6	91.5	94.2	95.2	97.1	98.3	100.4
3	53.7	75.0	79.7	82.6	86.3	88.1	90.7	92.4	95.6
4	44.0	64.6	69.7	72.9	77.5	79.6	82.6	84.7	88.7
5	36.1	55.2	60.2	63.8	68.4	70.5	73.8	76.1	80.9
6	29.4	47.1	51.7	55.3	60.0	62.6	66.0	68.5	73.5
7	24.2	40.1	44.7	47.8	52.5	54.9	58.2	60.9	66.6
8	19.7	33.8	38.1	41.1	45.9	47.8	51.2	53.8	60.1
9	16.1	28.6	32.5	35.3	39.8	41.5	45.1	47.6	53.7
10	13.1	24.2	27.8	30.4	34.3	36.1	39.6	41.7	47.9
11	10.8	20.5	23.7	26.0	29.7	31.2	34.5	36.6	42.4
12	8.8	17.4	20.2	22.3	25.6	27.0	30.1	32.0	37.4
13	7.2	14.6	17.2	19.1	22.1	23.4	26.3	28.0	33.1
14	5.9	12.3	14.6	16.4	19.0	20.4	22.9	24.6	29.1
15	4.9	10.5	12.4	14.0	16.4	17.5	19.9	21.6	25.7
16	4.0	8.8	10.7	12.0	14.1	15.2	17.4	19.0	22.6
17	3.4	7.5	9.1	10.3	12.3	13.1	15.1	16.6	19.9
18	2.8	6.3	7.7	8.8	10.6	11.3	13.2	14.6	17.5
19	2.3	5.3	6.6	7.6	9.1	9.8	11.5	12.8	15.4
20	1.9	4.5	5.6	6.5	7.8	8.5	10.0	11.3	13.6

H.V.L. 1.5 mm. Cu. F.S.D.: 80 cm.

Depth in cm.	Area of field in square centimetres								
	0	20	35	50	80	100	150	200	400
0	100.0	100.0	100.0	100.0	100.0	100.0	100.0	100.0	100.0
1	82.3	96.3	98.3	99.3	100.9	101.7	102.7	103.4	103.8
2	67.2	87.1	90.9	92.8	95.4	96.4	98.1	99.3	101.5
3	54.9	76.7	81.4	84.3	88.0	89.8	92.4	94.0	97.2
4	45.4	66.4	71.5	74.9	79.4	81.4	84.6	86.6	90.7
5	37.5	57.0	62.1	65.7	70.5	72.5	75.0	78.2	83.0
6	30.8	48.9	53.6	57.2	62.1	64.8	68.2	70.8	75.8
7	25.5	41.7	46.5	49.7	54.6	57.0	60.4	63.1	69.1
8	20.9	35.4	39.8	42.9	47.9	49.8	53.3	56.0	62.5
9	17.2	29.9	34.1	36.9	41.7	43.3	47.1	49.7	56.0
10	14.1	25.4	29.2	31.9	36.0	37.8	41.5	43.7	50.1
11	11.8	21.6	25.0	27.3	31.3	32.7	36.2	38.4	44.5
12	9.6	18.4	21.3	23.5	27.0	28.5	31.6	33.7	39.4
13	7.9	15.5	18.2	20.2	23.3	24.8	27.7	29.6	34.9
14	6.6	13.1	15.5	17.4	20.1	21.5	24.2	26.0	30.7
15	5.4	11.2	13.2	14.9	17.4	18.6	21.0	22.9	27.2
16	4.5	9.5	11.4	12.8	15.0	16.1	18.4	20.1	24.0
17	3.7	8.0	9.7	11.0	13.1	14.0	16.1	17.6	21.1
18	3.1	6.8	8.3	9.4	11.3	12.1	14.1	15.6	18.7
19	2.6	5.7	7.1	8.1	9.7	10.5	12.3	13.7	16.5
20	2.2	4.9	6.0	7.0	8.4	9.1	10.7	12.1	14.5

TABLE A-9
H.V.L. 2.0 mm. Cu. F.S.D.: 50 cm.

<i>Depth</i> <i>in cm.</i>	Area of field in square centimetres								
	0	20	35	50	80	100	150	200	400
0	100.0	100.0	100.0	100.0	100.0	100.0	100.0	100.0	100.0
1	81.4	95.0	96.9	97.9	99.4	99.9	101.0	101.6	102.4
2	66.5	85.5	88.5	90.3	92.7	93.8	95.4	96.6	99.0
3	54.0	74.3	78.6	81.3	84.8	86.3	88.8	90.5	93.7
4	44.2	63.9	68.7	71.8	75.8	77.6	80.7	82.8	87.0
5	36.2	54.9	59.5	62.8	67.0	68.8	71.9	74.2	79.2
6	29.6	46.5	51.2	54.5	58.8	61.0	64.2	66.5	71.8
7	24.3	39.6	44.0	47.2	51.5	53.4	57.0	59.2	64.8
8	19.9	33.5	37.7	40.8	44.8	46.8	50.3	52.7	58.5
9	16.4	28.4	32.4	35.2	39.2	40.9	44.4	46.5	52.4
10	13.4	24.0	27.7	30.3	33.9	35.7	38.9	41.3	46.7
11	11.1	20.4	23.7	26.0	29.4	31.0	34.0	36.3	41.6
12	9.1	17.2	20.2	22.3	25.4	27.0	29.7	31.8	36.9
13	7.5	14.7	17.3	19.2	21.9	23.4	26.0	28.0	32.7
14	6.2	12.5	14.8	16.5	19.0	20.3	22.8	24.7	28.9
15	5.1	10.6	12.6	14.1	16.4	17.7	19.9	21.7	25.5
16	4.2	8.9	10.8	12.1	14.2	15.3	17.4	19.1	22.6
17	3.5	7.6	9.2	10.4	12.3	13.3	15.2	16.8	20.0
18	2.9	6.5	7.8	8.9	10.7	11.6	13.3	14.8	17.7
19	2.4	5.5	6.7	7.7	9.2	10.0	11.6	13.0	15.6
20	2.0	4.7	5.7	6.6	7.9	8.7	10.2	11.4	13.8

H.V.L. 2.0 mm. Cu. F.S.D.: 60 cm.

<i>Depth</i> <i>in cm.</i>	Area of field in square centimetres								
	0	20	35	50	80	100	150	200	400
0	100.0	100.0	100.0	100.0	100.0	100.0	100.0	100.0	100.0
1	82.0	95.5	97.4	98.4	99.9	100.4	101.5	102.1	102.9
2	67.3	86.4	89.5	91.2	93.6	94.7	96.4	97.6	100.0
3	55.0	75.5	79.9	82.6	86.2	87.7	90.2	91.9	95.2
4	45.2	65.3	70.1	73.3	77.3	79.2	82.3	84.5	88.7
5	37.3	56.3	61.0	64.4	68.7	70.5	73.7	76.1	81.1
6	30.7	47.9	52.6	56.0	60.4	62.5	65.9	68.2	73.7
7	25.3	40.9	45.4	48.7	53.1	55.0	58.7	61.0	66.6
8	20.9	34.7	39.0	42.2	46.3	48.3	52.0	54.4	60.2
9	17.3	29.5	33.5	36.4	40.6	42.3	46.0	48.1	54.0
10	14.2	25.0	28.7	31.4	35.2	37.0	40.3	42.7	48.4
11	11.8	21.2	24.6	27.0	30.5	32.3	35.3	37.6	43.1
12	9.7	18.1	21.0	23.2	26.4	28.1	30.9	33.1	38.3
13	8.0	15.4	18.0	20.0	22.9	24.4	27.1	29.1	34.0
14	6.6	13.1	15.5	17.2	19.8	21.3	23.8	25.8	30.1
15	5.5	11.1	13.2	14.8	17.1	18.5	20.8	22.7	26.6
16	4.6	9.4	11.3	12.7	14.8	16.0	18.2	20.0	23.6
17	3.8	8.0	9.6	10.9	12.9	13.9	15.9	17.6	21.0
18	3.2	6.8	8.2	9.4	11.2	12.1	13.9	15.5	18.6
19	2.6	5.8	7.0	8.1	9.7	10.5	12.2	13.7	16.4
20	2.2	4.9	6.0	6.9	8.4	9.1	10.7	12.0	14.5

TABLE A-9
H.V.L. 2.0 mm. Cu. F.S.D.: 80 cm.

Depth in cm.	Area of field in square centimetres								
	0	20	35	50	80	100	150	200	400
0	100.0	100.0	100.0	100.0	100.0	100.0	100.0	100.0	100.0
1	82.9	96.1	98.0	99.0	100.5	101.0	102.1	102.7	103.4
2	68.5	87.6	90.6	92.5	94.8	96.0	97.6	98.8	101.2
3	56.3	77.1	81.4	84.1	87.8	89.1	91.7	93.5	96.7
4	46.6	67.1	71.9	75.2	79.2	81.0	84.2	86.4	90.7
5	38.7	58.1	62.9	66.3	70.7	72.6	75.8	78.2	83.2
6	32.1	49.7	54.5	58.0	62.6	64.8	68.1	70.6	76.0
7	26.7	42.6	47.3	50.6	55.2	57.1	60.9	63.2	69.1
8	22.1	36.3	40.7	44.1	48.3	50.4	54.1	56.6	62.8
9	18.4	30.9	35.2	38.2	42.3	44.3	48.0	50.3	56.6
10	15.3	26.3	30.2	33.0	36.9	38.8	42.2	44.7	50.7
11	12.8	22.5	26.0	28.5	32.1	33.9	37.1	39.6	45.3
12	10.6	19.1	22.3	24.5	27.9	29.6	32.5	34.8	40.4
13	8.8	16.3	19.1	21.2	24.1	25.8	28.6	30.8	35.9
14	7.3	13.9	16.4	18.3	21.0	22.5	25.2	27.3	31.8
15	6.1	11.8	14.0	15.7	18.2	19.6	22.0	24.0	28.2
16	5.1	10.1	12.1	13.5	15.8	17.0	19.4	21.3	25.1
17	4.3	8.6	10.3	11.7	13.7	14.9	17.0	18.8	22.3
18	3.6	7.3	8.8	10.1	12.0	13.0	14.9	16.6	19.8
19	3.0	6.3	7.6	8.7	10.3	11.3	13.1	14.6	17.5
20	2.5	5.3	6.5	7.4	9.0	9.8	11.5	12.9	15.6

H.V.L. 2.0 mm. Cu. F.S.D.: 100 cm.

Depth in cm.	Area of field in square centimetres								
	0	20	35	50	80	100	150	200	400
0	100.0	100.0	100.0	100.0	100.0	100.0	100.0	100.0	100.0
1	83.1	96.6	98.5	99.5	101.0	101.4	102.5	103.1	103.8
2	69.2	88.4	91.4	93.2	95.6	96.6	98.3	99.5	101.9
3	57.2	78.2	82.4	85.1	88.7	90.2	92.8	94.5	97.7
4	47.7	68.2	73.1	76.3	80.3	82.2	85.4	87.5	91.9
5	39.7	59.3	64.1	67.5	72.0	73.8	77.1	79.5	84.6
6	33.0	50.9	55.9	59.3	63.9	66.2	69.5	72.0	77.5
7	27.6	43.8	48.4	51.9	56.5	58.5	62.4	64.7	70.7
8	23.0	37.4	41.9	45.3	49.6	51.8	55.6	58.0	64.4
9	19.2	32.0	36.4	39.4	43.8	45.6	49.5	51.7	58.2
10	15.9	27.3	31.3	34.2	38.1	40.1	43.6	46.2	52.3
11	13.4	23.4	27.0	29.5	33.3	35.1	38.4	40.9	46.8
12	11.1	19.8	23.2	25.5	29.0	30.7	33.7	36.1	41.8
13	9.3	17.0	20.0	22.1	25.1	26.8	29.7	32.0	37.2
14	7.8	14.5	17.2	19.1	21.9	23.4	26.2	28.4	33.1
15	6.5	12.5	14.7	16.4	19.0	20.5	23.0	25.0	29.4
16	5.4	10.6	12.7	14.2	16.6	17.8	20.2	22.1	26.1
17	4.6	9.0	10.8	12.3	14.4	15.6	17.7	19.6	23.3
18	3.8	7.7	9.3	10.6	12.6	13.6	15.6	17.3	20.7
19	3.2	6.6	8.0	9.1	10.9	11.8	13.7	15.3	18.3
20	2.7	5.7	6.9	7.8	9.5	10.3	12.1	13.5	16.3

TABLE A-10
H.V.L. 3.0 mm. Cu. F.S.D. 50 cm.

Depth in cm.	Area of field in square centimetres								
	0	20	35	50	80	100	150	200	400
0	100.0	100.0	100.0	100.0	100.0	100.0	100.0	100.0	100.0
1	82.3	94.7	96.5	97.4	98.6	99.0	100.0	100.5	101.4
2	68.0	85.8	88.2	89.8	91.7	92.7	94.3	95.4	97.6
3	56.2	75.0	78.8	81.0	84.1	85.4	87.5	89.2	92.4
4	46.4	64.8	69.1	71.8	75.4	77.0	79.8	81.8	85.9
5	38.6	56.0	60.0	63.0	66.8	68.6	71.6	73.9	78.4
6	32.0	47.7	52.0	54.9	58.8	60.9	64.0	66.4	71.0
7	26.5	40.8	44.8	47.8	51.8	54.0	56.9	59.4	64.4
8	22.0	34.9	38.7	41.5	45.5	47.6	50.4	53.0	58.2
9	18.4	29.7	33.3	36.0	39.8	41.7	44.6	47.2	52.2
10	15.4	25.3	28.6	31.1	34.7	36.6	39.5	41.8	46.8
11	12.8	21.7	24.6	26.9	30.3	32.0	34.8	37.2	41.9
12	10.7	18.5	21.1	23.2	26.4	27.9	30.6	32.7	37.3
13	9.0	15.7	18.2	20.0	22.9	24.4	26.9	28.8	33.3
14	7.5	13.4	15.7	17.3	19.9	21.2	23.6	25.4	29.5
15	6.3	11.5	13.4	15.0	17.3	18.5	20.7	22.4	26.3
16	5.3	9.8	11.5	12.9	15.0	16.1	18.2	19.7	23.4
17	4.5	8.4	9.9	11.2	13.1	14.0	15.9	17.4	20.8
18	3.7	7.2	8.5	9.6	11.4	12.2	14.0	15.4	18.5
19	3.1	6.1	7.3	8.3	9.9	10.7	12.3	13.6	16.5
20	2.6	5.2	6.3	7.2	8.6	9.3	10.8	11.9	14.6

H.V.L. 3.0 mm. Cu. F.S.D.: 60 cm.

Depth in cm.	Area of field in square centimetres								
	0	20	35	50	80	100	150	200	400
0	100.0	100.0	100.0	100.0	100.0	100.0	100.0	100.0	100.0
1	82.9	95.3	97.1	98.0	99.2	99.5	100.6	101.1	102.0
2	68.8	86.7	89.2	90.8	92.7	93.7	95.3	96.4	98.7
3	57.3	76.2	80.1	82.3	85.4	86.8	88.9	90.6	93.9
4	47.5	66.1	70.5	73.2	76.8	78.5	81.3	83.3	87.4
5	39.8	57.5	61.4	64.5	68.3	70.2	73.2	75.5	80.1
6	33.2	49.1	53.4	56.4	60.3	62.5	65.6	68.1	72.8
7	27.6	42.2	46.2	49.3	53.3	55.6	58.6	61.1	66.2
8	23.1	36.2	40.0	42.9	47.0	49.1	52.0	54.7	60.0
9	19.4	30.9	34.6	37.3	41.2	43.2	46.2	48.9	54.0
10	16.3	26.4	29.8	32.3	36.1	38.0	41.0	43.3	48.5
11	13.6	22.7	25.7	28.0	31.5	33.3	36.2	38.6	43.4
12	11.4	19.4	22.1	24.2	27.5	29.1	31.9	34.1	38.8
13	9.6	16.5	19.1	20.9	24.0	25.5	28.1	30.1	34.8
14	8.1	14.2	16.5	18.1	20.9	22.2	24.7	26.6	30.9
15	6.8	12.2	14.2	15.7	18.2	19.5	21.8	23.6	27.6
16	5.8	10.4	12.2	13.6	15.8	17.0	19.2	20.8	24.6
17	4.9	8.9	10.5	11.8	13.9	14.8	16.8	18.4	21.9
18	4.1	7.6	9.1	10.2	12.1	12.9	14.8	16.3	19.6
19	3.5	6.5	7.9	8.9	10.5	11.4	13.1	14.4	17.5
20	2.9	5.6	6.8	7.7	9.2	9.9	11.5	12.7	15.6

TABLE A-10
H.V.L. 3.0 mm. Cu. F.S.D.: 80 cm.

Depth in cm.	Area of field in square centimetres								
	0	20	35	50	80	100	150	200	400
0	100.0	100.0	100.0	100.0	100.0	100.0	100.0	100.0	100.0
1	83.8	95.9	97.8	98.6	99.7	100.1	101.1	101.6	102.5
2	70.0	88.0	90.3	92.0	93.9	94.8	96.5	97.6	99.7
3	58.6	77.9	81.7	83.8	86.9	88.2	90.4	92.1	95.4
4	49.0	68.1	72.3	75.2	78.7	80.4	83.3	85.3	89.5
5	41.3	59.5	63.4	66.5	70.4	72.3	75.3	77.7	82.3
6	34.7	51.1	55.5	58.6	62.6	64.8	68.0	70.5	75.1
7	29.2	44.1	48.3	51.4	55.5	57.8	60.9	63.6	68.9
8	24.5	38.1	42.0	44.9	49.1	51.4	54.4	57.1	62.6
9	20.7	32.7	36.5	39.2	43.3	45.3	48.4	51.2	56.4
10	17.5	28.1	31.5	34.1	38.0	40.0	43.1	45.7	50.9
11	14.7	24.2	27.3	29.7	33.4	35.2	38.2	40.7	45.8
12	12.5	20.8	23.6	25.8	29.2	30.9	33.8	36.1	41.0
13	10.5	17.8	20.4	22.2	25.5	27.1	29.9	31.9	36.8
14	8.9	15.3	17.7	19.4	22.3	23.7	26.3	28.2	32.8
15	7.6	13.2	15.2	16.9	19.4	20.8	23.2	25.0	29.4
16	6.4	11.3	13.2	14.7	17.0	18.2	20.5	22.1	26.3
17	5.4	9.7	11.4	12.8	14.9	15.9	18.1	19.7	23.5
18	4.6	8.3	9.9	11.1	13.0	13.9	15.9	17.5	21.0
19	3.9	7.2	8.5	9.6	11.4	12.3	14.1	15.5	18.8
20	3.3	6.2	7.4	8.4	9.9	10.7	12.4	13.7	16.7

H.V.L. 3.0 mm. Cu. F.S.D.: 100 cm.

Depth in cm.	Area of field in square centimetres								
	0	20	35	50	80	100	150	200	400
0	100.0	100.0	100.0	100.0	100.0	100.0	100.0	100.0	100.0
1	84.0	96.4	98.1	99.0	100.1	100.5	101.5	101.9	102.8
2	70.7	88.8	91.1	92.7	94.5	95.5	97.0	98.2	100.3
3	59.6	79.0	82.7	84.8	87.9	89.2	91.4	93.0	96.3
4	50.1	69.3	73.5	76.3	79.8	81.5	84.4	86.4	90.6
5	42.4	60.8	64.7	67.8	71.7	73.6	76.7	79.1	83.7
6	35.7	52.4	56.8	59.9	63.9	66.1	69.3	71.8	76.6
7	30.1	45.5	49.6	52.8	56.9	59.3	62.3	65.0	70.3
8	25.4	39.3	43.4	46.3	50.6	52.8	55.8	58.6	64.1
9	21.6	33.9	37.7	40.6	44.7	46.7	49.8	52.6	58.0
10	18.3	29.2	32.7	35.4	39.3	41.4	44.5	47.0	52.4
11	15.4	25.2	28.4	30.9	34.6	36.5	39.5	42.1	47.3
12	13.1	21.7	24.6	26.9	30.4	32.1	35.0	37.4	42.4
13	11.1	18.6	21.3	23.4	26.6	28.2	31.0	33.1	38.0
14	9.5	16.1	18.5	20.4	23.3	24.7	27.4	29.4	34.0
15	8.1	13.8	16.0	17.8	20.4	21.7	24.2	26.1	30.5
16	6.9	11.9	13.9	15.4	17.8	19.0	21.4	23.1	27.3
17	5.8	10.3	12.1	13.5	15.6	16.7	18.9	20.5	24.4
18	5.0	8.9	10.5	11.7	13.7	14.6	16.7	18.2	21.9
19	4.2	7.6	9.2	10.2	12.0	12.9	14.7	16.2	19.6
20	3.6	6.6	7.9	8.9	10.5	11.3	13.0	14.3	17.5

TABLE A-11
H.V.L. 4.0 mm. Cu. F.S.D.: 50 cm.

Depth in cm.	Area of field in square centimetres								
	0	20	35	50	80	100	150	200	400
0	100.0	100.0	100.0	100.0	100.0	100.0	100.0	100.0	100.0
1	83.1	94.4	96.0	96.8	97.7	98.0	98.8	99.3	100.0
2	69.3	85.9	87.8	89.1	90.8	91.6	93.0	93.9	96.0
3	57.8	75.6	78.8	80.7	83.3	84.3	86.2	87.6	90.1
4	48.2	65.5	69.5	71.8	75.0	76.4	78.9	80.5	84.2
5	40.7	56.6	60.4	63.2	66.6	68.2	71.2	73.4	77.1
6	34.3	48.5	52.7	55.5	58.9	60.8	63.8	66.1	70.2
7	28.9	41.6	45.6	48.4	51.8	53.7	56.8	59.4	63.8
8	24.4	35.7	39.5	42.0	45.5	47.3	50.5	53.1	57.8
9	20.5	30.6	34.0	36.5	39.8	41.6	44.8	47.3	51.8
10	17.3	26.3	29.4	31.6	35.0	36.7	39.7	42.0	46.6
11	14.6	22.6	25.4	27.4	30.6	32.3	35.1	37.4	41.8
12	12.4	19.4	21.9	23.7	26.8	28.4	30.9	33.1	37.5
13	10.5	16.7	19.0	20.6	23.4	24.9	27.3	29.2	33.6
14	8.9	14.3	16.4	17.9	20.4	21.8	24.1	25.8	30.0
15	7.5	12.3	14.1	15.5	17.8	19.0	21.2	22.8	26.7
16	6.4	10.6	12.2	13.5	15.6	16.7	18.7	20.1	23.8
17	5.4	9.1	10.6	11.7	13.6	14.6	16.4	17.7	21.2
18	4.6	7.8	9.1	10.2	11.8	12.8	14.4	15.7	18.9
19	4.0	6.7	7.9	8.8	10.3	11.2	12.6	13.8	16.9
20	3.4	5.8	6.8	7.7	9.0	9.7	11.1	12.2	15.1

H.V.L. 4.0 mm. Cu. F.S.D.: 60 cm.

Depth in cm.	Area of field in square centimetres								
	0	20	35	50	80	100	150	200	400
0	100.0	100.0	100.0	100.0	100.0	100.0	100.0	100.0	100.0
1	83.7	94.9	96.5	97.3	98.2	98.5	99.3	99.8	100.5
2	70.1	86.8	88.6	89.9	91.6	92.4	93.8	94.7	96.8
3	58.9	76.8	79.9	81.8	84.5	85.5	87.3	88.7	91.7
4	49.4	66.9	70.8	73.1	76.4	77.9	80.3	81.9	85.6
5	41.9	58.1	61.8	64.7	68.1	69.8	72.8	74.9	78.6
6	35.5	50.1	54.1	57.0	60.5	62.4	65.5	67.9	71.9
7	30.1	43.1	47.1	49.9	53.4	55.4	58.6	61.2	65.5
8	25.5	37.2	41.0	43.5	47.1	49.0	52.2	54.9	59.5
9	21.6	32.0	35.4	38.0	41.4	43.2	46.5	49.1	53.5
10	18.3	27.6	30.8	32.9	36.5	38.2	41.3	43.7	48.3
11	15.5	23.9	26.7	28.7	32.0	33.8	36.7	39.0	43.5
12	13.2	20.6	23.1	24.9	28.0	29.7	32.4	34.7	39.2
13	11.2	17.8	20.0	21.7	24.6	26.2	28.7	30.7	35.2
14	9.5	15.3	17.4	18.9	21.5	23.0	25.4	27.2	31.5
15	8.1	13.2	15.0	16.4	18.8	20.1	22.4	24.1	28.2
16	6.9	11.4	13.0	14.4	16.5	17.8	19.8	21.4	25.3
17	5.9	9.8	11.3	12.5	14.5	15.6	17.5	18.9	22.6
18	5.1	8.5	9.8	10.9	12.6	13.7	15.4	16.7	20.2
19	4.3	7.3	8.5	9.5	11.2	12.0	13.6	14.8	18.2
20	3.7	6.3	7.4	8.3	9.7	10.5	12.0	13.1	16.3

TABLE A-11
H.V.L. 4.0 mm. Cu. F.S.D.: 80 cm.

Depth in cm.	Area of field in square centimetres								
	0	20	35	50	80	100	150	200	400
0	100.0	100.0	100.0	100.0	100.0	100.0	100.0	100.0	100.0
1	84.6	95.6	97.2	97.9	98.8	99.1	99.8	100.3	101.0
2	71.4	88.0	89.7	91.1	92.8	93.6	95.0	95.9	97.9
3	60.2	78.5	81.5	83.4	86.0	87.0	88.9	90.4	93.2
4	50.9	68.8	72.7	75.0	78.2	79.7	82.2	83.9	87.5
5	43.5	60.2	63.9	66.7	70.2	71.9	74.9	77.1	80.9
6	37.2	52.2	56.3	59.2	62.7	64.8	67.8	70.1	74.2
7	31.7	45.3	49.2	52.1	55.7	57.8	60.9	63.6	67.9
8	27.1	39.3	43.1	45.7	49.4	51.3	54.6	57.3	62.1
9	23.1	34.0	37.5	40.1	43.6	45.4	48.8	51.5	56.0
10	19.7	29.5	32.7	35.0	38.6	40.4	43.6	46.1	50.8
11	16.8	25.6	28.5	30.6	34.0	35.8	38.8	41.3	45.9
12	14.4	22.2	24.8	26.7	29.9	31.6	34.4	36.8	41.4
13	12.3	19.3	21.6	23.4	26.4	27.9	30.6	32.7	37.4
14	10.5	16.6	18.8	20.4	23.1	24.7	27.2	29.1	33.6
15	9.0	14.4	16.3	17.8	20.3	21.6	24.0	25.9	30.1
16	7.7	12.5	14.2	15.6	17.8	19.1	21.3	23.0	27.0
17	6.6	10.8	12.4	13.7	15.7	16.8	18.9	20.3	24.2
18	5.7	9.4	10.8	12.0	13.8	14.8	16.7	18.1	21.7
19	4.9	8.1	9.4	10.5	12.1	13.1	14.8	16.1	19.5
20	4.2	7.0	8.2	9.1	10.6	11.5	13.1	14.3	17.6

H.V.L. 4.0 mm. Cu. F.S.D.: 100 cm.

Depth in cm.	Area of field in square centimetres								
	0	20	35	50	80	100	150	200	400
0	100.0	100.0	100.0	100.0	100.0	100.0	100.0	100.0	100.0
1	84.8	96.0	97.5	98.3	99.2	99.4	100.1	100.6	101.3
2	72.1	88.8	90.5	91.8	93.5	94.3	95.6	96.5	98.5
3	61.3	79.6	82.5	84.4	87.0	87.9	89.7	91.2	94.0
4	52.0	70.1	73.9	76.2	79.4	80.8	83.2	84.9	88.6
5	44.7	61.5	65.2	68.0	71.5	73.1	76.2	78.4	82.0
6	38.3	53.5	57.7	60.6	64.1	66.1	69.1	71.5	75.5
7	32.8	46.6	50.7	53.5	57.1	59.1	62.3	65.0	69.4
8	28.2	40.6	44.5	47.1	50.8	52.7	56.0	58.7	63.6
9	24.0	35.3	38.8	41.4	45.0	46.8	50.2	52.9	57.5
10	20.6	30.8	34.0	36.3	39.9	41.8	45.0	47.5	52.3
11	17.7	26.8	29.8	31.9	35.3	37.1	40.2	42.6	47.4
12	15.2	23.3	26.0	27.9	31.2	33.0	35.7	38.1	42.8
13	13.0	20.3	22.8	24.5	27.6	29.1	31.8	33.9	38.6
14	11.2	17.6	19.9	21.5	24.2	25.8	28.2	30.2	34.8
15	9.6	15.3	17.3	18.8	21.3	22.6	25.1	26.9	31.2
16	8.3	13.3	15.1	16.5	18.8	20.0	22.2	23.9	28.1
17	7.1	11.5	13.2	14.4	16.5	17.7	19.7	21.3	25.2
18	6.1	10.0	11.5	12.6	14.5	15.6	17.5	19.0	22.6
19	5.3	8.7	10.0	11.1	12.8	13.8	15.4	16.9	20.4
20	4.6	7.6	8.7	9.7	11.3	12.1	13.7	15.0	18.3

TABLE A-12
H.V.L. 5.0 mm. Cu. F.S.D.: 50 cm.

Depth in cm.	Area of field in square centimetres								
	0	20	35	50	80	100	150	200	400
0	100.0	100.0	100.0	100.0	100.0	100.0	100.0	100.0	100.0
1	83.9	93.7	95.5	96.1	96.8	97.2	97.7	98.1	99.0
2	70.3	86.0	87.4	88.4	89.9	90.4	91.6	92.0	93.9
3	59.3	76.0	78.8	80.4	82.4	83.3	84.8	85.8	88.3
4	50.0	66.0	69.7	71.8	74.5	75.8	77.9	79.3	82.4
5	42.3	56.9	60.7	63.2	66.3	67.7	70.5	72.4	75.7
6	36.0	49.0	52.8	55.6	59.0	60.7	63.5	65.7	69.0
7	30.6	42.3	45.8	48.6	52.1	53.9	56.8	59.3	63.0
8	26.1	36.4	39.7	42.3	45.8	47.8	50.7	53.1	57.1
9	22.2	31.4	34.5	36.7	40.2	42.1	45.2	47.5	51.6
10	18.9	27.0	30.0	32.0	35.3	37.1	40.0	42.2	46.6
11	16.2	23.3	25.9	27.8	31.0	32.8	35.5	37.5	41.9
12	13.8	20.1	22.5	24.3	27.2	28.8	31.2	33.1	37.6
13	11.8	17.4	19.5	21.1	23.8	25.3	27.5	29.3	33.7
14	10.2	15.0	16.8	18.3	20.8	22.1	24.3	25.9	30.1
15	8.7	13.0	14.7	15.9	18.2	19.4	21.4	23.0	27.0
16	7.5	11.2	12.7	13.8	15.9	17.0	18.8	20.3	24.1
17	6.4	9.7	11.0	12.1	13.9	14.9	16.6	17.9	21.6
18	5.5	8.4	9.5	10.5	12.2	13.1	14.6	15.8	19.2
19	4.8	7.3	8.3	9.1	10.7	11.4	12.9	13.9	17.2
20	4.1	6.3	7.2	7.9	9.3	10.0	11.4	12.3	15.4

H.V.L. 5.0 mm. Cu. F.S.D.: 60 cm.

Depth in cm.	Area of field in square centimetres								
	0	20	35	50	80	100	150	200	400
0	100.0	100.0	100.0	100.0	100.0	100.0	100.0	100.0	100.0
1	84.5	94.2	95.9	96.5	97.2	97.6	98.1	98.5	99.3
2	71.1	86.8	88.1	89.1	90.6	91.1	92.3	92.7	94.7
3	60.4	77.1	79.8	81.4	83.5	84.4	85.9	86.8	89.4
4	51.2	67.4	70.9	73.0	75.8	77.1	79.2	80.6	83.8
5	43.6	58.4	62.1	64.6	67.7	69.1	72.0	73.9	77.2
6	37.3	50.7	54.3	57.1	60.6	62.3	65.2	67.4	70.7
7	31.9	44.0	47.4	50.2	53.8	55.6	58.6	61.1	64.7
8	27.4	38.1	41.3	43.9	47.5	49.6	52.5	54.9	58.9
9	23.4	33.1	36.1	38.2	41.9	43.9	47.0	49.3	53.4
10	20.0	28.6	31.5	33.5	36.9	38.8	41.8	44.0	48.4
11	17.2	24.8	27.3	29.2	32.6	34.4	37.2	39.3	43.7
12	14.7	21.4	23.8	25.6	28.6	30.3	32.8	34.8	39.3
13	12.6	18.6	20.7	22.3	25.2	26.7	29.1	30.9	35.4
14	11.3	16.1	17.9	19.4	22.1	23.4	25.8	27.4	31.8
15	9.4	14.0	15.7	16.9	19.4	20.7	22.8	24.4	28.6
16	8.1	12.1	13.7	14.8	17.0	18.2	20.1	21.7	25.7
17	7.0	10.6	11.9	13.0	14.9	16.0	17.8	19.2	23.2
18	6.0	9.2	10.3	11.3	13.2	14.1	15.7	17.0	20.7
19	5.2	8.0	9.0	9.9	11.6	12.3	14.0	15.1	18.6
20	4.5	6.9	7.9	8.6	10.1	10.9	12.4	13.4	16.8

TABLE A-12
H.V.L. 5.0 mm. Cu. F.S.D.: 80 cm.

Depth in cm.	Area of field in square centimetres								
	0	20	35	50	80	100	150	200	400
0	100.0	100.0	100.0	100.0	100.0	100.0	100.0	100.0	100.0
1	85.4	94.8	96.6	97.2	97.9	98.3	98.8	99.1	99.9
2	72.4	88.2	89.4	90.3	91.8	92.3	93.5	93.9	95.7
3	61.8	79.0	81.6	83.1	85.1	86.0	87.4	88.5	90.9
4	52.8	69.4	72.9	75.0	77.8	79.0	81.2	82.6	85.7
5	45.3	60.6	64.2	66.7	69.9	71.4	74.2	76.2	79.4
6	39.1	52.9	56.5	59.4	63.0	64.6	67.5	69.8	73.0
7	33.7	46.3	49.6	52.5	56.1	58.0	61.0	63.6	67.2
8	29.0	40.3	43.5	46.1	49.9	52.0	54.9	57.4	61.4
9	25.0	35.2	38.2	40.5	44.2	46.3	49.4	51.8	55.9
10	21.5	30.6	33.6	35.7	39.1	41.1	44.2	46.5	50.9
11	18.7	26.7	29.3	31.2	34.7	36.7	39.5	41.6	46.1
12	16.1	23.3	25.7	27.6	30.7	32.5	35.0	37.0	41.7
13	13.9	20.4	22.5	24.2	27.1	28.7	31.1	33.0	37.7
14	12.1	17.7	19.6	21.2	23.9	25.3	27.7	29.4	33.9
15	10.4	15.5	17.3	18.5	21.0	22.4	24.5	26.3	30.7
16	9.0	13.5	15.1	16.2	18.5	19.8	21.8	23.4	27.6
17	7.8	11.8	13.2	14.3	16.3	17.4	19.4	20.8	24.9
18	6.8	10.3	11.5	12.5	14.4	15.4	17.2	18.5	22.3
19	5.9	9.0	10.1	11.0	12.7	13.5	15.3	16.4	20.1
20	5.1	7.8	8.8	9.6	11.2	12.0	13.6	14.6	18.1

H.V.L. 5.0 mm. Cu. F.S.D.: 100 cm.

Depth in cm.	Area of field in square centimetres								
	0	20	35	50	80	100	150	200	400
0	100.0	100.0	100.0	100.0	100.0	100.0	100.0	100.0	100.0
1	85.7	95.3	96.9	97.5	98.2	98.6	99.0	99.4	100.2
2	73.1	88.9	90.1	91.1	92.5	92.9	94.2	94.5	96.3
3	62.9	80.0	82.6	84.1	86.1	86.9	88.4	89.3	91.8
4	54.0	70.7	74.2	76.3	78.9	80.1	82.3	83.7	86.8
5	46.4	62.0	65.6	68.1	71.2	72.6	75.4	77.3	80.6
6	40.2	54.3	58.0	60.8	64.4	66.0	68.9	71.1	74.4
7	34.7	47.8	51.1	54.0	57.6	59.5	62.4	64.9	68.6
8	30.1	41.8	45.0	47.6	51.3	53.5	56.4	58.9	62.9
9	26.0	36.6	39.7	41.9	45.7	47.7	50.9	53.3	57.5
10	22.5	32.0	35.0	37.1	40.6	42.6	45.6	47.9	52.4
11	19.6	28.0	30.7	32.6	36.1	38.0	40.9	43.0	47.6
12	16.9	24.5	27.0	28.8	32.0	33.8	36.3	38.4	43.1
13	14.6	21.5	23.7	25.4	28.3	30.0	32.3	34.2	39.1
14	12.8	18.8	20.7	22.3	25.0	26.5	28.9	30.6	35.2
15	11.1	16.5	18.3	19.6	22.1	23.5	25.7	27.4	31.9
16	9.6	14.4	16.0	17.2	19.5	20.8	22.8	24.4	28.7
17	8.4	12.7	14.1	15.3	17.2	18.4	20.3	21.7	25.9
18	7.3	11.1	12.3	13.4	15.3	16.3	18.0	19.3	23.3
19	6.4	9.7	10.8	11.8	13.5	14.3	16.0	17.2	21.0
20	5.6	8.5	9.6	10.3	11.9	12.7	14.3	15.3	18.9

TABLE A-13. COBALT 60 RADIATION
 (Average photon energy 1.25 M.e.v., H.V.L. 1.1. mm. Pb.)
 Source to skin distance 50 cm.

Depth (cm.)	Area of field in square centimetres					
	0	20	50	100	200	400
0.5	100.0	100.0	100.0	100.0	100.0	100.0
1	94.6	96.2	97.0	97.5	97.6	97.7
2	85.2	89.2	90.6	91.4	91.8	92.1
3	76.8	82.3	84.2	85.4	86.1	86.8
4	69.3	75.7	78.2	79.6	80.6	81.6
5	62.6	69.5	72.4	74.0	75.3	76.6
6	56.4	63.7	66.8	68.6	70.2	71.8
7	51.0	58.3	61.4	63.4	65.3	67.1
8	46.1	53.3	56.4	58.5	60.7	62.7
9	41.7	48.7	51.7	53.9	56.2	58.6
10	37.8	44.5	47.4	49.7	52.2	54.9
11	34.3	40.6	43.5	45.8	48.4	51.2
12	31.1	37.1	40.0	42.2	45.0	47.8
13	28.2	33.9	36.7	39.0	41.7	44.7
14	25.6	31.0	33.7	36.0	38.7	41.7
15	23.3	28.4	30.9	33.2	36.0	39.0
16	21.1	26.0	28.4	30.6	33.4	36.5
17	19.3	23.8	26.1	28.3	31.1	34.2
18	17.5	21.8	24.0	26.2	28.9	32.0
19	15.9	19.9	22.2	24.2	26.9	29.9
20	14.5	18.2	20.3	22.4	25.0	28.1

Cobalt 60. Source to skin distance 60 cm.

Depth (cm.)	Area of field in square centimetres					
	0	20	50	100	200	400
0.5	100.0	100.0	100.0	100.0	100.0	100.0
1	95.0	96.7	97.1	97.8	97.9	98.1
2	86.0	90.1	91.2	92.2	92.6	93.0
3	77.9	83.7	85.4	86.6	87.4	88.0
4	70.7	77.6	79.7	81.2	82.3	83.2
5	64.2	71.7	74.2	75.9	77.3	78.4
6	58.3	66.1	68.9	70.7	72.4	73.7
7	53.0	60.8	63.7	65.7	67.6	69.2
8	48.2	55.8	58.8	60.9	63.0	65.0
9	43.9	51.2	54.2	56.4	58.6	60.9
10	39.9	46.9	49.9	52.2	54.5	57.1
11	36.3	43.0	46.0	48.3	50.7	53.4
12	33.1	39.4	42.4	44.7	47.2	50.0
13	30.2	36.1	39.1	41.4	44.0	47.0
14	27.5	33.1	36.0	38.3	41.0	44.0
15	25.1	30.4	33.2	35.5	38.2	41.2
16	22.9	27.9	30.6	32.9	35.6	38.6
17	20.9	25.7	28.2	30.5	33.2	36.2
18	19.1	23.7	26.0	28.3	31.0	34.1
19	17.4	21.8	24.0	26.2	28.9	32.0
20	15.9	20.0	22.1	24.2	27.0	30.0

TABLE A-13

Cobalt 60, Source to skin distance 80 cm.

Depth (cm.)	Area of field in square centimetres					
	0	20	50	100	200	400
0.5	100.0	100.0	100.0	100.0	100.0	100.0
1	95.4	97.0	97.7	98.2	98.4	98.5
2	87.1	91.0	92.5	93.4	93.7	94.0
3	79.5	85.3	87.2	88.4	89.0	89.6
4	72.7	79.6	82.0	83.4	84.4	85.2
5	66.5	74.1	76.9	78.5	79.9	80.8
6	60.8	68.9	71.8	73.7	75.2	76.4
7	55.6	63.8	66.8	68.9	70.7	72.1
8	50.9	58.9	62.1	64.2	66.3	68.0
9	46.6	54.3	57.5	59.8	62.1	64.1
10	42.7	50.1	53.3	55.7	58.1	60.3
11	39.2	46.2	49.4	51.8	54.3	56.7
12	35.9	42.6	45.8	48.2	50.8	53.3
13	32.9	39.3	42.4	44.9	47.6	50.1
14	30.2	36.3	39.3	41.8	44.5	47.1
15	27.7	33.5	36.4	38.9	41.8	44.3
16	25.4	31.0	33.8	36.2	39.0	41.7
17	23.3	28.7	31.3	33.8	36.5	39.2
18	21.4	26.5	29.0	31.4	34.2	36.9
19	19.6	24.5	27.0	29.3	32.0	34.7
20	18.0	22.6	25.0	27.3	30.0	32.7

Cobalt 60, Source to skin distance 100 cm.

Depth (cm.)	Area of field in square centimetres					
	0	20	50	100	200	400
0.5	100.0	100.0	100.0	100.0	100.0	100.0
1	95.9	97.2	97.9	98.6	98.8	98.8
2	87.9	91.7	93.0	94.0	94.5	94.6
3	80.7	86.3	88.1	89.4	90.1	90.5
4	73.8	81.0	83.2	84.8	85.7	86.4
5	67.8	75.7	78.4	80.2	81.3	82.3
6	62.3	70.6	73.6	75.6	76.9	78.2
7	57.3	65.7	68.8	71.0	72.5	74.1
8	52.7	61.0	64.2	66.5	68.3	70.1
9	48.5	56.5	59.7	62.1	64.2	66.2
10	44.7	52.3	55.5	57.9	60.3	62.5
11	41.2	48.4	51.6	54.0	56.6	58.8
12	38.0	44.8	48.0	50.4	53.1	55.4
13	35.0	41.5	44.6	47.1	49.8	52.2
14	32.2	38.5	41.5	44.0	46.7	49.2
15	29.6	35.7	38.6	41.1	43.8	46.4
16	27.2	33.1	35.9	38.4	41.1	43.7
17	25.0	30.7	33.4	35.9	38.6	41.2
18	23.0	28.5	31.1	33.6	36.3	38.8
19	21.2	26.4	29.0	31.4	34.1	36.6
20	19.5	24.4	27.0	29.2	32.0	34.5

TABLE A-14
22 Mev. Betatron Radiation with Copper
Compensating Filter

<i>Depth</i>	<i>F.S.D. — 70 cm.</i>	<i>F.S.D. — 100 cm.</i>
0.0	20	19
0.5	51.0	50.0
1.0	71.0	70.0
2.0	92.8	90.1
3.0	99.2	98.0
4.0	100.0	100.0
5.0	98.2	99.5
6.0	93.3	96.6
7.0	89.0	93.0
8.0	84.9	89.1
9.0	81.0	85.3
10.0	77.1	81.9
11.0	73.5	78.5
12.0	70.0	75.5
13.0	66.7	72.5
14.0	63.6	69.6
15.0	60.5	67.0
16.0	57.7	64.2
17.0	55.0	61.6
18.0	52.4	59.1
19.0	49.9	56.8
20.0	47.5	54.5

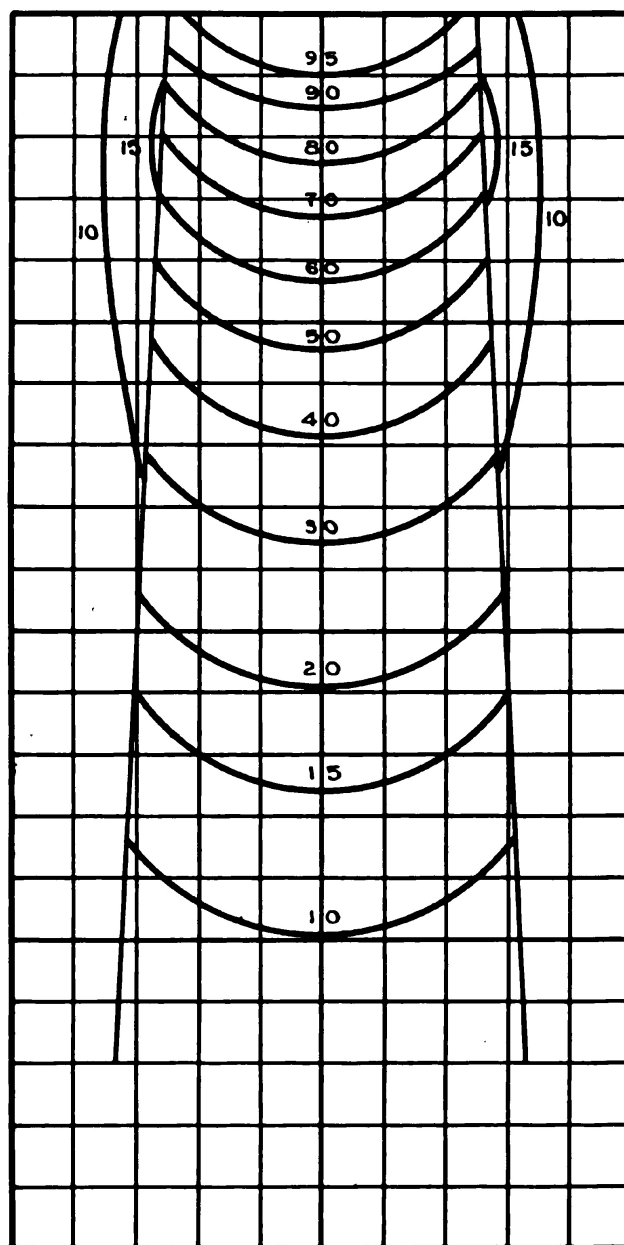


Figure A-1. 5 cm. circular field; 200 K. V.,
F.S.D.: 50 cm. H.V.L. 1.5 mm. Cu.

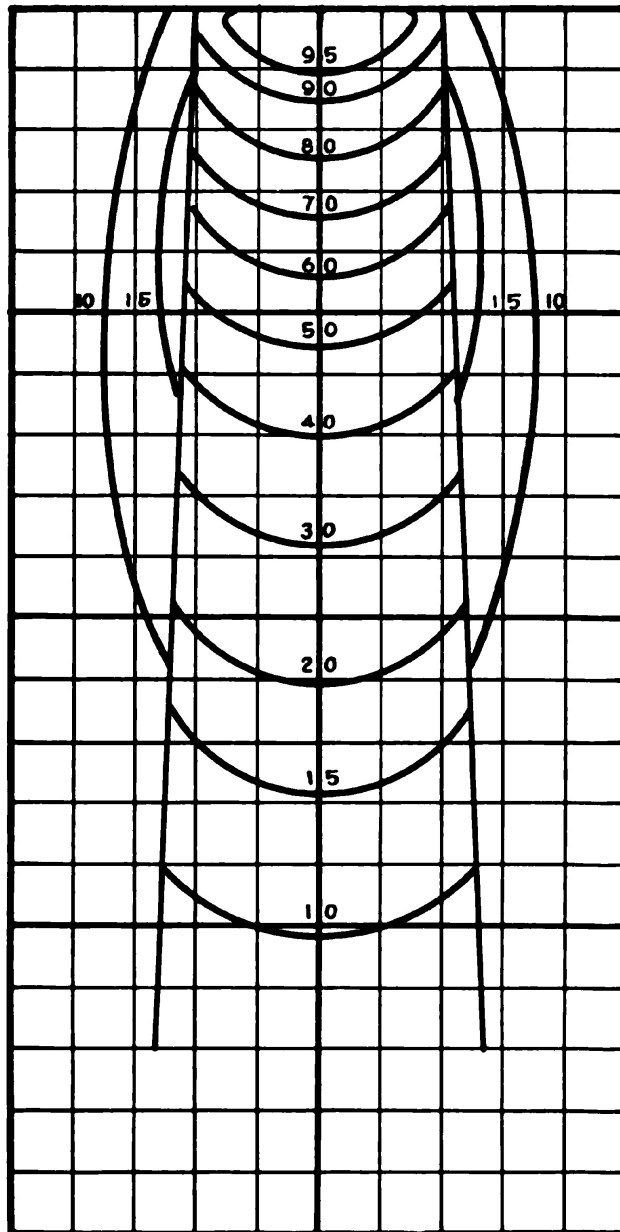


Figure A-2. 4 x 6 cm. rectangular field, short axis; 200 K.V., F.S.D.: 50 cm., H.V.L. 1.5 mm. Cu.

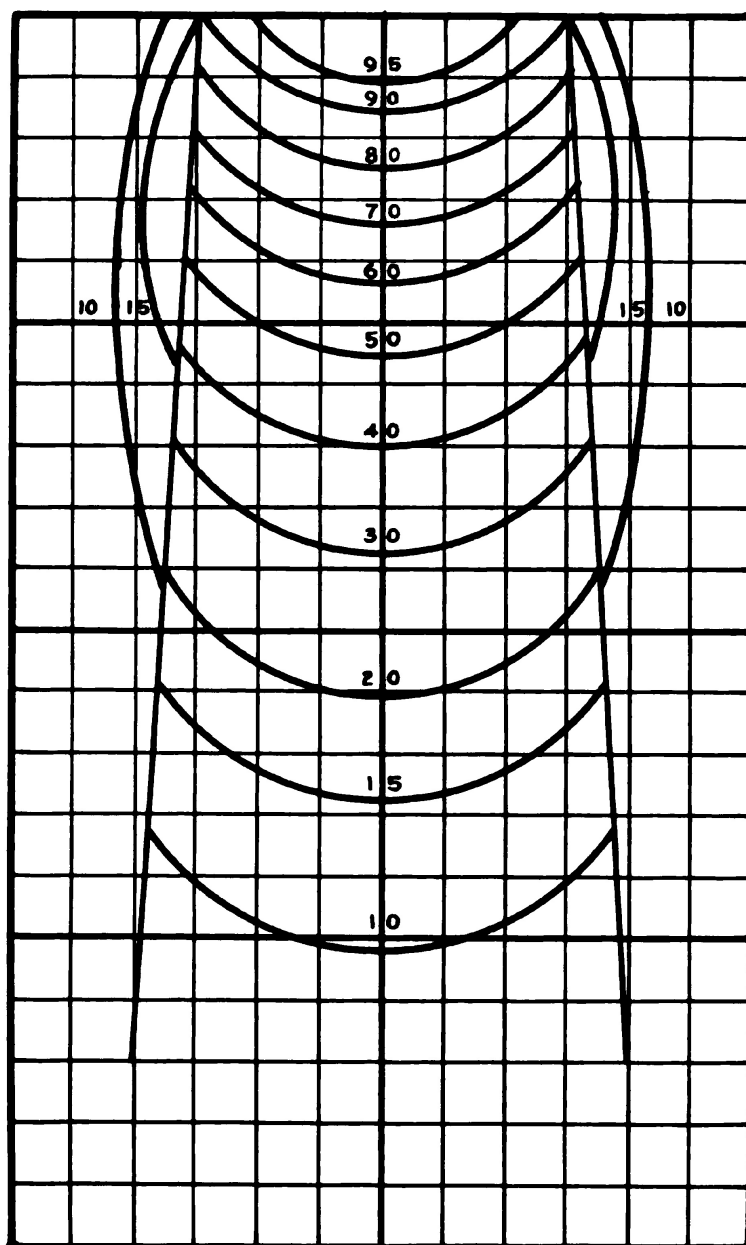


Figure A-3. 6 x 4 cm. rectangular field, long axis; 200 K.V., F.S.D.: 50 cm. H.V.L. 1.5 mm. Cu.

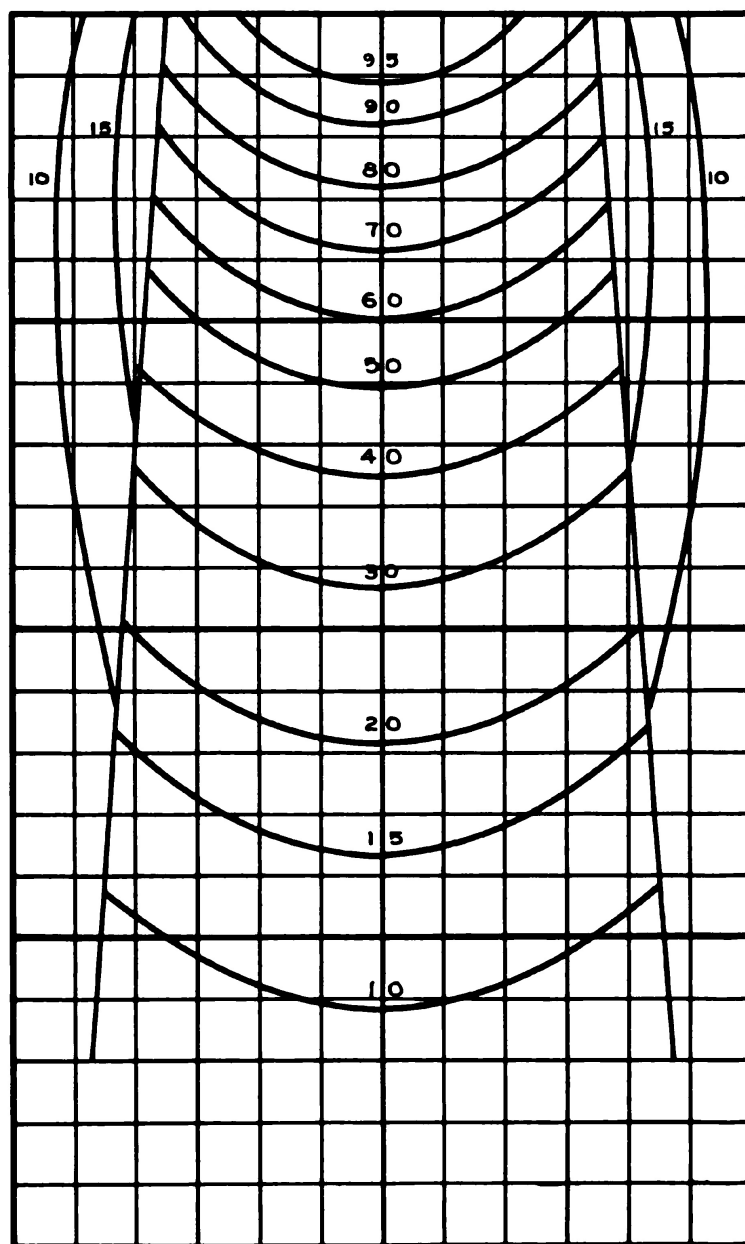


Figure A-4. 7 cm. circular field; 200 K. V., F.S.D.: 50 cm. H.V.L. 1.5 mm. Cu.

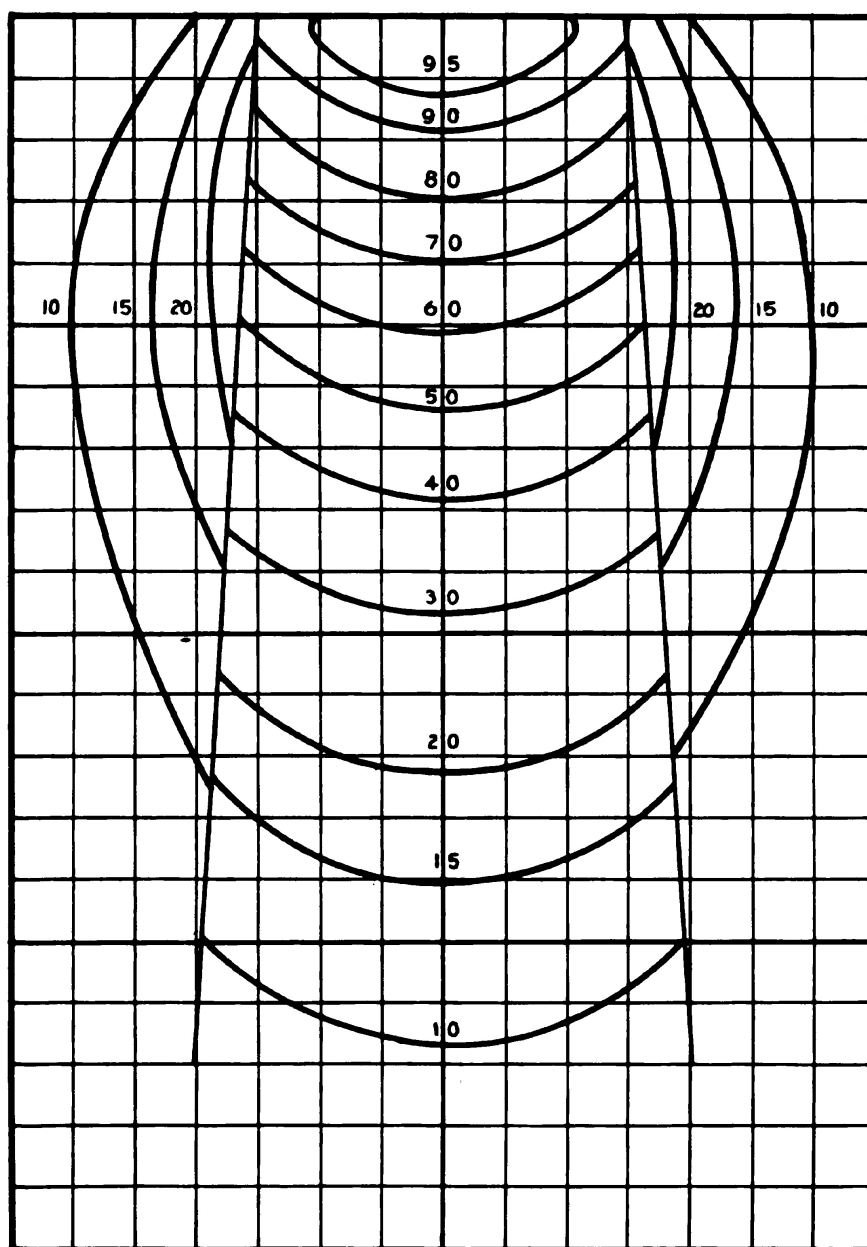


Figure A-5. 6 x 8 cm. rectangular field; short axis; 200 K.V., F.S.D.: 500 cm., H.V.L. 1.5 mm. Cu.

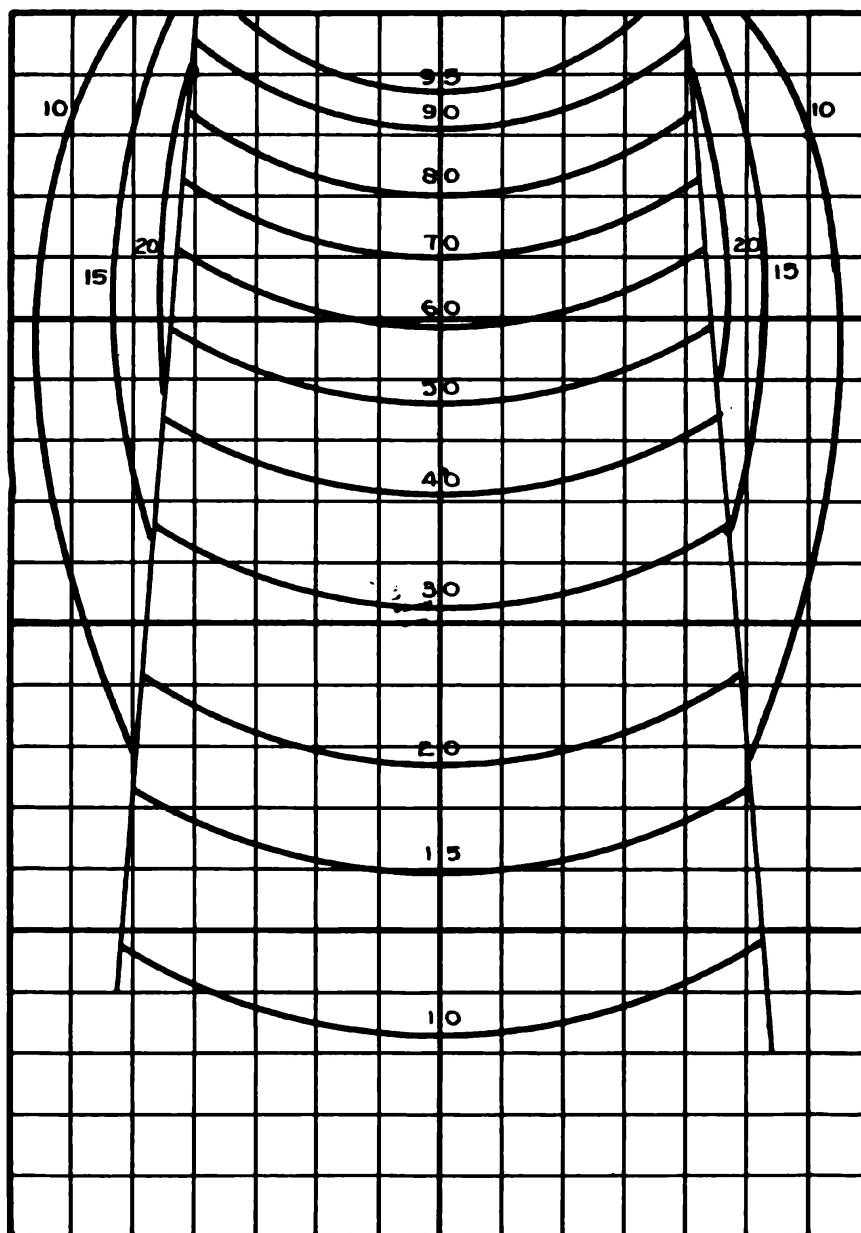


Figure A-6. 8 x 6 rectangular field; long axis; 200 K.V., F.S.D.: 50 cm., H.V.L. 1.5 mm. Cu.

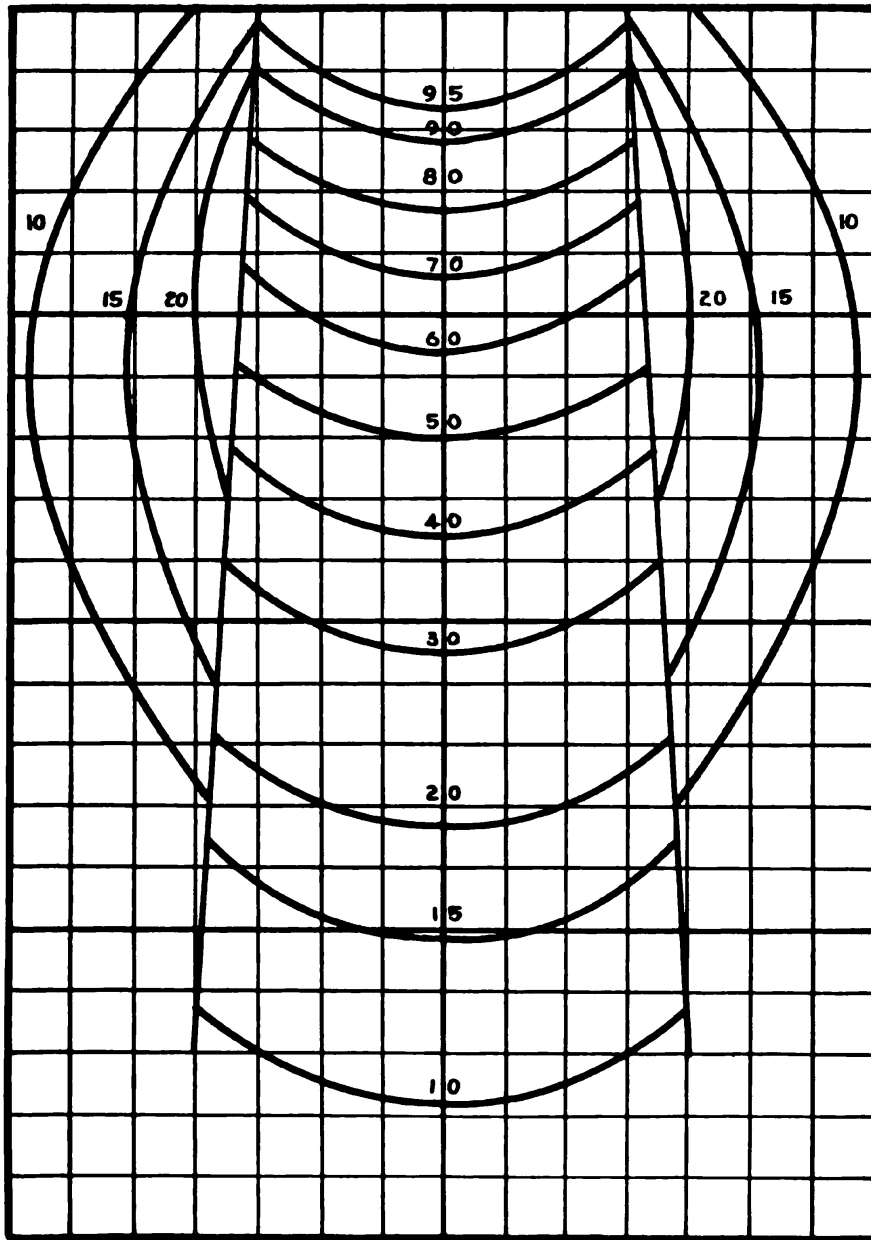


Figure A-7. 6 x 15 cm. rectangular field; short axis; 200 K.V., F.S.D.: 50 cm., H.V.L. 1.5 mm. Cu.

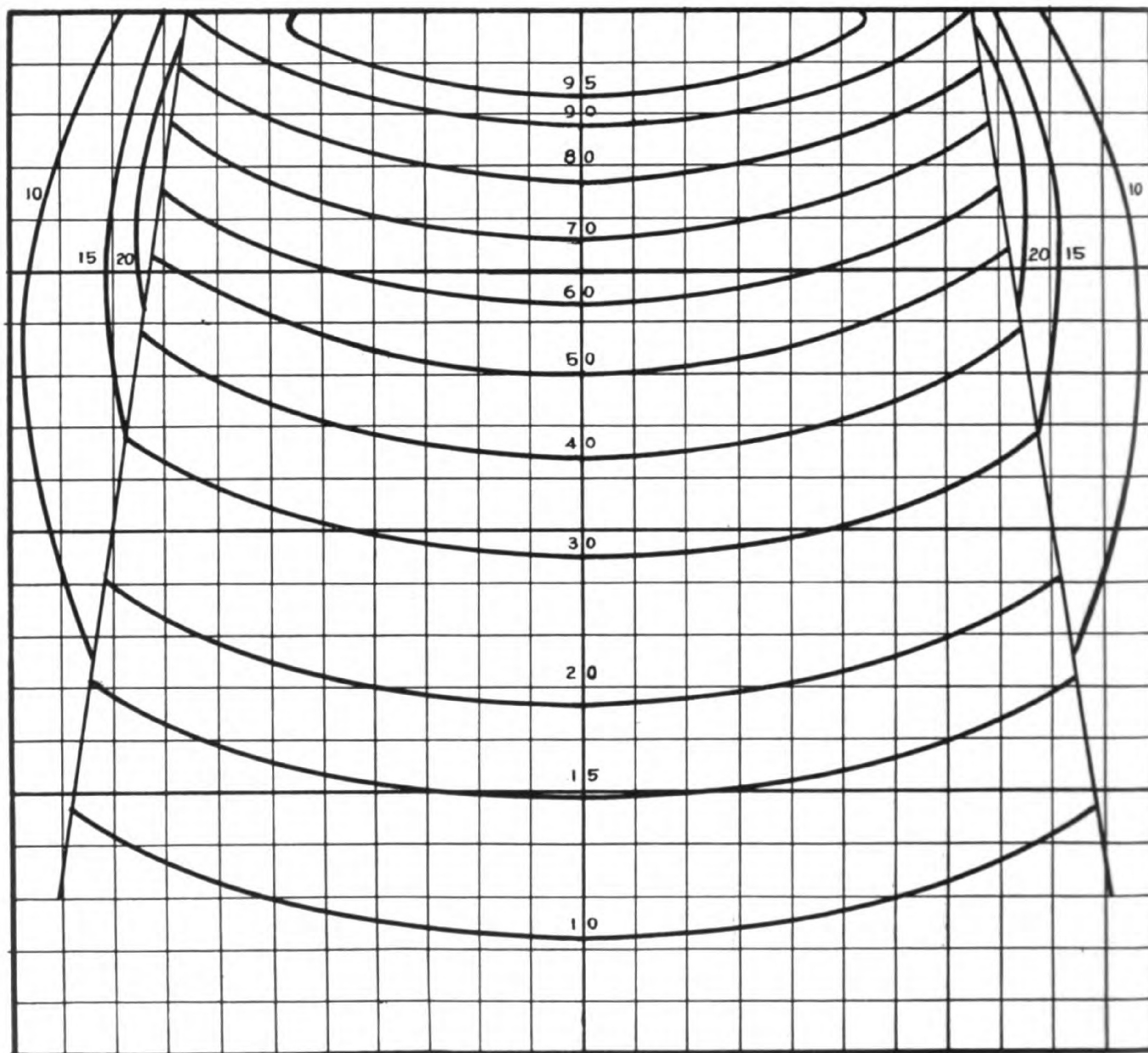


Figure A-8. 15 x 6 cm. rectangular field; long axis; 200 K.V., F.S.D.: 50 cm., H.V.L. 1.5 mm. Cu.

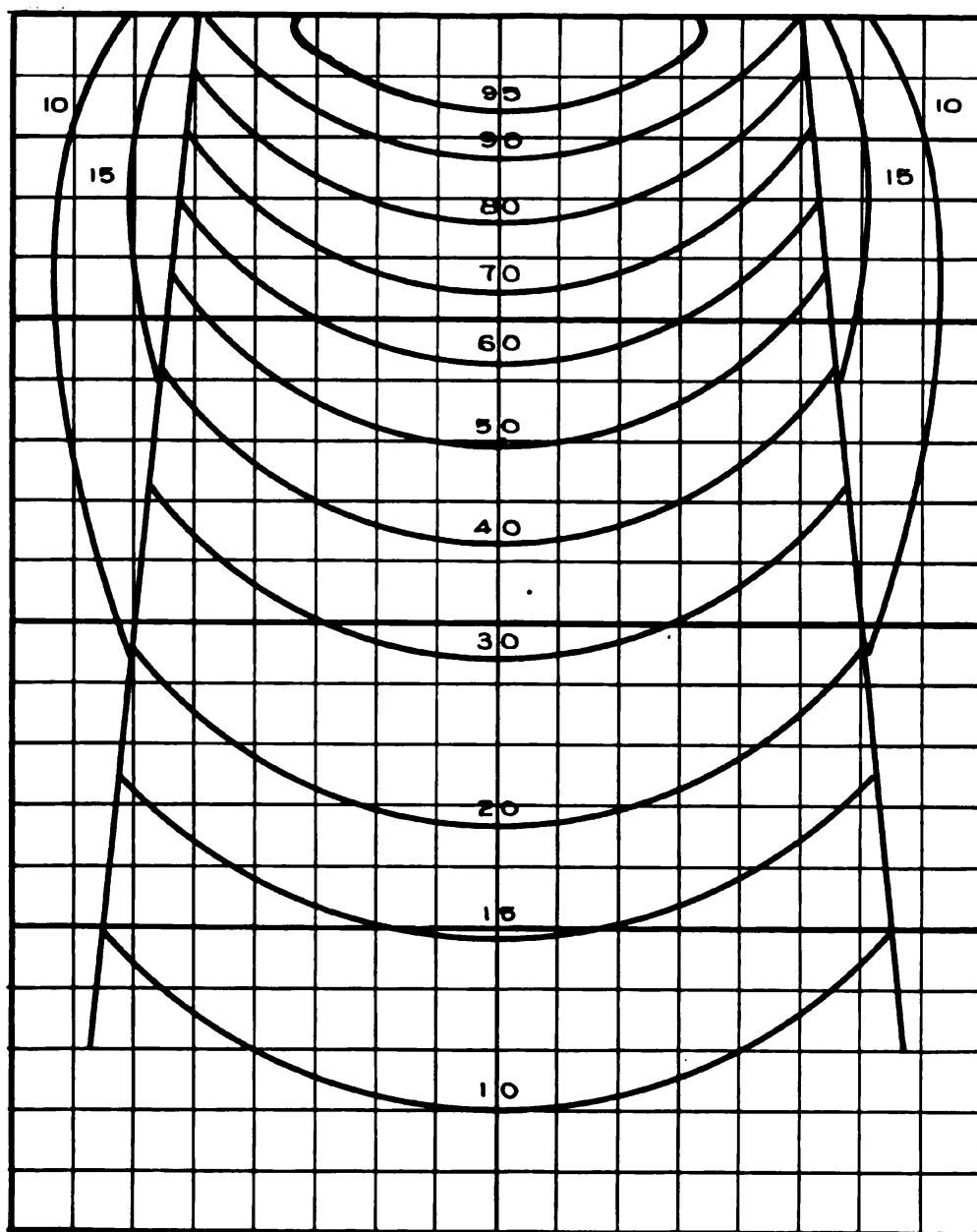


Figure A-9. 10 cm. circular field; 200 K.V., F.S.D.: 50 cm., H.V.L. 1.5 mm. Cu.

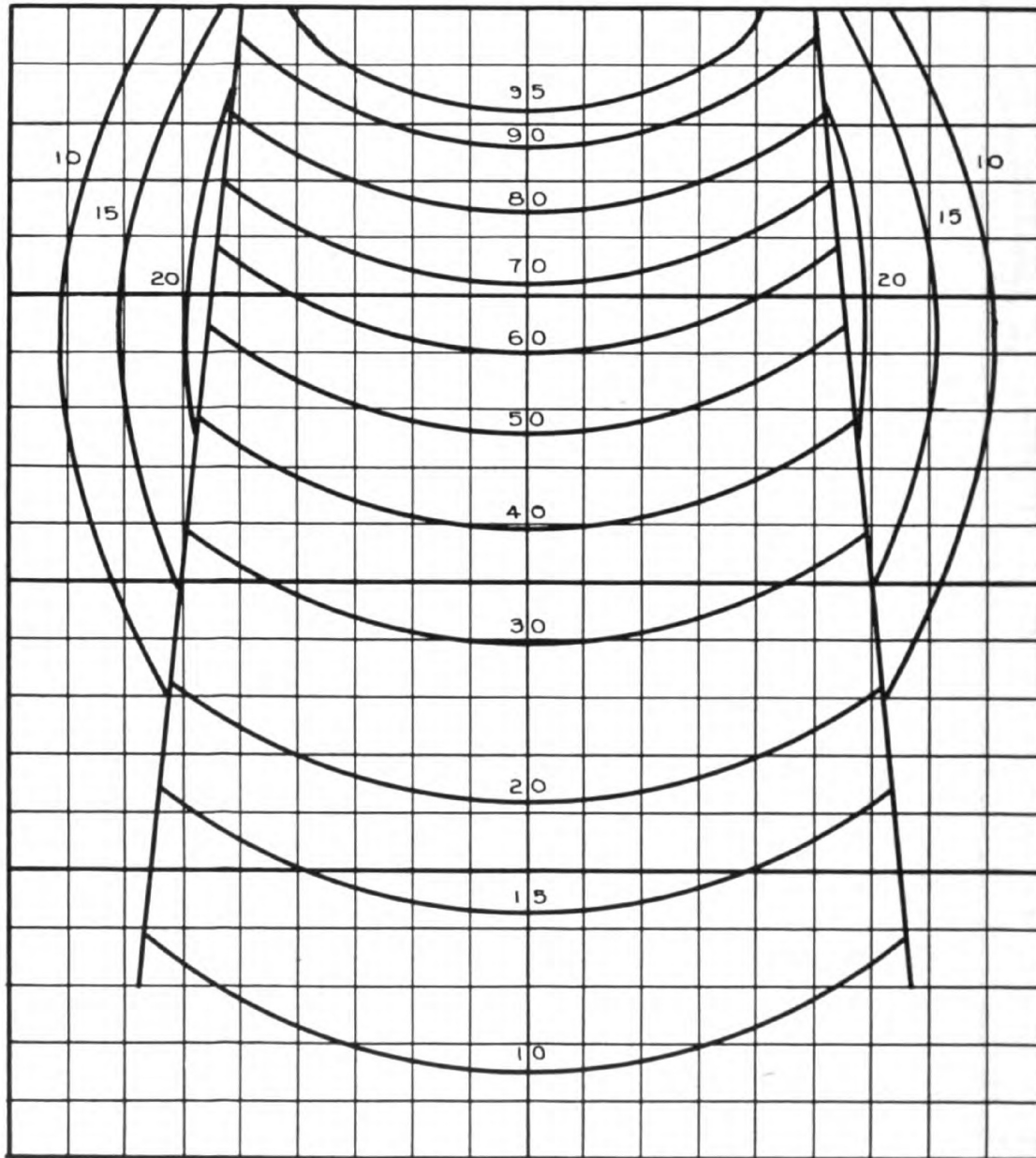


Figure A-10. 10 x 10 square field; 200 K.V., F.S.D.: 50 cm. H.V.L. 1.5 mm. Cu.

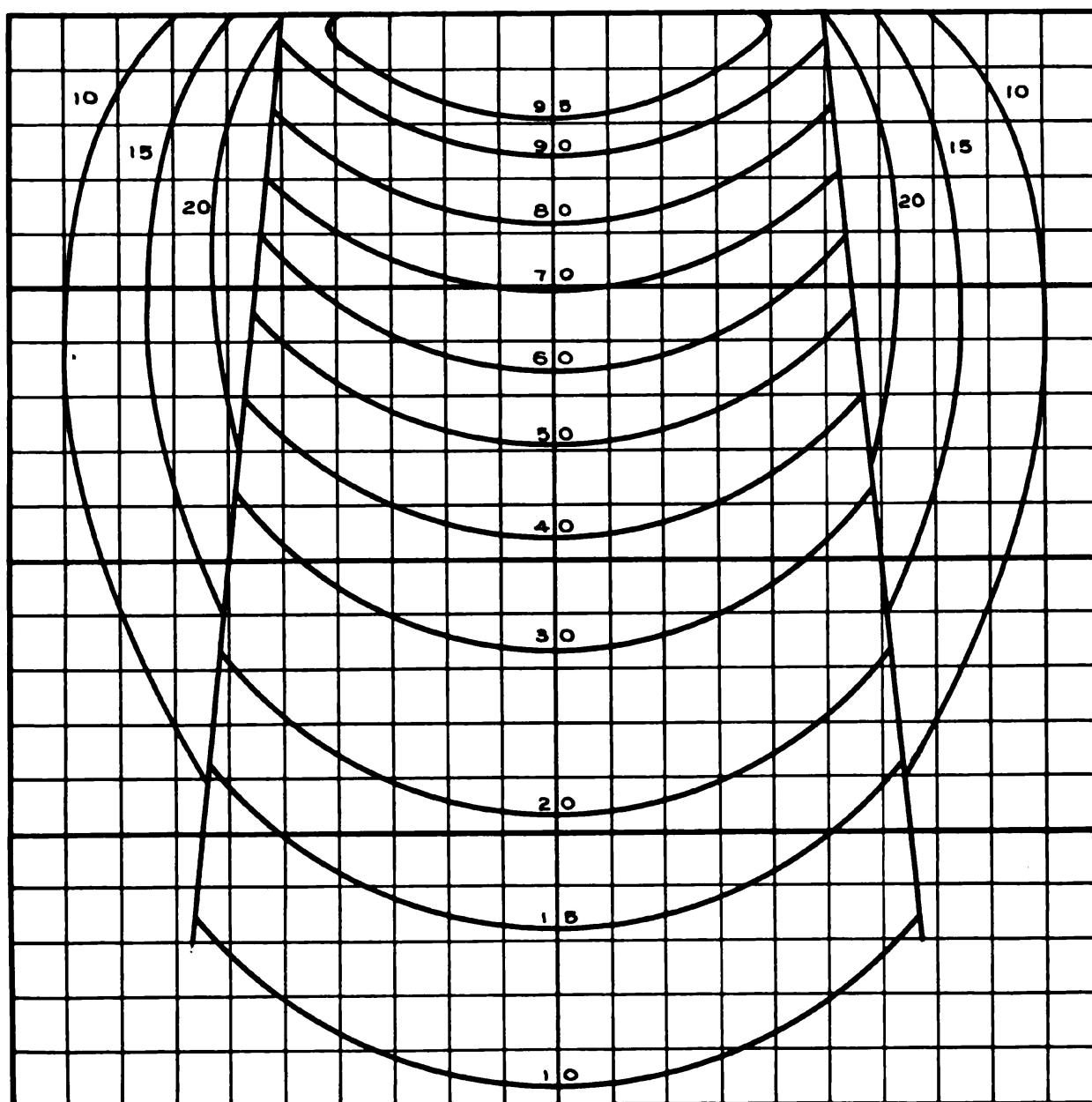


Figure A-11. 10 x 15 rectangular field; short axis; 200 K.V., F.S.D.: 50 cm., H.V.L. 1.5 mm. Cu.

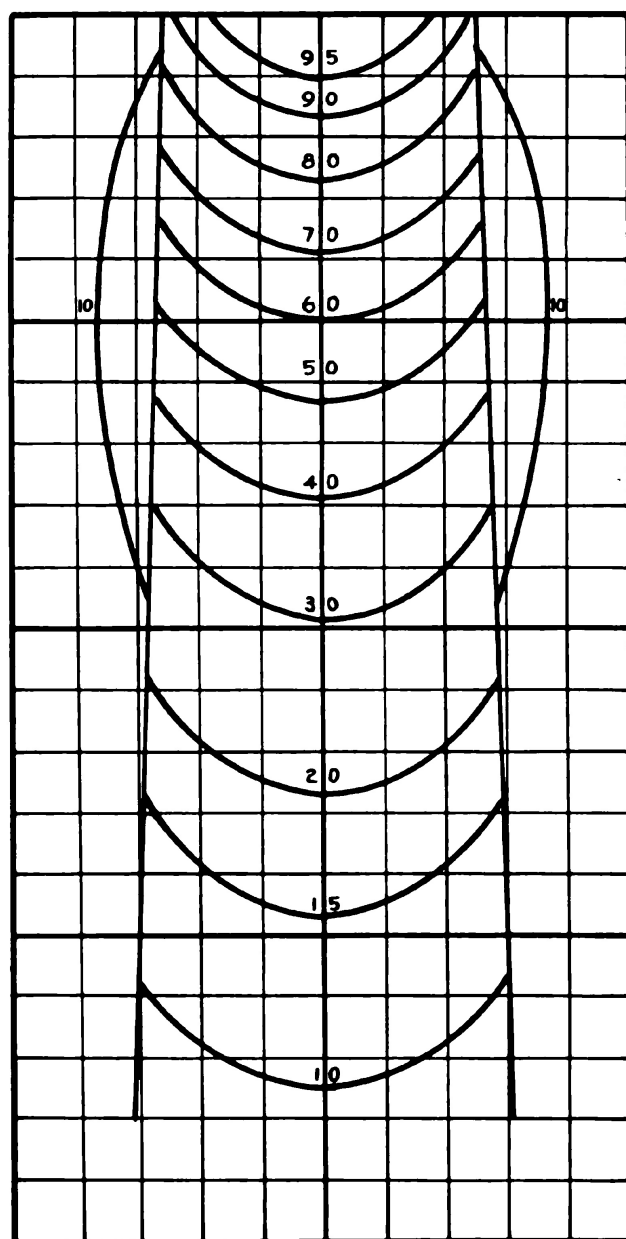


Figure A-12. 5 cm. circular field; 400 K.V.P.,
F.S.D.: 80 cm., H.V.L. 4.0 mm. Cu.

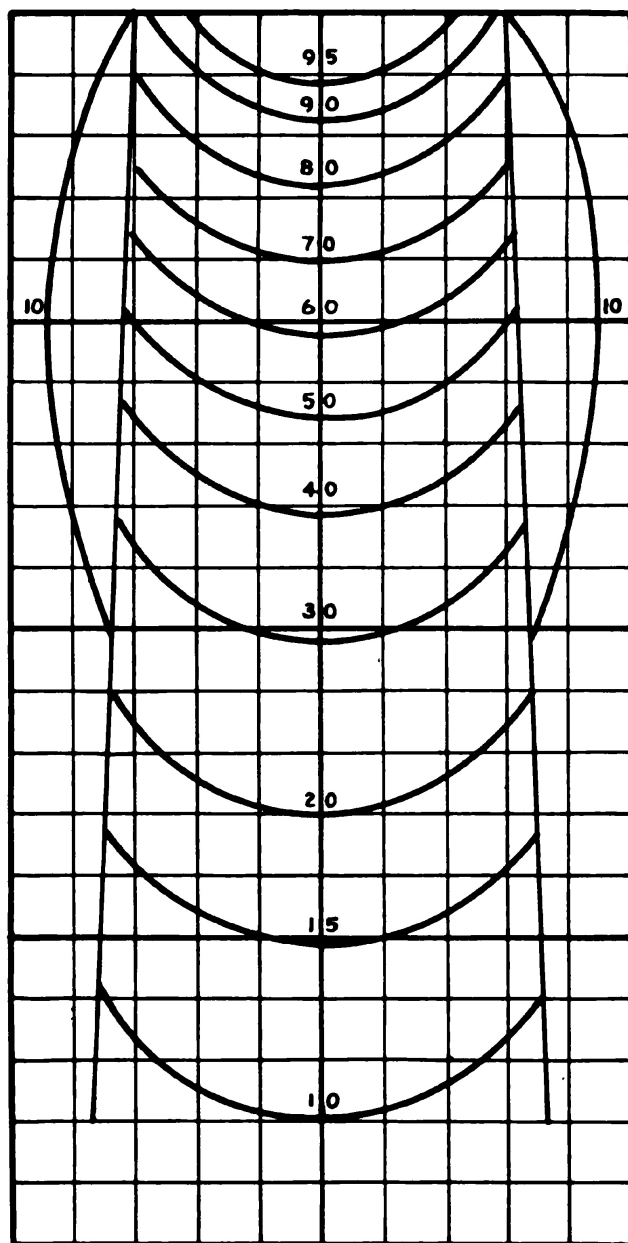


Figure A-13. 6 cm. circular field; 400 K.V.P.,
F.S.D.: 80 cm., H.V.L. 4.0 mm. Cu.

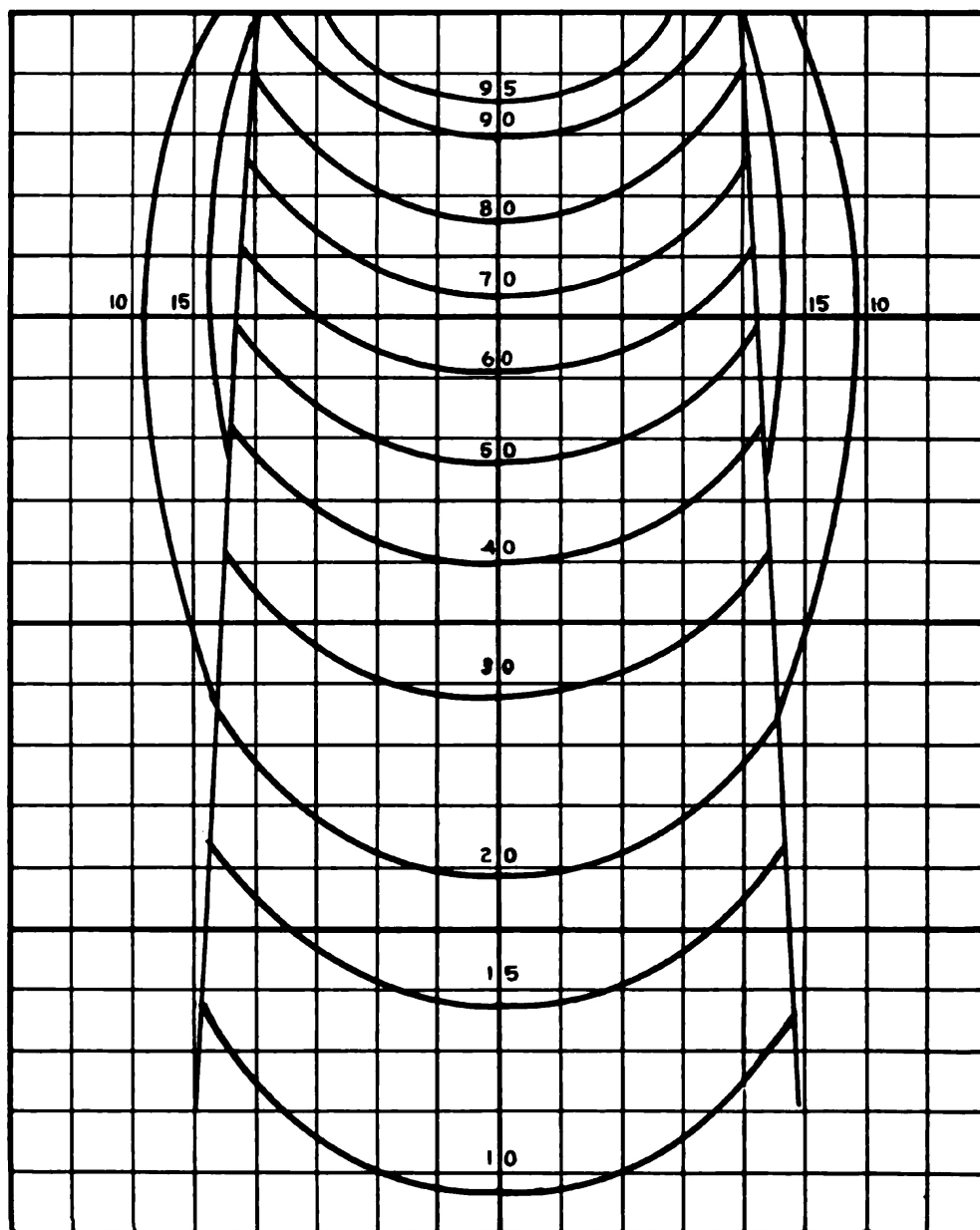


Figure A-14. 8 cm. circular field; 400 K.V.P., F.S.D.: 80 cm., H.V.L. 4.0 mm. Cu.

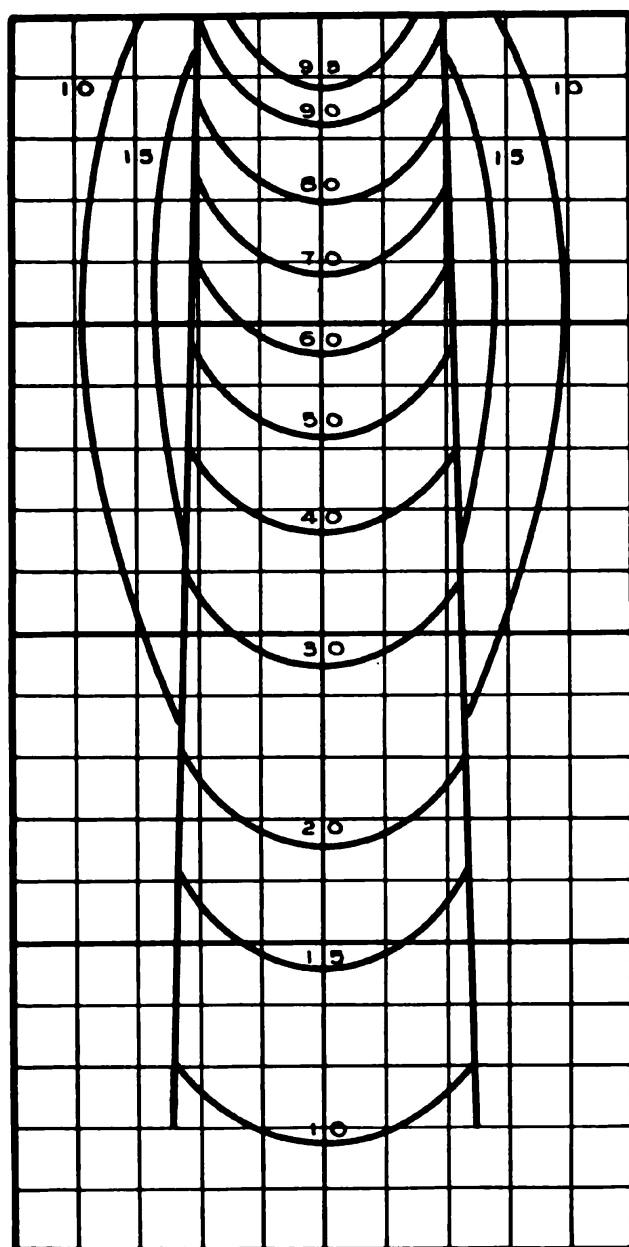


Figure A-15. 4 x 10 cm. rectangular field; short axis; 400 K.V.P., F.S.D.: 80 cm., H.V.L. 4.0 mm. Cu.

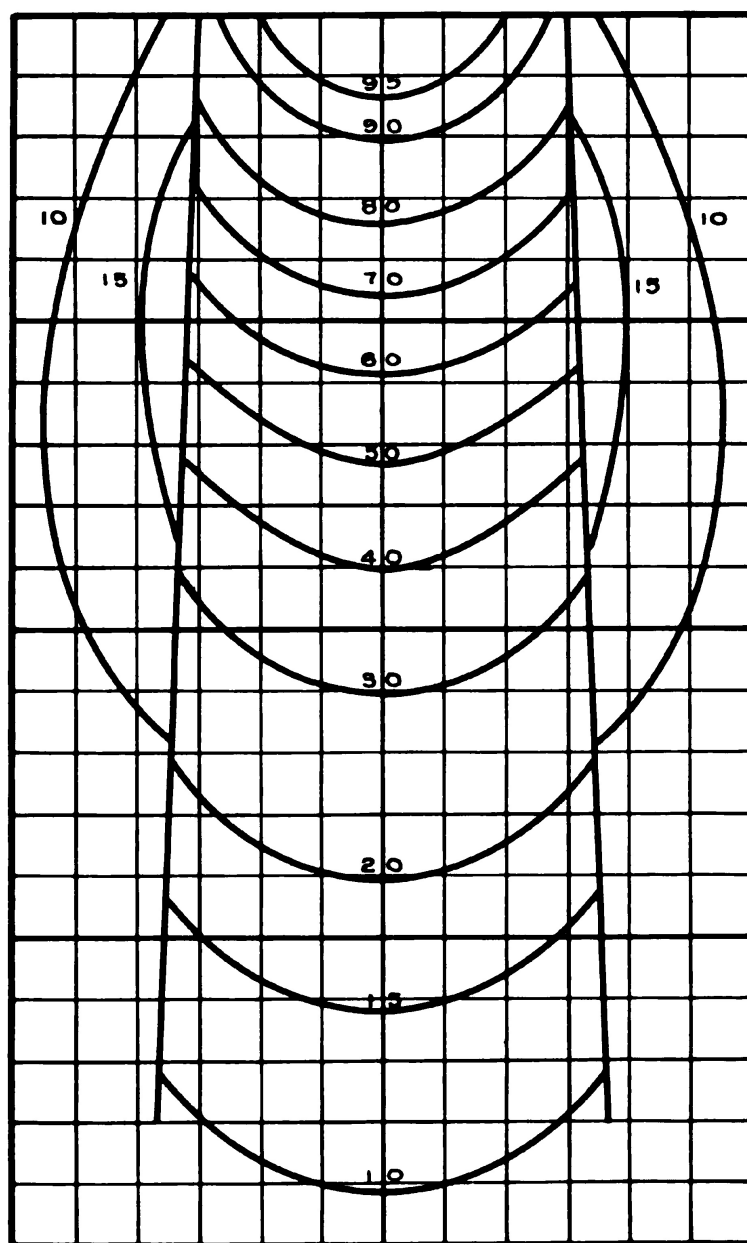


Figure A-16. 6 x 8 cm. rectangular field; short axis; 400 K.V.P., F.S.D.: 80 cm., H.V.L. 4.0 mm. Cu.

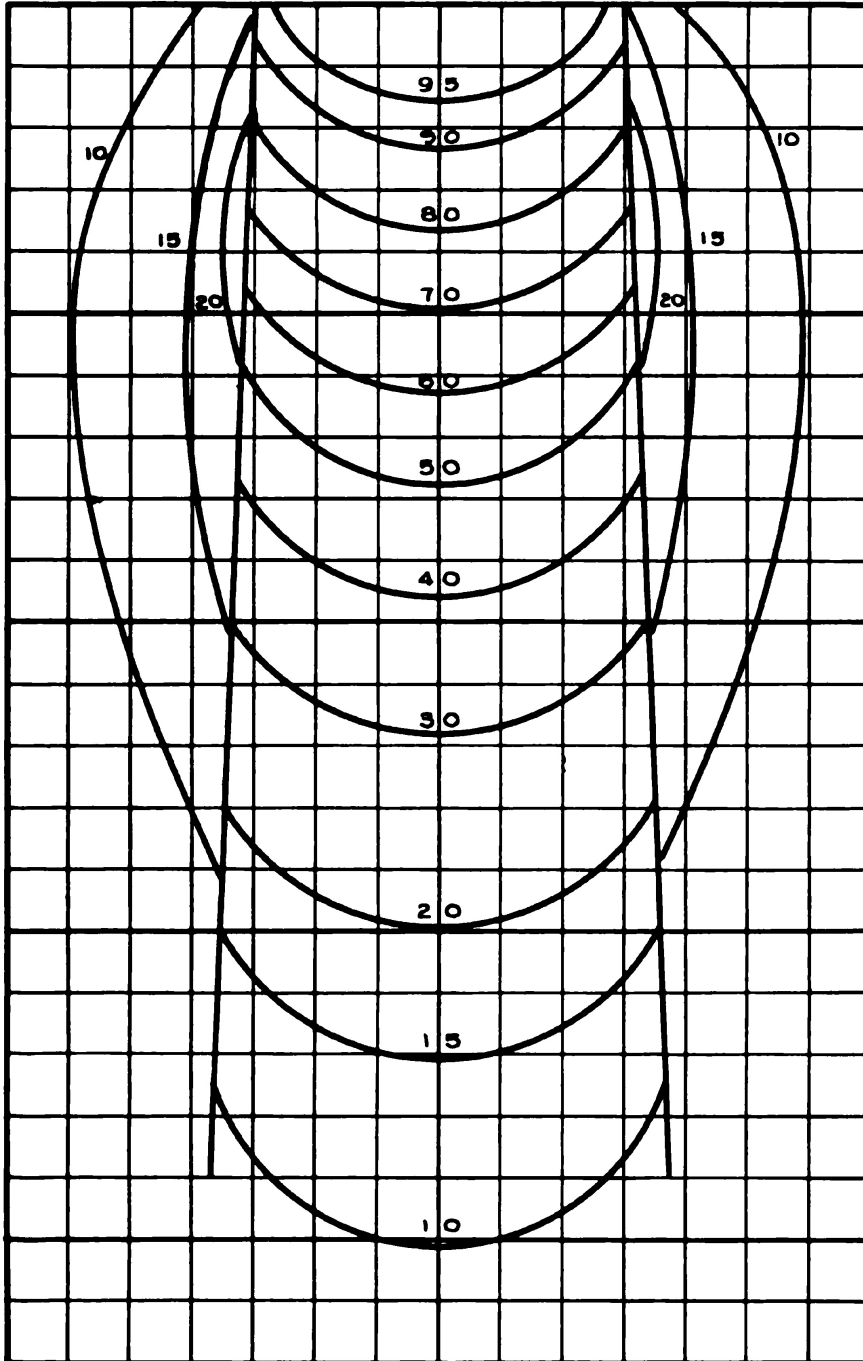


Figure A-17. 6 x 15 cm. rectangular field; short axis; 400 K.V.P., F.S.D.: 80 cm., H.V.L. 4.0 mm. Cu.

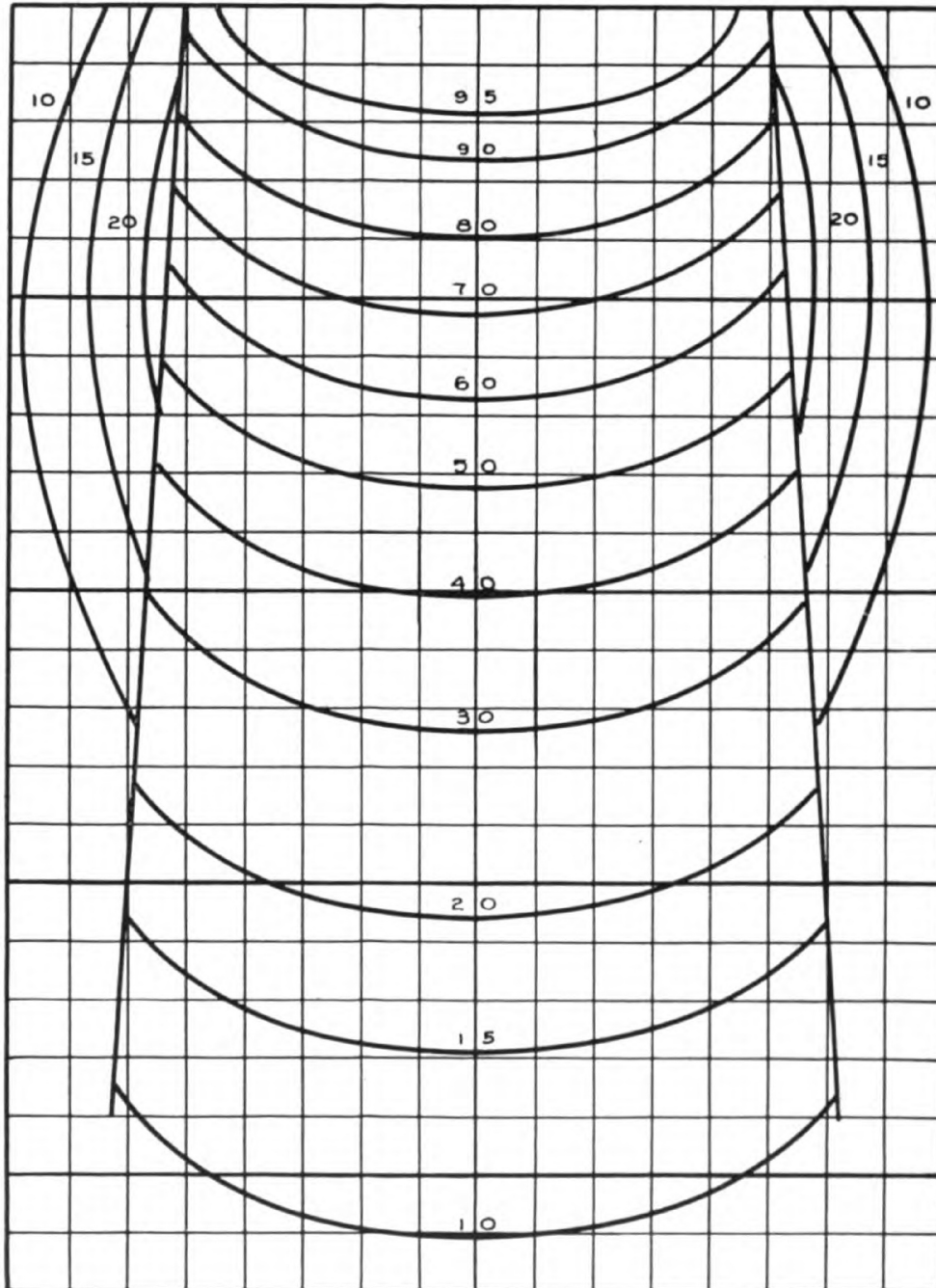


Figure A-18. 10 x 10 square field; 400 K.V.P., F.S.D.: 80 cm., H.V.L. 4.0 mm. Cu.

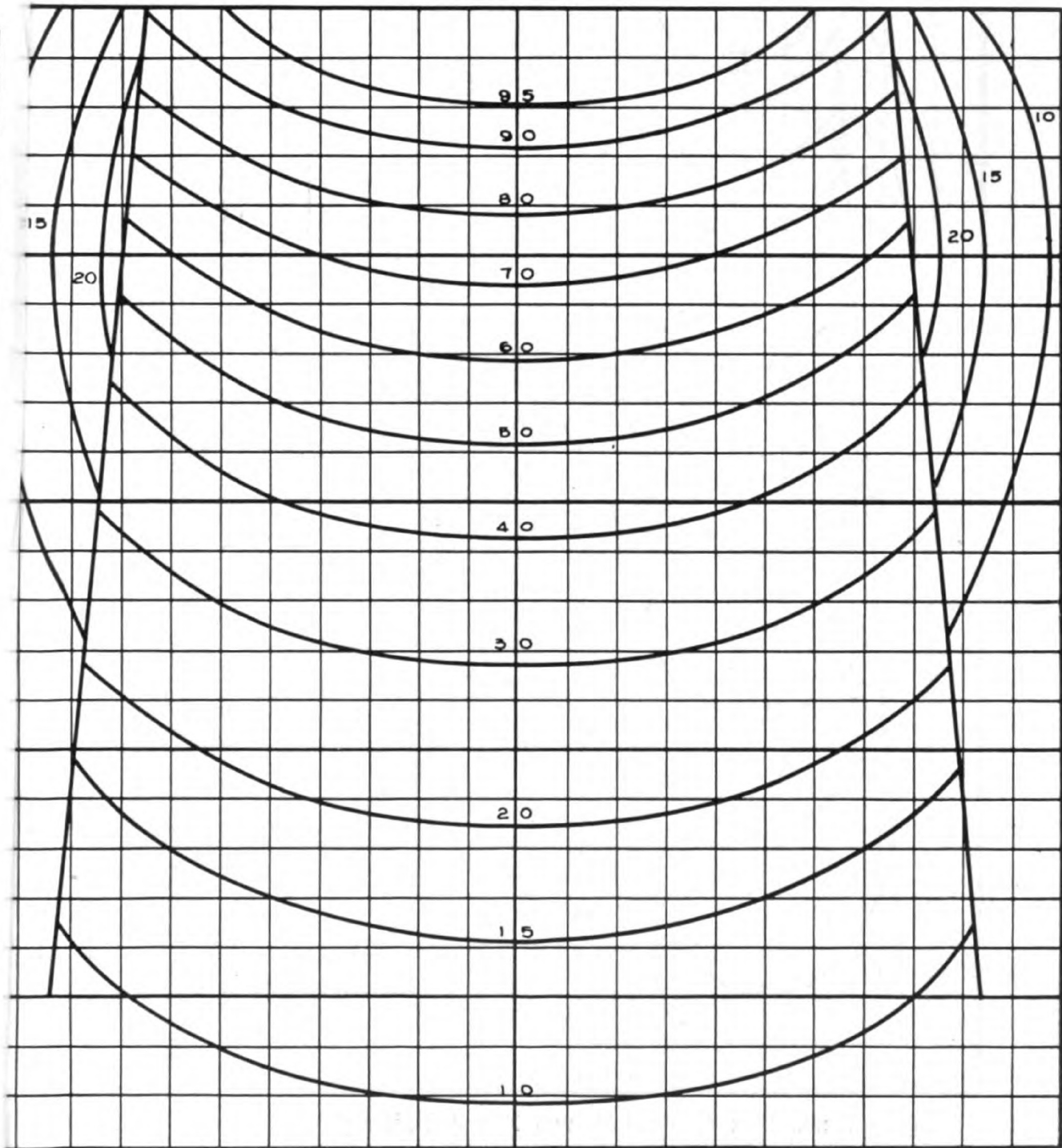


Figure A-19. 15 x 10 cm. rectangular field; long axis; 400 K.V.P., F.S.D.: 80 cm., H.V.L. 4.0 mm. Cu.

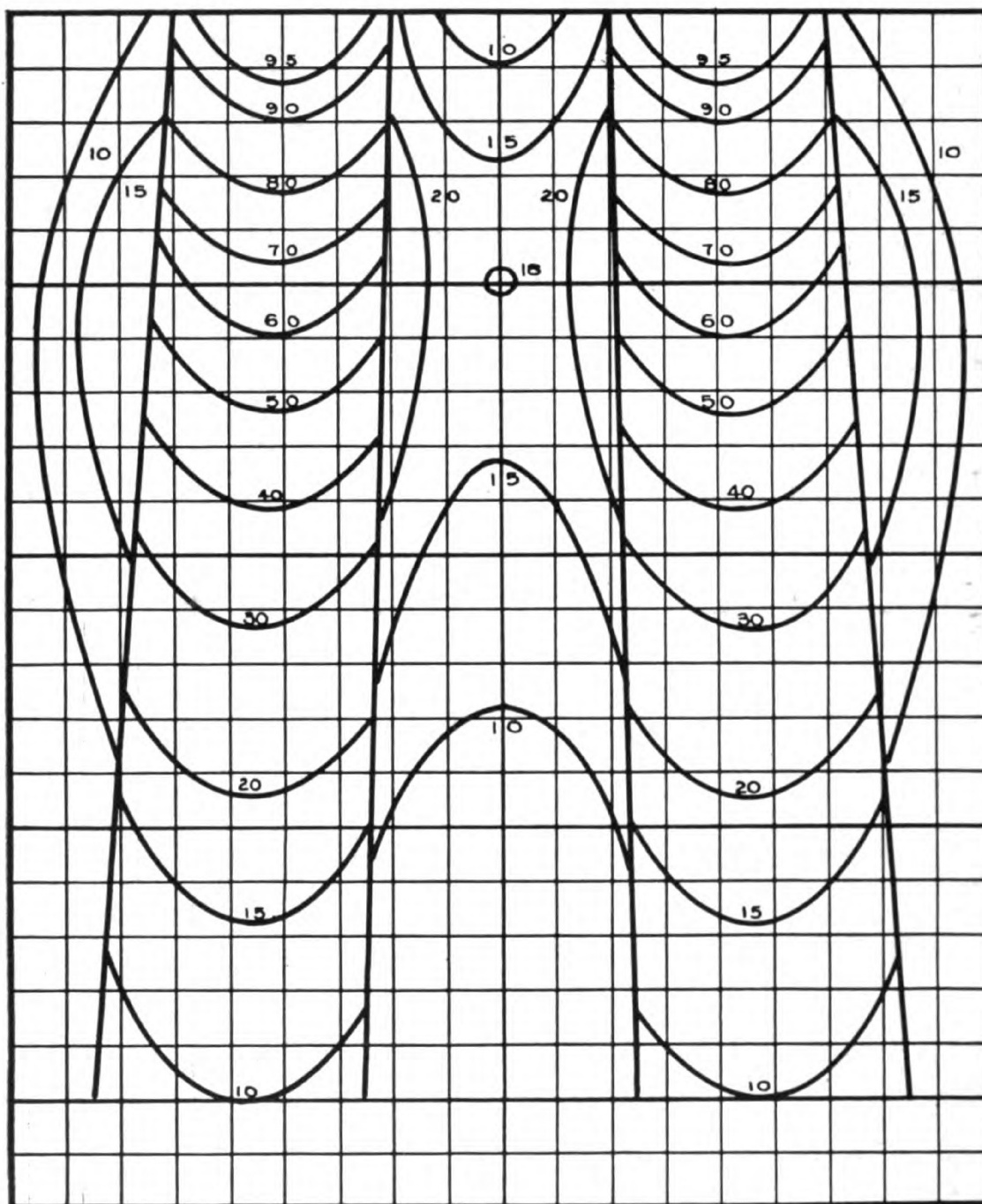


Figure A-20. 10 x 4 split field, two 10 x 4 fields separated by a 4 cm. gap. 400 K.V.P., F.S.D.: 80 cm., H.V.L. 4.0 mm. Cu. Such a composite field is useful in treating the parametria after radium has been placed in the uterus and vagina (see Section 10.11).

Appendix B

SPECTRAL DISTRIBUTIONS

The spectral distribution of an x-ray beam may be determined by a method discussed by Greening⁽¹⁾. This method involves an accurate determination of the absorption of the x-ray beam by standard absorbers such as Al., Cu. or Sn. The resulting transmission curve can be analyzed to yield a spectral distribution. This has been done for (a) 200 K.V.P., H.V.L. 1.8 mm. Cu. (b) 250 K.V.P., H.V.L. 2.6 mm. Cu. and (c) 400 K.V.P., H.V.L. 4.0 mm. Cu. The author is

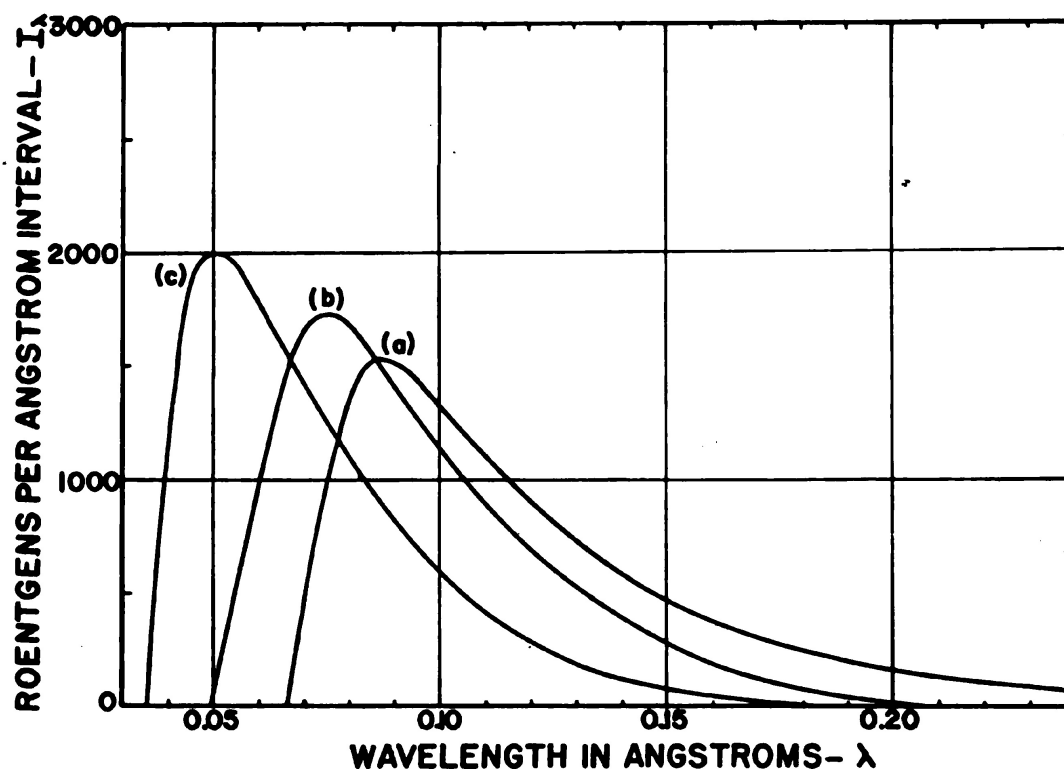


Figure B-1. Graph giving the dose in roentgens per angstrom interval for three radiations - (a) 200 K.V.P., H.V.L. - 1.8 mm. Cu.; (b) 250 K.V.P., H.V.L. - 2.6 mm. Cu.; (c) 400 K.V.P., H.V.L. - 4.0 mm. Cu. The graphs all correspond to a dose of 100 roentgens and give the distribution of this dose at the different wavelengths. For example, for curve (c) (400 K.V.P.) the maximum dose is produced by a wave length of 0.05 Å. For curve (a) (200 K.V.P.) the maximum dose is delivered by photons of wavelength 0.09 Å.

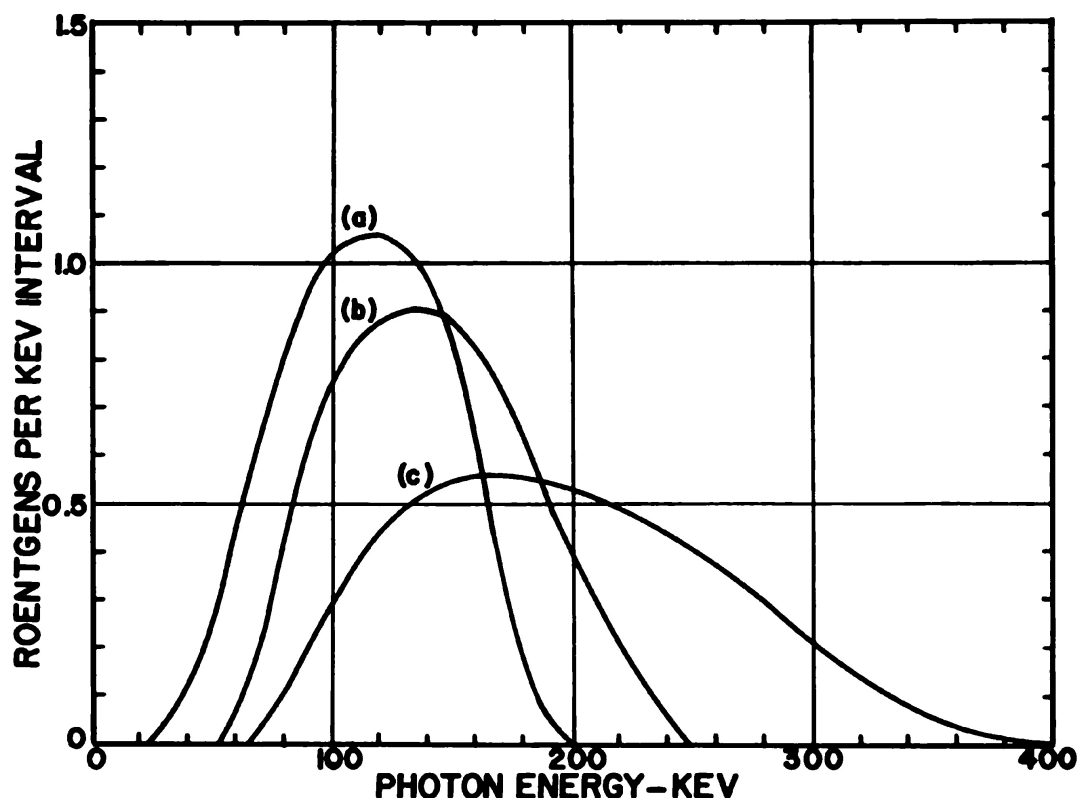


Figure B-2. Graph giving the dose in roentgens per Kev. interval for three radiations, (a) 200 K.V.P., H.V.L. — 1.8 mm. Cu.; (b) 250 K.V.P., H.V.L. — 2.6 mm. Cu.; (c) 400 K.V.P., H.V.L. — 4.0 mm Cu. It is seen that for 200 K.V.P. (Curve a) most of the dose is produced by photons in the interval 90 to 160 K.V. For 400 K.V.P. (Curve c) photons in the interval 100 to 300 K.V. produce most of the dose. The area under each of the curves corresponds to a dose of 100 roentgens.

indebted to Mr. D. V. Cormack, graduate student of the Physics Department of the University of Saskatchewan, for the calculations on distributions "a" and "c," and to Mr. J. Dresner, Physicist at the Hospital for Joint Diseases, New York, for the measurements and calculations of distribution "b."

Spectral distributions may be presented in a number of different forms. In Figure B-1, the dose in roentgens in each angstrom interval is given for (a), (b) and (c). The areas under these curves have been adjusted to give 100 r. For example, curve (a) has a mean height of about 500 and the wave-length interval is about 0.2 Å, giving an areas of $500 (0.2) = 100$. The short wave-length limit is fixed by the maximum energy applied to the x-ray machine.

The spectral distribution of Figure B-1 may be altered to give the number of roentgens in each Kev. interval. The results are shown

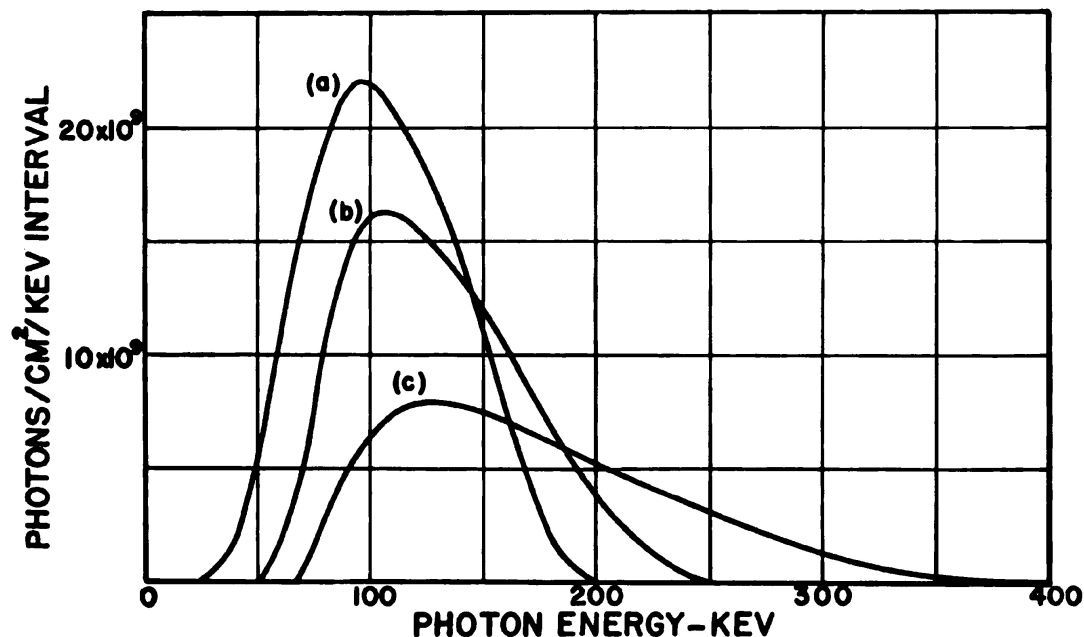


Figure B-3. Graph showing the number of photons per cm^2 in each Kev. interval for three radiations — (a) 200 K.V.P., H.V.L. — 1.8 mm. Cu.; (b) 250 K.V.P., H.V.L. — 2.6 mm. Cu.; (c) 400 K.V.P., H.V.L. — 4.0 mm. Cu. The graph shows the number of photons of each energy which cross a square centimeter perpendicular to the beam. All three curves correspond to a dose of 100 roentgens but the areas under the curves are not all equal since photons of different energy are not all equally efficient in producing a dose measured in roentgens.

in Figure B-2. Finally in Figure B-3 appear the same distributions plotted as a number of photons per cm^2 per Kev. interval. It should be emphasized that each of the three methods of presenting the spectral distributions give the same fundamental information, but in a different way. All curves have been normalized to correspond to a dose of 100 r.

From a knowledge of the spectral distributions given in Figure B-3, it is possible to determine the number of photoelectrons and Compton electrons liberated in 1 cm^3 of water. These calculations have been carried out and the results are given in Table B-1 for the three qualities of radiation. It is immediately apparent that there are a very large number of low energy electrons set into motion, when these radiations interact with water. Table B-1 may be of value in radiobiological investigations.

(1) Greening, J. R.: *Brit. J. Radiol.*, 22:71, 1947.

TABLE B-1

Number of electrons set in motion per 100 r. per cm.³ of water by radiations with H.V.L. 1.8 mm. of Cu. (200 K.V.); 2.6 mm. of Cu. (250 K.V.) and 4.0 mm. of Cu. (400 K.V.). The table gives the number of electrons in each energy interval. For example, for H.V.L. 1.8 mm. Cu. we see that there are 58×10^8 electrons set in motion per cm.³ of water with energies in the interval 45 to 50 Kv.

<i>Electron Energy Interval</i>	<i>H.V.L. = 1.8</i>	<i>H.V.L. = 2.6</i>	<i>H.V.L. = 4.0</i>
<i>Kv.</i>			
0 — 5	800 x 10 ⁸	475 x 10 ⁸	233 x 10 ⁸
5 — 10	655	410	202
10 — 15	505	343	175
15 — 20	373	281	151
20 — 25	271	230	130
25 — 30	201	185	113
30 — 35	147	147	97
35 — 40	108	119	84
40 — 45	79	96	73
45 — 50	58	76	63
50 — 55	43	60	54
55 — 60	31	48	47
60 — 65	23	38	41
65 — 70	17	30	35
70 — 75	13	24	31
75 — 80	9.6	19	28
80 — 85	8.0	15.3	24
85 — 90	7.0	12.1	22
90 — 95	6.0	9.5	19
95 — 100	5.1	7.4	16.4
100 — 105	4.3	5.6	14.2
105 — 110	3.6	4.2	12.2
110 — 115	3.0	3.0	10.5
115 — 120	2.5	2.3	8.9
120 — 125	2.1	1.8	7.6
125 — 130	1.7	1.5	6.4
130 — 135		1.3	5.3
135 — 140		1.1	4.3
140 — 145			3.4
145 — 150			2.7
150 — 155			2.0
155 — 160			1.7
160 — 165			1.4
165 — 170			1.2
170 — 175			1.0

AUTHOR INDEX

A

Adams, G. D., 34, 84, 213
Aebersold, P. C., 195, 213
Agnew, H. M., 164
Allen-Williams, D. J., 56
Allison, S. K., 44, 56
Almy, G. M., 34, 84, 213
Appleyard, R. K., 44, 56
Atlee, Z. J., 34

B

Behnken, H., 73
Bell, H. G., 229
Bierbaum, O. S., 229
Blomfield, G. W., 191, 192
Braestrup, C. B., 213, 233
Buckingham, R. A., 56
Burkell, C. C., 129, 147

C

Charlton, E. E., 213
Clarkson, J. R., 81, 82, 83, 84, 126, 129, 135, 148
Cloud, R. W., 109, 213
Compton, A. H., 35, 42, 43, 44, 46, 47, 48, 49, 50, 52, 53, 54, 55, 56, 66, 81, 137, 141
Coolidge, W. D., 34
Cormack, D. V., 276
Cosman, B. J., 109

D

Dancoff, S. M., 34, 84, 213
Darby, E. K., 34, 84, 109, 129, 147, 213
Davisson, C. M., 44, 56
Dempster, L. E., 213
Dobbie, J. L., 129
Dresner, J., 276
Dresser, R., 109

E

Einstein, A., 195
Ellis, F., 129
Epp, E. R., 233
Evans, R. D., 214, 226, 228

F

Failla, G., 73, 109, 192
Farmer, F. T., 73, 109
Fedoruk, S. O., 233
Flanders, P. H., 129
Fowler, R. H., 56

Fricke, H., 73

Friedlander, G., 218, 229

G

Glasser, O., 73
Gray, L. H., 67, 73
Green, A., 129
Greening, J. R., 275
Grimmett, L. G., 129

H

Hahn, O., 202
Hall, B. E., 221, 229
Hamilton, J. J. S., 109
Hanson, A. O., 34, 84, 213
Happey, F., 109
Harrington, E. L., 34, 84, 109, 164, 213
Haslam, R. N. H., 34, 84, 109, 213
Hay, G. A., 109
Heitler, W., 44, 56
Herbert, R. J. T., 109
Honerjager, R., 32, 33, 34
Honeyburne, J., 129
Hulme, H. R., 44, 56

J

Johns, H. E., 34, 84, 94, 95, 97, 109, 124, 129, 147, 164, 192, 213
Jones, D. E. A., 90, 93, 109, 192

K

Katz, L., 34, 84, 109, 213
Kernp, L. A. W., 109
Kerst, D. W., 34, 84, 213
Klumpar, J., 109
Koch, H. W., 34, 84, 213
Kornelson, R. O., 233
Kulenkampff, H., 28, 29, 34

L

Lamerton, L. F., 84, 89, 92, 98, 105, 109, 129, 233
Lanzl, E. F., 213
Lanzl, L. H., 34, 84, 213
Laughlin, J. S., 34, 84, 213
Lawrence G. C., 109, 148,
Lawrence, J. H., 195, 213
Layne, D. A., 229
Lea, D. E., 44, 56
Low-Beer, B. V. A., 221, 229

M

Mabbs, D. V., 90, 109
Marinelli, L. D., 192

Martin, J. H., 229

Mayneord, W. V., 64, 65, 66, 73, 80, 81, 82, 83, 84, 89, 92, 98, 102, 105, 108, 109, 119, 120, 129, 131, 132, 135, 138, 148, 189, 192, 221, 229, 233

Meredith, W. J., 104, 109, 129, 166, 167, 174, 176, 177, 192

Moore, C. V., 229

Moore, S., 229

Moster, C. R., 213

MacVicar, W., 178, 192

McCorkle, H. J., 229

McDougall, J., 56

N

Neary, G. J., 104, 109, 191, 192

O

Oliver, R., 92, 109

P

Parker, H. M., 162, 166, 168, 170, 192, 222, 229

Paterson, R., 95, 109, 118, 129, 162, 166, 168, 170, 177, 192

Perlman, I., 229

Perlman, M. L., 218, 229

Portmann, U. V., 73

Q

Quastler, H., 34, 84, 213

Quimby, E. H., 87, 88, 92, 102, 109, 128, 148, 220, 229, 233

R

Read, J., 109

Reinhard, E. H., 221, 229

Riesen, D. E., 34, 84, 213

Roberts, J. E., 64, 66, 73, 192

Robertson, J. K., 34

Robinson, C. S., 34, 84, 213

Robinson, C. V., 229

Rude, J. C., 109

S

Schiff, L. I., 33, 34

Seaborg, G. T., 214, 229

Seitz, V. B., 73

Selverstone, B., 221, 229

Sievert, R. M., 73, 186, 192

Singer, G., 73, 192

Skaggs, L. S., 34, 84, 199, 200, 213

Smith, B. C., 220, 229

Smithers, D. W., 126, 129, 134, 148

Spencer, E. W., 164, 192

Spiers, F. W., 42, 56, 109, 141, 146, 147, 148, 191, 192

Stephenson, S. K., 192

Stone, R. S., 195, 213, 229

Strassmann, F., 202

Strong, J. A., 126, 129

Sweet, W. H., 229

T

Taft, R. B., 73

Taylor, L. S., 73, 192

Thoracius, R., 84

Tod, M. C., 192

Trump, J. G., 94, 95, 97, 109, 199, 212, 213

U

Uhlmann, E. M., 213

Ungar, E. M., 120, 123, 124, 129

V

Van de Graaff, R. J., 199, 200, 204, 206, 212, 213

Victoreen, J. A., 44, 56, 63, 65, 67, 69, 72, 73, 74, 90

W

Watson, T. A., 129, 147

Westendorp, F. W., 213

White, T. N., 192

Wilson, C. W., 120, 129, 147, 148

Wilson, R. R., 196, 213

Wyckoff, H. O., 213

SUBJECT INDEX

A

- Absorption coefficients, 35-56
 - apparent linear, 35-40
 - Compton, 44, 48, 49, 52
 - electronic, 40-42
 - linear, 35-40
 - mass, 40-47
 - pair, 44, 50, 51, 52
 - photoelectric, 43-48
 - real, 44, 49, 51, 53
 - real for air, 137, 138
 - relation between, 42
 - table of, 44
 - total, 52, 53
 - variation with atomic number and energy, 54, 55
- Absorption of x-rays, 35-56
 - copper, 75
 - edges in tin, 77
 - filter, 75, 77, 78, 79
 - graphs and tables illustrating, 37, 38, 39
 - importance of different mechanisms in biological material 53, 54, 55
- Air dose, 108
- Air wall material, 64
- Alpha particle, 149, 150
 - nuclear reactions induced by, 215
 - from radium, 153
 - track, 150
- Angstrom, unit of length, 11
- Annihilation radiation, 51
- Anode of x-ray tube, 17, 21
 - emission from, 23
 - rotating, 22
- Applicator, beta ray, 190, 191 (*see* radium dosage)
- Area of field
 - dependence of backscatter on, 88, 89, 233
 - dependence of depth dose on, 92, 93, 94, 234-253
- Atom, 3
- Atomic number, 4, 5
 - biological material, 42, 141
 - effective, 42, 64
- Auto-transformer, 19
- Average life, 156
- Avogadro's number, 42

B

- Backscatter, 85, 86
 - Variation with
 - area, 88, 89, 233
 - elongation factor, 91
 - half value layer, 89
 - thickness of underlying tissue, 87
- Balanced tumor dose, 118
- Beam director, 114, 115, 116
- Beta
 - decay, 150-153, 217
 - particles and tracks, 150
- Betatron
 - activity induced in biological materials, 216, 217
 - angular distribution of radiation, 33
 - depth dose, 94, 95, 254
 - integral dose, 134
 - operation, 196-199
 - response of thimble chamber to, 66
 - treatment of oesophagus, 127
- Biasing of fields, 113
- Bolus material, 123
- Bone
 - atomic number, 141
 - effect of, on depth dose and energy absorption, 144-147
 - preferential energy absorption, 119

C

- Calibration of x-ray machine, 62, 67-70
- Calorie, unit of heat, 21, 131
- Calorie and gram roentgen, 131
- Carbon, electronic structure, 7
- Carbon dioxide, electronic structure, 7
- Cervix
 - radium in treatment of, 187-190
 - split field for use in treatment of, 274
- Chlorine electronic structure, 7
- Cobalt isotopes, 6
- Cobalt 60
 - calculation of dosage rate from, 227
 - decay of, 220
 - depth dose from, 96, 212
 - depth dose tables, 252, 253
 - disintegration scheme, 225, 226
 - energy of decay particles, 220
 - telecurie units, 206, 208-212, 228
- Coefficients (*see* absorption coefficients)

- Combination of x-ray fields, 110 (*see* isodose distributions of radiation)
- Compensating filter for high energy x-ray beams, 34, 95
- Compton process, 35, 43, 44, 48, 49, 52 (*see* absorption coefficients)
- Condenser, 27
- Cone, treatment, 86
- Contour projector, 119, 120, 123
- Coplanar fields, 110 (*see* isodose distributions of radiation)
- Copper
- absorption of x-rays by, 46, 77
 - mass absorption coefficients (Table), 44
 - photoelectric absorption in, 78
- Corpuscular radiation, 58, 59
- Curie, definition of, 160
- Cyclotron, 193-196, 226
- D**
- Density, 41
- of biological material (Table), 42, 141
- Depth dose
- definition, 91
 - diagram illustrating, 86
 - effect of bone and fat, 144-147
 - measurement of, 231-233
 - tables, 233-254
 - variations with
 - area of field, 92, 93, 94, 234-253
 - depth, 92, 93, 94, 95
 - F.S.D., 100-103
 - half value layer, 94-98
 - quality, 94-98
- Detection of radiation using geiger counter, 72
- Deuteron, 5
- Diaphragm, limiting, 86
- Disintegration
- schemes for radioactive materials, 153, 225
 - types in artificial radioactivity, 218
- Distributions of radiation (*see* isodose distributions of radiation)
- spectral, 28, 29, 77, 78, 79, 275-278
- Dosage
- from radioactive isotopes, 223, 224, 225
 - in air, 108
 - in radiotherapy, 127, 128, 129
 - rate from gamma emitters, 228
- Dyne, 3
- E**
- Effective atomic number, 42, 64, 141
- Einstein
- energy equation, 50, 216
 - mass equation, 195
- Electric field, 61
- Electron, 3, 4
- absorption coefficients, 40-43 (*see* absorption coefficients)
 - acceleration, 18
 - depth dose obtained using, 200
 - emission, 20
 - energy loss, 41
 - number per gram, 42, 141
 - range, 62, 97
 - stopping power, 67
 - structure of atoms, 6, 7, 8
 - volt, 9
- Electromagnetic radiation, 10
- Electrostatic machine, 204, 205
- Electrostatic unit, 3
- ion pairs per, 130
- Ellipse, area of, 136
- Elongation factor
- effect on backscatter, 90, 91
 - effect on depth dose, 93
- Energy absorption
- biological material, 140-144
 - per gram roentgen, 130, 222
 - preferential, 119
 - variation with energy for biological material, 142, 147
- Energy conservation in beta decay, 151
- Energy distribution of beta particles in beta decay, 151
- Energy flux, 137
- per roentgen, 137, 138, 139, 227
- Energy levels in atoms, 8
- Entrance point of x-ray beam, 114
- Equivalent kilovoltage, 79
- relation to wavelength, 79 (*see* wavelength)
 - variation of depth dose with, 98
- Erg, unit of energy, 8
- Erythema, skin, 128
- Exit point of x-ray beam, 114
- Exponential absorption, 38, 39, 40
- F**
- F-factor for depth dose conversion, 100-104
- Fat, effect on depth dose, 144-147

Filament of x-ray tube, 17

Filter, 77

radiation from, 78

Thoraeus, 78

Filtration corrections for radium dosage,
167, 174, 177

Fission of uranium, 201-204, 217, 226

Fluorine, electronic structure, 7

Flux, of energy (*see* energy flux)

neutron, 206

Focal skin distance

conversion factors for depth dose, 100-
104

effect on depth dose, 96, 99, 100-104

Focussing device for electrons, 17

Fractionation of dose, 128

Frequency of radiation, 10, 11

G

Gamma emitters, dosage rate from, 227,
228

Gamma ray, 150, 153, 154

from radium, 153, 158, 159

reactions induced by, 216

track, photograph, 150

Geiger counter, 72

Geometrical edge of beam, 86

isodose curves near, 104, 105, 106

Gram roentgen, 130

Graph paper, logarithmic, 39, 40

Gray's formula, response of thimble cham-
ber, 67

H

Half life, relation to transformation con-
stant, 155

Half value layer, 38, 39, 40

graph illustrating, 38, 39, 75

measurement of, 74

relation to equivalent kilovoltage, 80

Helium

electronic structure of, 6

isotopes of, 5

Homogeneity of tumor dose, 113, 118, 127

Hospital Physicist's Association, 108

Hydrogen, 5, 6

Implant (*see* radium dosage)

Infra red radiation, 13

Integral dose, 129, 131

calculation for circular x-ray field, 132,
133

calculation for isotopes, 224

I

Integrating meter, 71

Internal field, 111, 112, 113, 118

Inverse cycle, 23

Inverse square law, 67, 68, 69

effect on depth dose, 99, 101

Iodine, 131

disintegration scheme, 225

dosage calculations for, 225

Ion pair, energy to liberate, 130

Ionization chamber

corrections for temperature and pressure,
62, 69, 70

double, 81

energy absorbed in, 67

equilibrium wall, 66

Gray's formula, 67

practical types, 62

standard, 58-61

Victoreen condenser, 62-66

wall effect, 64, 66

Ionization current, 60

Ionizing radiation, units, 222

Isobar, 6, 218

Isobaric lines, 217, 218

Isodose curves, 104 (*see* isodose distribu-
tions of radiation)

Isodose distributions of radiation

betatron, 107, 127

combinations of fields, 110, 111, 112,
122, 126, 127, 274

coplanar fields, 110

paraxial plane, 120-124

peripheral plane, 123, 124, 126

principal plane, 108, 123, 124

radium sources, 186, 187

rectangular fields, 123, 124

skin surface, 122

space, 110

standard fields, 400 KV, 105, 108, 266-
274

standard fields, 200 KV, 106, 108, 255-
265

treatment of oesophagus, 124-127

Isodose surfaces, 104, 110

Isotopes, 5, 214-218

list of radioactive, 226

J

Joule

energy unit, 21, 131

K

- K-capture, 217
- K-radiation, 9
 - tin, 77
 - tissue, 16
 - tungsten, 15, 29, 77
- Kilovoltage, equivalent, 79
 - equivalent wavelength, relation to, 80
 - half value layer, relation to, 80
- Kilovoltage, selection by auto-transformer, 19
- Klein-Nishina formula, 89

L

- L-radiation, 9
 - tungsten, 15
- Larynx, 113
 - calculation for treatment of, 116-119
 - mould, 115
- Lead mass absorption coefficients
 - graph of, 46
 - table of, 44
- Light, velocity of, 10
- Line focus, x-ray tube, 22
- Lines, spectral
 - K of tungsten, 29, 77
 - L of tungsten, 9, 15
- Lithium, electronic structure, 7
- Logarithm, base of natural, 38
- Logarithmic graph paper, 39, 40

M

- M-radiation, 9
- Magnification of x-ray images, 114, 115
- Manchester system (*see* radium dosage)
- Mass
 - number, 5, 217, 218
 - relation to velocity, 195
- Mass absorption coefficient, 40 (*see* absorption of radiation)
- Mass of atoms, 3, 4, 5
- Measurement of radiation
 - integrating types, 71
 - protection devices, 72
 - standard chamber, 58-61
 - Victoreen condenser r meter, 62-70
- Megagram roentgen, *see* gram roentgen
- Mesotron, 4
- Mev., unit of energy, 9
- Microcurie, 160
- Millicurie, 160
 - destroyed, 162
 - hour, 161

Monochromatic radiation, 74

Mould for beam direction, 114, 115, 116, 125

N

- Neon, electronic structure, 7
- Neutron, 3, 4, 214
 - reactions induced by, 215
- Neutrino, 3, 4, 151
- Nuclear reactor (pile), 203, 204, 206, 208, 214, 226
- Nucleii, 3, 4
 - chart of, 214, 217
 - stability of, 217

O

- Oesophagus
 - treatment, 124-127
 - integral dose in treatment, 134
- Optical radiation, 9
- Oxygen, electronic structure, 7

P

- Pair process, 35, 44, 50, 51, 52
- Paraxial plane, 120-124
- Percentage depth dose (*see* depth dose)
- Peripheral plane, 123, 124, 126
- Phantoms, 85
- Phosphorous, isotopes, 6
- Phosphorous radioactive, (P^{32})
 - disintegration scheme, 225
 - dosage with, 223, 224
 - energy distribution of beta particles, 151
 - tracer studies, 220, 221
 - use of, for blood disorders, 221
- Photoelectric process, 35, 43, 44
- Photonuclear reaction, 216
- Pile, nuclear reactor, 203, 204, 206, 208, 214, 226
- Pinch spot, 126
- Planck's constant, 11
- Planar implants, dosage table, 167 (*see* radium dosage)
- Planetary electrons, 6
- Plaster of paris moulds, 114, 115, 116, 125
 - effect on depth dose, 119
- Positron, 4
- Power, 21
- Principal plane, 108, 123, 124
- Projector, contour, 119, 120, 123
- Protection, health, 139, 140, 212, 213
- Proton, 3
 - reactions induced by, 215

Q

- Quality of radiation, 74-84
 - dependence of backscatter on, 87, 89
 - dependence of depth dose on, 92-99
 - measurement, 74, 75, 76
 - variation of, in scattering medium, 81-83
- Quantity of radiation, measurement of, 57-73
- Quantum nature of radiation, 11

R

- Radiation, electromagnetic, 10-16 (*see* x-rays)
 - radiation of energy by, 15, 16
 - spectrum, 12-15
 - quantum nature, 11, 12
 - wavelength, 10, 11
- Radiation of energy, 15
- Radio waves, 13
- Radioactive
 - disintegration, 154-157
 - equilibrium, 158
 - series, 156, 157
- Radioactive isotopes
 - dosage with, 223, 224, 225
 - strength of, 160
- Radium
 - active deposits, 158
 - beam unit, 95, 145, 146
 - decay products, 156, 157
 - disintegration scheme, 153
 - dosage calculator, 162, 163, 166, 168
 - dosage rate from, 165
 - energy levels, 153
- Radium distribution rules
 - circles, 169
 - concave and convex surfaces, 170
 - cylindrical surfaces, 170
 - ideal, 168
 - rectangles, 169, 171, 172
 - squares, 169, 171, 172
 - surface applicators, 166, 168, 169, 180, 181
 - volume implants, 175
- Radium dosage, 165-192
 - cervix, 187-190
 - depth dose for surface applicators, 170
 - examples, 179-186
 - filtration corrections, 167, 174, 177
 - interstitial implants, 170, 171, 172, 181, 182

- linear sources, 175, 176, 177, 183, 186, 187
- linear sources for homogeneity, 178, 184
- Manchester system, 165
- radiographic control, 177-181
- sandwich mould, 184-186
- summary, 191, 192
- surface applicators, 166-170
- two plane implant, 172, 173, 184, 185, 186
- volume implant, 173, 174, 182, 183
- Radium gamma rays
 - depth dose, 95
 - response of thimble chamber to, 65, 66
- Radon
 - disintegration of, 156
 - emitted dose from, 161
 - growth and decay of activity, 155, 162, 163, 164
 - table of decay, 161
- Range of electrons, 62
- Rectangular fields, 118
 - distribution in space for, 123, 124
- Rectification,
 - full wave, 26
 - mechanical, 23
 - self, 18, 19
 - valve, 22-25
- Resonant transformer, 206-208
- Rheostat, 19
- Roentgen, 57, 58
- Roentgen equivalent mammal (rem.), 222
- Roentgen equivalent physical (rep.), 222-224
- Rutherford, activity unit, 161

S

- Saturation ionization current, 60
- Scattered radiation, 40, 76, 86
 - angular distribution of, 89
 - Compton, 48
 - effect on depth dose, 99
- Scattering medium, interaction of x-rays with, 85
- Shells of atoms, 7, 16
- Sigma, sum of, 133
- Skin dose, 108, 117
- Skin surface
 - depth dose near, 94
 - distributions on, 122
- Sodium, electronic structure, 7

Soft x-rays

- depth dose and energy absorption using, 144, 145
- tube, 25

Spectral distribution of x-rays, 28, 29, 275-278

Spectrum

- continuous, 30
- electromagnetic, 12
- radium gamma ray, 158, 159

Standard ionization chamber, 58-61

Supervoltage equipment, 193-212

Surface backscatter (*see* backscatter)

Synchrotron, 201

T

Target of x-ray tube, 17, 31

Thimble chamber, 62-66

Thoria filter, 78, 79

Tin

- filter, 77, 78, 79
- photoelectric effect in, 77, 78

Tracer studies, 220

Transformation, constant, 154

Transformer

- auto, 19
- constant voltage, 26
- filament, 19, 20
- high tension, 19
- step down, 20

Trunk, mean dose in radiation of, 136

Tungsten

- energy levels, 9, 15, 43
- K-lines, 29
- shells of, 9

U

Ultra violet radiation, 14

V

Vacuum inside x-ray tube, 18

Valence electron, 9

Van de Graaff generator, 204, 205

- depth dose from, 95, 212

Vertebra, treatment of, 124

Victoreen condenser r meter, 62-70

Villard circuit, 27

Visible radiation, 14

Voltage doubling circuit, 27

W

Water, mass absorption coefficients of, 44, 47

Watt, unit of power, 21

Wavelength, 10

- change in, 48
- minimum, 15, 29

Wavelength, equivalent, 79

- relation to equivalent kilovoltage, 80
- variation in scattering medium, 81, 82, 83

- measurement of, using double chamber, 81

Wax man, 135

White radiation, 29, 30

Whole body irradiation, 135

X

X-ray

- absorption of (*see* absorption of x-rays)
- angular distribution of, 32
- characteristic, 29
- continuous, 29, 30
- energy of, 12
- interaction with scattering medium, 85-109
- measurement of, 57-73
- production of, 17-29
- properties of, 17, 29-34
- quality of, 74-84
- quantity of, 57-73
- types of, 14, 15
- wavelength of, 14, 15
- white, 29, 30

X-ray circuits, 22, 23, 26, 27, 28

X-ray machine

- calibration of, 67-70
- supervoltage types, 193-212

X-ray tube, 17

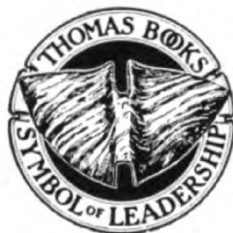
- diagnostic, 22
- soft, 25

This Book

THE PHYSICS OF RADIATION THERAPY

By HAROLD ELFORD JOHNS, M.A., PHD., F.R.S.C.

was set, printed, and bound by The Marvin D. Evans Company of Fort Worth, Texas. The page trim size is 6½ x 10 inches. The type page is 28 x 48 picas. The type face is Caledonia, set 11 point on 13 point. The text paper is 70-pound Enamel. The cover is Roxite, LS Vellum 5175 11-M, Two-tone Black Morocco.



With THOMAS BOOKS careful attention is given to all details of manufacturing and design. It is the Publisher's desire to present books that are satisfactory as to their physical qualities and artistic possibilities and appropriate for their particular use. THOMAS BOOKS will be true to those laws of quality that assure a good name and good will.

UNIVERSITY OF CALIFORNIA

THE LIBRARY
UNIVERSITY OF CALIFORNIA
San Francisco Medical Center

THIS BOOK IS DUE ON THE LAST DATE STAMPED BELOW

Books not returned on time are subject to fines according to the Library Lending Code.

Books not in demand may be renewed if application is made before expiration of loan period.

<p>14 DAY JUN 29 1964 JUN 7 1964 14 DAY NOV 9 1964 14 DAY DEC 31 1965 RETURNED JAN 10 1966</p>	<p>14 DAY JUN 2 1967 RETURNED JUN 5 1967 14 DAY NOV 30 1969 14 DAY DEC 14 1969 RETURNED NOV 30 1969</p>	<p>14 DAY JUL 5 1974 RETURNED JUN 2 1974 80m-10,'61(C3941s4)4128</p>
--	---	---

00448 963



3 1378 00448 9632

RM849 Johns, H. E. 89955
J65 The physics of radiation
1953 therapy.

~~Oba~~
~~Oba~~
~~Oba~~
~~Oba~~
UG 8 1955
~~EC K...~~
~~EC K...~~
~~Q...~~

